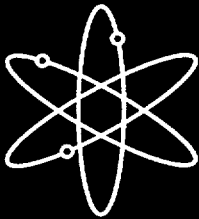
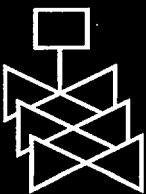


FRAPTRAN: Integral Assessment



Pacific Northwest National Laboratory



**U.S. Nuclear Regulatory Commission
Office of Nuclear Regulatory Research
Washington, DC 20555-0001**



AVAILABILITY OF REFERENCE MATERIALS IN NRC PUBLICATIONS

NRC Reference Material

As of November 1999, you may electronically access NUREG-series publications and other NRC records at NRC's Public Electronic Reading Room at www.nrc.gov/NRC/ADAMS/index.html.

Publicly released records include, to name a few, NUREG-series publications; *Federal Register* notices; applicant, licensee, and vendor documents and correspondence; NRC correspondence and internal memoranda; bulletins and information notices; inspection and investigative reports; licensee event reports; and Commission papers and their attachments.

NRC publications in the NUREG series, NRC regulations, and *Title 10, Energy*, in the Code of *Federal Regulations* may also be purchased from one of these two sources.

1. The Superintendent of Documents
U.S. Government Printing Office
Mail Stop SSOP
Washington, DC 20402-0001
Internet: bookstore.gpo.gov
Telephone: 202-512-1800
Fax: 202-512-2250
2. The National Technical Information Service
Springfield, VA 22161-0002
www.ntis.gov
1-800-553-6847 or, locally, 703-605-6000

A single copy of each NRC draft report for comment is available free, to the extent of supply, upon written request as follows:

Address: Office of the Chief Information Officer,
Reproduction and Distribution
Services Section
U.S. Nuclear Regulatory Commission
Washington, DC 20555-0001
E-mail: DISTRIBUTION@nrc.gov
Facsimile: 301-415-2289

Some publications in the NUREG series that are posted at NRC's Web site address www.nrc.gov/NRC/NUREGS/indexnum.html are updated periodically and may differ from the last printed version. Although references to material found on a Web site bear the date the material was accessed, the material available on the date cited may subsequently be removed from the site.

Non-NRC Reference Material

Documents available from public and special technical libraries include all open literature items, such as books, journal articles, and transactions, *Federal Register* notices, Federal and State legislation, and congressional reports. Such documents as theses, dissertations, foreign reports and translations, and non-NRC conference proceedings may be purchased from their sponsoring organization.

Copies of industry codes and standards used in a substantive manner in the NRC regulatory process are maintained at—

The NRC Technical Library
Two White Flint North
11545 Rockville Pike
Rockville, MD 20852-2738

These standards are available in the library for reference use by the public. Codes and standards are usually copyrighted and may be purchased from the originating organization or, if they are American National Standards, from—

American National Standards Institute
11 West 42nd Street
New York, NY 10036-8002
www.ansi.org
212-642-4900

Legally binding regulatory requirements are stated only in laws; NRC regulations; licenses, including technical specifications; or orders, not in NUREG-series publications. The views expressed in contractor-prepared publications in this series are not necessarily those of the NRC.

The NUREG series comprises (1) technical and administrative reports and books prepared by the staff (NUREG-XXXX) or agency contractors (NUREG/CR-XXXX), (2) proceedings of conferences (NUREG/CP-XXXX), (3) reports resulting from international agreements (NUREG/IA-XXXX), (4) brochures (NUREG/BR-XXXX), and (5) compilations of legal decisions and orders of the Commission and Atomic and Safety Licensing Boards and of Directors' decisions under Section 2.206 of NRC's regulations (NUREG-0750).

DISCLAIMER: This report was prepared as an account of work sponsored by an agency of the U.S. Government. Neither the U.S. Government nor any agency thereof, nor any employee, makes any warranty, expressed or implied, or assumes any legal liability or responsibility for any third party's use, or the results of such use, of any information, apparatus, product, or process disclosed in this publication, or represents that its use by such third party would not infringe privately owned rights.

FRAPTRAN: Integral Assessment

Manuscript Completed: September 2001

Date Published: September 2001

Prepared by

M.E. Cunningham, C.E. Beyer, F.E. Panisko, P.G. Medvedev, PNNL

G.A. Berna, GABC

H.H. Scott, NRC

Pacific Northwest National Laboratory

Richland, WA 99352

Subcontractor:

G.A. Berna Consulting

2060 Sequoia Drive

Idaho Falls, ID 83404

H. Scott, NRC Project Manager

Prepared for

Division of Systems Analysis and Regulatory Effectiveness

Office of Nuclear Regulatory Research

U.S. Nuclear Regulatory Commission

Washington, DC 20555-0001

NRC Job Code W6200



ABSTRACT

An integral assessment has been performed of the FRAPTRAN transient fuel behavior code designed to analyze fuel rod thermal and mechanical behavior during a range of transients with fuel burnup to 65 GWd/MTU. This assessment was performed for the U.S. Nuclear Regulatory Commission by Pacific Northwest National Laboratory to quantify the predictive capabilities of FRAPTRAN. The FRAPTRAN predictions are shown to compare satisfactorily to a selected set of experimental data from reactivity-initiated accident (RIA), loss-of-coolant-accident (LOCA), and other transient operating conditions.

CONTENTS

ABSTRACT	iii
EXECUTIVE SUMMARY	xv
FOREWORD	xvii
ACKNOWLEDGMENTS	xix
ACRONYMS/ABBREVIATIONS.....	xxi
1 INTRODUCTION	1.1
2 ASSESSMENT DATA DESCRIPTION.....	2.1
3 SEPARATE EFFECTS ASSESSMENTS.....	3.1
4 REACTIVITY INITIATED ACCIDENTS ASSESSMENT.....	4.1
4.1 NSRR Test Rods.....	4.5
4.2 CABRI Test Rods.....	4.12
4.3 IGR H5T Case	4.13
4.4 Summary of RIA Assessment Results.....	4.14
5 LOSS-OF-COOLANT-ACCIDENT ASSESSMENTS.....	5.1
5.1 MT-1 Assessment	5.1
5.2 MT-4 Assessment	5.2
5.3 MT-6A Assessment	5.2
5.4 PBF LOC-11C Assessment	5.4
5.5 TREAT FRF-2 LOCA Assessment	5.6
5.6 Summary of LOCA Assessment Results.....	5.6

6	OTHER TRANSIENT ASSESSMENTS	6.1
6.1	FRAP-T6 Standard Problem.....	6.1
6.2	IFA-508, Rod 11	6.4
6.3	IFA-533.2.....	6.5
6.4	PBF IE-1, Rod 7	6.6
6.5	PBF PR-1	6.8
7	SUMMARY AND CONCLUSIONS	7.1
8	REFERENCES	8.1
	APPENDIX A - DESCRIPTION OF CASES	A.1
	APPENDIX B - FRAPTRAN INPUT FILES.....	B.1

FIGURES

3.1	Comparison of Predicted and Measured Fuel Centerline.....	3.2
3.2	Comparison of Predicted and Measured Fuel Centerline.....	3.2
3.3	Comparison of Predicted and Measured Fuel Centerline.....	3.3
3.4	Comparison of Predicted and Measured Cladding.....	3.3
3.5	Comparison of Predicted and Measured Cladding.....	3.5
3.6	Comparison of Predicted and Measured Gas Pressure.....	3.5
4.1	Predicted vs. Measured Cladding Permanent Hoop Strain for RIAs.....	4.3
4.2	Predicted vs. Measured Cladding Permanent Axial Strain for RIAs.....	4.3
4.3	Predicted vs. Measured Peak Cladding Elongation for RIAs.....	4.4
4.4	Predicted vs. Measured Peak Fuel Elongation for RIAs.....	4.4
4.5	Comparison of Measured and Predicted Axial Elongation for HBO-6.....	4.6
4.6	Comparison of Measured and Predicted Axial Elongation for MH-3.....	4.6
4.7	Comparison of Measured and Predicted Axial Elongation for GK-1.....	4.7
4.8	Comparison of Measured and Predicted Axial Elongation for OI-2.....	4.7
4.9	Comparison of Measured and Predicted Axial Elongation for TS-5.....	4.8
4.10	Comparison of Measured and Predicted Axial Elongation for FK-1.....	4.8
4.11	Comparison of Measured and Predicted Axial Elongation for REP-Na3.....	4.9
4.12	Comparison of Measured and Predicted Axial Elongation for REP-Na4.....	4.9
4.13	Comparison of Measured and Predicted Axial Elongation for REP-Na5.....	4.10
4.14	Predicted Cladding and Fuel Axial Elongation for IGR H5T.....	4.10
4.15	Predicted Rod Gas Pressure and Cladding-Average Temperature for IGR H5T.....	4.13

5.1	Comparison of Measured and Predicted Plenum Gas Pressure for MT-1.....	5.3
5.2	Comparison of Measured and Predicted Plenum Gas Pressure for MT-4.....	5.3
5.3	Comparison of Measured and Predicted Plenum Gas Pressure for MT-6A.....	5.4
5.4	Comparison of Measured and Predicted Fuel Centerline Temperature for LOC-11C.....	5.5
5.5	Comparison of Measured and Predicted Cladding Axial Elongation for LOC-11C.....	5.5
5.6	Comparison of Measured and Predicted Gas Pressure for FRF-2.....	5.7
5.7	Measured and Predicted Permanent Hoop Strain for FRF-2.....	5.7
6.1	Comparison of FRAP-T6 and FRAPTRAN.....	6.2
6.2	Comparison of FRAP-T6 and FRAPTRAN Fuel Centerline.....	6.2
6.3	Comparison of FRAP-T6 and FRAPTRAN Cladding Elongation for Standard Problem.....	6.3
6.4	Comparison of FRAP-T6 and FRAPTRAN Gas Pressure for Standard Problem.....	6.3
6.5	Comparison of Measured and Predicted Cladding Elongation During.....	6.4
6.6	Comparison of Measured and Predicted Difference Between Fuel.....	6.5
6.7	Comparison of Measured and Predicted Cladding Elongation for IE-1, Rod 7.....	6.7
6.8	Comparison of Measured and Predicted Cladding Elongation for IE-1,.....	6.7
A.1	Measured Fuel Centerline Temperatures for Rod 1 (standard gap) of IFA-432.....	A.2
A.2	Measured Fuel Centerline Temperatures for Rod 3 (small gap) of IFA-432.....	A.3
A.3	Measured Fuel Centerline Temperatures for Rod 6 (23% xenon) of IFA-513.....	A.3
A.4	Measured Cladding Elongation for Rod 3 (small gap) of IFA-432.....	A.4
A.5	Measured Cladding Elongation and Gas Pressure.....	A.4
A.6	Example RIA Power History for NSRR.....	A.7
A.7	Cladding Surface Temperature History for HBO-6, Thermocouples #1 and #3.....	A.11

A.8 Fuel Pellet Stack Elongation History for HBO-6	A.12
A.9 Cladding Surface Temperature History for MH-3.....	A.13
A.10 Pellet Stack and Cladding Elongation History for MH-3	A.14
A.11 Cladding Surface Temperature History for GK-1	A.15
A.12 Rod Internal Gas Pressure History for GK-1.....	A.15
A.13 Fuel and Cladding Axial Elongation History for GK-1.....	A.16
A.14 Cladding Surface Temperature History for OI-2.....	A.17
A.15 Rod Internal Gas Pressure History for OI-2	A.17
A.16 Fuel and Cladding Elongation History for OI-2	A.18
A.17 Cladding Temperature History for TS-5.....	A.19
A.18 Rod Internal Gas Pressure History for TS-5.....	A.20
A.19 Cladding Elongation History for TS-5.....	A.20
A.20 Cladding Temperature History for FK-1	A.21
A.21 Rod Internal Gas Pressure History for FK-1	A.22
A.22 Fuel and Cladding Elongation History for FK-1	A.22
A.23 Cladding Elongation History for REP-Na3	A.26
A.24 Double Peak Power History for REP-Na4.....	A.27
A.25 Cladding Elongation History for REP-Na4	A.27
A.26 Cladding Elongation History for REP-Na5	A.28
A.27 Power History for IGR H5T	A.31
A.28 Cladding Inner Surface Temperature for MT-1.....	A.34
A.29 Representative Plenum Pressure for MT-1, Rod 5C (unfailed).....	A.35

A.30 Representative Post-Test Diameter Profile for MT-1 Rods	A.35
A.31 Cladding Inner Surface Temperature for MT-4.....	A.36
A.32 Rod Gas Pressure for MT-4	A.37
A.33 Representative Permanent Strain for MT-4 Rods.....	A.38
A.34 Cladding Inner Surface Temperatures for MT-6A	A.39
A.35 Plenum Gas Pressure for MT-6A.....	A.39
A.36 LOC-11C Cladding Surface Temperature History	A.41
A.37 LOC-11C Fuel Centerline Temperature History	A.41
A.38 LOC-11C Cladding Elongation History	A.42
A.39 LOC-11C Axial Strain History	A.42
A.40 Post-Test Cladding Diameters for Test Rods in LOC-11C	A.43
A.41 Cladding Permanent Hoop Strain for Test Rods in LOC-11C	A.43
A.42 Cladding OD Temperature History for TREAT FRF-2.....	A.45
A.43 Rod Plenum Pressure History for TREAT FRF-2	A.46
A.44 Cladding Permanent Diameter Increase for FRF-2	A.46
A.45 FRAP-T6 Standard Problem Cladding Temperature History.....	A.48
A.46 FRAP-T6 Standard Problem Fuel Centerline Temperature History.....	A.48
A.47 FRAP-T6 Standard Problem Cladding Elongation History.....	A.49
A.48 FRAP-T6 Standard Problem Rod Gas Pressure History	A.49
A.49 Initial Power Ascension for IFA-508, Rod 11	A.51
A.50 Initial Cladding Elongation History for HPR-508, Rod 11	A.51
A.51 Fuel Centerline Temperature History for Rod 808R of IFA-533.2	A.53

A.52 Rod-Average Power and Coolant Flow History for Rod 7, PBF IE-1.....	A.55
A.53 Measured Cladding Axial Elongation and Gas Pressure.....	A.56
A.54 Measured Cladding Temperature During Flow Reduction for Rod 7, PBF IE-1	A.56
A.55 Measured Cladding Axial Elongation During Flow Reduction for Rod 7, PBF IE-1	A.57
A.56 Linear Heat Rate and Coolant Flow History for PR-1.....	A.58
A.57 Measured Cladding Elongation History for PR-1, Cycle 17	A.59
A.58 Measured Cladding Surface Temperature for PR-1, Cycle 17	A.59
B.1 Comparison of Potential RIA Power Histories for Rod FK-1	B.7
B.2 FRAPTRAN Coolant Temperature Input History for HBO-6.....	B.8
B.3 FRAPTRAN Coolant Temperature Input History for FK-1	B.16
B.4 Axial Power Profiles for CABRI RIA Tests.....	B.18
B.5 Coolant Temperature History for REP-Na3	B.19
B.6 Coolant Temperature History for REP-Na4	B.21
B.7 Coolant Temperature History for REP-Na5	B.23
B.8 Axial Power Profile for IGR HST	B.30
B.9 MT-6A Cladding Temperature History	B.31
B.10 Pretransient Axial Temperature Profile for MT-4.....	B.33
B.11 Assumed MT-4 Cladding/Coolant Temperature History	B.34
B.12 Assumed MT-1 Cladding/Coolant Temperature History	B.37
B.13 Assumed Axial Power Profile for NRU LOCA Tests	B.39
B.14 Assumed Coolant Temperature History for LOC-11C.....	B.41
B.15 Assumed Axial Power Profile for LOC-11C.....	B.41

B.16	Transient Power History for FRF-2.....	B.44
B.17	Axial Power Profile for FRF-2	B.44
B.18	Assumed Input Cladding Temperature History for FRF-2.....	B.45
B.19	Axial Power Profile for IFA-508, Rod 11	B.50
B.20	Axial Power Profile for IFA-533.2.....	B.53
B.21	Axial Power Profile for PBF IE-1, Rod 7	B.55
B.22	Axial Power Profile for PBF PR-1.	B.58

TABLES

2.1	Integral Assessment Cases for FRAPTRAN	2.2
4.1	Comparison of RIA Mechanical Results	4.2
5.1	Summary of Measured and Predicted Results for LOCA Assessment Cases	5.2
6.1	Comparison of Measured Data and FRAPTRAN Results for PR-1, Cycle 17	6.8
A.1	Design Parameters for Rods 1 and 3 of IFA-432 and Rod 6 of IFA-513	A.2
A.2	Summary of RIA Data Collection and Post-Test Results	A.6
A.3	Summary of NSRR RIA Test Rod Parameters	A.8
A.4	Summary of CABRI RIA Test Rod Parameters	A.24
A.5	Summary of IGR H5T Test Rod Parameters	A.30
A.6	Summary of NRU Test Parameters and Results	A.33
A.7	Basic Parameters for the LOC-11C Test	A.40
A.8	Basic Parameters for the TREAT FRF-2 Test	A.45
A.9	Fuel Rod Design for FRAP-T6 Standard Problem	A.47
A.10	Basic Parameters for the IFA-508 Test, Rod 11	A.50
A.11	Basic Parameters for IFA-533.2, Rod 808R	A.53
A.12	Basic Design Parameters for Rod 7, PBF IE-1	A.54
A.13	Basic Design Parameters for PBF PR-1 Test	A.58
B.1	FRAPTRAN Input for IFA-432, Rod 1 Assessment Case	B.2
B.2	FRAPTRAN Input for IFA-432, Rod 3 Assessment Case	B.4
B.3	FRAPTRAN Input for IFA-513, Rod 6 Assessment Case	B.5
B.4	Measured and Assumed Power Histories for NSRR RIA Cases	B.7

B.5	FRAPTRAN Input for HBO-6 Assessment Case	B.9
B.6	FRAPTRAN Input for MH-3 Assessment Case	B.10
B.7	FRAPTRAN Input for GK-1 Assessment Case.....	B.12
B.8	FRAPTRAN Input for OI-2 Assessment Case	B.13
B.9	FRAPTRAN Input for TS-5 Assessment Case.....	B.15
B.10	FRAPTRAN Input for FK-1 Assessment Case	B.17
B.11	Measured and Assumed Power Histories for CABRI RIA Cases	B.18
B.12	FRAPTRAN Input for REP-Na3 Assessment Case.....	B.20
B.13	FRAPTRAN Input for REP-Na4 Assessment Case.....	B.22
B.14	FRAPTRAN Input for REP-Na5 Assessment Case.....	B.24
B.15	FRAPTRAN Input for IGR H5T Assessment Case.....	B.26
B.16	FRAPTRAN Input for MT-6A Assessment Case.....	B.31
B.17	FRAPTRAN Input for MT-4 Assessment Case	B.35
B.18	FRAPTRAN Input for MT-1 Assessment Case	B.37
B.19	FRAPTRAN Input for LOC-11C Assessment Case.....	B.42
B.20	FRAPTRAN Input for FRF-2 Assessment Case	B.46
B.21	FRAPTRAN Input for FRAP-T6 Standard Problem Assessment Case	B.48
B.22	FRAPTRAN Input for IFA-508, Rod 11 Assessment Case	B.51
B.23	FRAPTRAN Input for IFA-533.2 Assessment Case	B.53
B.24	FRAPTRAN Input for PBF IE-1, Rod 7 Assessment Case	B.56
B.25	FRAPTRAN Input for PBF PR-1 Assessment Case.....	B.59

EXECUTIVE SUMMARY

An integral assessment was performed for the U.S. Nuclear Regulatory Commission of the transient fuel rod behavior code FRAPTRAN. The code was developed to calculate the thermal and mechanical behavior of light-water reactor fuel rods during reactor power and coolant transients such as reactivity accidents, boiling-water reactor power oscillations without scram, and loss-of-coolant accidents at burnup levels up to 65 GWd/MTU. The code calculates the variation with time, power, and coolant conditions of fuel rod variables such as fuel and cladding temperatures, cladding stress, elastic and plastic strain, and fuel rod gas pressure. To provide calculations for fuel at high burnup levels, FRAPTRAN utilizes a fuel thermal conductivity model and cladding mechanical properties that are appropriate for high burnup fuel. Volume 1 (Cunningham et al. 2001) of this report provides a complete description of the code and the input instructions.

The assessment was performed by comparing FRAPTRAN code calculations to data from selected integral irradiation experiments and postirradiation examination programs.

The cases used for code assessment were selected on the criteria of having well-characterized design and operational data, and spanning the ranges of interest for both design and operating conditions. Three principal sets of data were used: a) data from recent reactivity-initiated accident (RIA) test programs, b) data from loss-of-coolant-accident (LOCA) test programs, and c) other miscellaneous data sets. The code assessment data base consists of three separate effects and 20 integral assessment cases, as discussed in Section 2. A description of each assessment case is provided in Appendix A and the FRAPTRAN input for each case is provided in Appendix B.

The comparisons of the FRAPCON calculations to the experimental data are provided in Section 3 (separate effects), Section 4 (reactivity initiated accidents), Section 5 (loss of coolant accidents), and Section 6 (other transients). FRAPTRAN generally performed well in the comparisons to data. Additional conclusions for this code-data assessment are:

Comparison of code predictions with data have provided assurance that the basic models are working satisfactorily; i.e., temperature, gap conductance, gas pressure, and thermal expansion.

- Comparisons of predicted and measured fuel centerline temperature during scrams show that the code consistently calculates faster temperature decreases than were measured. This is likely due to FRAPTRAN calculating lower thermal resistances in the fuel or the fuel-cladding gap than are operating in the fuel rods.
- Rod internal gas pressure is correctly calculated when other parameters that determine gas pressure, such as available volume and corresponding temperatures, are correctly input and calculated. In addition, when gas pressure is correctly predicted for the LOCA cases, then reasonable agreement between predicted and measured time to failure is obtained.

- The experimental steady-state data for cladding elongation as a function of heat rate indicate fuel compliance (creep) that is not modeled by the code; i.e., the observed transition for cladding axial elongation from being driven by thermal expansion to expansion driven by fuel-cladding mechanical interaction is more gradual than predicted by the code. This observation is based on steady-state data that may not be appropriate for rapid transient response; i.e., rapid transients may not involve fuel creep.
- FRAPTRAN provided reasonable predictions of cladding axial elongation for fast transients but, as expected, did not follow the fuel and cladding relaxation when steady-state power conditions were achieved.
- FRAPTRAN consistently underpredicted permanent cladding hoop strain for the RIA tests conducted in the NSRR. This is indicative of fuel-cladding mechanical interaction occurring in these tests that is not modeled by the code. This failure to predict some aspects of the mechanical behavior of these tests has been observed for other codes. There is evidence to suggest there is actual fuel behavior resulting in additional cladding radial stress/strain that is not accounted for by the transient codes.

This assessment has identified some areas of work that are still needed for FRAPTRAN; these include:

- Improvements to the convergence of the mechanical solution model. The mechanical solution scheme is sensitive to rapid strain rates and may not iteratively converge if the time step is too large during periods of high strain rate for cases such as RIAs or high cladding temperature and low yield strength for cases such as LOCAs.
- Comparisons to the experimental data indicate the need for some fuel compliance, particularly for slow transients, to lessen the predicted abrupt mechanical transition from no fuel-cladding interaction to solid fuel-cladding interaction.
- Gaseous fission gas release and fuel swelling have been proposed as contributors to the cladding permanent hoop strain during RIAs. However, models for these phenomena are not included in FRAPTRAN and should be developed.

FOREWORD

The U.S. industry is in the process of increasing fuel burnup in nuclear power plants and introducing new cladding alloys that are needed to withstand associated challenges. High burnup fuel brings considerable economic benefits including a reduced number of fuel assemblies that need to be manufactured and a reduction in the overall volume of nuclear waste. To assure the safety of these newer fuel designs and operating conditions, analysis is needed within the industry and at NRC with transient fuel rod computer codes. NRC's code, FRAPTRAN, has recently been updated to handle these situations. To earn the public's confidence and the industry's acceptance, this code has been assessed against a variety of test data and has been subjected to a peer review. That assessment and review are described herein. Although this code, like other NRC and industry codes, still has limitations, we will continue to work on improvements to increase the accuracy of our work and to maintain the trust we owe to our constituents.

Jack E. Rosenthal, Chief
Safety Margins and Systems Analysis Branch

ACKNOWLEDGMENTS

The authors acknowledge Dr. Ralph Meyer of the U.S. Nuclear Regulatory Commission (NRC) for his technical guidance on the development, assessment, and peer review of FRAPTRAN. The NRC has agreements with the Japan Atomic Energy Research Institute and the Institute for Protection and Nuclear Safety in France. The authors acknowledge their assistance in providing the reactivity initiated accident data used in this assessment.

ACRONYMS/ABBREVIATIONS

ATWS	anticipated transient without scram
BWR	boiling-water reactor
FGR	fission gas release
FRAPTRAN	Fuel Rod Analysis Program TRANsient
FRAP-T6	Fuel Rod Analysis Program-Transient
HBWR	Halden Boiling Water Reactor
IGR	Impulse Graphite Reactor
IPSN	Institute for Protection and Nuclear Safety
JAERI	Japan Atomic Energy Research Institute
LHGR	linear heat generation rate
LWR	light-water reactor
LOCA	loss-of-coolant-accident
NSRR	Nuclear Safety Research Reactor
NRC	U.S. Nuclear Regulatory Commission
NRU	National Reactor Universal
PBF	Power Burst Facility
PCM	power-cooling-mismatch
PNNL	Pacific Northwest National Laboratory
PWR	pressurized-water reactor
RIA	reactivity-initiated accident
RRC-KI	Russian Research Centre "Kurchatov Institute"
TFBP	Thermal Fuels Behavior Program
TREAT	Transient Reactor Test Facility

1 INTRODUCTION

The ability to accurately calculate the performance of light-water reactor (LWR) fuel during irradiation, both long-term steady-state and various operational transients and hypothetical accidents, is an objective of the reactor safety research program conducted by the U.S. Nuclear Regulatory Commission (NRC). To achieve this objective, the NRC has sponsored an extensive program of analytical computer code development and both in-reactor and out-of-reactor experiments to generate the data necessary for development and verification of the computer codes. Provided in this report is an assessment of the performance of the FRAPTRAN (Fuel Rod Analysis Program TRANSient) code developed to calculate the response of single fuel rods to operational transients and hypothetical accidents at burnup levels up to 65 GWd/MTU (Cunningham et al. 2001). The FRAPTRAN code is the successor to the FRAP-T (Fuel Rod Analysis Program-Transient) code series developed in the 1970s and 1980s (Siefken et al. 1981; Siefken et al. 1983). FRAPTRAN is also a companion code to the FRAPCON-3 code (Berna et al. 1997) developed to calculate the steady-state response high burnup response of a single fuel rod.

FRAPTRAN is an analytical tool that calculates LWR fuel rod behavior when power and/or coolant boundary conditions are rapidly changing. The code calculates the variation with time, power, and coolant conditions of fuel rod variables such as fuel and cladding temperatures, cladding stress, elastic and plastic strain, and fuel rod gas pressure. To provide calculations for fuel at high burnup, FRAPTRAN utilizes a fuel thermal conductivity model and cladding mechanical properties that are appropriate for high burnup fuel. Provided in Volume 1 of this report (Cunningham et al. 2001) are descriptions of the fuel performance models, the code structure and limitations, and the code input instructions.

Provided in this report (Volume 2) are the results of the assessment of the integral code predictions to measured data for various transient types. The assessment data sets are summarized in Section 2.0 with detailed descriptions of each individual data set provided in Appendix A.

The results of the code-data assessments are provided in Sections 3, 4, 5, and 6. Because transient performance is dependent on the integrated thermal-mechanical response (and calculations), the assessment results are discussed by transient type rather than model response (i.e., thermal, mechanical, specific model, etc.). Provided in Section 3 are comparisons of the code to selected separate effects data. Following the separate effects comparisons, the code is compared to three main types of transients: reactivity-initiated accidents (RIAs) are discussed in Section 4; loss-of-coolant accidents (LOCAs) are discussed in Section 5; and other miscellaneous transients are discussed in Section 6. These three groups of transients represent the major applications that FRAPTRAN will be applied to by the NRC in evaluating transient fuel behavior. The input files for FRAPTRAN are provided in Appendix B, along with discussions of considerations applicable to setting up and making the assessment runs with FRAPTRAN. A summary and conclusions for the assessment are provided in Section 7.

2 ASSESSMENT DATA DESCRIPTION

A variety of assessment cases were selected to perform the assessment of FRAPTRAN. Three separate effects cases were selected to evaluate characteristics such as temperature or gas pressure; descriptions of these cases are provided in Section 3, along with the assessment results. Twenty integral assessment cases that have transient and/or post-irradiation examination data were selected to perform the integral assessment of the FRAPTRAN code. These integral assessment cases are of three principal types: a) data from reactivity-initiated accident (RIA) test programs, b) data from loss-of-coolant-accident (LOCA) test programs, and c) other miscellaneous data sets.

The objective of the code assessment was to assess FRAPTRAN against a limited set of qualified data that span a range of operational conditions for commercial light-water reactors for which the code will be applied. The cases in this limited group were selected using criteria regarding the completeness and the quality of the fuel rod performance data, as follows:

- The cases should provide pre-irradiation and postirradiation characterization data for the fuel rods of interest.
- The cases should provide well-qualified in-reactor fuel performance data such as power history, temperature history, and mechanical behavior history.
- The cases were chosen to include both low and high fuel burnup under the limiting conditions of interest.
- The cases should be of non-failed rods because of the difficulty in predicting failure and interpreting data from failed rods. (A couple of cases with failed rods are included because they were previously used in the assessment of FRAP-T6.)

The selected cases generally fulfill the above criteria. As shown below, there is a mix of fuel rod types among the assessment cases.

Assessment Type	# of PWR Cases	# of BWR Cases	# of VVER Cases
Separate Effects	0	3	0
RIA	7	2	1
LOCA	4	1	0
Other	2	3	0

A listing of the selected integral assessment cases is provided in Table 2.1. More information on the integral assessment cases is provided in Appendix A. Descriptions of how the FRAPTRAN runs were set up are provided in Appendix B, along with copies of the input files.

Table 2.1 Integral Assessment Cases for FRAPTRAN				
Case	Rod Type	Transient Reactor	Rod-Average Burnup	Other Comments
A. RIAs				
1) HBO-6	PWR 17x17	NSRR	49 MWd/kgM	80 cal/g, 4.4ms, 1.2% diametral strain
2) MH-3	PWR 14x14	NSRR	39 MWd/kgM	65 cal/g, 4.5ms, 1.6% diametral strain
3) GK-1	PWR 14x14	NSRR	42 MWd/kgM	93 cal/g, 4.6ms, 2.5% diametral strain
4) OI-2	PWR 17x17	NSRR	39 MWd/kgM	108 cal/g, 4.4ms, 4.8% diametral strain
5) TS-5	BWR 7x7	NSRR	26 MWd/kgM	98 cal/g, 4.6ms, 0% diametral strain
6) FK-1	BWR 8x8	NSRR	45 MWd/kgM	112 cal/g, 3.5ms, 0.9% diametral strain
7) REP-Na 3	PWR	CABRI	53 MWd/kgM	125 cal/g, 9.5ms, 2.0% diametral strain
8) REP-Na 4	PWR	CABRI	62 MWd/kgM	96 cal/g, 64ms, 0.4% diametral strain
9) REP-Na 5	PWR	CABRI	64 MWd/kgM	115 cal/g, 9ms, 1.1% diametral strain
10) IGR-H5T	VVER	IGR	50 MWd/kgM	153 cal/g, 760 ms, 6.5% diametral strain, failed
B. LOCAs				
11) NRU MT-1	PWR	NRU	0	11 full-length rods, adiabatic heatup
12) NRU MT-4	PWR	NRU	0	11 full-length rods, adiabatic heatup
13) NRU MT-6A	PWR	NRU	~0	21 full-length rods
14) PBF LOC-11C	PWR	PBF	0	4-rod test train; scram plus LOCA
15) TREAT FRF-2	BWR	TREAT	0	power ramp, adiabatic heatup
C. Other Cases				
16) FRAP-T6 Standard Problem	PWR	Assumed PWR	0	hypothetical PWR double-ended cold leg break
17) IFA-508, Rod 11	BWR	HBWR	0	initial power ascension
18) IFA-533.2, Rod 808R	BWR	HBWR	44 MWd/kgUO ₂	reinstrumented rod, scram
19) PBF IE-1, Rod 7	PWR-type	PBF	6.8 MWd/kgM	power-cooling mismatch
20) PBF PR-1	BWR-type	PBF	0 MWd/kgM	4-rod test train, 1 failed

During the process of performing the assessment, and getting the assessment cases to run, errors in the FRAPTRAN coding were identified and corrected.^a However, FRAPTRAN was not “tuned” to provide agreement with the assessment cases. For cases where cladding temperature data were available, the FRAPTRAN runs were made so that the calculated cladding temperatures matched the data; the purpose of this was to eliminate the effect of the thermal-hydraulic models in evaluating the performance of the fuel and cladding behavior models. FRAPTRAN is not intended to be used for predicting thermal-hydraulic performance because other codes have been developed for that purpose. The purpose of FRAPTRAN is to predict the thermal response of the fuel and its impact on the mechanical response of the cladding. The approach to assigning cladding temperatures for each case is provided in Appendix B.

Much of the mechanical data used in the assessment are axial elongation data for the cladding and fuel. These data are often quoted as an absolute length change, and occasionally as a % length change. For comparing the data and predicted length changes, the results will be presented here as % elongation. However, this does result in an issue of making appropriate comparisons because, for the experiments, the cladding length change is relative to the total rod length (active fuel length plus plenum length plus end plugs) while, for FRAPTRAN, cladding length change is calculated only over the active fuel length. For some test rods, the non-active length of the rod may be as long as the active length, thus defining the gage length to calculate % elongation is important to evaluating the data-prediction comparisons.

^aWhere applicable, these changes are included in the code description provided in Volume 1 (Cunningham et al. 2001).

For the assessments presented in the following sections, the cladding % elongation will be relative to the pre-transient active fuel length. This convention will be used because, in general, the non-active length of the cladding will be at coolant temperature and the contribution to the total cladding length change from the non-active lengths will be significantly less than the cladding length change along the active fuel section of the rod.

An input option for FRAPTRAN is to use an initialization file generated by using FRAPCON3 to simulate the steady-state irradiation prior to the transient. This initialization file defines burnup dependent parameters for FRAPTRAN such as radial dimensions, gas composition and pressure, and radial power and burnup profiles. This option was used for the assessment cases involving rods tested with burnup.

3 SEPARATE EFFECTS ASSESSMENTS

A few experiments were selected to provide what may be called separate effects data. These experiments are those where the experiment design and measured results are relatively unambiguous and may be used to demonstrate that specific models in FRAPTRAN are working correctly.

The selected tests were the IFA-432 and IFA-513 experiments irradiated in the Halden Boiling Water Reactor. These tests irradiated well-characterized BWR-type rods that were instrumented with fuel centerline thermocouples, gas pressure sensors, and cladding elongation sensors. Data obtained from the initial power ascension are used to compare against the FRAPTRAN predictions as a function of power (and temperature). Three rods have been selected because of design differences. Rod 1 of IFA-432 may be considered the standard rod with an initial fill gas of 100% helium and a fuel-cladding diametral gap of 0.009 inches (0.229 mm). Rod 3 of IFA-432 had a small diametral gap of 0.003 inch (0.076 mm). Rod 6 of IFA-513 had a diametral gap of 0.008 inch (0.203 mm) but an initial fill gas mixture of 77% helium and 23% xenon. The design parameters and irradiation data for these tests are provided in Appendix A and the input files are provided in Appendix B.

Predicted versus measured fuel centerline temperatures are provided in Figure 3.1 for Rod 1 of IFA-432, the "standard" rod. For this beginning-of-life, first power ascension case, the predicted temperatures are less than the measured temperatures with the difference approaching 100K at 30 kW/m. This under-prediction may be attributed to the simplified implementation of fuel relocation in FRAPTRAN where relocation occurs immediately during the initial power ascension. While this results in underpredicting temperatures for an initial power ascension, it results in better temperature predictions for later in an irradiation history.

Predicted versus measured fuel centerline temperatures are provided in Figure 3.2 for Rod 3 of IFA-432, the "small gap" rod. The difference between predicted and measured fuel centerline temperature is within approximately 50K from 0 to 20 kW/m rod-average linear heat generation rate (LHGR). Above 20kW/m, the overprediction of measured fuel centerline temperature begins to increase as the slope of the measured temperature as a function of LHGR begins to decrease. Also at the LHGR of 20 kW/m is when the measured cladding elongation data indicate increasing fuel-cladding mechanical interaction (see Figure 3.4). Because this rod had fuel-cladding contact during much of the initial power ascension, the agreement of predicted and measured fuel centerline temperature indicates that a) the gap conductance model under solid contact conditions is operating correctly, and b) the fuel thermal conductivity model at zero burnup is acceptable.

Predicted versus measured fuel centerline temperatures are provided in Figure 3.3 for Rod 6 of IFA-513, the "mixed gas" rod. FRAPTRAN underpredicts fuel centerline temperature for this normal gap rod with a mixed gas by ~200K at 30 kW/m. However, this behavior is very similar, and of the same order of magnitude, as seen for FRAPCON-3 (Lanning, Beyer, and Berna 1997).

These three temperature comparisons indicate that FRAPTRAN should predict fuel-cladding gap conductance and fuel temperature satisfactorily under conditions of mostly helium fill gas after fuel

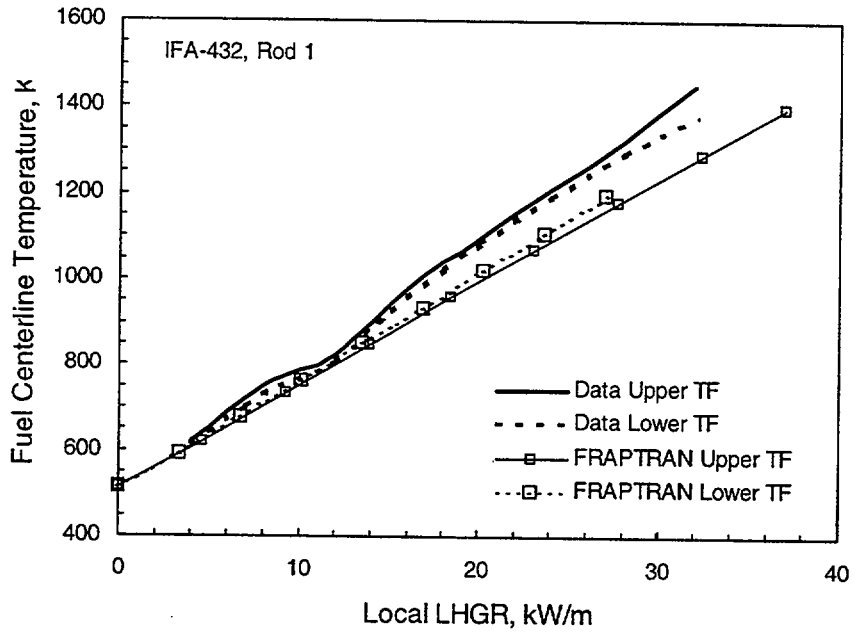


Figure 3.1 Comparison of Predicted and Measured Fuel Centerline Temperatures for Rod 1 of IFA-432 (standard rod)

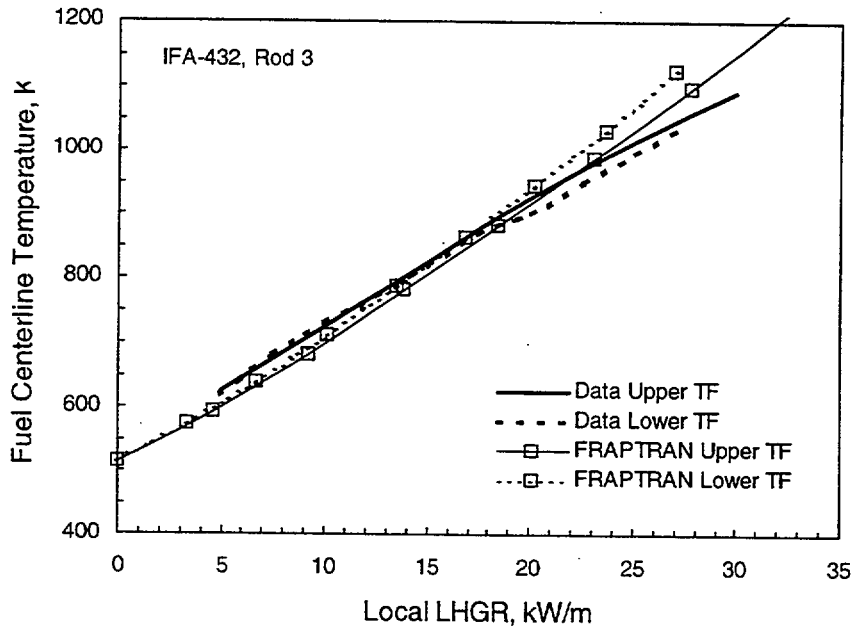


Figure 3.2 Comparison of Predicted and Measured Fuel Centerline Temperatures for Rod 3 of IFA-432 (small gap)

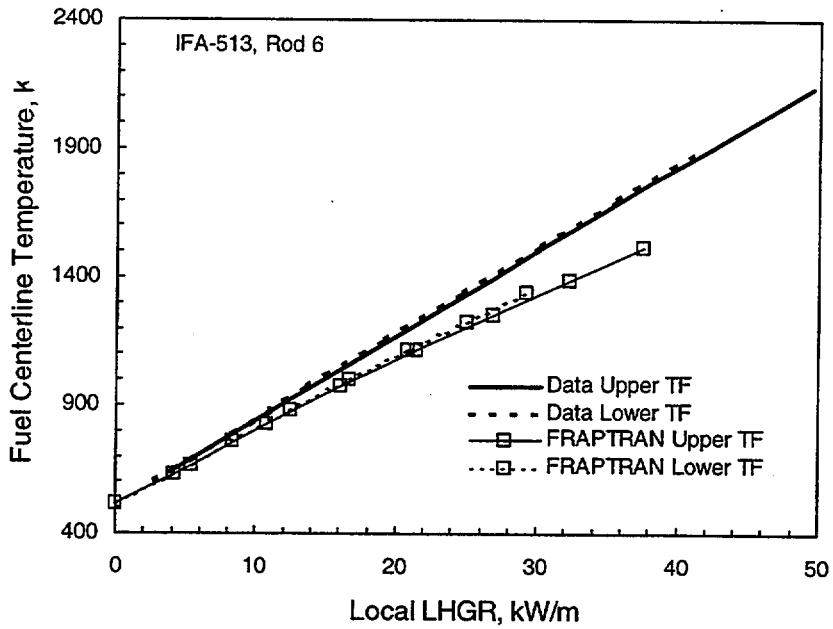


Figure 3.3 Comparison of Predicted and Measured Fuel Centerline Temperatures for Rod 6 of IFA-513 (mixed gas)

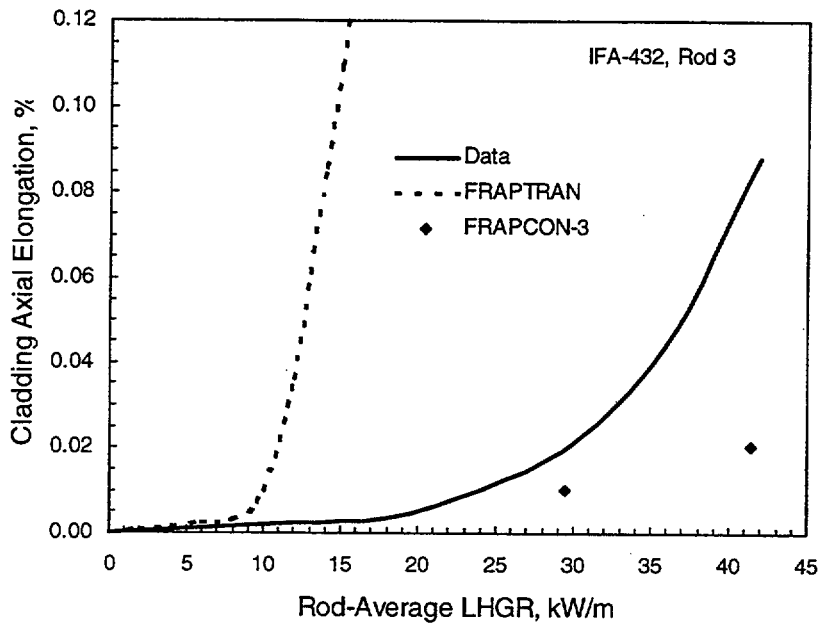


Figure 3.4 Comparison of Predicted and Measured Cladding Elongation for Rod 3 of IFA-432 (small gap)

relocation has decreased the initial fuel-cladding gap, or when the fuel and cladding are in contact; i.e., conditions of mid-to-high burnup with low fission gas release. For conditions of high fission gas release and degraded gas composition, FRAPTRAN may overpredict fuel-cladding gap conductance and underpredict fuel temperatures.

Predicted versus measured cladding elongation is provided in Figure 3.4 for Rod 3 of IFA-432. The prediction has fuel-cladding contact occurring at a lower power than was observed from the data. In addition, the prediction has a higher rate of elongation after contact than was observed from the data, with the data indicating more initial fuel compliance upon contact. This is an expected result because the FRAPTRAN fuel model has instantaneous fuel relocation and no fuel compliance or creep.

Predicted versus measured cladding elongation is provided in Figure 3.5 for Rod 6 of IFA-513. The predicted elongation has a higher thermal expansion slope than the data, and has fuel-cladding interaction occurring at a higher heat rate than indicated by the data. This result would indicate that the initial fuel-cladding gap may have been too large, while the underprediction of temperature would indicate a gap too small, relative to the data. The predicted thermal expansion slope for this rod is the same as for Rod 3 of IFA-432 and suggests that fuel compliance is needed for FRAPTRAN for slow increases in power.

For comparison, FRAPCON-3 (Berna et al. 1997) predicted cladding elongation for Rod 3 of IFA-432 and Rod 6 of IFA-513 are included in Figures 3.4 and 3.5, respectively. For Rod 3 of IFA-432, FRAPCON-3 predicted only axial thermal expansion to a rod-average LHGR of 30 kW/m and then a slight amount of cladding elongation due to fuel-cladding interaction at higher power levels. For Rod 6 of IFA-513, FRAPCON-3 predicted only thermal expansion to a rod-average LHGR of 36 kW/m. Thus, FRAPCON-3 tends to underpredict the initial mechanical behavior of these two rods while FRAPTRAN overpredicts the mechanical behavior. As with the FRAPTRAN temperature calculations, this is due to FRAPTRAN assuming too much fuel relocation at the start of an irradiation. However, FRAPTRAN would be expected to provide better comparisons to higher burnup data.

These cladding elongation comparisons illustrate the effect of FRAPTRAN not having a fuel compliance model for when fuel and cladding initially come into contact under slowly varying conditions such as an ascension to steady-state power levels. However, fuel compliance may not be as important for predicting mechanical response for conditions of very rapidly increasing powers (see Section 4.)

Predicted versus measured gas pressure is provided in Figure 3.6 for Rod 6 of IFA-513. Both prediction and measurement show approximately the same relative change in pressure with power, although the prediction starts at a slightly higher pressure level. This indicates the gas pressure calculation is working as expected.

These code-data comparisons provide evidence that the basic models in FRAPTRAN (i.e., temperature, gap conductance, and thermal expansion) are operating acceptably, although possibly "tuned" better for mid-to-high burnup conditions rather than beginning-of-life conditions.

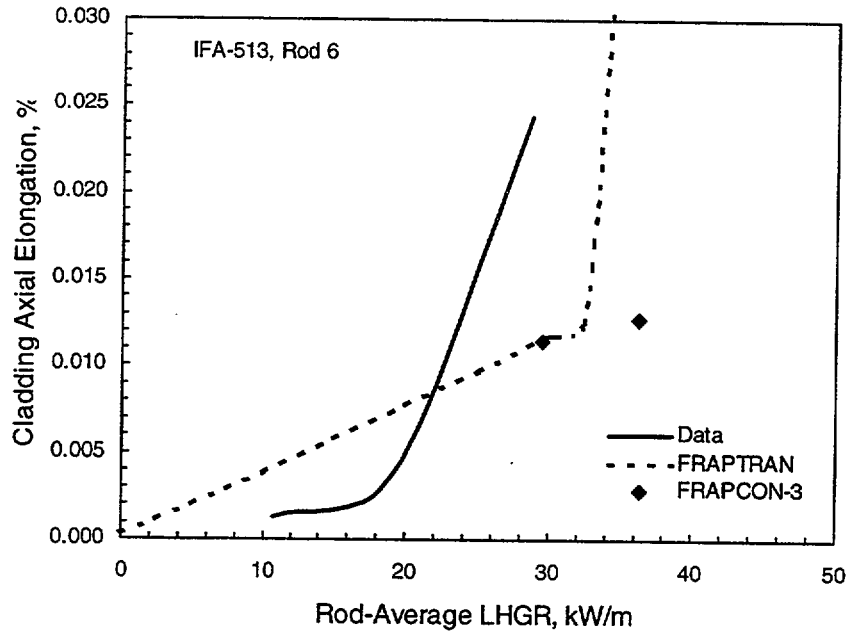


Figure 3.5 Comparison of Predicted and Measured Cladding Elongation for Rod 6 of IFA-513 (mixed gas)

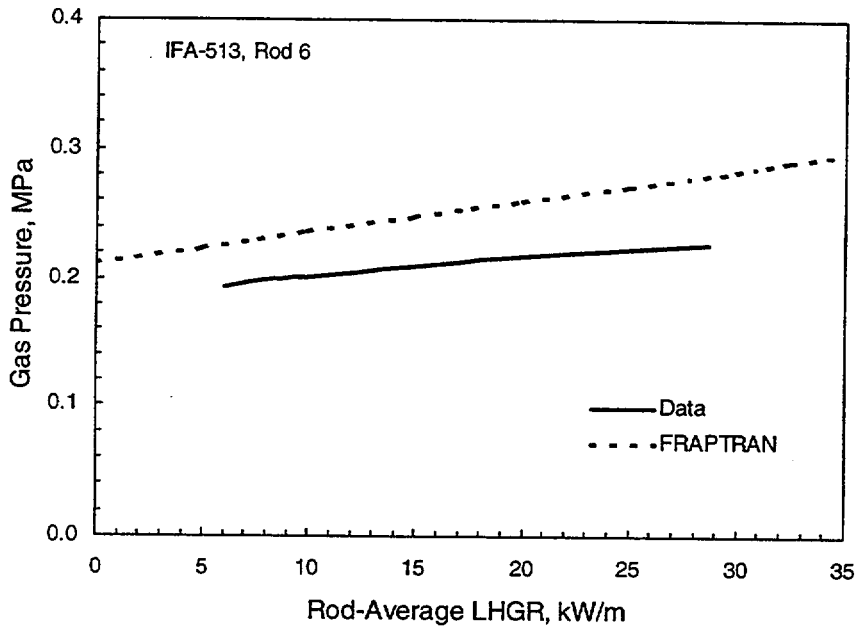


Figure 3.6 Comparison of Predicted and Measured Gas Pressure for Rod 6 of IFA-513 (mixed gas)

4 REACTIVITY INITIATED ACCIDENTS ASSESSMENT

Reactivity initiated accidents are very quick, high energy deposition transients that typically are most severe when beginning from a zero power condition. At high burnup levels, the radial power profile across the fuel is highly peaked at the fuel edge, thus the energy is deposited in the outer portions of the fuel. This results in the outer portions of the fuel heating up first, followed by the cladding and the inner portions of the fuel. For zero or low burnup rods, the radial power distribution across the fuel is more uniform. The rapid heating and thermal expansion of the fuel, and subsequent pellet-cladding mechanical interaction (PCMI) may result in permanent cladding strain, and if the energy deposit is sufficient, the cladding may fail from the induced strain.

Instrumentation during transient experiments to simulate RIAs may include cladding axial elongation, fuel column axial elongation, rod gas pressure, coolant conditions (temperature and pressure), and power deposition (magnitude and rate). Post-test examinations may include metrology (diameter and length), fission gas release, and metallography. Test rods typically are prepared from previously irradiated fuel rods, and characterization and irradiation history data on the "mother" rod are often available.

Noting that mechanical data are the principal data available from the RIA experiments, the assessment of code performance concentrates on the predictions of mechanical response for the test rods. Thus, strain history (fuel and cladding axial elongation when available) during the transient and post-test cladding permanent strain (hoop and axial) are the primary parameters of comparison. As discussed in Appendix B, cladding temperature data were used to define the input coolant histories for the RIA calculations. Provided in Table 4.1 is a summary of the principal measured and predicted mechanical results for the RIA assessments; these data and results are visually presented in Figures 4.1 through 4.4.^a

Predicted versus measured permanent cladding hoop strain results are presented in Figure 4.1. It may be seen from this figure that permanent hoop strain was generally underpredicted by FRAPTRAN. This is particularly the case for the NSRR tests where little or no permanent hoop strain was predicted while measured permanent hoop strain ranged up to ~5%.

Predicted versus measured permanent cladding axial strain results are presented in Figure 4.2. In contrast to consistently underpredicting the permanent hoop strain, FRAPTRAN generally overpredicted cladding permanent axial strain, with the CABRI tests being strongly overpredicted.

Predicted versus measured peak cladding elongation values are presented in Figure 4.3. In general, the results trend along the 1-to-1 line, but with a fairly wide scatter.

Predicted versus measured peak fuel elongation values for the NSRR tests are presented in Figure 4.4 (fuel elongation was not measured for the CABRI tests). As with the cladding peak elongation, the results trend along the 1-to-1 line, but with less scatter than for the peak cladding elongation comparison.

^aThe IGR H5T case is not included in Figures 4.1 through 4.4.

Table 4.1 Comparison of RIA Mechanical Results (Specified Coolant Boundary Condition)

Test	Permanent Hoop Strain, %		Permanent Axial Strain, %		Peak Cladding Elongation, mm (%)		Peak Fuel Elongation, mm (%)	
	Experiment	FRAPTRAN	Experiment	FRAPTRAN	Experiment	FRAPTRAN	Experiment	FRAPTRAN
HBO-6	1.2	0.20	0.05	0.30	NM	0.97 0(0.71)	1.3 (0.95)	1.71 (1.25)
MH-3	1.6	0.00	0.36	0.00	1.12 (0.92)	0.14 (0.12)	1.2 (0.98)	1.10 (0.90)
GK-1	2.5	0.16	0.15	0.26	1.16 (0.95)	0.82 (0.68)	1.3 (1.07)	1.74 (1.43)
OI-2	4.8	0.30	0.1	0.47	2.8 (2.11)	1.17 (0.88)	2.8 (2.11)	2.23 (1.68)
TS-5	0	0.0	0	0.0	0.55 (0.44)	0.10 (0.08)	NM	1.78 (1.41)
FK-1	0.9/3.0	0.45	NM	0.62	1.1 (1.04)	1.44 (1.36)	1.5 (1.42)	2.43 (2.29)
REP-Na3	2.0	0.87	0.8	1.22	6	6.76 (1.54)	NM	8.33 (1.89)
REP-Na4	0.4	0.48	0.07	0.72	4	5.23 (0.92)	NM	8.49 (1.50)
REP-Na5	1.1	1.07	0.35	1.54	6	9.83 (1.74)	NM	9.83 (1.74)
IGR H5T	3.1-6.5 FAILED	18.8	NM?	3.0	NM	3.24 (2.08)	NM	4.00 (2.56)

NM = not measured

^aFRAPTRAN elongation values for REP-Na3, REP-Na4, and REP-Na5 are corrected for initial axial thermal expansion from room temperature to coolant temperature because measured data were zeroed at coolant temperature. Initial axial thermal expansion values are:

REP-Na3: 0.50 mm cladding, 1.12 mm fuel
 REP-Na4: 0.64 mm cladding, 1.45 mm fuel
 REP-Na5: 0.76 mm cladding, 1.45 mm fuel

^b% axial elongation values are relative to initial active fuel length

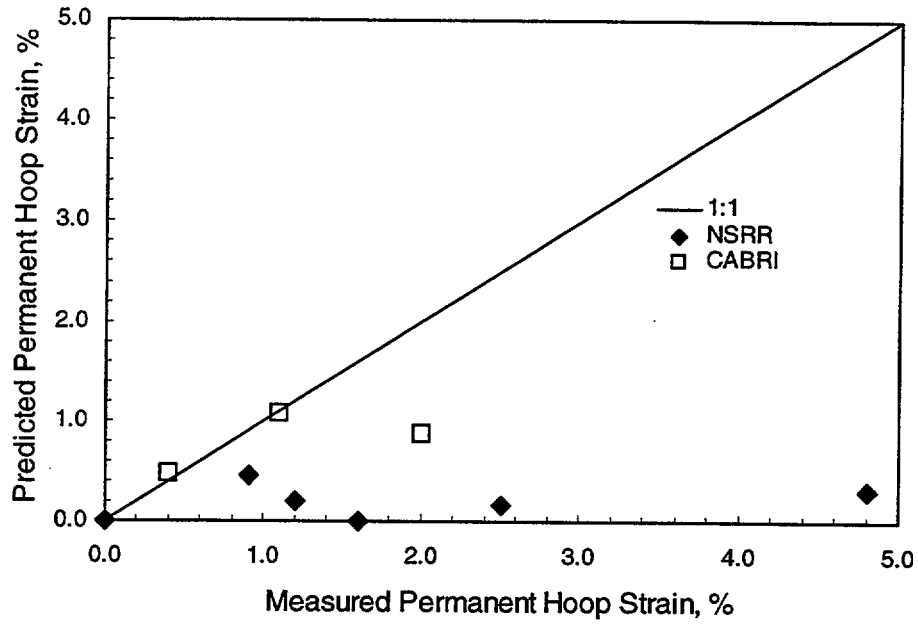


Figure 4.1 Predicted vs. Measured Cladding Permanent Hoop Strain for RIAs

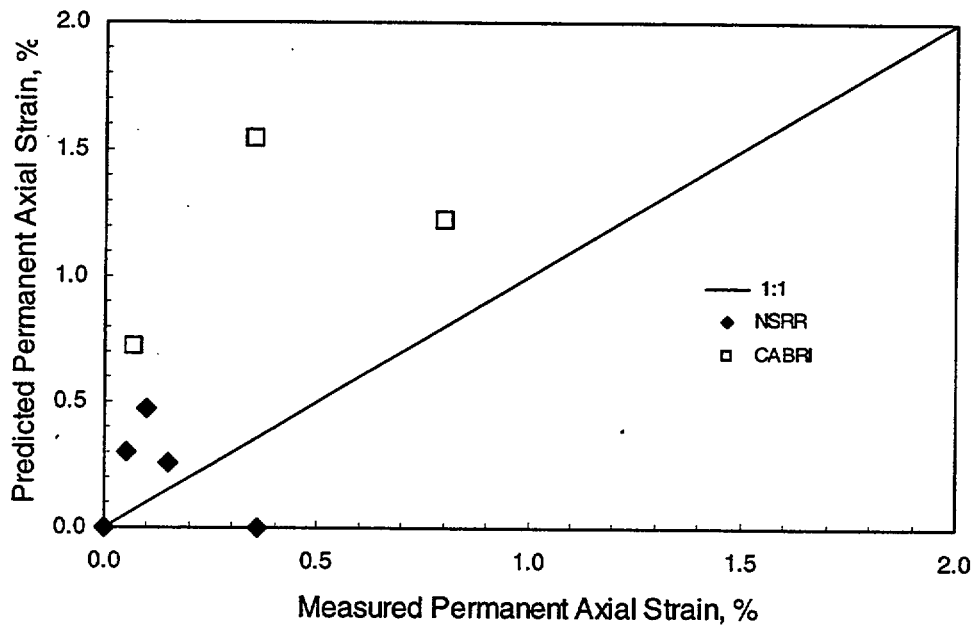


Figure 4.2 Predicted vs. Measured Cladding Permanent Axial Strain for RIAs

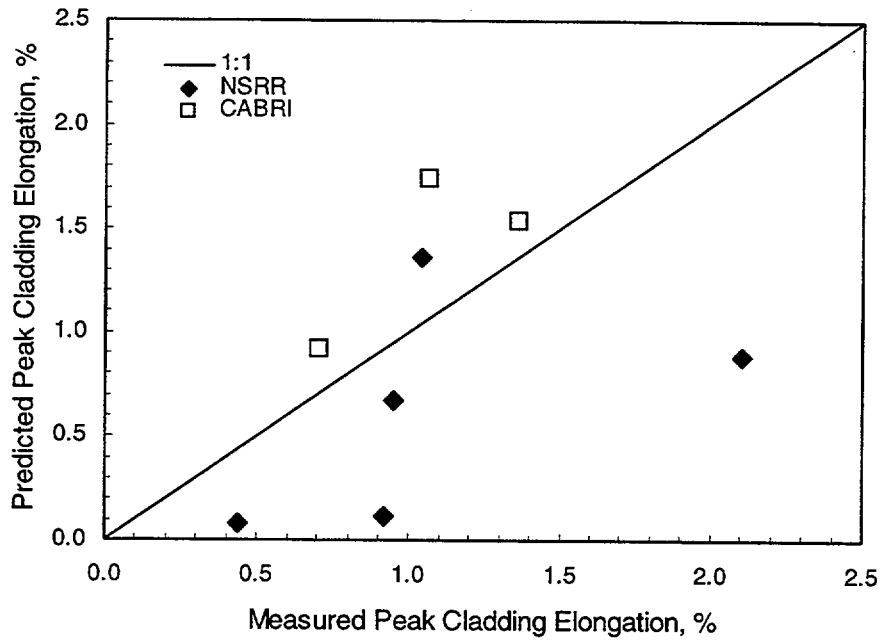


Figure 4.3 Predicted vs. Measured Peak Cladding Elongation for RIAs

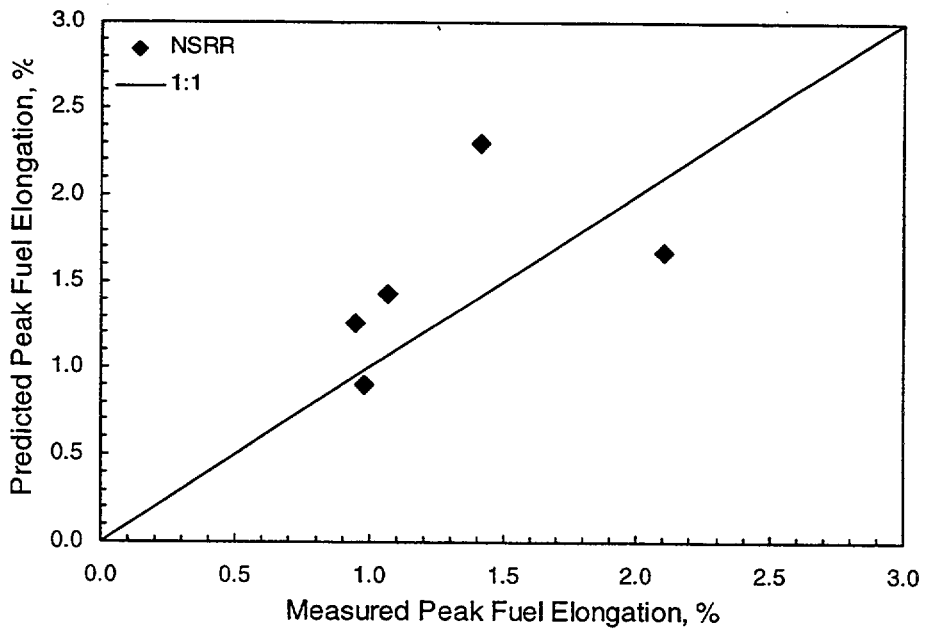


Figure 4.4 Predicted vs. Measured Peak Fuel Elongation for RIAs

The results presented in Table 4.1 and Figures 4.1 through 4.4 provide some initial indications of FRAPTRAN's predictive performance for these RIA tests. The general agreement with the peak fuel elongation data (Figure 4.4), which is due to fuel axial thermal expansion driven by fuel temperature, indicates that fuel temperatures predicted by FRAPTRAN are likely in general agreement with the temperatures experienced by the fuel rods during the tests.

Noting that predicted peak cladding and fuel axial elongations were reasonably predicted by FRAPTRAN (Figures 4.3 and 4.4, respectively), but that cladding permanent hoop strain was significantly under-predicted (Figure 4.1), it is apparent that the FRAPTRAN-predicted radial stress imposed on the cladding during the fuel-cladding mechanical interaction was less than that experienced by the rods. The lower fuel-cladding interaction in the hoop direction predicted by FRAPTRAN, than was apparent from the data, may be due to several factors. First, the initial fuel-cladding gap used by FRAPTRAN, and obtained from FRAPCON-3 predictions, may be greater than actually existed in the rods, and thus less fuel-cladding interaction was predicted than actually experienced. Second, the correct fuel-cladding gap may have been used by FRAPTRAN, but the refabrication process resulted in fuel pieces being jammed or cocked against the cladding which would result in more mechanical interaction during the RIAs than predicted. Third, fuel behavior during the RIAs is not being fully modeled by FRAPTRAN; a prime example would be the postulated behavior of the rim region (such as gaseous fuel swelling and/or fission gas release) during an RIA providing additional stress on the cladding.

The predicted time history of cladding and fuel axial elongation for the ten RIA cases is presented in Figures 4.5 through 4.14. This behavior also needs to be reviewed in addition to the discussion above in order to provide an evaluation of FRAPTRAN's performance for RIA transients. Each of the RIAs is discussed in the following.

The reported cladding axial elongation history data for the CABRI test rods (REP-Na3, REP-Na4, and REP-Na5) are relative to a zero value at the beginning of the transient, i.e., axial thermal expansion from room temperature to coolant temperature (280°C) is not included in the measured value. However, the FRAPTRAN values of axial elongation are relative to a reference temperature of room temperature. Therefore, the FRAPTRAN values of total axial elongation presented in this report for the three CABRI rods have had the initial axial thermal expansion to the coolant temperature subtracted out in order to provide a better comparison to the data. This correction was not necessary for the NSRR cases because those tests were initiated at temperatures close to room temperature.

4.1 NSRR Test Rods (HBO-6, MH-3, GK-1, OI-2, TS-5, and FK-1)

The NSRR test rods all had fast power transients of approximately 4.5 ms pulse half-width, peak fuel enthalpy values between 67 and 130 cal/g, and rod-average burnup values between 26 and 49 GWd/MTM. Comparisons of measured and predicted histories of cladding and fuel axial elongation are provided in Figures 4.5 through 4.10.

The FRAPTRAN comparison to measured permanent cladding hoop strain for the NSRR test rods in Table 4.1 and Figure 4.1 demonstrates a significant underprediction of the data for all six rods. No permanent hoop strain was predicted for PWR Rod MH-3, while permanent hoop strain was measured.

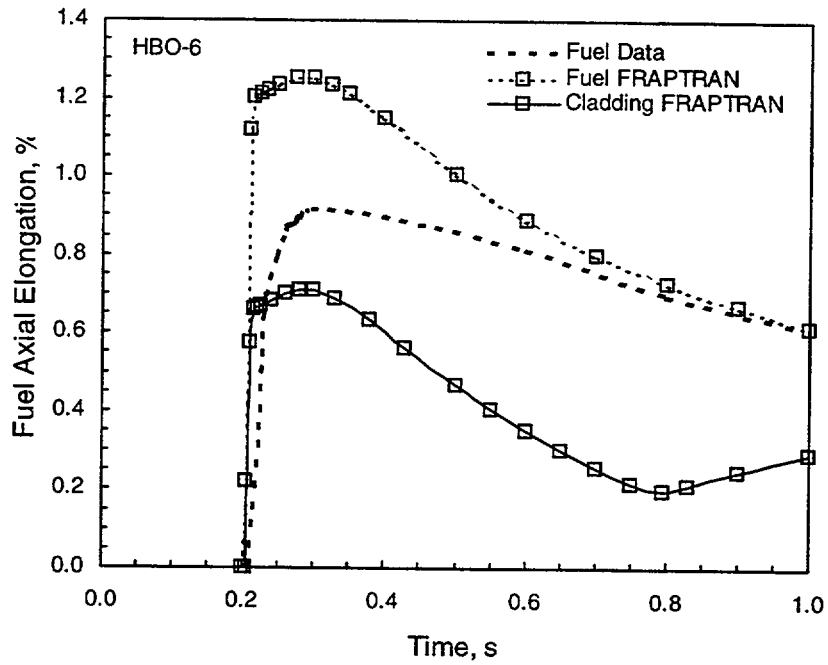


Figure 4.5 Comparison of Measured and Predicted Axial Elongation for HBO-6 (no cladding axial elongation data)

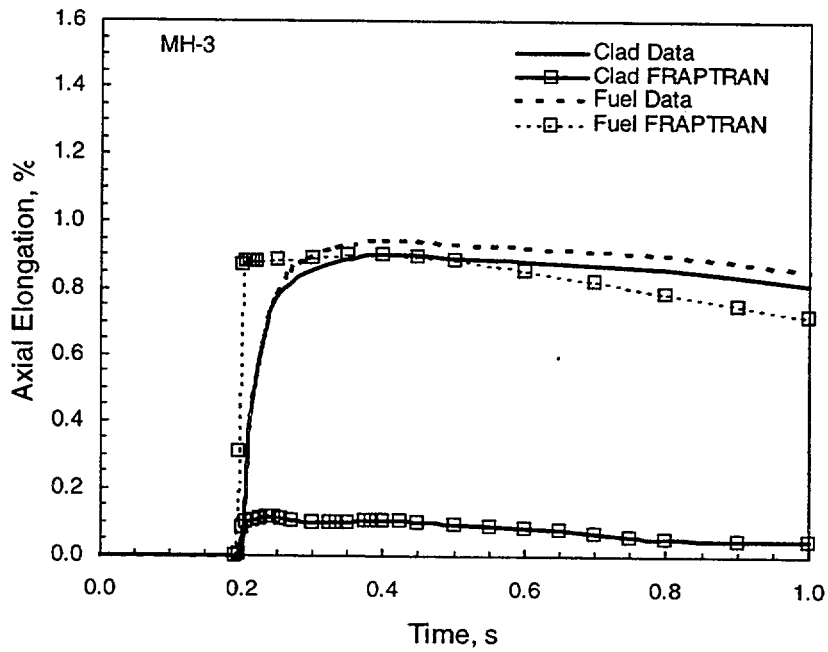


Figure 4.6 Comparison of Measured and Predicted Axial Elongation for MH-3

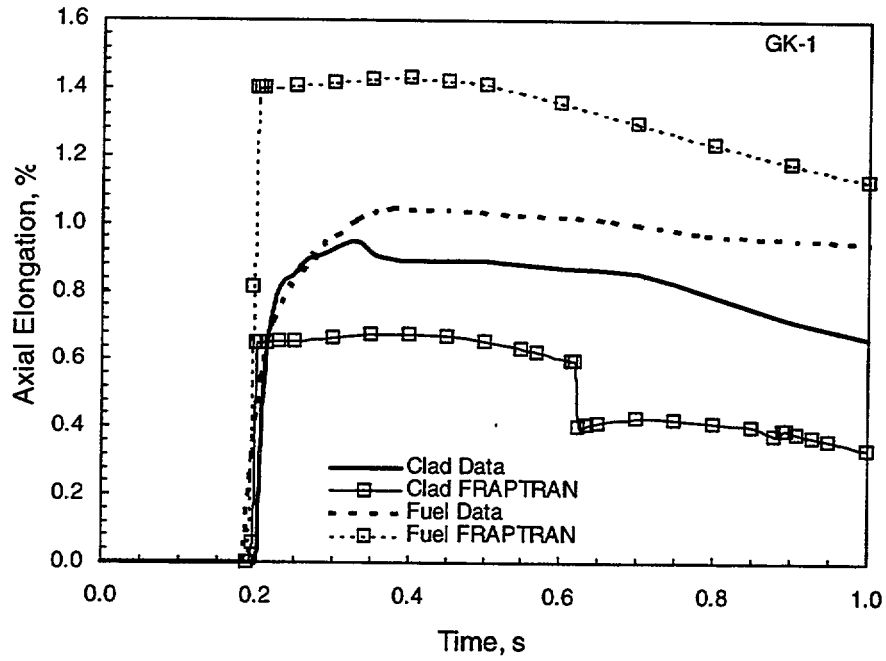


Figure 4.7 Comparison of Measured and Predicted Axial Elongation for GK-1

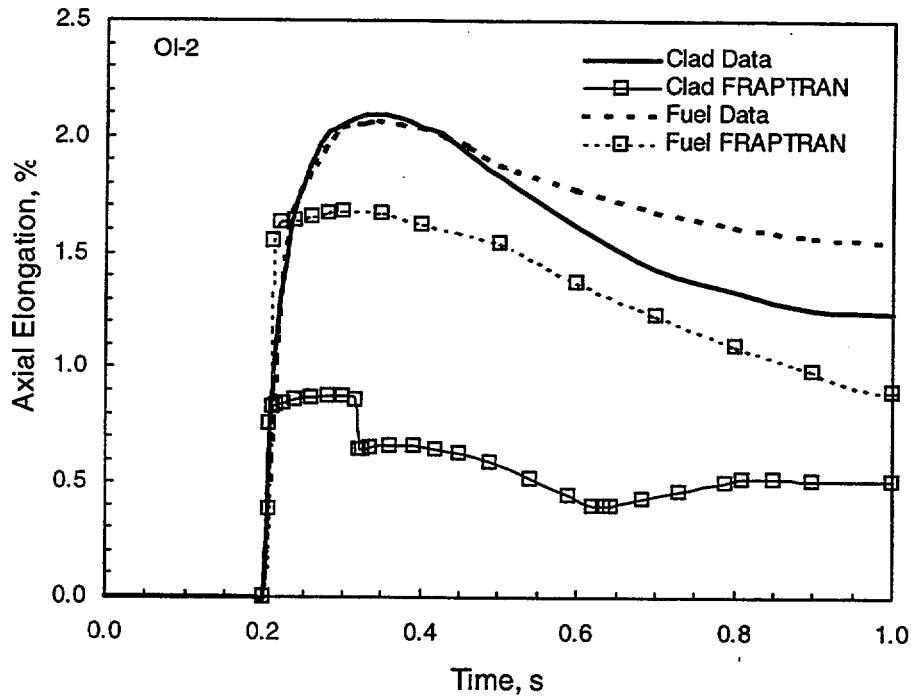


Figure 4.8 Comparison of Measured and Predicted Axial Elongation for OI-2

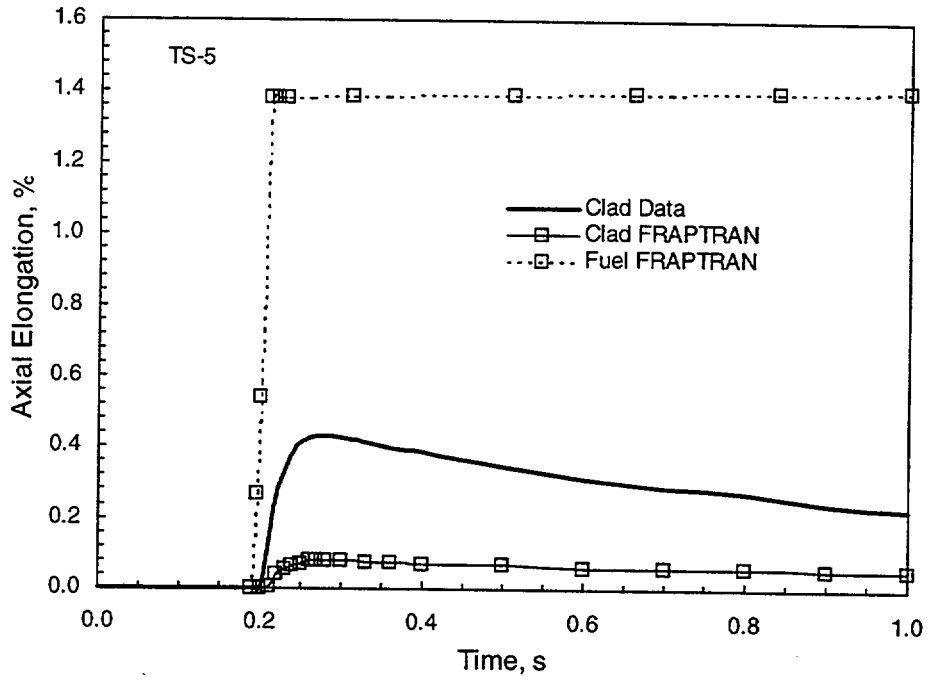


Figure 4.9 Comparison of Measured and Predicted Axial Elongation for TS-5

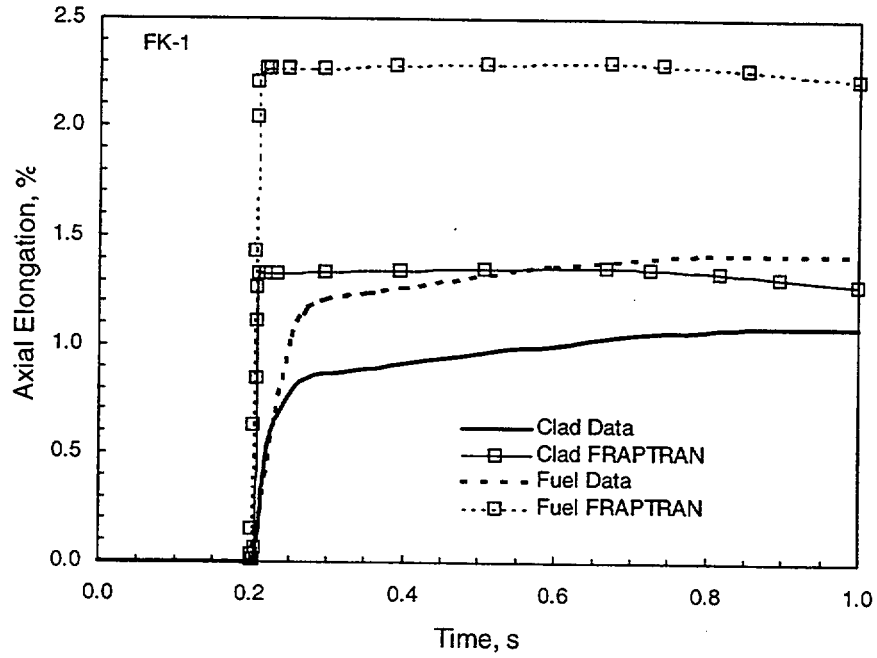


Figure 4.10 Comparison of Measured and Predicted Axial Elongation for FK-1

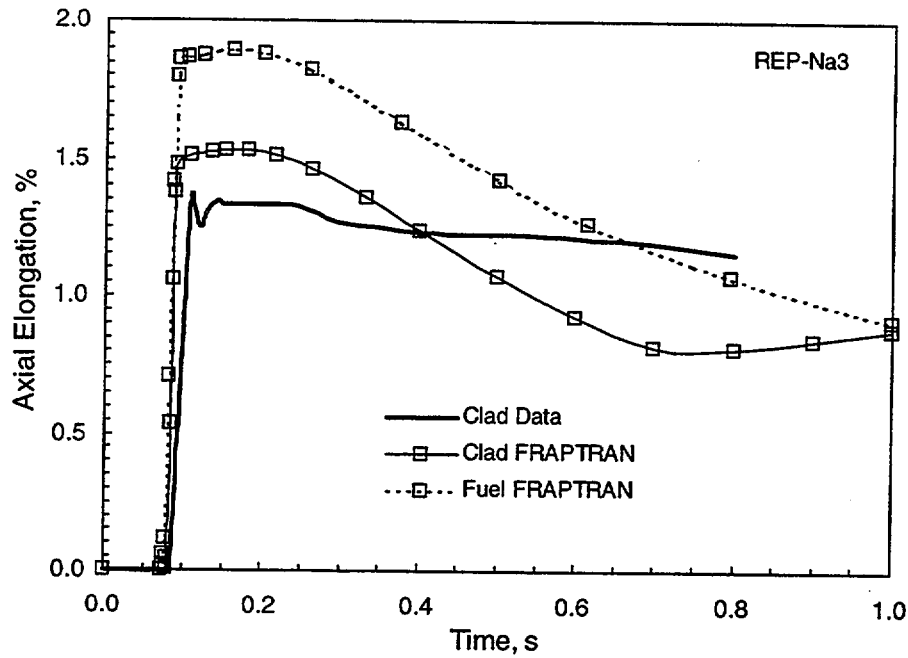


Figure 4.11 Comparison of Measured and Predicted Axial Elongation for REP-Na3

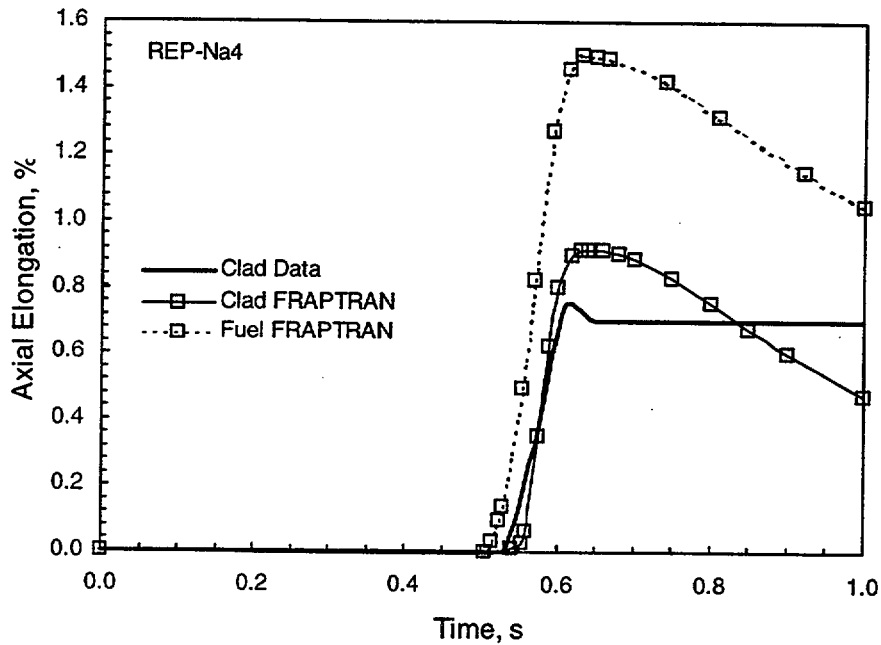


Figure 4.12 Comparison of Measured and Predicted Axial Elongation for REP-Na4

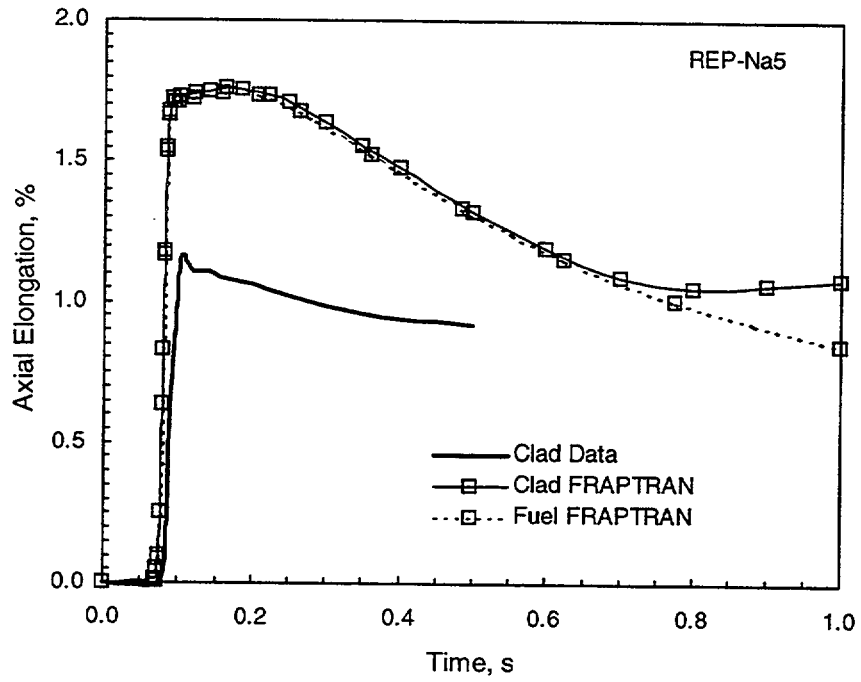


Figure 4.13 Comparison of Measured and Predicted Axial Elongation for REP-Na5

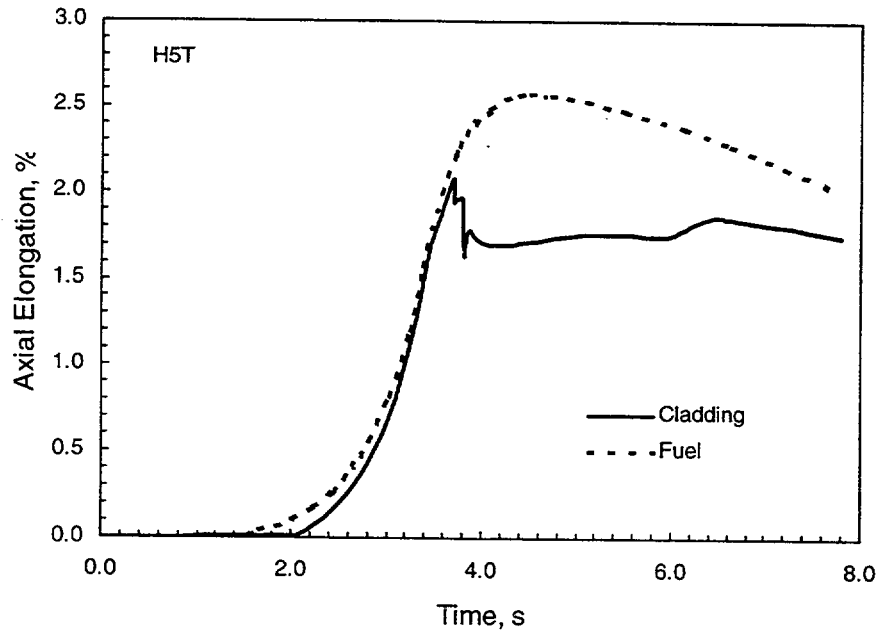


Figure 4.14 Predicted Cladding and Fuel Axial Elongation for IGR H5T

Similarly, no permanent hoop strain was predicted or measured for TS5, a BWR rod. Similar results for permanent axial strain were obtained for these two rods, i.e., no predicted strain while strain was measured for MH-3 but not for TS-5. The close correspondence of measured fuel and cladding elongation for MH-3 (Figure 4.6) suggests that the fuel-cladding gap was closed (or nearly closed) for this rod at the start of the transient while FRAPTRAN predicted an initial open gap.

Although no permanent axial strain was predicted for rods MH-3 and TS-5, the cladding permanent axial strain was overpredicted for two of the PWR rods. For Rod HBO-6, 0.30% strain was predicted versus 0.05% measured. At the same time, the fuel peak elongation was also overpredicted (1.25% versus 0.95% measured). For Rod OI-2, 0.47% permanent axial strain was predicted, versus 0.1% measured. However peak cladding elongation was underpredicted (0.88% predicted versus 2.11% measured) and peak fuel elongation was slightly underpredicted (1.68% predicted versus 2.11% measured).

The time history of cladding and fuel elongation for Rod HBO-6 (PWR) is presented in Figure 4.5. The fuel elongation is initially overpredicted, relative to the data, then matches the data after approximately 0.6s. This is indicative of probably a fairly good agreement between predicted and actual fuel temperatures since fuel elongation is from fuel axial thermal expansion which is temperature dependent. No measured history for cladding elongation is available; however, the predicted cladding elongation is less than the predicted fuel elongation. HBO-6 had much more cladding permanent hoop strain than was predicted (Table 4.1), thus indicating fuel-cladding mechanical interaction that was not predicted by FRAPTRAN.

The time history of cladding and fuel elongation for Rod MH-3 (PWR) is presented in Figure 4.6. For this case, the predicted fuel elongation is in good agreement with both the measured fuel and cladding elongation histories while the predicted cladding elongation history is substantially less than the measured history. In addition, no permanent cladding strain was predicted by FRAPTRAN while there was measured permanent strain. The agreement for measured and predicted fuel elongation implies a good prediction of fuel temperatures. The close agreement for the measured fuel and cladding elongation histories, plus the large measured cladding permanent strains indicates that the fuel and cladding were locked up from early in the transient. However, FRAPTRAN predicted an open (though nearly closed) fuel-cladding gap during the transient which resulted in the low predicted cladding elongation due only to thermal expansion, even though predicted fuel elongation was in good agreement with the measured data.

The time history of cladding and fuel elongation for Rod GK-1 (PWR) is presented in Figure 4.7. For this case, predicted fuel elongation was greater than measured while the predicted cladding elongation was less than measured. Comparing the measured fuel and cladding elongation, it would appear that the cladding was released from the fuel at approximately 0.35s when a decrease in the measured cladding elongation is observed. Similarly, the predicted cladding elongation shows a decrease at approximately 0.6s when the fuel-cladding gap is predicted to reopen. As with other rods, cladding permanent hoop strain is underpredicted even though cladding permanent axial strain is overpredicted (Table 4.1).

The time history of cladding and fuel elongation for Rod OI-2 (PWR) is presented in Figure 4.8. Measured fuel and cladding elongation are nearly the same indicating that the fuel and cladding are locked up from the beginning of the transient. Predicted fuel elongation is less than the measured fuel elongation

indicating that fuel temperatures are probably underpredicted for this rod. Predicted cladding elongation shows a sharp decrease at approximately 0.3s when the fuel-cladding gap reopens. This rod had substantial measured cladding permanent hoop strain that was not predicted by FRAPTRAN. Interestingly, even though the fuel and cladding elongation histories were underpredicted, the cladding permanent axial strain was overpredicted for this rod (Table 4.1).

The time history of cladding and fuel elongation for Rod TS-5 (BWR) is presented in Figure 4.9. The predicted cladding elongation is less than the measured elongation, and the fuel-cladding gap was predicted to remain open during the transient, thus there was no predicted fuel-cladding interaction. There was no measured fuel elongation data to compare to the predicted fuel elongation. This rod likely experienced little fuel-cladding mechanical interaction during the transient since there was no measured cladding permanent strain and no predicted cladding permanent strain (Table 4.1).

The time history of cladding and fuel elongation for Rod FK-1 (BWR) is presented in Figure 4.10. Elongation for both fuel and cladding for this rod was overpredicted relative to the measured elongation data. However, cladding permanent hoop strain was again underpredicted as observed for the other rods (Table 4.1). There was no measurement of cladding permanent axial strain, but based on results for the other rods, it may be conjectured that FRAPTRAN likely overpredicted the cladding permanent axial strain.

In summary, FRAPTRAN apparently did a reasonable job on predicting fuel temperatures for these cases tested in the NSRR (based on comparisons of predicted versus measured fuel elongation histories), yet still underpredicted fuel-cladding interaction as evidenced by fuel-cladding gaps opening during the transients and underpredicting cladding permanent hoop strain.

4.2 CABRI Test Rods (REP-Na3, REP-Na4, REP-Na5)

The REP-Na3 and REP-Na5 test rods had relatively fast power transients (~9.5 ms half-width) while REP-Na4 had a slower pulse (~64 ms half-width) with a double peak (see Appendix A). All three test rods had peak fuel enthalpy values between 99 to 125 cal/g and the test rod burnups were between 53 to 64 GWd/MTM. Comparisons of measured and predicted histories of cladding elongation and predicted fuel axial elongation (no measured fuel elongation data for the NSRR cases) are provided in Figures 4.11 through 4.13.

The time history of cladding and fuel elongation for Rod REP-Na3 (PWR) is presented in Figure 4.11. The predicted cladding elongation is in general agreement with the measured cladding elongation. The predicted cladding permanent axial strain is greater than measured while the predicted cladding permanent hoop strain is less than measured. However, the predicted cladding permanent strain values are larger than were predicted for any of the NSRR cases (Table 4.1).

The time history of cladding and fuel elongation for Rod REP-Na4 (PWR, double peak power history) is presented in Figure 4.12. As for REP-Na3, the predicted cladding peak elongation is near to the measured

value, but then drops below the measured values. Predicted cladding permanent axial strain was significantly overpredicted while the predicted cladding permanent hoop strain was fairly close to the measured value (0.47% vs. 0.4%, respectively).

The time history of cladding and fuel elongation for Rod REP-Na5 (PWR) is presented in Figure 4.13. For this case the predicted cladding elongation was greater than measured. This result is also reflected in the predicted cladding permanent axial strain being much greater than measured. Predicted cladding permanent hoop strain was in good agreement with the measured value (1.04% vs. 1.1%, respectively).

In general, FRAPTRAN predicted the behavior of the CABRI rods better than the NSRR rods. Predicted values of cladding peak elongation and cladding permanent hoop strain are in fair agreement with the data even though cladding permanent axial strain was overpredicted. The lack of measured fuel elongation data does not allow for an evaluation of how well FRAPTRAN predicted the fuel temperatures.

4.3 IGR H5T Case

This assessment case was included, even though the rod failed and there is a lack of measured in-reactor data, because of the long pulse width (800 msec half-width), the Zr-1%Nb cladding, and an interest in seeing what FRAPTRAN would predict. Measured hoop strain was 6.5% at the failure site and 3.1% away from the failure site. Presented in Figure 4.14 are the predicted time histories of fuel and cladding elongation for this rod. The predicted gas pressure and cladding average temperature histories are presented in Figure 4.15. It can be seen that FRAPTRAN predicted that the fuel and cladding were in

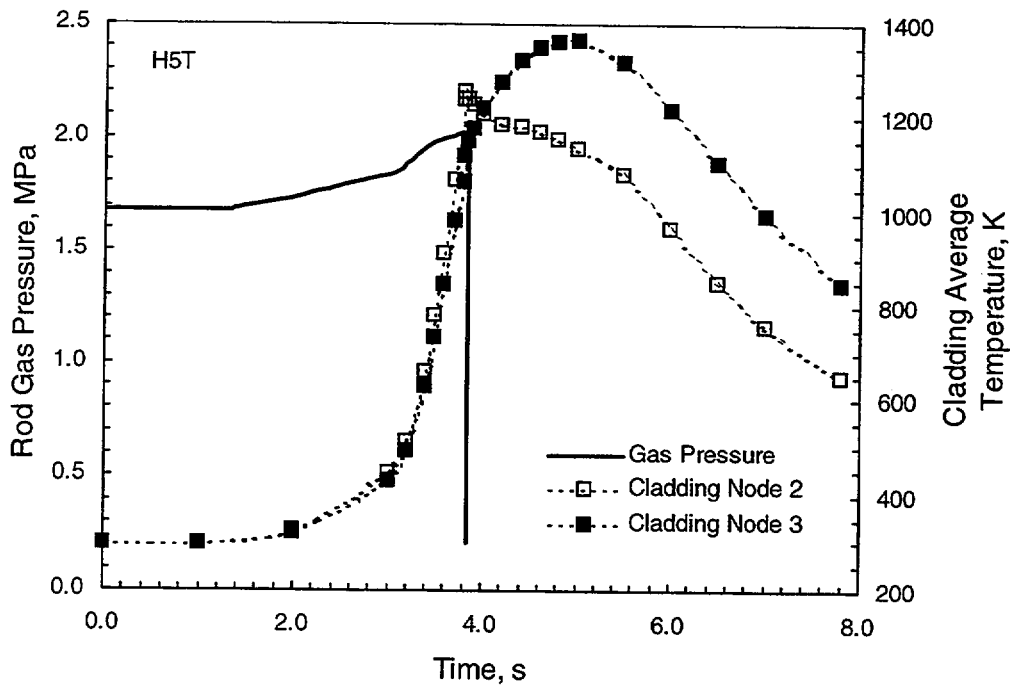


Figure 4.15 Predicted Rod Gas Pressure and Cladding-Average Temperature for IGR H5T

contact during the power increase until the predicted time of failure at approximately 3.8s. FRAPTRAN predicted failure at approximately 3.8 seconds as evidenced by the decrease in cladding elongation (Figure 4.14) and rod gas pressure (Figure 4.15). The predicted time of failure is approximately 0.44 seconds after the power peak (there was no measured time of failure).

Predicted values of cladding permanent hoop and axial strain are 18.8% and 3.0%, respectively, for the H5T rod. The predicted permanent hoop strain (18.8%) is much larger than the strain measured at the failure site (6.5%). This is the only RIA case where predicted cladding permanent hoop strain was much greater than what was measured. This is attributed to the predicted cladding hoop strain for H5T being due to ballooning while the cladding hoop strain for the other RIA cases was due to fuel-cladding mechanical interaction. The predicted cladding temperatures (Figure 4.15) show that failure occurred with a cladding average temperature of approximately 1250K. These predicted cladding temperatures are much higher than those measured for the other RIA assessment cases.

As noted in Appendix B, this assessment case was run with an assumption of 8% fission gas release occurring by 4 seconds into the transient. A run was made with no assumed fission gas release. For that case, the cladding elongation history is the same as shown in Figure 4.14 through the time of failure; however, after failure, the predicted cladding elongation is a little less than shown in Figure 4.14. Similarly, the predicted gas pressure history was a little lower than shown in Figure 4.15, with a peak of 1.88 MPa versus the peak of 2.02 MPa in Figure 4.15. Predicted permanent hoop strain was 17.6% for the no fission gas release case versus 18.8% for the fission gas release case. Thus, the assumption of fission gas release did not have a large effect for these FRAPTRAN predictions.

4.4 Summary of RIA Assessment Results

From these comparisons of FRAPTRAN predictions to experimental data obtained from RIA-type experiments, it may be concluded that:

- General agreement between predicted and measured fuel elongation histories for the NSRR cases implies that predicted fuel temperatures were representative of actual (unmeasured) fuel temperatures.
- Predicted cladding elongation histories were generally less than measured for the NSRR cases but in agreement with the measured histories for the CABRI cases.
- FRAPTRAN consistently underpredicted cladding permanent hoop strain relative to permanent axial strain. When predicted and measured permanent axial strains were in agreement, permanent hoop strain was underpredicted (NSRR cases). When predicted and measured permanent hoop strains were in agreement, permanent axial strain was overpredicted (CABRI cases).
- The consistent underprediction of cladding permanent hoop strain relative to permanent axial hoop strain indicates that the radial stress/strain behavior resulting in permanent hoop strain for these RIA test rods is not well modeled by FRAPTRAN.

Users of other codes have also noted that they are unable to obtain sufficient permanent cladding hoop strain for the RIA tests when assuming that only thermal expansion strain from the fuel is responsible for the cladding strain. It has been conjectured and discussed that additional strain components come from transient gaseous fission gas release and fuel swelling during the RIA. For this assessment, FRAPTRAN did not provide any strain to the cladding other than that from thermal expansion of the fuel (i.e., no transient fission gas release or transient fuel swelling). FRAPTRAN predicted two of the CABRI test rods (REP-Na4 and REP-Na5 with pulse widths of 64 and 9 ms, respectively) hoop strains very well, but underpredicted REP-Na3 (with a 9 ms pulse width) by over a factor of 2. For nearly all of the NSRR test rods (with a pulse width of 4.5 ms), hoop strains were significantly underpredicted indicating that there may be fuel behavior operating that is not modeled by FRAPTRAN. These fast power ramps with pulse widths less than 9 ms may have additional fuel expansion due to, perhaps, fission gas expansion at grain boundaries.

5 LOSS-OF-COOLANT-ACCIDENT ASSESSMENTS

Loss-of-coolant accidents typically occur from full power conditions, are initiated with a scram, coolant flow is lost, and then eventually coolant flow is restored (reflood and quench). The energy is already present in the fuel at the time of the scram, with a continuing low level of energy deposition in the fuel from decay heat. Another component of energy deposition during the transient, depending on conditions, may be heat generation in the cladding from Zircaloy oxidation. The response of the fuel rods is cladding heatup, while the fuel cools down, and subsequent straining and ballooning of the cladding with failure from either excessive strain or departure from nucleate boiling.

Instrumentation during LOCA transient experiments typically consists of cladding outer surface thermocouples, fuel centerline thermocouples, fuel rod gas pressure (and occasionally plenum temperature), cladding axial elongation, and coolant conditions (temperature, pressure, flow). The data base used for this assessment consists of essentially non-irradiated fuel rods; the rods did acquire some minimal burnup during power calibration and decay heat buildup periods prior to the LOCA transients. Post-test examinations may include metrology (diameter and rupture location) and metallography.

Noting the typically available data for LOCAs, the assessment of code performance concentrates on both the thermal and mechanical performance of the test rods. Key parameters for comparison to data are time to rupture, axial location of rupture and ballooning, cladding elongation history, and rod gas pressure history.

As discussed in Appendix B, measured cladding temperature data were used to define coolant conditions where possible to minimize the impact of the thermal-hydraulic models and to thus allow this assessment to focus on the fuel and cladding thermal and mechanical models.

It was found that the reported gas pressures for the MT cases in the NRU were dependent on a volume of gas being outside the core and thus at nearly room temperature. An external gas volume cannot be modeled by FRAPTRAN and not accounting for this design characteristic resulted in initially predicting gas pressures much higher than were measured. For these assessment cases, the FRAPTRAN input was adjusted so that predicted pressures at the beginning of the transient were matched to the measured pressures. This is discussed further in Appendix A. A similar difficulty exists with the TREAT FRF-2 case, but an adjustment, via input control, was made to control the plenum temperature which resulted in predicted and measured gas pressures being in good agreement.

Provided in Table 5.1 is a summary of the key measured and predicted parameters for the LOCA assessment cases. Each of the cases is discussed separately in the following.

5.1 MT-1 Assessment

In general, good agreement was obtained between the FRAPTRAN prediction and the experimental data for rod gas pressure and time to failure. The predicted gas pressure history is compared in Figure 5.1 to

		MT-1	MT-4	MT-6A	LOC-11C	TREAT FRF-2
Rupture Time, s						
	Measured	70(60-95)	55(52-58)	58-64	No failures	30-35
	FRAPTRAN	65	42.5	40	Failure not predicted	28
Rupture Location, m						
	Measured	2.0	2.68	NM	No failures	~0.35
	FRAPTRAN	~2	~2	~2	Failure not predicted	~0.28
Rupture Hoop Strain, %						
	Measured	43	72	"Large"	No failures	35-50
	FRAPTRAN	25 at node 7	22 at node 7	32 at node 7	8% at top of rod	355
Pressure at Rupture, MPa						
	Measured	Not stated (9.7 Peak)	5.6-6.5 (9.3 peak)	6.1-7.9 (9.3 peak)	No failures; NM	~0.6 (1.0 peak)
	FRAPTRAN	2.5 (4.8 peak)	5.6 (10.1 peak)	4.90 (10.0 peak)	Failure not predicted (10.4 MPa peak)	0.3 (1.0 peak)

the measured rod gas pressure history for an MT-1 rod that did not fail; good agreement is obtained through about 40 seconds at which time FRAPTRAN predicts ballooning and failure. Although the test rod in Figure 5.1 did not fail, it did apparently begin to balloon at about 40s as indicated by the measured pressure decrease at that time. (The measured pressure data in Figure 5.1 begin to increase again at about 70s, but that behavior is not evaluated here.) Predicted time to failure is about 65 seconds while the measured rupture times, based on pressure data from rods in the test that did fail, were from 60 to 90 seconds. The predicted permanent hoop strain of 25% was less than the measured hoop strain at the failure site of 43% (Table 5.1).

5.2 MT-4 Assessment

For this case, FRAPTRAN provided a good comparison to the measured gas pressures but underpredicted the time to failure. Predicted and measured gas pressures for MT-4 are compared in Figure 5.2. At the time of rod failure, measured rod gas pressures were 5.6 to 6.5 MPa (peak values of 8.9 to 9.3 MPa) and cladding temperature was 1086 to 1114K. The FRAPTRAN predicted value of peak pressure is 10.1 MPa with a failure pressure of 5.6 MPa, and cladding temperature of about 1000K. Predicted time to failure was about 42 seconds while measured times to failure were 52 to 58 seconds.

The region of maximum ballooning for the MT-4 rods was observed to be at an elevation of approximately 2.54 m while FRAPTRAN predicted maximum ballooning at about 2.0 m. FRAPTRAN also underpredicted the maximum ballooning strain (23% predicted versus about 70% measured).

5.3 MT-6A Assessment

Measured time to rupture for the MT-6A rods was between 58 to 64 seconds while FRAPTRAN predicted time to rupture of 40 seconds (similar to the MT-4 test). The predicted and measured gas pressure histories are compared in Figure 5.3. The peak pressures are similar, but FRAPTRAN predicted failure at a lower burst pressure (4.9 MPa predicted versus 6 to 8 MPa measured).

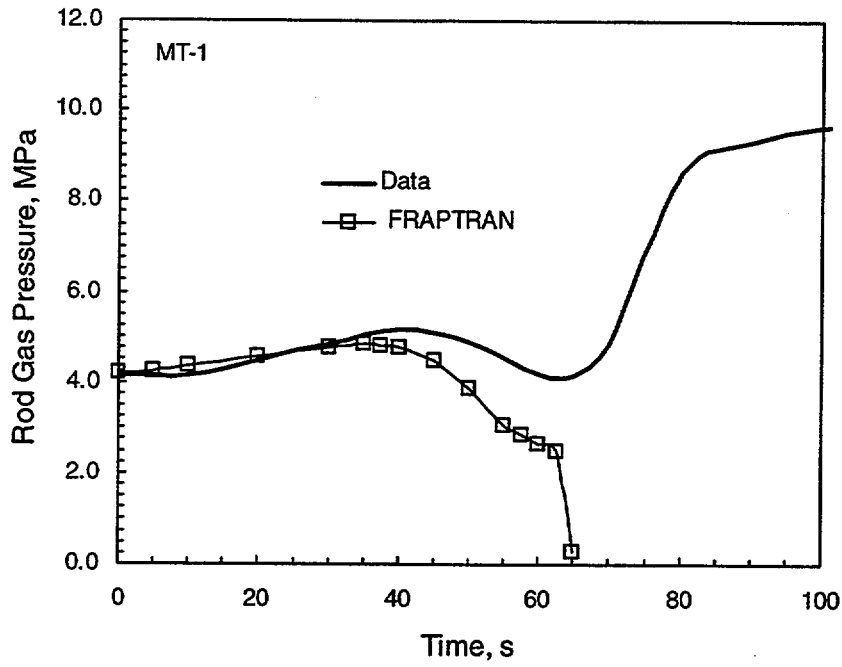


Figure 5.1 Comparison of Measured and Predicted Plenum Gas Pressure for MT-1

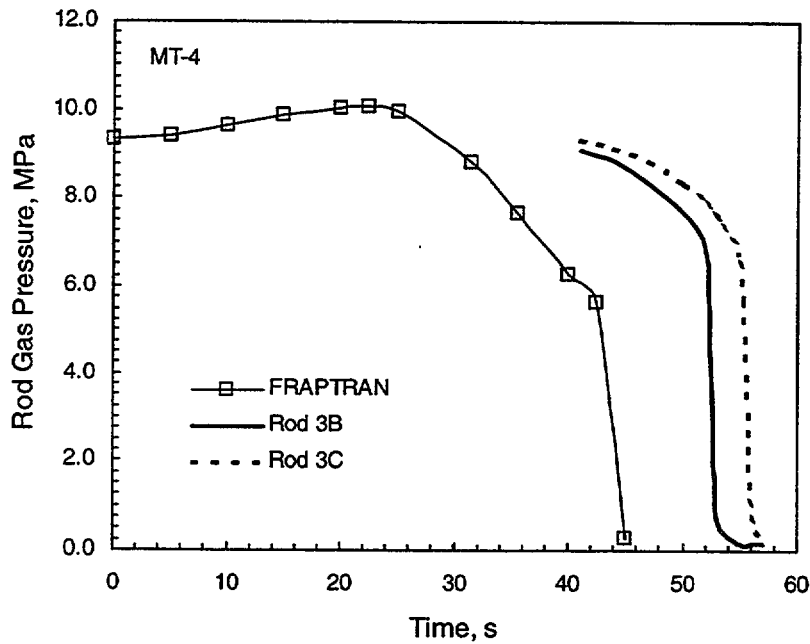


Figure 5.2 Comparison of Measured and Predicted Plenum Gas Pressure for MT-4

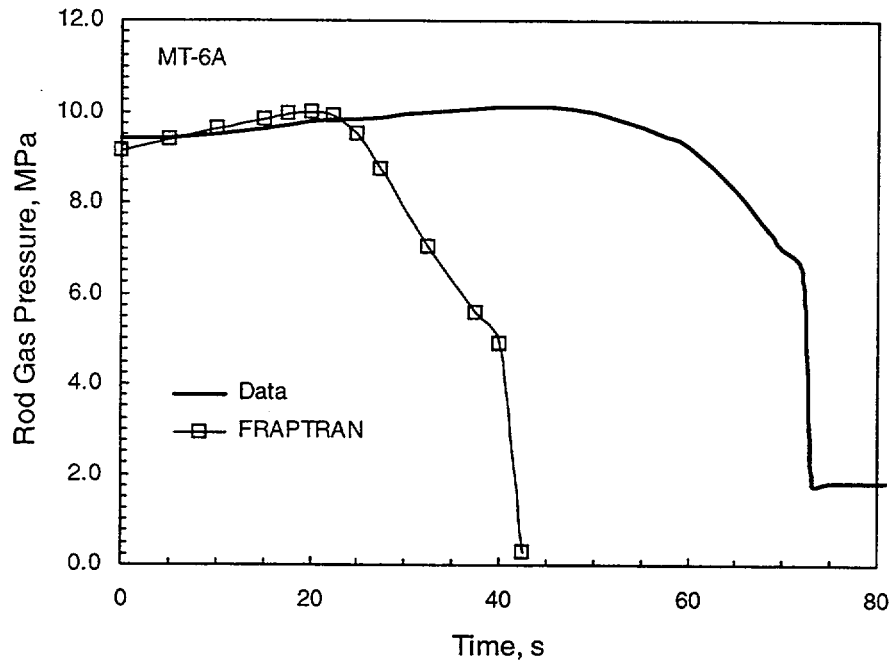


Figure 5.3 Comparison of Measured and Predicted Plenum Gas Pressure for MT-6A

The axial location of ballooning was not determined for this test bundle because post-irradiation examinations were not performed. However, FRAPTRAN predicted the rupture region to be at approximately 2.0 m, which was consistent with the MT-1 and MT-4 predictions. Predicted permanent cladding hoop strain at the failure region was 32%.

5.4 PBF LOC-11C Assessment

The LOC-11C test was initiated with a scram and predicted and measured fuel centerline temperatures are compared in Figure 5.4. FRAPTRAN predicted a slightly faster decrease in fuel centerline temperature than was measured. FRAPTRAN also predicted a starting fuel centerline temperature approximately 200K higher than was measured (2764K predicted versus 2550 measured).

Predicted and measured cladding axial elongation histories for LOC-11C are presented in Figure 5.5. The FRAPTRAN predicted response is in general agreement with the measured data from two rods. At the time of the scram (0s on the plot), the predicted decrease in cladding elongation is greater than was measured. For the balance of the history, the magnitude of the predicted increase in cladding elongation is similar to the measured response.

No rods failed during this test, nor are any gas pressure data available. FRAPTRAN did not predict failure, with a predicted peak gas pressure of 10 MPa at the beginning of the transient, then decreasing. FRAPTRAN predicted 5.8% permanent cladding hoop strain at an elevation of 0.3m while the measured permanent hoop strain was 2.4% at an elevation of 0.3m.

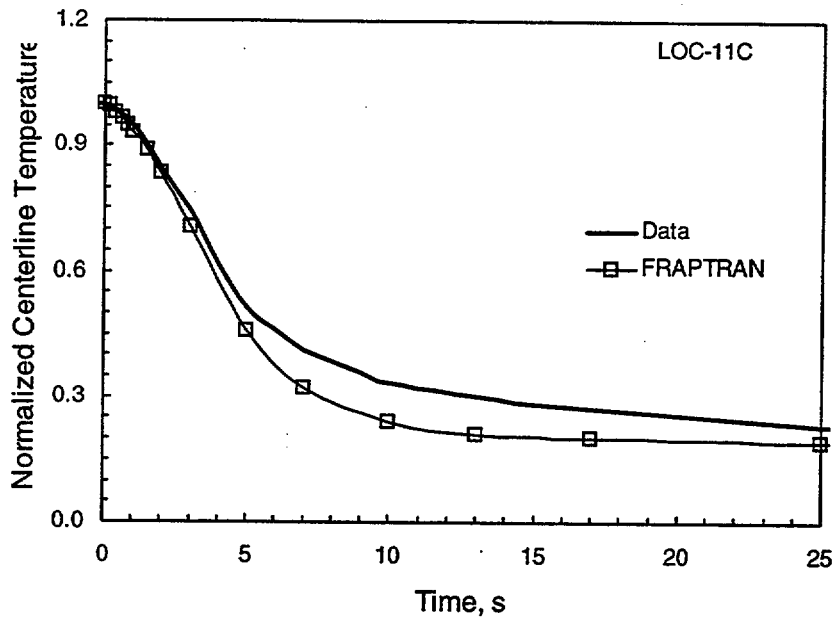


Figure 5.4 Comparison of Measured and Predicted Fuel Centerline Temperature for LOC-11C

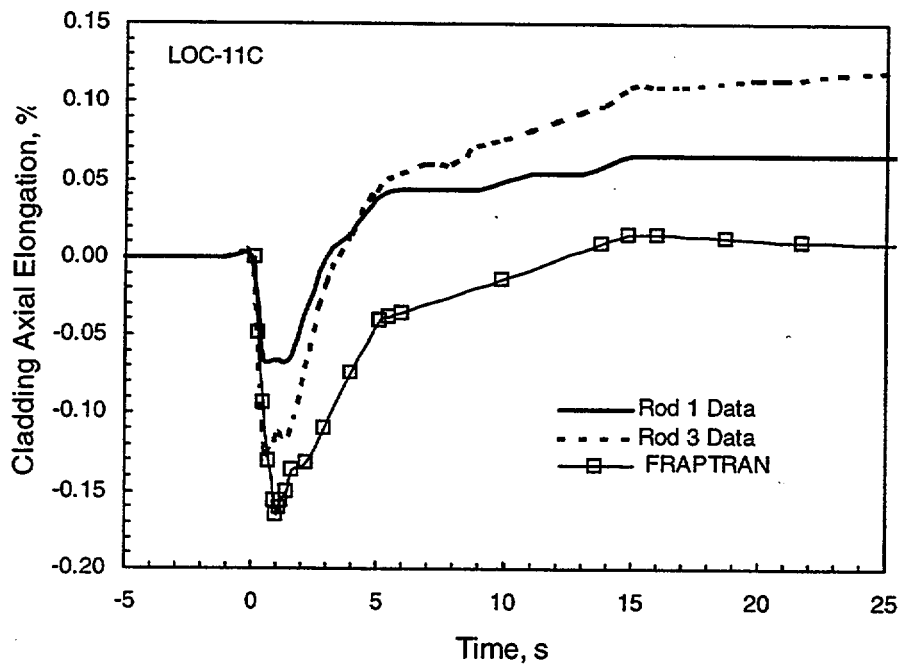


Figure 5.5 Comparison of Measured and Predicted Cladding Axial Elongation for LOC-11C

5.5 TREAT FRF-2 LOCA Assessment

Provided in Figure 5.6 is a comparison of measured and calculated gas pressures for the FRF-2 LOCA case. The measured gas pressure history for two rods is provided, both similar in behavior with rod failure occurring between 30 and 35 second. As presented in Section A.3.3, cladding temperatures for these rods reached 1600K before being quenched and there were large hoop strains measured for the rods.

Two different calculated gas pressure histories are presented in Figure 5.6 to illustrate the importance of understanding an experiment when performing assessments of this type. The first calculated curve (FRAPTRAN #1) shows a large pressure increase prior to failure. When this was evaluated against the data, it became apparent that the experimental gas pressure increase was not as large would have been expected based on the measured cladding temperatures. Subsequent investigation revealed three significant gas volumes for this test: the fuel-cladding gap (35% of the total), the fuel rod plenum (49% of the total), and a pressure cell (16% of the total) held at about 400K during the test. Thus there was a large volume of gas that did not see a significant temperature rise during the test.

The second FRAPTRAN run (FRAPTRAN #2) in Figure 5.6 was based on controlling the plenum (with a volume totaling the plenum and the pressure cell) at a much lower temperature (<450K) than the rest of the rod. For this case, the pressure history matches well with the measured pressure data and predicted rod failure occurred at about 28 seconds, which is in reasonable agreement, though earlier, with the actual failure times of 31-34 seconds.

The predicted cladding ballooning (hoop strain) as a function of axial position is compared to the data in Figure 5.7. The predicted peak ballooning strain was much larger than measured and occurred at a lower elevation than was measured.

5.6 Summary of LOCA Assessment Results

Good results were obtained in comparing FRAPTRAN to the LOCA test data. In general:

- FRAPTRAN was conservative in predicting time to failure for these experiments; i.e., the code underpredicted the time to failure.
- FRAPTRAN underpredicted the permanent cladding hoop strain for the failed NRU MT rods while overpredicting the length of the axial region of the cladding having significant hoop strain. This result is likely dependent on the specified axial node structure.
- If gas pressures were correctly predicted, then the general rod behavior was predicted in reasonable agreement with the data. FRAPTRAN cases run with higher rod gas pressures resulted in earlier times to failure, as would be expected.

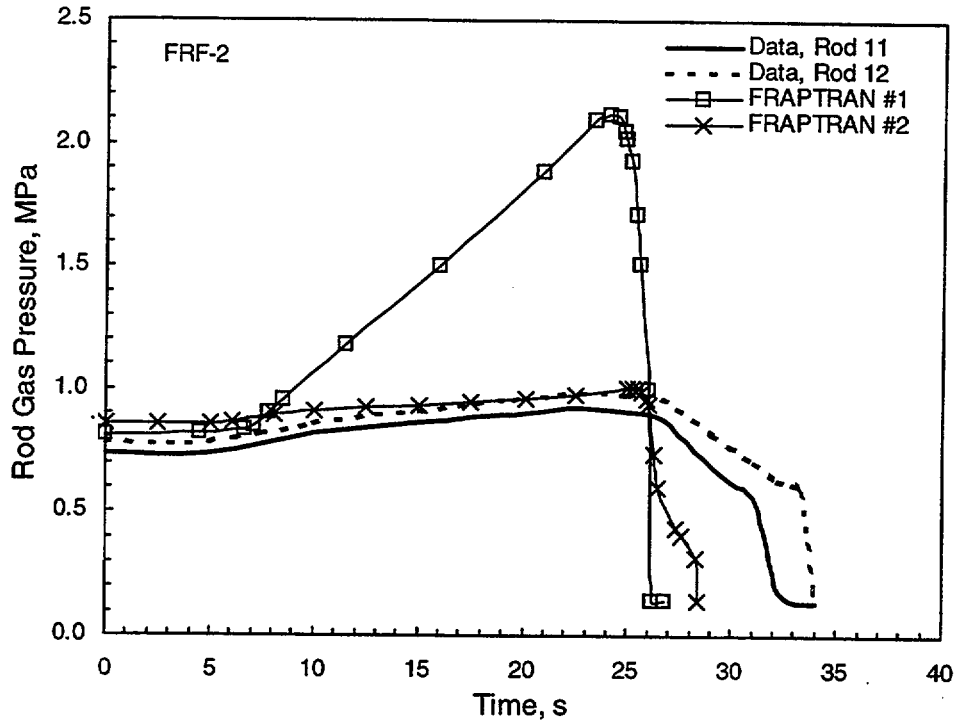


Figure 5.6 Comparison of Measured and Predicted Gas Pressure for FRF-2

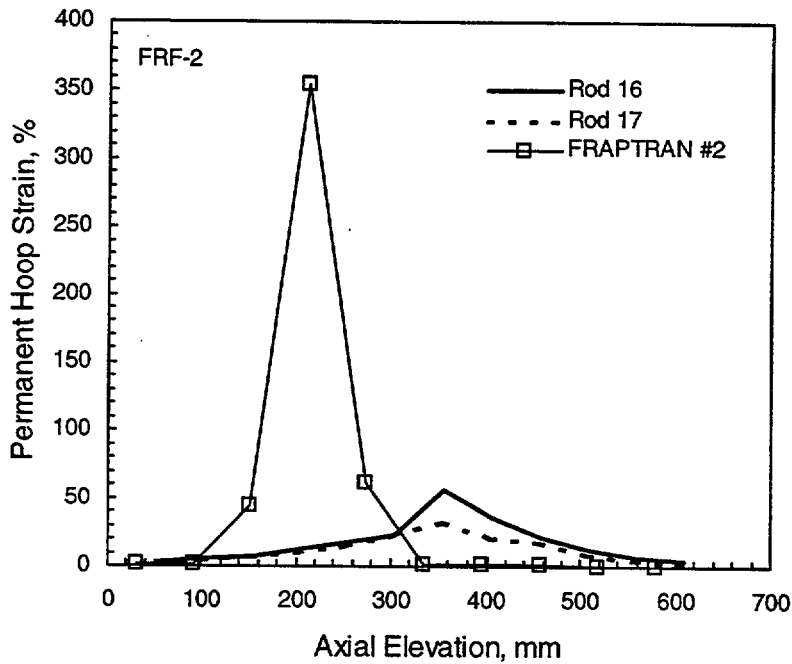


Figure 5.7 Measured and Predicted Permanent Hoop Strain for FRF-2

- Good comparisons to cladding axial elongation data, while controlling the cladding temperatures, again provide confirmation that the cladding thermal expansion model is working correctly.
- No comparison to cladding oxidation data was performed, thus the cladding oxidation models were not evaluated.

6 OTHER TRANSIENT ASSESSMENTS

Provided in this section are assessment results for FRAPTRAN predictions of a variety of transient experiments. The cases presented in this section are:

- A comparison with the standard problem developed for FRAP-T6. FRAPTRAN will be compared against the reported FRAP-T6 results for this problem which simulates a LOCA.
- A comparison with cladding elongation data obtained during the initial power ascension of IFA-508 irradiated in the Halden Boiling Water Reactor (HBWR). This power ascension incorporated hold points where fuel and cladding relaxation were observed.
- A comparison with fuel centerline temperature data obtained during the scram of an irradiated, re-instrumented rod at a burnup level of 44 MWd/kgUO₂. This rod was in the IFA-533.2 test assembly irradiated in the HBWR.
- Two comparisons with cladding axial elongation data obtained during power-cooling mismatch experiments conducted in the Power Burst Facility (PBF). The IE-1 test used four previously irradiated PWR rods while the PR-1 test used four non-irradiated BWR-type rods.

6.1 FRAP-T6 Standard Problem

The FRAP-T6 standard problem was included in the documentation (Siefken et al. 1981) when FRAP-T6 was first issued. Results from FRAPTRAN, using the input specified in the FRAP-T6 documentation, are presented here to illustrate possible changes that have occurred since FRAP-T6 was first issued. The FRAP-T6 standard problem description and results are provided in Section A.4.1.

Provided in Figure 6.1 is a comparison of cladding inner surface temperature between the two code calculations, and in Figure 6.2 is a comparison of fuel centerline temperature. For both cases the FRAPTRAN calculation results in lower temperatures than the FRAP-T6 results reported by Siefken et al. (1981). Examination of Figure 6.1 would suggest that FRAP-T6 predicted a lower coolant-cladding heat transfer coefficient than FRAPTRAN. If so, this would result in higher cladding and fuel temperatures for the FRAP-T6 calculation. It is noted that the coolant heat transfer models in FRAPTRAN have not been changed, although programming errors have been found and corrected for some of these models. The FRAPTRAN results are for the peak node, which is also the mid-plane node.

Presented in Figure 6.3 is a comparison between the two codes of cladding axial elongation and in Figure 6.4 is a comparison of rod gas pressure. For both these parameters, FRAPTRAN generally calculates the higher values. This is an interesting result since, in contrast, FRAPTRAN calculates the lower fuel and cladding temperatures. However, both codes provide the same general response with time although there are differences in the absolute values. In addition, the FRAPTRAN cladding elongation history is in agreement with the cladding temperature history; i.e., the elongation peaks at about 11 seconds as does

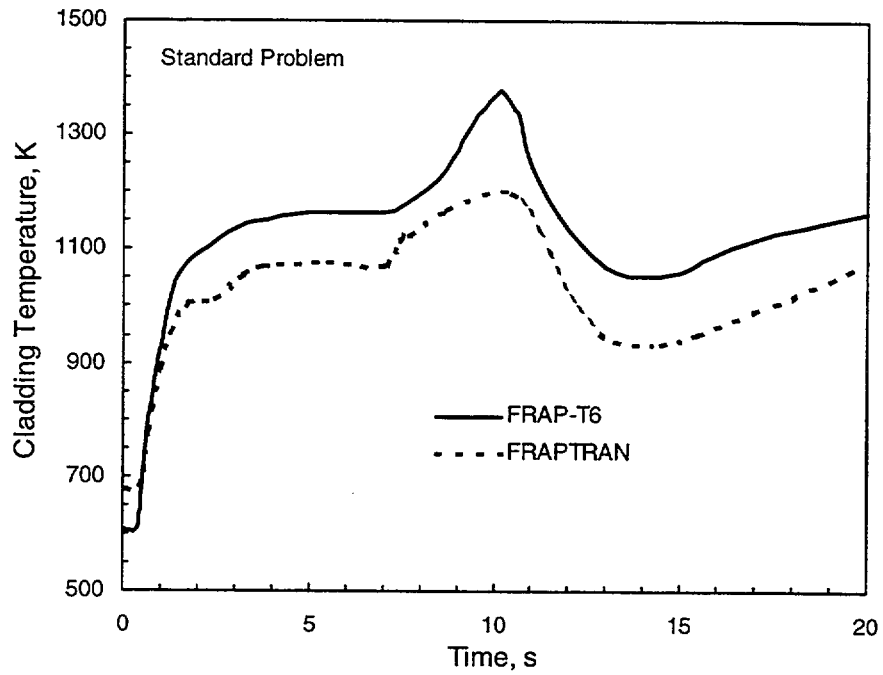


Figure 6.1 Comparison of FRAP-T6 and FRAPTRAN Cladding Temperature for Standard Problem

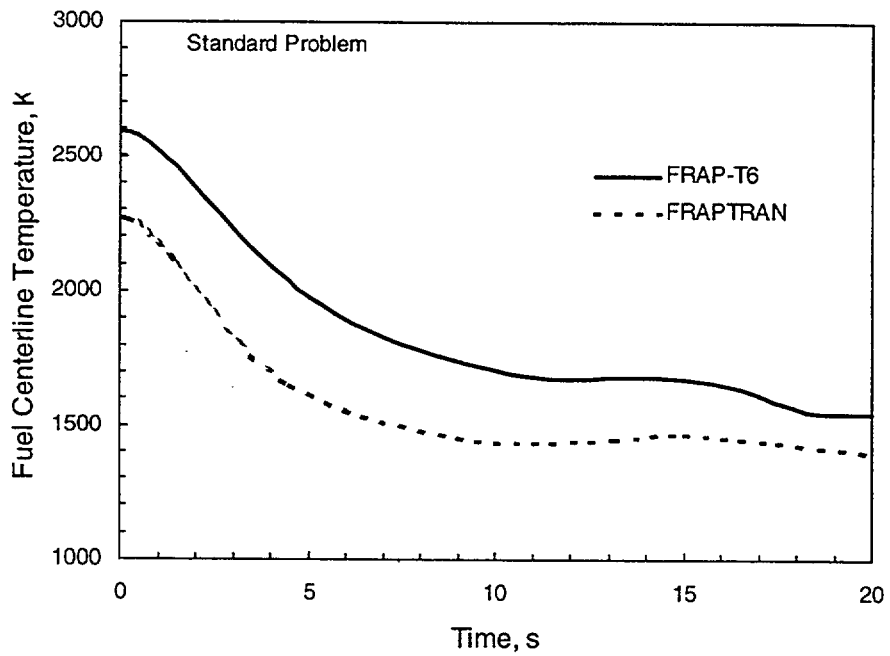


Figure 6.2 Comparison of FRAP-T6 and FRAPTRAN Fuel Centerline Temperature for Standard Problem

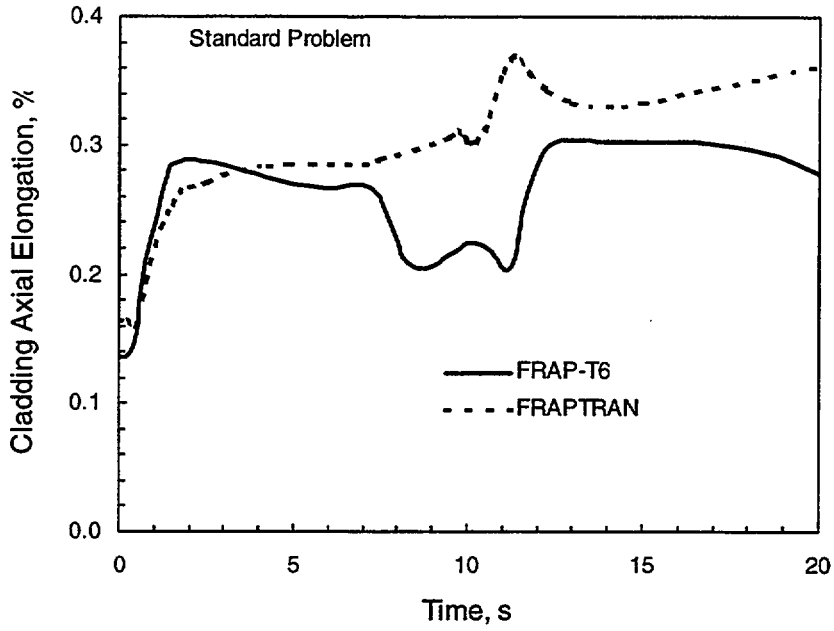


Figure 6.3 Comparison of FRAP-T6 and FRAPTRAN Cladding Elongation for Standard Problem

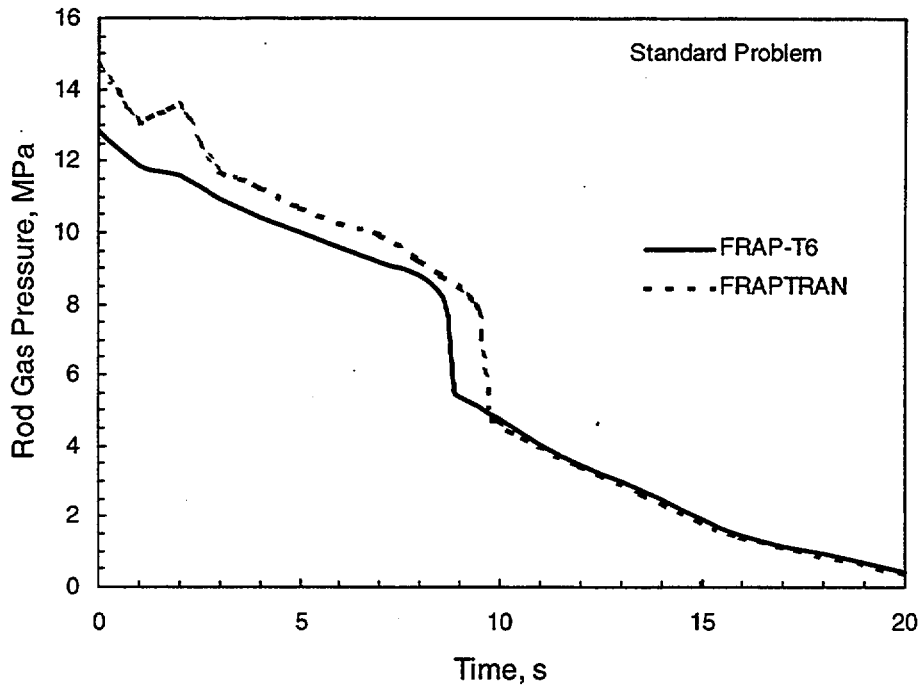


Figure 6.4 Comparison of FRAP-T6 and FRAPTRAN Gas Pressure for Standard Problem

the cladding temperature. Since the FRAP-T6 calculation showed an elongation decrease during this period of peaking cladding temperature, it may indicate that there was a problem with the FRAP-T6 calculation.

Since the 1981 version of FRAP-T6 is not available, it is not possible to do an evaluation of the code changes that might contribute to the observed calculational results. Known differences that would impact temperatures would include changes in fuel thermal conductivity and between the two codes' gap conductance models.

6.2 IFA-508, Rod 11

The initial power ascension for IFA-508 was performed in a stair-step approach. It was observed during the holds at each power level that cladding elongation decreased due to fuel and cladding relaxation. This behavior would not be expected for FRAPTRAN because the code does not have a fuel relaxation model.

Predicted and measured cladding elongation for Rod 11 of IFA-508 during the initial power ascension is presented in Figure 6.5. The data illustrate that the fuel and cladding relaxed during the power step holds. However, because FRAPTRAN, using the FRACAS-1 mechanical model, has no model for this phenomena, no relaxation during the holds at power is calculated. The comparison of cladding elongation slope between FRAPTRAN and the data (using the fuel gage length) shows good agreement. In addition, the power level at which fuel-cladding interaction is predicted to begin (approximately 18 kW/m) is in

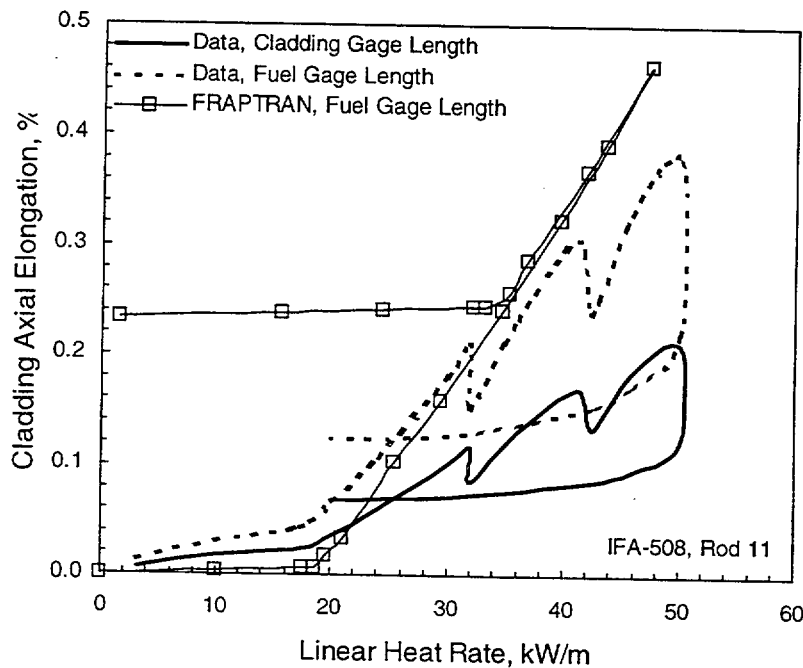


Figure 6.5 Comparison of Measured and Predicted Cladding Elongation During Initial Power Ascension for IFA-508, Rod 11

good agreement with the data. FRAPTRAN predicts a higher level of residual cladding axial strain after the power ramp than the data. This case demonstrates that FRAPTRAN provides reasonable predictions of cladding axial elongation for fast transients but, as expected, does not follow the fuel and cladding relaxation when steady-state power conditions are achieved.

6.3 IFA-533.2

The IFA-533.2 irradiation consisted of rods that were pre-irradiated in IFA-409 and then re-instrumented with fuel centerline thermocouples. A key feature of the IFA-533.2 irradiation is periodic scrams from power where fuel centerline temperature is measured during the scram and analyses of the temperature data can indicate changes in fuel performance with burnup.

Presented in Figure 6.6 is a comparison of the difference between measured and predicted fuel centerline temperatures and the coolant temperature (523K) during the first scram of IFA-533.2 at a burnup of 44 MWd/kgUO₂. The temperatures are presented on a natural log plot to emphasize the time constant of the fuel during the scram. Two FRAPTRAN calculations are presented: a “base” calculation and a calculation assuming additional thermal resistance in the fuel.

The initial centerline temperature for the base calculation is in good agreement with the data (~1375K) indicating a good steady-state temperature calculation by FRAPTRAN using the initialization values

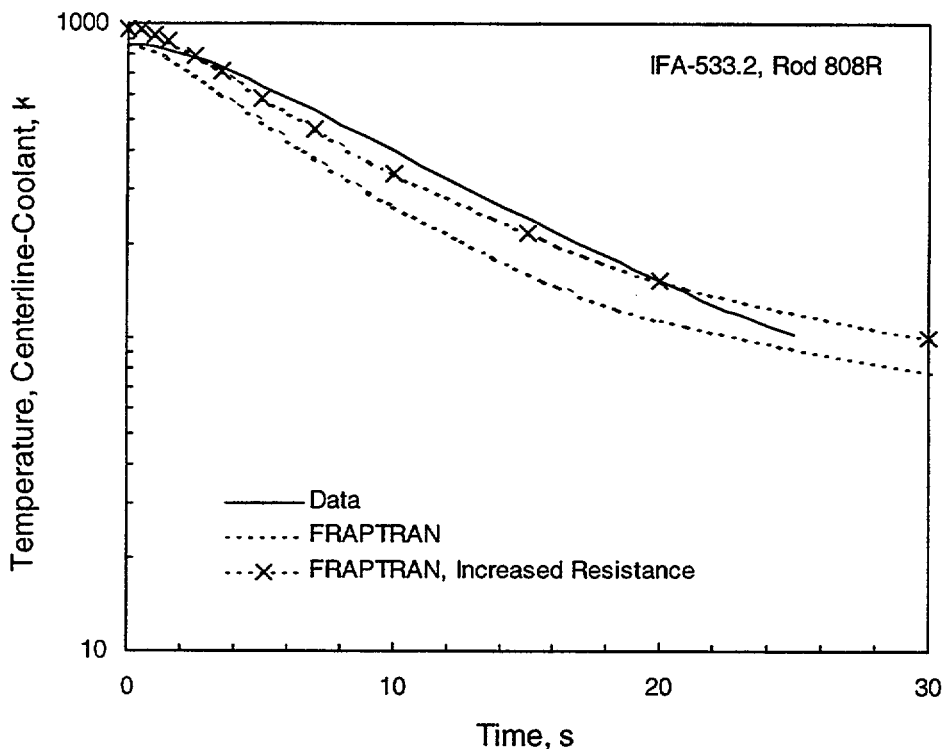


Figure 6.6 Comparison of Measured and Predicted Difference Between Fuel Centerline Temperature and Coolant for IFA 533.2, Rod 808R

provided by FRAPCON-3 for this case. This case also assumes a 100% helium fill gas from the refabrication process. The base FRAPTRAN calculation shows a faster time constant than the measured data; i.e., a steeper slope for the predicted temperature curve.

The second FRAPTRAN curve presented assumes a gas mixture of 90% helium and 10% xenon to simulate fission gas release that might have occurred during the initial portion of the IFA-533.2 irradiation; the early IFA-533.2 irradiation was at a significantly higher LHGR than the end of the IFA-409 irradiation. In addition, the fuel thermal conductivity, which was already decreased because of the burnup effect, was decreased by an additional 10% to increase the predicted fuel thermal resistance during the scram. For this case, the initial FRAPTRAN temperature was 100K higher than the measurement (1475K vs. 1375K, respectively), which would indicate that these assumptions are not as good for the steady-state conditions. However, better agreement in the fuel time constant is obtained with these assumptions; i.e., a better agreement in the temperature slope between prediction and measurement. It could be hypothesized that greater thermal resistance deduced for the fuel rod may be due to the refabrication process creating cracks or gaps in the fuel that were not completely healed during the irradiation period prior to the scram. The greater thermal resistance could also indicate that the fuel thermal conductivity burnup degradation in FRAPTRAN (and FRAPCON-3) needs to be increased; i.e., greater degradation is needed. This has been proposed as a future change to the thermal conductivity model in FRAPCON-3 (Lanning, Beyer, and Cunningham 2000).

The faster temperature decrease predicted by FRAPTRAN than was experimentally measured is consistent with the behavior observed for the TREAT FRF-2 assessment case (Section 5).

6.4 PBF IE-1, Rod 7

The PBF IE-1 test subjected four previously irradiated PWR rods to a variety of power and coolant conditions. During the sixth cycle of this test, the rods were brought to power, held at power, and then coolant flow was decreased until the rods experienced departure from nucleate boiling. Cladding elongation data from this test are used for comparison to FRAPTRAN.

Presented in Figure 6.7 is a comparison of measured and calculated cladding elongation for Rod 7 in the IE-1 test. As presented in Section A.4.4, this test began with a stairstep ascension to power followed by decreasing coolant flow. The large measured cladding elongation increase seen at the end of the history in Figure 6.7 is the period when coolant flow was decreased sufficiently to drive the rod into departure from nucleate boiling and thus increase cladding temperature to approximately 660K.

The predicted and measured cladding elongation is in reasonable agreement during the stair step ascension, particularly the cladding elongation at peak power approximately 2500 seconds into the transient (Figure 6.7).

The FRAPTRAN calculation during the coolant flow decrease portion of the test (after 2600 seconds) was very sensitive to the input coolant flow; this period is presented in Figure 6.8. With the code input as specified in Table B.24, the code calculated more cooling than was demonstrated by the data. Therefore,

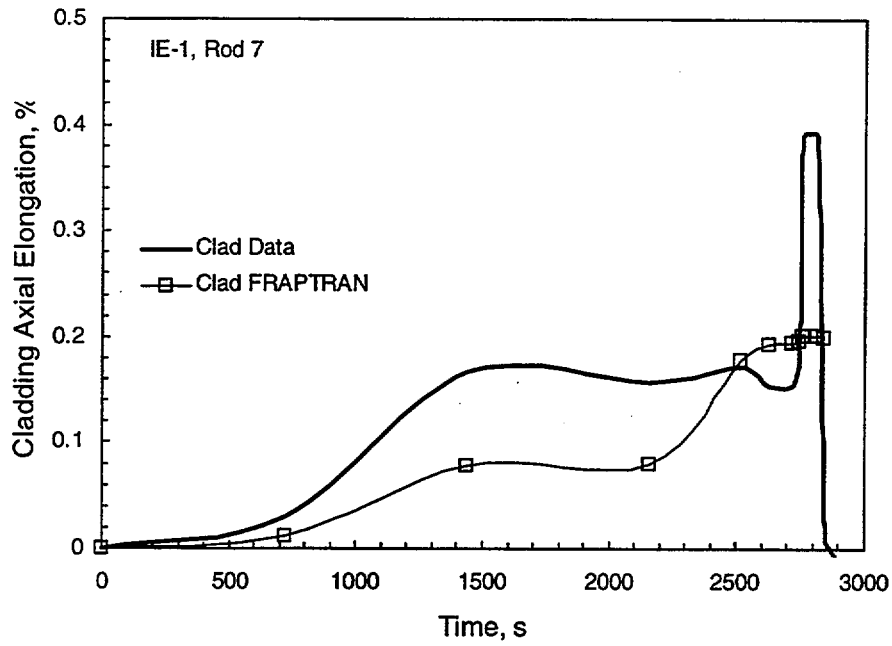


Figure 6.7 Comparison of Measured and Predicted Cladding Elongation for IE-1, Rod 7

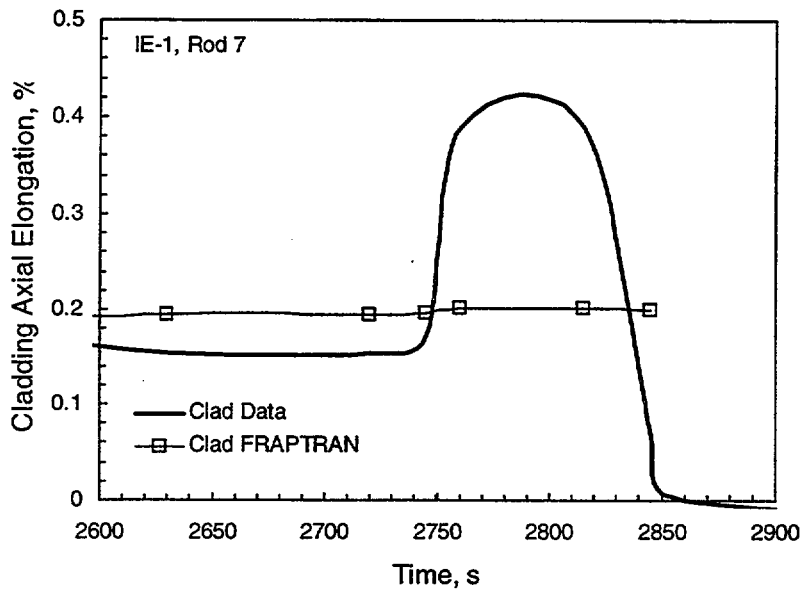


Figure 6.8 Comparison of Measured and Predicted Cladding Elongation for IE-1, Rod 7 During Power-Cooling Mismatch Period

for this case, FRAPTRAN did not calculate well the onset of departure from nucleate boiling and again the need is emphasized to use a thermal-hydraulic code to provide coolant conditions for complicated coolant heat transfer test conditions.

6.5 PBF PR-1

The PBF PR-1 test subjected four non-irradiated BWR-type rods to a variety of power and coolant conditions, including some RIA-type conditions at the end of the test series. During cycle 17 of this test the rods were held at a constant power of approximately 34 kW/m while the flow was reduced (see Section A.4.5). Cladding and fuel centerline temperature, cladding elongation, and rod gas pressure were measured and used for comparison with the FRAPTRAN prediction.

The four rods had a variety of initial fuel densities and fill gas composition as noted in Section A.4.5. The FRAPTRAN prediction for cycle 17 (see Section B.6) was based on the Rod 524-2 design with an added assumption of fuel densification from the as-fabricated 92% TD to 95% TD with a concurrent decrease in the fuel pellet diameter and increase in the fuel-cladding gap. This fuel densification assumption was made because of the observable increase in fuel centerline temperature (at a constant power level) as the testing proceeded through the various cycles.

Provided in Table 6.1 is a comparison of measured data and predicted results for cycle 17 of the PR-1 test sequence. Even with the assumed fuel densification and increase in fuel-cladding gap, FRAPTRAN underpredicted the measured fuel centerline temperatures by 200-300K. This implies that densification was greater than assumed, or that other factors affected the measured fuel centerline temperatures.

Measured cladding elongation for Rods 524-1, 524-2, and 524-3 was an increase of ~0.1 mm during the period of flow reduction while the FRAPTRAN prediction was for an increase of ~0.06 mm. Corresponding to the cladding elongation, measured cladding surface temperature for Rod 524-3 showed no increase at the 60-degree orientation but a greater than 200K increase at the 180-degree orientation. This indicates potentially very localized departure from nucleate boiling during the period of flow reduction. FRAPTRAN predicted a cladding surface temperature increase of approximately 30K for axial node 4 (of 5) and a smaller increase for axial node 5. The FRAPTRAN-predicted cladding elongation is consistent with the predicted cladding temperature increase and in reasonable agreement with the measured data. This would indicate that there was some cladding temperature increase during the flow reduction, but not a great increase over a significant length of the cladding.

Parameter	Measured	FRAPTRAN Predicted
Fuel Centerline Temperature	524-1: 1885K 524-2: 1785K	1590K
Peak Cladding Surface Temperature	524-3@60°: 625K 524-3@180°: 860K	653K for axial node 4
Increase in Cladding Elongation During Flow Reduction	~0.1 mm	~0.06 mm
Rod Gas Pressure	524-1: 9.0 MPa 524-2: 9.7 MPa	9.5 MPa

7 SUMMARY AND CONCLUSIONS

The FRAPTRAN transient fuel behavior computer code has been assessed against a selected set of experimental fuel rod transient data. The selected data are from tests simulating RIAs, LOCAs, and other transients. Because of the sensitivity of the code calculations to the assumed thermal-hydraulic conditions, an effort was made to minimize the impact of the thermal-hydraulic calculations on the calculated fuel and cladding thermal and mechanical behavior. The FRAPCON-3 code was used to initialize burnup-dependent parameters for FRAPTRAN.

The FRAPTRAN predictions compared reasonably well to the experimental data. A number of specific observations and conclusions about the performance of FRAPTRAN have been reached; they are summarized in the following.

- Comparison of code predictions with data have provided assurance that the basic models are working satisfactorily; i.e., temperature, gap conductance, gas pressure, and thermal expansion.
- When the cladding outer surface temperature is controlled to match experimental data (by controlling the coolant temperature), and there is no fuel-cladding mechanical interaction, predicted cladding axial elongation is generally in good agreement with the experimental data. This indicates that the cladding thermal elongation model is appropriate.
- Comparisons of predicted and measured fuel elongation for the RIAs were in general agreement, thus providing some assurance that predicted fuel temperatures were reasonable for the RIAs. In addition, the general agreement also indicates that calculating fuel axial thermal expansion using the temperature at the shoulder of the fuel pellet dish rather than the peak radial fuel temperature is acceptable.
- Comparisons of predicted and measured fuel centerline temperature during scrams (LOC-11C and IFA-533.2) show that the code consistently calculates faster temperature decreases than were measured. This is likely due to FRAPTRAN calculating lower thermal resistances in the fuel and/or the fuel-cladding gap than are operating in the fuel rods.
- Rod internal gas pressure is correctly calculated when other parameters that determine gas pressure, such as available volume and corresponding temperatures, are correctly input and calculated (NRU MT cases). In addition, when gas pressure is correctly predicted for the LOCA cases, then reasonable agreement between predicted and measured time to failure is obtained.
- The experimental steady-state data for cladding elongation as a function of LHGR indicate fuel compliance (creep) that is not modeled by the code; i.e., the observed transition for cladding axial elongation from being driven by thermal expansion to expansion driven by fuel-cladding mechanical interaction is more gradual than predicted by the code (IFA-432, Rod 3). This observation is based on steady-state data that may not be appropriate for rapid transient response.

- FRAPTRAN provided reasonable predictions of cladding axial elongation for fast transients but, as expected, did not follow the fuel and cladding relaxation when steady-state power conditions are achieved (IFA-508).
- FRAPTRAN consistently underpredicted permanent cladding hoop strain for the RIA tests conducted in the NSRR. This is indicative of fuel-cladding mechanical interaction occurring in these tests that is not modeled by the code. This failure to predict some aspects of the mechanical behavior of RIA tests has been observed for other codes. There is evidence to suggest there is fuel behavior resulting in additional cladding radial stress/strain that is not accounted for by the transient codes.
- The FRAPTRAN results were often sensitive to the input, particularly coolant conditions. For complicated transients, attention needs to be paid to the input thermal-hydraulic conditions and input from a thermal-hydraulic code should be considered.
- The FRAPTRAN mechanical results are strongly dependent on the input fuel-cladding gap size.

This assessment has identified some areas of work that are still needed for FRAPTRAN. In addition, other work is planned that was not indicated by this assessment. Planned future FRAPTRAN work includes:

- Improvements to the convergence of the mechanical solution model. The mechanical solution scheme is sensitive to rapid strain rates and may not interactively converge if the time step is too large during periods of high strain rate for cases such as RIAs or high cladding temperatures and low yield strength for cases such as LOCAs.
- Comparisons to the experimental data indicate the need for some fuel compliance to lessen the predicted abrupt mechanical transition from no fuel-cladding interaction to solid fuel-cladding interaction.
- Gaseous fission gas release and fuel swelling have been proposed as contributors to the cladding permanent hoop strain during RIAs. However, models for these phenomena are not included in FRAPTRAN. Future work will include developing and implementing simple models in FRAPTRAN. The code user does have the option to specify the amount of fission gas release fuel swelling during a transient.
- One transient type that was not evaluated in this assessment, because of a lack of experimental data, was a BWR anticipated transient without scram (ATWS). This postulated transient is characterized by multiple cycles of power and coolant variations. To assist in analyzing ATWS transients, the use of thermal-hydraulic models other than those currently in FRAPTRAN may be explored.

During the development of FRAPTRAN and during the code assessment, some insight into the operation of FRAPTRAN and guidance in preparing input files was developed. Following are some comments relative to the general use of FRAPTRAN.

- As mentioned above, the mechanical solution scheme is sensitive to rapid strain rates. To assist the user in determining when such conditions exist, the code will stop operation and print warning messages to both the computer prompt window and the output file. These messages (see Section 3.5 of Cunningham et al. 2001) will inform the user that the plastic strain increment is too large and that the time step should be reduced.
- The cladding strain rate may also become too high when elevated cladding temperatures result in very low yield strength values, i.e., <6 MPa. For these cases, the code does not stop but goes to a simplified mechanical solution for strain that ignores elastic strain. A warning message for the user is printed to both the computer prompt window and the output file.
- Guidelines for time step sizes are provided in Section 3.5 of Cunningham et al. (2001).
- The input files in Appendix B provide examples of setting up FRAPTRAN to run RIA, LOCA, and other cases
- The input instructions in Appendix A of Cunningham et al. (2001), identify an option to specify a file (FILE66) for graphics data output. This file is designed to be read by a PNNL-developed routine that works with EXCEL® software. The EXCEL® routine and user instructions will be provided along with the FRAPTRAN code to users.

8 REFERENCES

Berna, G. A., et al. 1997. FRAPCON-3: A Computer Code for the Calculation of Steady-State, Thermal-Mechanical Behavior of Oxide Fuel Rods for High Burnup. NUREG/CR-6534, Vol. 2 (PNNL-11513), Pacific Northwest National Laboratory, Richland, Washington.

Cunningham, M. E., et al. 2001, FRAPTRAN: A Computer Code for the Transient Analysis of Oxide Fuel Rods. NUREG/CR-6739 (PNNL-13576), Vol. 1, Pacific Northwest National Laboratory, Richland, Washington.

Lanning, D. D., C. E. Beyer, and M. E. Cunningham. 2000. "FRAPCON-3 Fuel Rod Temperature Predictions with Fuel Thermal Conductivity Degradation Caused by Fission Products and Gadolinia Additions," in Conference Proceedings of the 2000 International Topical Meeting on Light Water Reactor Fuel Performance, Park City, Utah, April 10-13, 2000, American Nuclear Society.

Lanning, D. D., C. E. Beyer, and G. A. Berna. 1997. FRAPCON-3: Integral Assessment. NUREG/CR-6534, Vol. 3 (PNNL-11513), Pacific Northwest National Laboratory, Richland, Washington.

Siefken, L. J., et al. 1981. FRAP-T6: A Computer Code for the Transient Analysis of Oxide Fuel Rods. NUREG/CR-2148 (EGG-2104), EG&G Idaho, Inc., Idaho Falls, Idaho.

Siefken, L. J., et al. 1983. FRAP-T6: A Computer Code for the Transient Analysis of Oxide Fuel Rods. NUREG/CR-2148 Addendum (EGG-2104 Addendum), EG&G Idaho, Inc., Idaho Falls, Idaho.

APPENDIX A

DESCRIPTION OF CASES

APPENDIX A

DESCRIPTION OF CASES

Experimental data from four basic types of experiments have been selected and compiled for the assessment of FRAPTRAN: separate effects tests from steady-state experiments; reactivity initiated accident (RIA) tests; loss-of-coolant-accident (LOCA) tests; and other selected miscellaneous transient tests. The selected tests and data sets are described in this appendix. The input files used for the FRAPTRAN runs are provided in Appendix B along with other information relevant to setting up the FRAPTRAN cases.

The measurement units reported in this appendix for the design and operation variables for each experiment are generally those used or reported in the references. Standardization of units to the SI system is provided when presenting the assessment results in Sections 3 through 6.

A.1 Separate Effects Tests

A few experiments were selected to provide what may be called separate effects data. These experiments are those where the experiment design and measured results are relatively unambiguous and may be used to demonstrate that specific models in FRAPTRAN are working correctly.

The selected tests are the IFA-432 and IFA-513 experiments irradiated in the Halden Boiling Water Reactor. These tests irradiated well-characterized BWR-type rods that were instrumented with fuel centerline thermocouples, gas pressure sensors, and cladding elongation sensors. Data obtained from the initial power ascension is used to compare against the FRAPTRAN predictions as a function of power (and temperature). Three rods have been selected because of design differences. Rod 1 of IFA-432 may be considered the standard rod with an initial fill gas of 100% helium and a fuel-cladding diametral gap of 0.009 inches. Rod 3 of IFA-432 is a small gap (0.003 inch diametral) rod. Rod 6 of IFA-513 had a gap of 0.008 inch but an initial fill gas mixture of 77% helium and 23% xenon. Provided in Table A.1 is a summary of the design characteristics of the three rods.

These three rods provide a check of FRAPTRAN's performance for different gap sizes and fill gas compositions, and thus a check of the temperature calculations. Provided in Figures A.1 through A.3 are the measured fuel centerline temperatures for these three rods as a function of power during the initial power ascension. It can be seen that there was some variation in temperature versus power response between the upper and lower thermocouples in these rods. This is believed to be due to uncertainties in defining the local power at the thermocouple positions.

Provided in Figure A.4 is the measured cladding elongation data for Rod 3 of IFA-432 (small gap) during the initial power ascension. It may be seen that fuel-cladding interaction began at a rod-average power of approximately 20 kW/m.

Parameter	Rod 1, IFA-432	Rod 3, IFA-432	Rod 6, IFA-513
Rod Overall Length	25 in.	25 in.	32.4 in.
Active Fuel Length	22.8 in.	22.8 in.	30.7 in.
Cladding Type	Zircaloy-2	Zircaloy-2	Zircaloy-2
Cladding Outer and Inner Diameters	0.5035 and 0.4295 in.	0.5035 and 0.4295 in.	0.5039 and 0.4291 in.
Cladding Thickness	0.0370 in.	0.0370 in.	0.0374 in.
Pellet Diameter	0.4204 in.	0.4204 in.	0.4213 in.
Fuel-Cladding Radial Gap	0.0045 in.	0.0015 in.	0.0039 in.
Fuel Pellet Length	0.50 in.	0.50 in.	0.50 in.
Pellet Hole Diameter	0.069 in.	0.069 in.	0.069 in.
Pellet Density	95% TD	95% TD	95% TD
Pellet Enrichment	10% U-235	10% U-235	9.9% U-235
Fill Gas	100% He 0.1 MPa at 300K	100% He 0.1 MPa at 300K	77% He/23%Xe 0.1 MPa at 300K
Coolant Inlet Conditions	240°C at 3.4 MPa	240°C at 3.4 MPa	240°C at 3.4 MPa

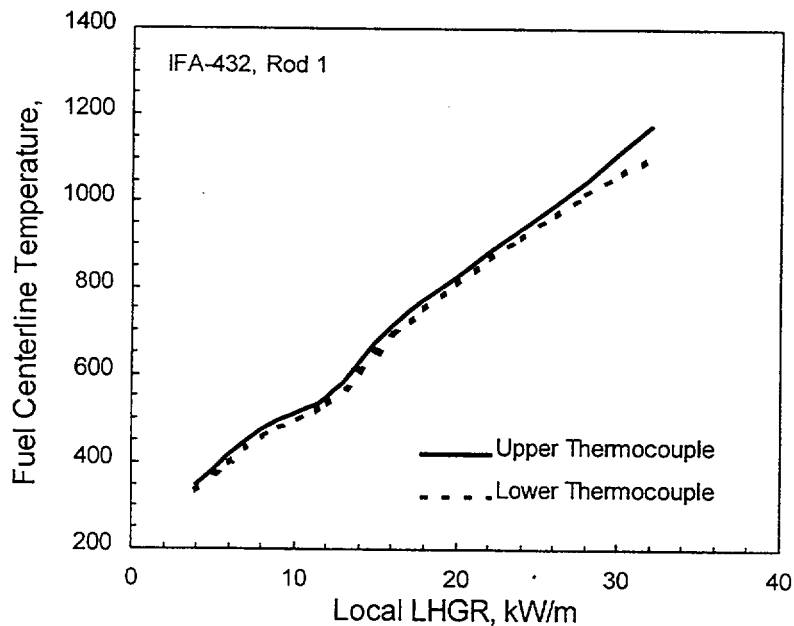


Figure A.1 Measured Fuel Centerline Temperatures for Rod 1 (standard gap) of IFA-432

Provided in Figure A.5 are the measured cladding elongation and gas pressure for Rod 6 of IFA-513 (23% xenon). Fuel-cladding mechanical interaction for this rod began at a rod-average power of approximately 20 kW/m.

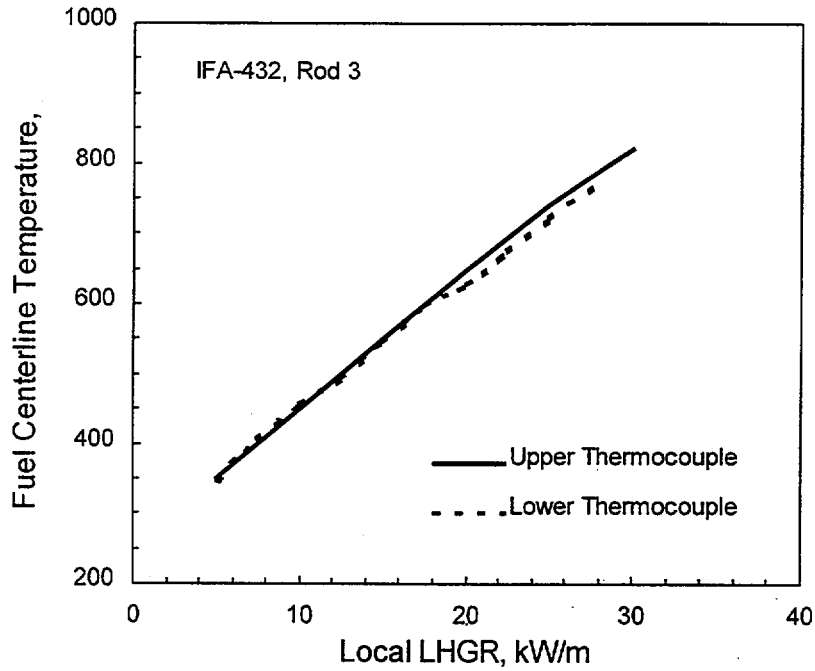


Figure A.2 Measured Fuel Centerline Temperatures for Rod 3 (small gap) of IFA-432

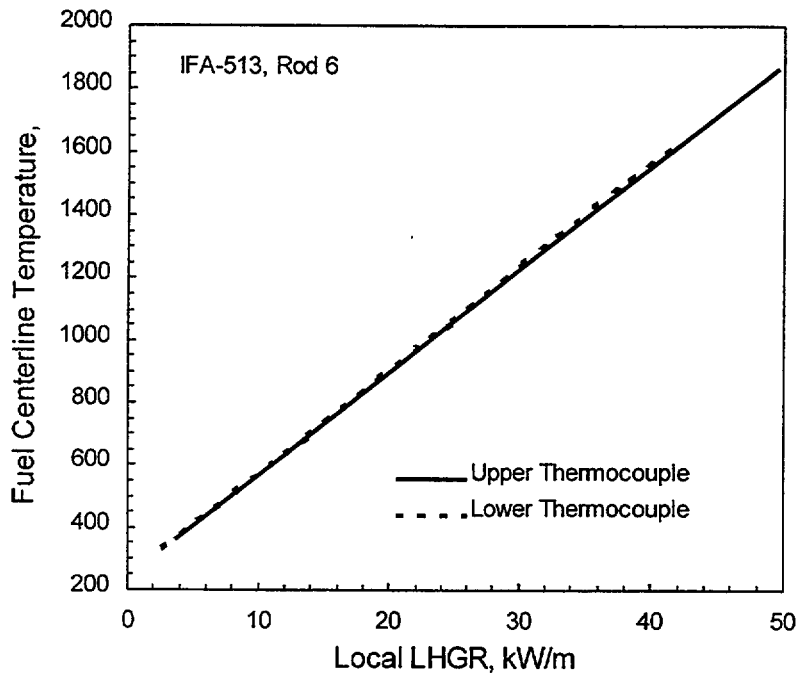


Figure A.3 Measured Fuel Centerline Temperatures for Rod 6 (23% xenon) of IFA-513

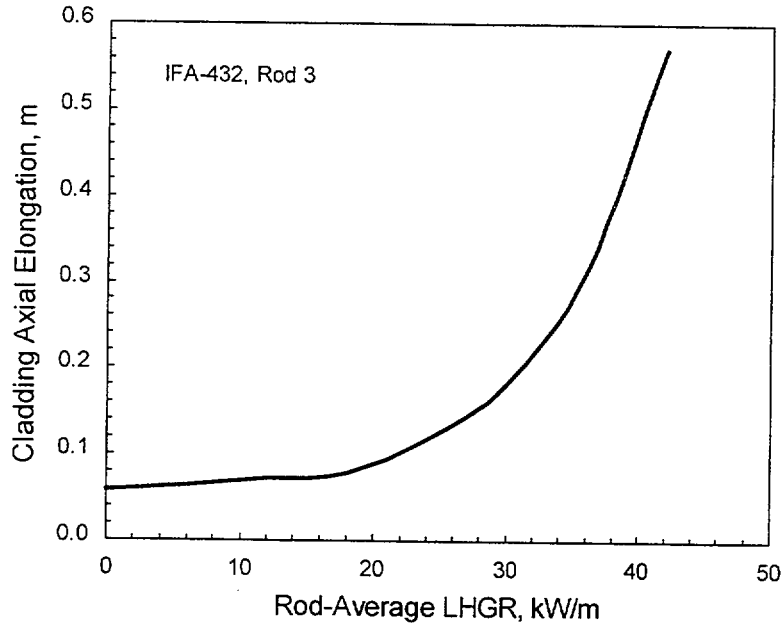


Figure A.4 Measured Cladding Elongation for Rod 3 (small gap) of IFA-432

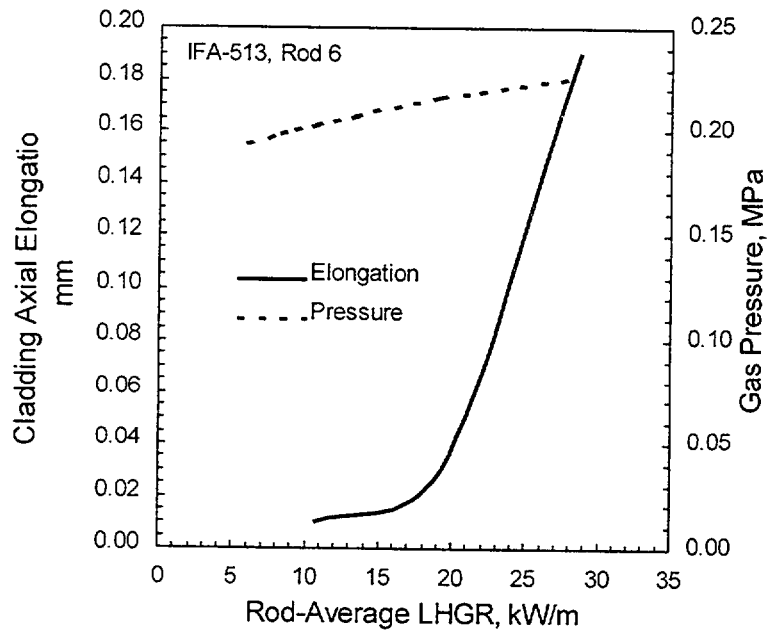


Figure A.5 Measured Cladding Elongation and Gas Pressure for Rod 6 (23% xenon) of IFA-513

Sources

Bradley, E. R., et al. 1979. *Precharacterization Report for Instrumented Nuclear Fuel Assembly IFA-513*. NUREG/CR-1077 (PNL-3156), Pacific Northwest National Laboratory, Richland, Washington.

Bradley, E. R., et al. 1981. *Data Report for the Instrumented Fuel Assembly IFA-513*. NUREG/CR-1838 (PNL-3637), Pacific Northwest National Laboratory, Richland, Washington.

Hann, C. R., et al. 1977. *Test Design, Precharacterization and Fuel Assembly Fabrication for Instrumented Fuel Assemblies IFA-431 and IFA-432*. NUREG/CR-0332 (BNWL-1988), Pacific Northwest National Laboratory, Richland, Washington.

Lanning, D. D., and E. R. Bradley. 1984. *Irradiation History and Interim Postirradiation Data for IFA-432*. NUREG/CR-3071 (PNL-4543), Pacific Northwest National Laboratory, Richland, Washington.

A.2 Reactivity-Initiated Accident (RIA) Test Cases

Reactivity-initiated accidents (RIAs) are of concern to regulatory agencies for high burnup fuels. Therefore, a number of RIA tests have been run in test reactors during the 1990s. The principal programs and facilities, testing modern design fuels and providing data for the assessment of FRAPTRAN, are:

- The Nuclear Safety Research Reactor (NSRR) operated by the Japan Atomic Energy Research Institute (JAERI); both PWR and BWR commercial fuel have been tested.
- The CABRI test facility operated by the French Nuclear Safety and Protection Institute (IPSN) and with the tests sponsored by IPSN and Electricite de France (EDF); PWR commercial UO₂ and mixed oxide fuel have been tested.
- The Impulse Graphite Reactor (IGR) managed by the Russian Research Centre "Kurchatov Institute" (RRC-KI); VVER fuel has been tested.

Data collected during RIAs as a function of time typically consist of power, coolant conditions (temperature and pressure), cladding temperature, fuel stack and cladding elongation, and fuel rod gas pressure. Standard post-irradiation examination data include rod profilometry for evaluation of cladding permanent strain (diametral and length) and rod puncture for fission gas release. Provided in Table A.2 is a summary of the RIA tests and experimental data selected for comparison to the FRAPTRAN calculations.

A.2.1 Tests Conducted in the NSRR

The Japan Atomic Energy Research Institute (JAERI) has conducted a series of RIA-type tests in the Nuclear Safety Research Reactor (NSRR). The objective of these tests is to provide a data base for regulation of light-water reactors. Numerous experiments have been performed to evaluate the thresholds, modes, and consequences of fuel rod failure in terms of fuel enthalpy, coolant conditions, and

Table A.2 Summary of RIA Data Collection and Post-Test Results

Test	Fuel Rod Data Collected During Test				Post-RIA Results		
	Cladding Temperature	Fuel Elongation	Cladding Elongation	Rod Gas Pressure	Permanent Cladding Hoop Strain, %	Permanent Cladding Axial Strain, %	Fission Gas Release, %
HBO-6	yes	yes	no	yes	1.2	0.05	10
MH-3	yes	yes	yes	yes	1.6	0.36	3.8
GK-1	yes	yes	yes	yes	2.5	0.15	14
OI-2	yes	yes	yes	yes	4.8		10
TS-5	yes	no	yes	yes	~0	~0	8
FK-1	yes	yes	yes	yes	0.9 ave/3.0 max	not measured	8
REP-Na3	no	yes ^a	yes	no	2.0	0.80	13.7
REP-Na4	no	yes ^a	yes	no	0.4	0.07	8.3
REP-Na5	no	yes ^a	yes	no	1.1	0.35	15.1
IGR H5T	no	no	no	no	6.5@failure site 3.1 away from failure	not measured	rod failed

^aFuel elongation measured by hodoscope.

fuel design. Six NSRR RIA test cases were selected for the assessment of FRAPTRAN. All six RIA tests used pre-irradiated fuel, with the test rods spanning a range of fuel designs and burnup levels. None of the six test rods used for the FRAPTRAN assessment failed during their RIA test.

The NSRR was designed exclusively to conduct power transient experiments. The NSRR is a modified TRIGA-ACP (annular core pulse) reactor using uranium-zirconium hydride fuel-moderator elements. A dry irradiation space is located in the center of the reactor core, while the core is cooled by natural circulation of the pool water. The test capsules used for the RIA irradiations are of a double capsule design. The instrumented test rods, within the capsules, are in stagnant water at atmospheric pressure (~ 0.1 MPa) and ambient temperature ($\sim 20^\circ\text{C}$). An example RIA power history is provided in Figure A.6.

Typical test instrumentation consists of cladding surface thermocouples (0.2 mm bare-wire type-R thermocouples) spot-welded to the cladding; coolant water temperature measured by type-K thermocouples; and a strain gauge-type pressure sensor to measure capsule internal pressure. Instrumentation was also included to measure fuel stack and cladding elongation during the transients.

Summary results of the six NSRR RIA tests used for the assessment are provided in Table A.3. Because of the variety of fuel designs and RIA test conditions, the test rod responses (such as permanent diametral strain) varied from test to test. Measured in-reactor elongation data are relative to the pre-transient temperature of 20°C . Each test will be individually presented in the following sections.

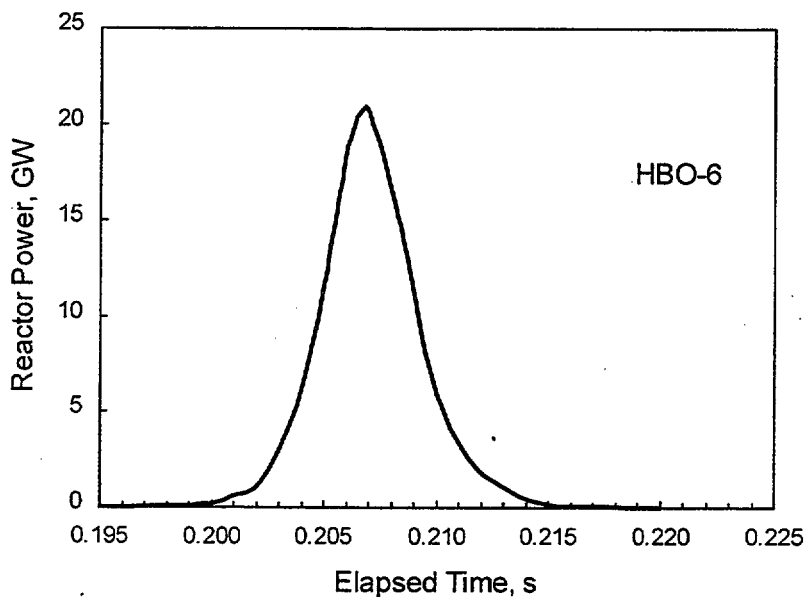


Figure A.6 Example RIA Power History for NSRR

Table A.3 Summary of NSRR RIA Test Rod Parameters

Parameter	NSRR RIA Test					
	HBO-6	MH-3	GK-1	OI-2	TS-5	FK-1
Rod Type	PWR 17x17	PWR 14x14	PWR 14x14	PWR 17x17	BWR 7x7	BWR 8x8BJ
Basic Design						
Cladding Type	Zry-4	Zry-4	Zry-4	Zry-4	Zry-2	Zry-2 w/Zr liner
Clad OD, mm	9.5	10.72	10.72	9.5	14.30	12.27
Clad Wall Thickness, mm	0.64	0.62	0.62	0.59	0.810	0.86
Fuel OD, mm	8.05	9.29	9.29	8.05	12.37	10.31
Fuel Length, mm	3648	3642	3642	3648	3657	360
Rod Length, mm	3852	3856	3856	3852	3964	510
Fill Gas	He@3.3 MPa	He@3.2 MPa	He@3.2 MPa	He@3.3 MPa	He@1.0 MPa	He@0.3 MPa
Fuel Enrichment, %U-235	3.2	2.6	3.4	3.2	2.79	3.9
Fuel Density, %	95	95	95	95	91-97	95
SS Irradiation						
Reactor	Ohi Unit 1, Kansai Electric Power Co., Inc.	Mihama Unit 2, Kansai Electric Power Co., Inc.	Genkai Unit 1, Kansai Electric Power Co., Inc.	Ohi Unit 2, Kansai Electric Power Co., Inc.	Tsuruga Unit 1, Japan Atomic Power Co.	Fukushima 1, Unit 3
Rod Number	full length Rod B15/N01G13, cut at 2015-2170 mm above bottom)	cut at 1832-1980 mm above the bottom	full length Rod C33/F10, cut at 2115-2237 mm above the bottom	full length,	full length Rod JAB73/B6, cut at ~1500 mm)	segmented rod D7-5 (5th segment)
Irradiation Dates	1982-1987	1978-1983	1975-1979	1985-1988	1972-1978	1984-1990
Average LHGR, kW/m	15.2	19.8	20.1	20.7		20.4
Burnup, MWd/kgM	50.4	38.9	42.0	39.2	26.6	45.3
Cladding Corrosion, μm	20-30	< 20; 41 ppm H ₂	< 20	< 20	not available	~15 max
Steady State Fission Gas Release, %	0.78% FGR (97.5% He)	0.15% FGR (99.3% He)	0.4% FGR (96.9% He)	< 1% (98.6% He)	19.7% FGR (18.1% He, 71.9% Xe, 8.6% Kr)	~8% FGR (79.9% He, 18.1% Xe, 2% Kr)
RIA Irradiation						
Data of RIA test	2/6/96	10/31/90	3/12/91	1/27/93	1/21/93	11/21/96
Fuel Length, mm	136.5 (15 pellets)	122 (8 pellets)	122 (8 pellets)	133 (14 pellets)	126.0 (6 pellets)	106 (10 pellets)
Pre-RIA Rod Length, mm	309.2	298.7	299.5	307	312	280.4

A.8

Table A.3 (contd)

Parameter	NSRR RIA Test					
	HBO-6	MH-3	GK-1	OI-2	TS-5	FK-1
Pre-RIA Rod Diameter, mm	9.444	10.656 min=10.643 max=10.690	10.666	9.467	14.3 nominal for mother rod	min=12.254 max=12.273
Fill Gas	He@0.1 MPa	He@4.6 MPa @0°C	He@4.7 MPa	He@0.1 MPa	1.1 MPa (72.0% Xe, 9.3% Kr, 18.7% He)	He@0.3 MPa
Energy Deposited, cal/g	90	87	114	139	117	125
Fuel Enthalpy, cal/g	85	67	93	108	98	130
Pulse Width, ms		4.5	4.6	4.4	4.8	
Coolant	stagnant water @20°C, 0.1 MPa	stagnant water @20°C, 0.1 MPa	stagnant water @20°C, 0.1 MPa	stagnant water @20°C, 0.1 MPa	stagnant water @20°C, 0.1 MPa	stagnant water @20°C, 0.1 MPa
RIA Results						
Peak Pellet Stack Elongation, mm	1.3	1.19	1.29	2.8	not measured	1.5
Peak Cladding Elongation, mm	not measured	1.12	1.16	2.8	0.55	1.1
Post- RIA Rod Length, mm	309.36	299.78	299.95	307.28	306.24	not measured?
Post- RIA Rod Diameter, mm	ave ~9.56	max=10.83	max~10.93	~9.77 (from plots)	min=14.25 max=14.33	12.2-12.4
Cladding Residual Hoop Strain, %	ave~1.2	max=1.6	~2.5	4.8	~0	0.9 ave 3.0 max
Cladding Residual Axial Strain, %	0.05	0.36	0.15	3.2	~0	not measured
Peak Gas Pressure Increase, MPa	1.7	0.2	1.93	2.3	1.5	1.6
Fission Gas Release	10% FGR (33.7% He, 51.9% Xe, 5.0% Kr, 8.0% H ₂)	3.8% FGR (94.8% He, 2.0% Xe, 0.2% Kr, 1.5% H ₂)	14% FGR (90.8% He, 7.4% Xe, 0.7% Kr, 0.4% H ₂)	12.0% FGR (19.8% He, 39.5% Xe, 4.3% Kr, 25.0% H ₂ , 5.1% N ₂)	8% FGR (18.7% He, 67.9% Xe, 9.7% Kr)	8.2% FGR (46.2% He, 35.1% Xe, 3.9% Kr, 10.4% H ₂ , 2.6% N ₂)
Peak Cladding Temperature, °C	162	200, DNB	310	380 @ 380 ms	170	360

A.9

Sources

Fuketa, T., et al. 1995. "Behavior of High Burnup PWR Fuel Under a Simulated RIA Condition in the NSRR," *Transient Behavior of High Burnup Fuel, Proceedings of the CSNI Specialist Meeting, Cadarache, France, 12-14 September 1995*. NEA/CSNI/R(95)22 [OCDE/GD(96)197].

Fuketa, T., et al. 1996. "NSRR/RIA Experiments with High-Burnup PWR Fuels," *Nuclear Safety*, Vol. 37, No. 4., October-December 1996, pg. 328-342.

Fuketa, T. et al. 1996. "New Results from the NSRR Experiments Reactor with High Burnup Fuel," in *Proceedings of Twenty-Third Water Reactor Safety Information Meeting*, NUREG/CP-0149, Volume 1, U.S. NUCLEAR REGULATORY COMMISSION, Washington, D.C.

Fuketa, T., et al. 1997. "NSRR/RIA Experiments with High Burnup PWR Fuels," in *Proceedings of 1997 International Topical Meeting on Light Water Reactor Fuel Performance*. March 1997, pp 669-676.

Fuketa, T., et al. 1999. "NSRR Pulse Irradiation Experiments and Tube Burst Tests," in *Proceedings of Twenty-Sixth Water Reactor Safety Information Meeting*, NUREG/CP-0166, Volume 3, U.S. NUCLEAR REGULATORY COMMISSION, Washington, D.C.

Fuketa, T., et al. 2000. "JAERI Research on Fuel Rod Behavior During Accident Conditions," in *Proceedings of Twenty-Seventh Water Reactor Safety Information Meeting*, NUREG/CP-0169, U.S. NUCLEAR REGULATORY COMMISSION, Washington, D.C.

Fuketa, T., T. Nakamura, and K. Ishigima. 1998. "The Status of the RIA Test Program in the NSRR," in *Proceedings of Twenty-Fifth Water Reactor Safety Information Meeting*, NUREG/CP-0162, Volume 2, U.S. NUCLEAR REGULATORY COMMISSION, Washington, D.C.

Ishihima, K., and T. Fuketa. 1997. "Progress of the RIA Experiments with High Burnup Fuels," in *Proceedings of Twenty-Fourth Water Reactor Safety Information Meeting*, NUREG/CP-0157, Volume 1, U.S. NUCLEAR REGULATORY COMMISSION, Washington, D.C.

Nakamura, T., et al. 1994. "Boiling Water Reactor Fuel Behavior at Burnup of 26 GWd/tonne Under Reactivity-Initiated Accident Conditions," *Nuclear Technology*, 108(1994)45-59.

Sasajima, H., et al. 1995. *Behavior of Irradiated PWR Fuel Under a Simulated RIA Condition (Results of NSRR Test MH-3)*. JAERI-Research 95-087, Japan Atomic Research Institute, Tokai-Mura, Japan.

A.2.1.1 HBO-6 (PWR 17x17)

The HBO-6 test rod was fabricated from a PWR 17x17 full-length commercial rod irradiated in the Ohi Unit 1 reactor operated by Kansai Electric Power Co., Inc. The commercial rod (Rod B15 of Assembly N01G13) was irradiated from 1981 to 1987. After the steady-state irradiation, post-irradiation characterization of the commercial rod was performed with examinations including visual and photography, profilometry, gamma scanning, X-radiography, eddy current, and rod puncture and gas analysis. The average linear heat rate during the 4-cycle commercial irradiation was 15.2 kW/m and the end-of-life fission gas release was 0.8% with a gas composition of 97.5% helium.

The commercial rod was sectioned from 2015 to 2170 mm above the bottom of the rod to fabricate test rod HBO-6. The fill gas for HBO-6 was helium at 1.1 MPa. Pre-RIA characterization was performed, including visual and photography, profilometry, gamma scanning, X-radiography, and eddy current. Key results of these characterization activities are provided in Table A.3. Cladding corrosion for the rod segment used for HBO-6 was 20 to 30 μm .

The HBO-6 test rod was instrumented with three cladding surface thermocouples (one of which failed early in the transient), fuel stack elongation, and fuel rod gas pressure. Examples of measured responses during the RIA transient are presented in Figures A.7 and A.8. Principal results from the in-reactor instrumentation are summarized in Table A.3. Maximum cladding surface temperature was 162°C, peak fuel elongation was 1.3 mm, and peak gas pressure increase was 1.7 MPa. Cladding elongation was not measured during the transient.

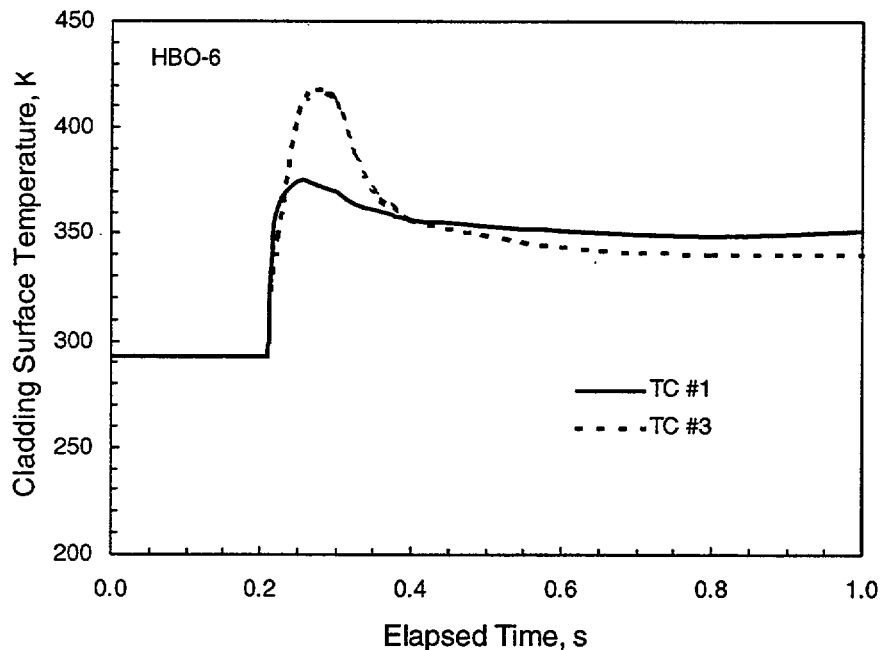


Figure A.7 Cladding Surface Temperature History for HBO-6, Thermocouples #1 and #3

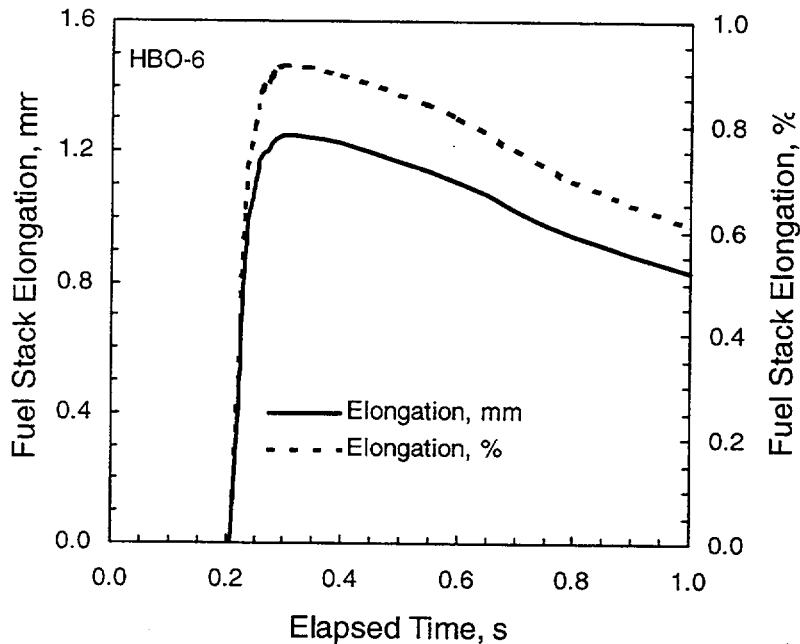


Figure A.8 Fuel Pellet Stack Elongation History for HBO-6

Post-RIA examinations of HBO-6 included: visual and photography, X-radiography, profilometry, gamma scanning, rod puncture and gas analysis, fuel density, cladding hardness, metallography, and electron probe microanalysis. The residual cladding diametral strain was 1.2% and the residual cladding length strain was 0.05%. The fission gas release during the RIA was determined to be 10% with a final gas mixture of 33.7% He, 51.9% Xe, 5.0% Kr, and 8.0% hydrogen.

A.2.1.2 MH-3 (PWR 14x14)

The MH-3 test rod was fabricated from a PWR 14x14 full-length commercial rod irradiated in the Mihama Unit 2 reactor operated by Kansai Electric Power Co., Inc. The commercial rod was irradiated from 1978 to 1983. After the steady-state irradiation, post-irradiation characterization of the commercial rod was performed with examinations including visual and photography, profilometry, gamma scanning, X-radiography, eddy current, and rod puncture and gas analysis. The average linear heat rate during the 4-cycle commercial irradiation was 19.8 kW/m to a rod-average burnup of 38.9 MWd/kgM and the end-of-life fission gas release with 0.15% with a gas composition of 99.3% helium.

The commercial rod was sectioned from 1832-1980 mm above the bottom of the rod to fabricate test rod MH-3. The fill gas for MH-3 was helium at 4.6 MPa. The burnup of MH-3 test rod was 38.9 MWd/kgM. Pre-RIA characterization was performed, including visual and photography, profilometry, gamma scanning, X-radiography, and eddy current. Key results of these characterization activities are provided in Table A.3. Cladding corrosion for the rod segment used for MH-3 was <20 μm .

The MH-3 test rod was instrumented with one cladding surface thermocouple (located at the fuel mid-plane), fuel stack elongation, cladding elongation, and fuel rod gas pressure. Examples of measured responses during the RIA transient are presented in Figures A.9 and A.10. Principal results from the in-reactor instrumentation are summarized in Table A.3. Maximum cladding surface temperature was 200°C with DNB indicated, peak fuel elongation was 1.19 mm, peak cladding elongation was 1.3 mm, and peak gas pressure increase was 0.2 MPa.

Post-RIA examinations of MH-3 included: visual and photography, X-radiography, profilometry, gamma scanning, rod puncture and gas analysis, fuel density, cladding hardness, metallography, and electron probe microanalysis. The residual cladding diametral strain was 1.6% and the residual cladding length strain was 0.36%. The fission gas release during the RIA was determined to be 3.8% with a final gas mixture of 94.8% He, 2.0% Xe, 0.2% Kr, and 1.5% hydrogen.

A.2.1.3 GK-1 (PWR 14x14)

The GK-1 test rod segment was fabricated from a PWR 14x14 full-length commercial rod irradiated in the Genkai Unit 1 reactor operated by Kansai Electric Power Co., Inc. The commercial rod (Rod C33/F10) was irradiated from 1975 to 1979. After the steady-state irradiation, post-irradiation characterization of the commercial rod was performed with examinations including visual and photography, profilometry, gamma scanning, X-radiography, eddy current, and rod puncture and gas analysis. The average linear heat rate during the 3-cycle commercial irradiation was 20.1 kW/m to a rod-average burnup of 42.0 MWd/kgM and an end-of-life fission gas release of 0.4% with a gas composition of 96.9% helium.

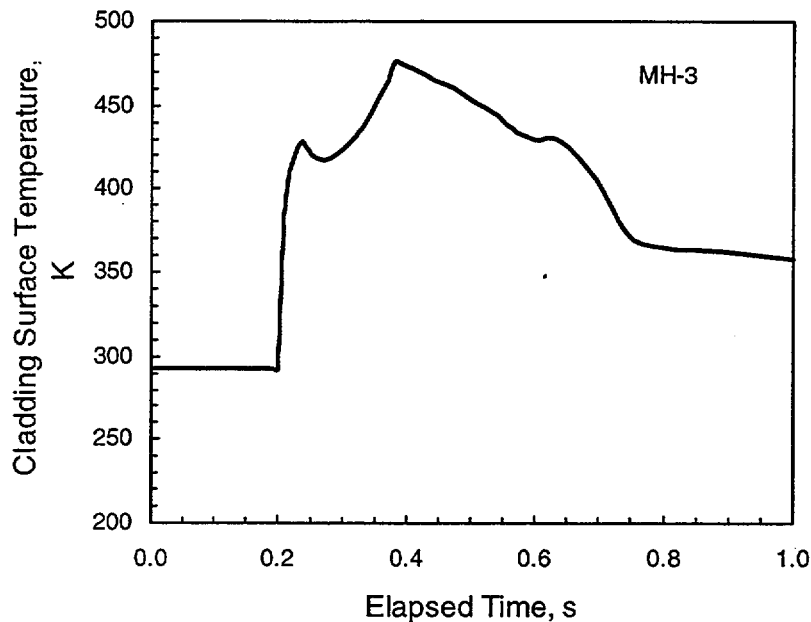


Figure A.9 Cladding Surface Temperature History for MH-3

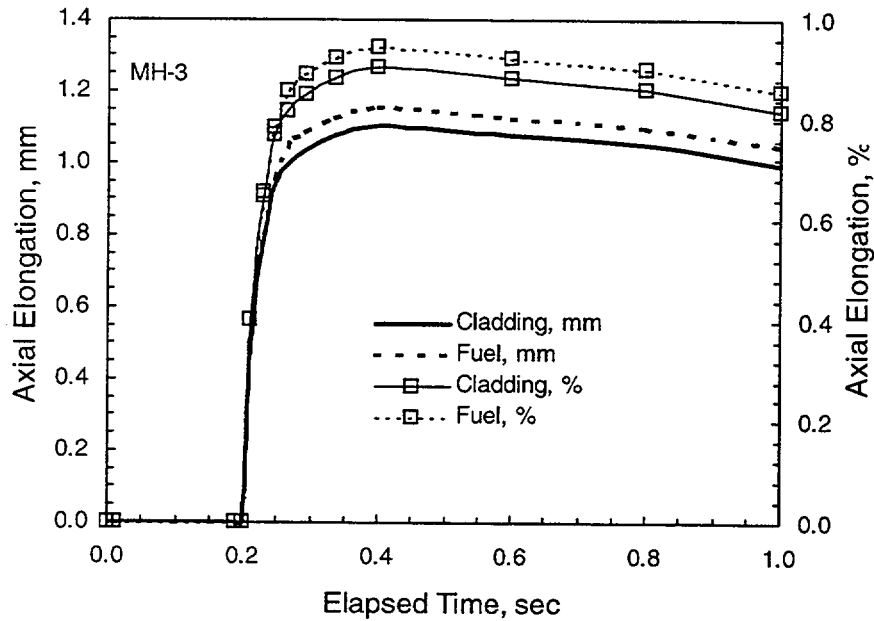


Figure A.10 Pellet Stack and Cladding Elongation History for MH-3

The commercial rod was sectioned from 2115-2237 mm above the bottom of the rod to fabricate test rod GK-1. The fill gas for GK-1 was helium at 4.7 MPa. The burnup of the GK-1 test rod was 42.1 MWd/kgM. Pre-RIA characterization was performed, including visual and photography, profilometry, gamma scanning, X-radiography, and eddy current. Key results of these characterization activities are provided in Table A.3. Cladding corrosion for the rod segment used for GK-1 was <math><20\ \mu\text{m}</math>.

The GK-1 test rod was instrumented with one cladding surface thermocouple (located at fuel mid-plane), fuel stack elongation, cladding elongation, and fuel rod gas pressure. Examples of measured responses during the RIA transient are presented in Figures A.11 through A.13. Principal results from the in-reactor instrumentation are summarized in Table A.3. Maximum cladding surface temperature was 310°C with DNB indicated, peak fuel elongation was 1.29 mm, peak cladding elongation was 1.16 mm, and peak gas pressure increase was 1.93 MPa.

Post-RIA examinations of GK-1 included: visual and photography, X-radiography, profilometry, gamma scanning, rod puncture and gas analysis, fuel density, cladding hardness, metallography, and electron probe microanalysis. The residual cladding diametral strain was approximately 2.5% and the residual cladding length strain was 0.15%. The fission gas release during the RIA transient was 14% with a final gas mixture of 90.8% He, 7.4% Xe, 0.7% Kr, and 0.4% hydrogen.

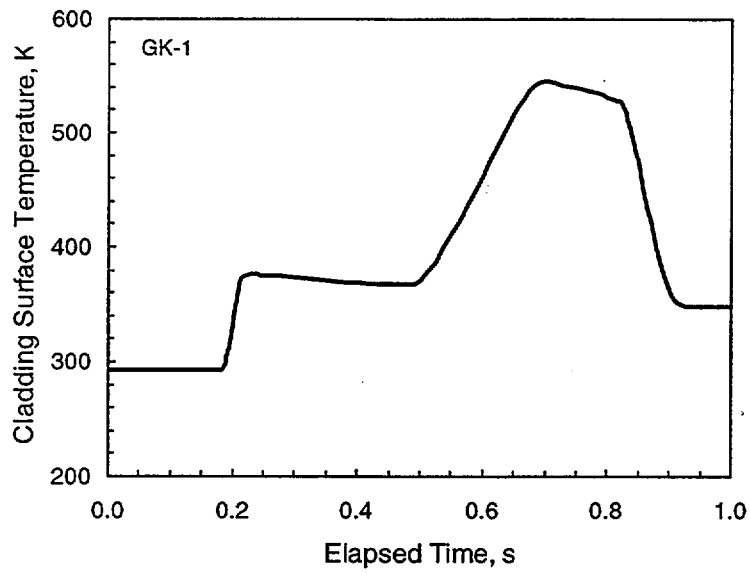


Figure A.11 Cladding Surface Temperature History for GK-1

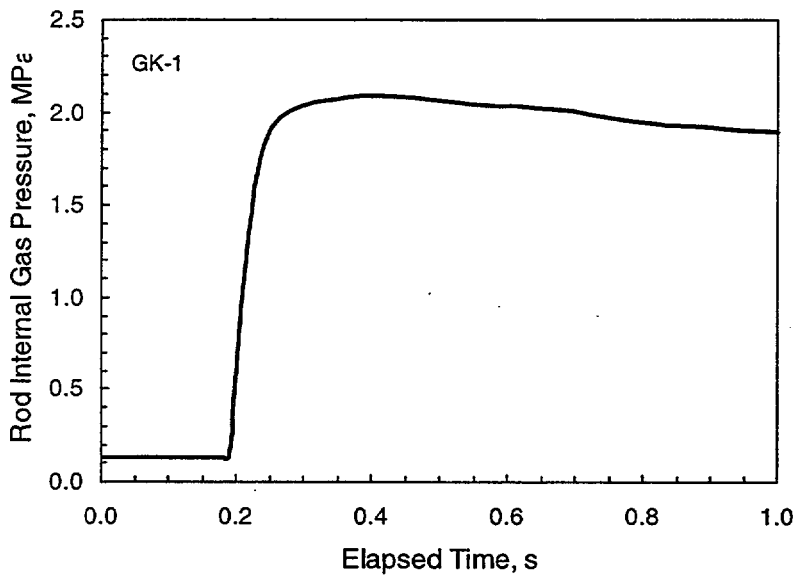


Figure A.12 Rod Internal Gas Pressure History for GK-1

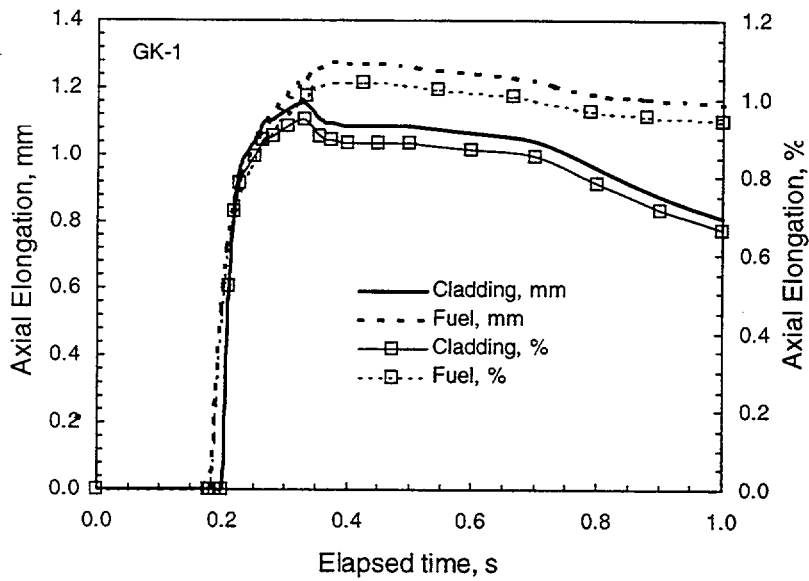


Figure A.13 Fuel and Cladding Axial Elongation History for GK-1

A.2.1.4 OI-2 (PWR 17x17)

The OI-2 test rod segment was fabricated from a PWR 17x17 full-length commercial rod irradiated in the Ohi Unit 2 reactor operated by Kansai Electric Power Co., Inc. The commercial rod (Rod J2R-I10) was irradiated from 1985 to 1988. After the steady-state irradiation, post-irradiation characterization of the commercial rod was performed with examinations including visual and photography, profilometry, gamma scanning, X-radiography, eddy current, and rod puncture and gas analysis. The average linear heat rate during the 2-cycle commercial irradiation was 20.7 kW/m to a rod-average burnup of 39.2 MWd/kgM and an end-of-life fission gas release of <1% with a gas composition of 98.6% helium.

The commercial rod was sectioned from 2115-2237 mm above the bottom of the rod to fabricate test rod OI-2. The fill gas for OI-2 was helium at 0.1 MPa. The burnup of the OI-2 test rod was 39.2 MWd/kgM. Pre-RIA characterization was performed, including visual and photography, profilometry, gamma scanning, X-radiography, and eddy current. Key results of these characterization activities are provided in Table A.3. Cladding corrosion for the rod segment used for OI-2 was <20 μm .

The OI-2 test rod was instrumented with one cladding surface thermocouple (located at the fuel mid-plane), fuel stack elongation, cladding elongation, and fuel rod gas pressure. Examples of measured responses during the RIA transient are presented in Figures A.14 through A.16. Principal results from the in-reactor instrumentation are summarized in Table A.3. Maximum cladding surface temperature was 380°C with DNB indicated, peak fuel elongation was 2.9 mm, peak cladding elongation was 2.8 mm, and peak gas pressure increase was 2.3 MPa.

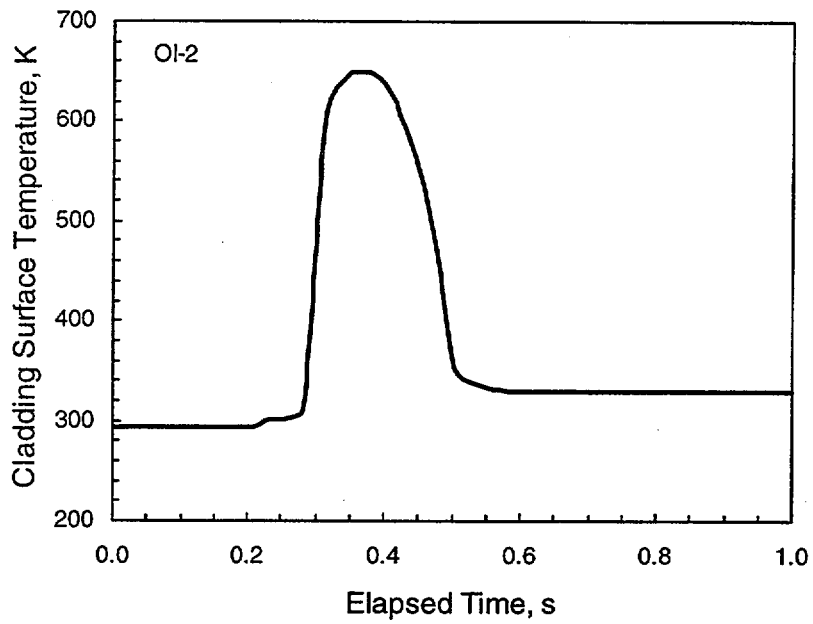


Figure A.14 Cladding Surface Temperature History for OI-2

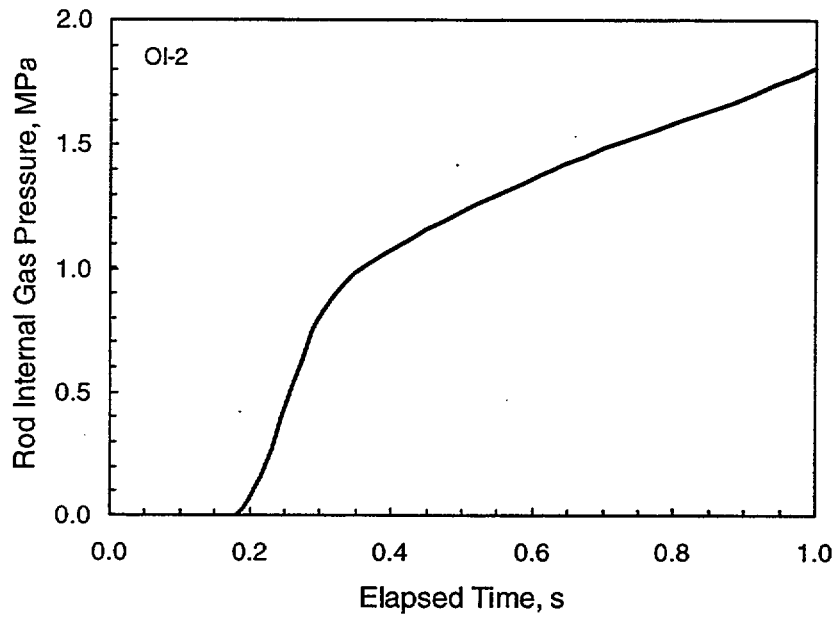


Figure A.15 Rod Internal Gas Pressure History for OI-2

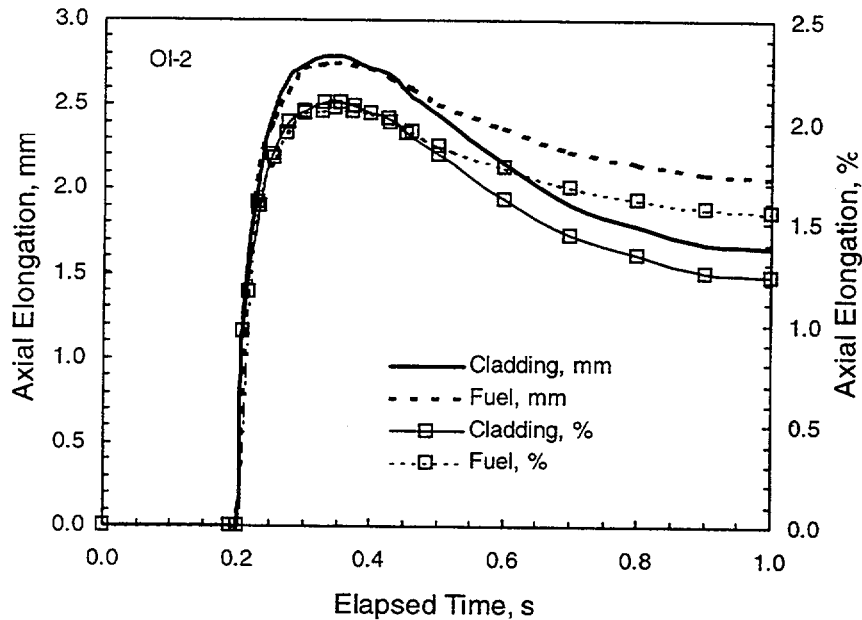


Figure A.16 Fuel and Cladding Elongation History for OI-2

Post-RIA examinations of OI-2 included: visual and photography, X-radiography, profilometry, gamma scanning, rod puncture and gas analysis, fuel density, cladding hardness, metallography, and electron probe microanalysis. The residual cladding diametral strain was approximately 5% and the residual cladding length strain was 3.2%. The fission gas release during the RIA transient was 12% with a final gas mixture of 19.8% He, 39.5% Xe, 4.1% Kr, 25.0% hydrogen, and 5.1% nitrogen.

A.2.1.5 TS-5 (BWR 7x7)

The TS-5 test rod segment was fabricated from a BWR 7x7 full-length commercial rod irradiated in the Tsuruga Unit 1 reactor operated by Japan Atomic Power Co. The commercial rod (Rod JAB73/B6) was irradiated from 1972 to 1978. After the steady-state irradiation, post-irradiation characterization of the commercial rod was performed with examinations including visual and photography, profilometry, gamma scanning, X-radiography, eddy current, and rod puncture and gas analysis. The average linear heat rate during the 6-cycle commercial irradiation was 20.7 kW/m to a rod-average burnup of 26.6 MWd/kgM and an end-of-life fission gas release of 19.7% with a gas composition of 18.1% He, 71.9% Xe, and 8.6% Kr.

The commercial rod was sectioned from approximately 2260 to 2425 mm above the bottom of the rod to fabricate test rod TS-5. The fill gas for TS-5 was 18.7% He, 72% Xe, and 9.3% Kr at 1.1 MPa to simulate the end of steady-state condition. The burnup of the TS-5 test rod was 26.6 MWd/kgM. Pre-RIA characterization was performed, including visual and photography, profilometry, gamma scanning, X-radiography, and eddy current. Key results of these characterization activities are provided in Table A.3. Cladding corrosion for the rod section used for TS-5 was not available.

The TS-5 test rod was instrumented with five cladding surface thermocouples (two at 32 mm below the fuel mid-plane, one at the fuel mid-plane, and two at 32 mm above the fuel mid-plane), cladding elongation, and fuel rod gas pressure. Examples of measured responses during the RIA transient are presented in Figures A.17 through A.19. Principal results from the in-reactor instrumentation are summarized in Table A.3. Maximum cladding surface temperature was 170°C, peak cladding elongation was 0.55 mm, and peak gas pressure increase was 1.5 MPa.

Post-RIA examinations of TS-5 included: visual and photography, X-radiography, profilometry, gamma scanning, rod puncture and gas analysis, fuel density, cladding hardness, metallography, and electron probe microanalysis. The residual cladding diametral strain was approximately 0% and the residual cladding length strain was 0%. The fission gas release during the RIA transient was 8% with a final gas mixture of 18.7% He, 67.9% Xe, 9.7% Kr, and 2.9% hydrogen.

A.2.1.6 FK-1 (BWR 8x8)

The FK-1 test rod was fabricated from a six-segment BWR 8x8 rod irradiated in the First Fukushima plant unit 3 reactor of Tokyo Electric Power Company, Inc. (TEPCO). The commercial rod (Rod D7-5) was irradiated from 1984 to 1990. After the steady-state irradiation, post-irradiation characterization of the commercial rod was performed with examinations including visual and photography, profilometry, gamma scanning, X-radiography, eddy current, and rod puncture and gas analysis. The average linear heat rate during the 5-cycle commercial irradiation was 20.4 kW/m to a rod-average burnup of 45.3 MWd/kgM and an end-of-life fission gas release of 8% with a gas composition of 79.9% He, 18.1% Xe, and 2.0% Kr.

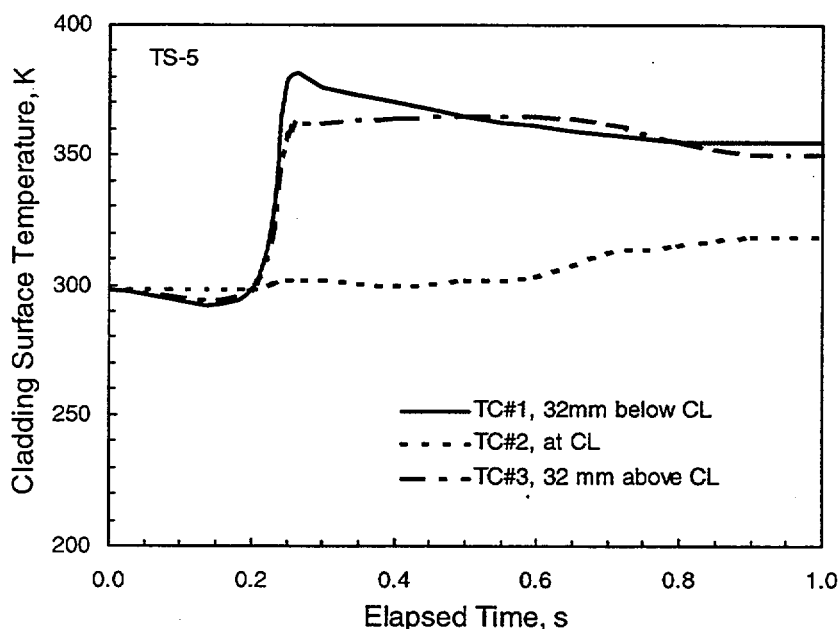


Figure A.17 Cladding Temperature History for TS-5

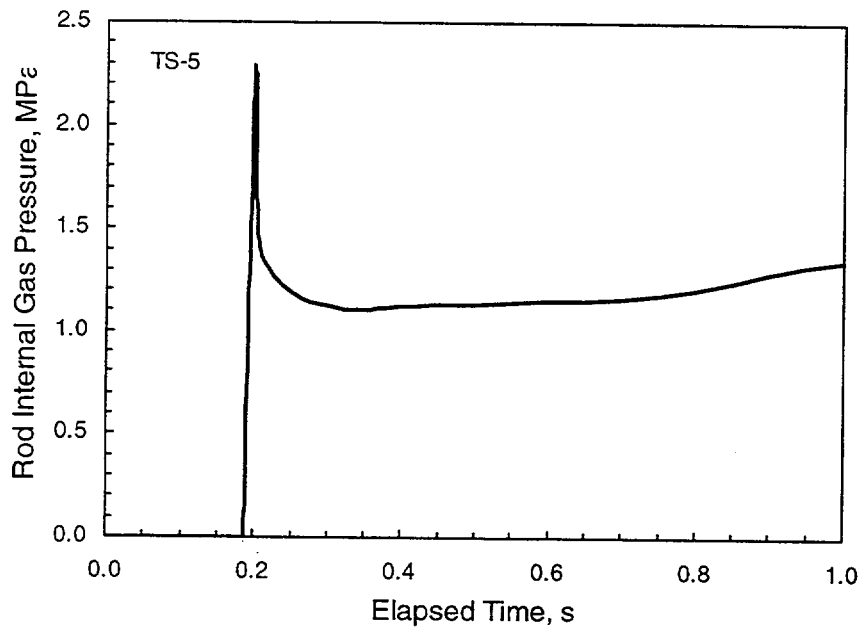


Figure A.18 Rod Internal Gas Pressure History for TS-5

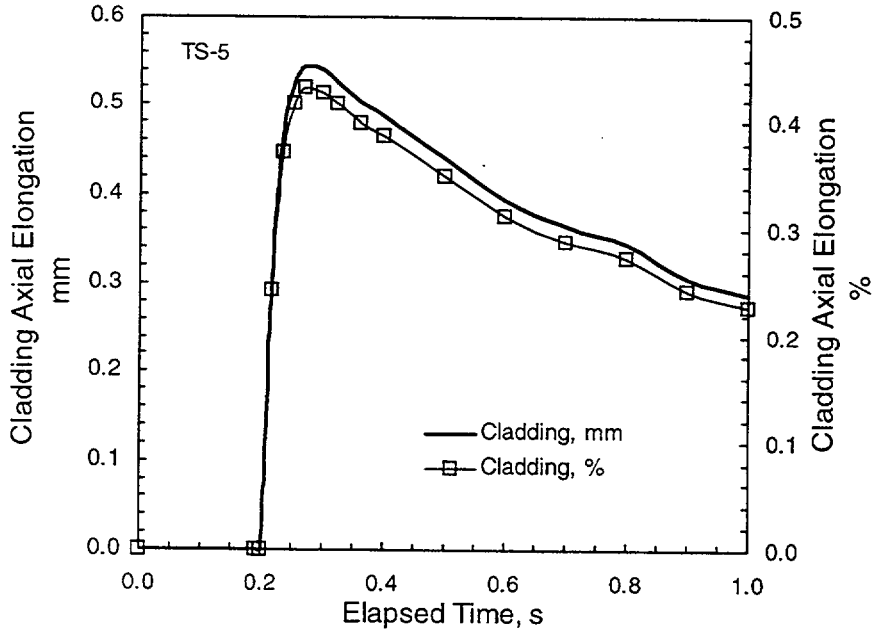


Figure A.19 Cladding Elongation History for TS-5

Test rod FK-1 was fabricated from the fifth segment (from the bottom) of the commercial rod (approximately 2000 mm above the bottom of the commercial rod). The fill gas for FK-1 was helium at 0.3 MPa. The burnup of the FK-1 test rod was 45.3 MWd/kgM. Pre-RIA characterization was performed, including visual and photography, profilometry, gamma scanning, X-radiography, and eddy current. Key results of these characterization activities are provided in Table A.3. Cladding corrosion for the rod segment used for TS-5 was 20 μm .

The FK-1 test rod was instrumented with three cladding surface thermocouples (one at 32 mm below the fuel mid-plane, one at the fuel mid-plane, and one at 32 mm above the fuel mid-plane), fuel stack elongation, cladding elongation, and fuel rod gas pressure. Examples of measured responses during the RIA transient are presented in Figures A.20 through A.22. Principal results from the in-reactor instrumentation are summarized in Table A.3. Maximum cladding surface temperature was 360°C, peak fuel elongation was 1.5 mm, peak cladding elongation was 1.1 mm, and peak gas pressure increase was 1.6 MPa.

Post-RIA examinations of FK-1 included: visual and photography, X-radiography, profilometry, gamma scanning, rod puncture and gas analysis, fuel density, cladding hardness, metallography, and electron probe microanalysis. The residual cladding diametral strain was approximately 0.9% (average) and the residual cladding length strain was not measured (no pre-RIA rod length measurement). The fission gas release during the RIA transient was 8.2% with a final gas mixture of 46.2% He, 35.1% Xe, 3.9% Kr, 10.4% hydrogen, and 2.6% nitrogen.

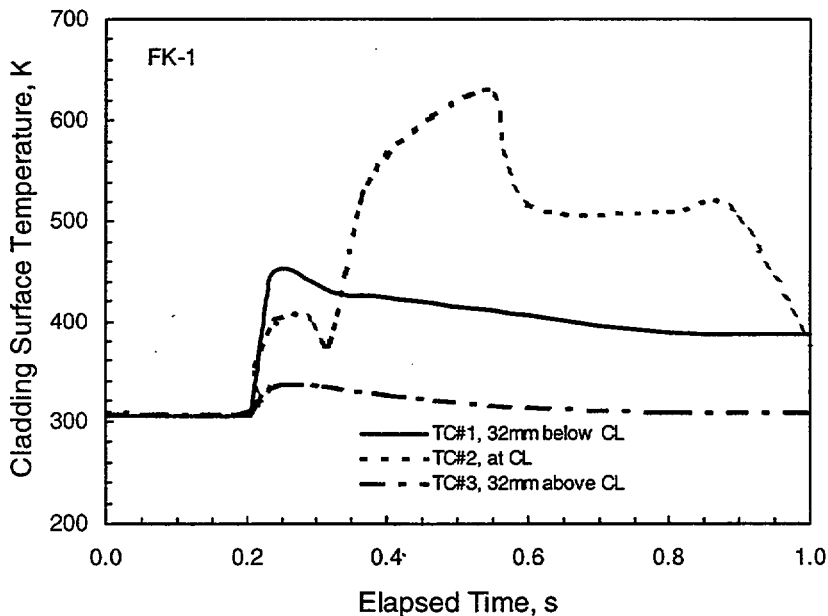


Figure A.20 Cladding Temperature History for FK-1

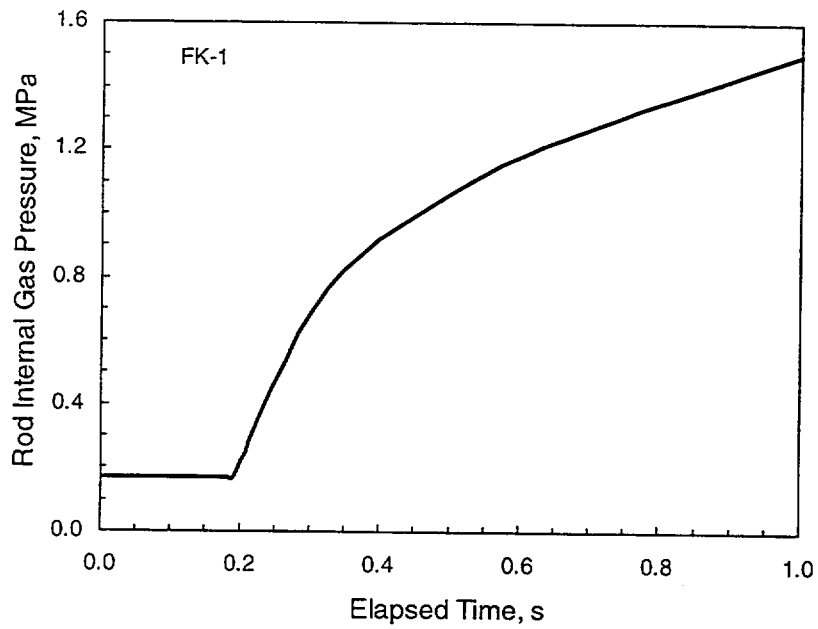


Figure A.21 Rod Internal Gas Pressure History for FK-1

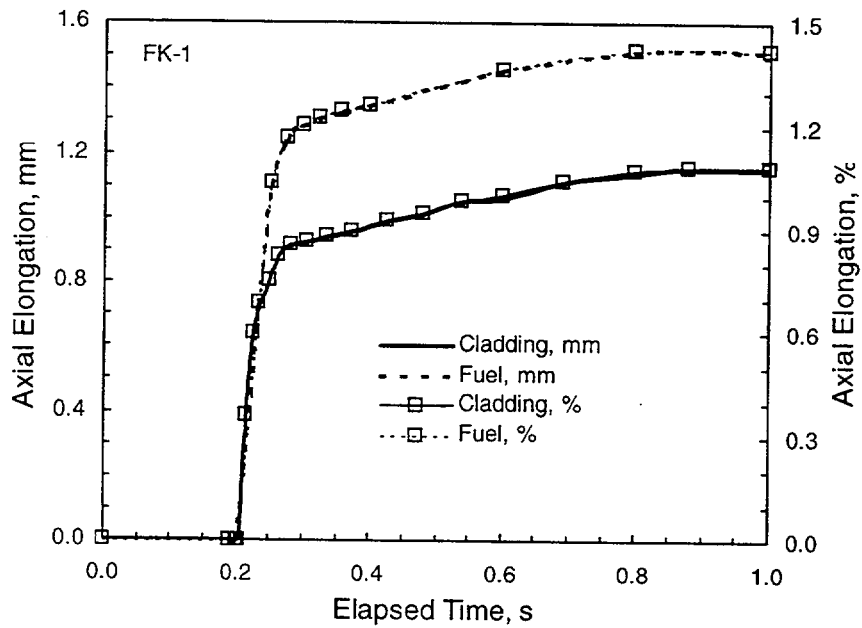


Figure A.22 Fuel and Cladding Elongation History for FK-1

A.2.2 CABRI, IPSN/EDF

In response to increasing burnup levels, the Institute for Protection and Nuclear Safety (IPSN) initiated studies on fuel response during RIAs. The program was initiated using the CABRI test reactor and is testing a variety of commercial LWR and mixed-oxide fuels. The experimental work focuses on pellet-cladding mechanical interaction during the first phase of a power transient when cladding-coolant heat transfer has a minor effect.

The CABRI reactor consists of a driver core in a water pool. The reactor core houses a central flowing sodium loop for experimental testing of fuel rods. The RIA experiments consist primarily of fast pulses (<10 ms half-width). The test rods selected for the FRAPTRAN assessment cases were fabricated from commercially irradiated PWR fuel rods and did not fail during the RIA pulses. Test rods REP-Na4 and REP-Na5 were from the same commercial rod, but had different oxidation levels and different RIA power histories.

Typical instrumentation for a RIA test includes loop flowrate measurements using inlet and outlet flowmeters; test loop pressure from strain gauges located near the top and bottom of the test section; sodium coolant temperature using thermocouples; microphones for detecting acoustic events associated with the testing; and a cladding elongation transducer for the test rod. The test rods were not instrumented for either internal gas pressure or fuel axial elongation.

Summary results of the three CABRI RIA tests used for the FRAPTRAN assessment are provided in Table A.4. Because of the variety of cladding oxidation levels and RIA test conditions, the test rod responses (such as permanent diametral strain) varied from test to test. Measured in-reactor elongation data are relative to the pre-transient temperature of 280°C. Each test is individually presented in the following.

Sources

Anselmet-Vitiello, M. C., et al. 1995. "The Experimental Test Programme for the Study of High Burnup PWR Rods Under RIA Conditions in the CABRI Core," *Transient Behavior of High Burnup Fuel, Proceedings of the CSNI Specialist Meeting, Cadarache, France, 12-14 September 1995*. NEA/CSNI/R(95)22 [OCDE/GD(96)197].

Frizonnet, J. M., et al. 1997. "The Main Outcomes from the Interpretation of the CABRI REP-Na Experiments for RIA Study," in *Proceedings of 1997 International Topical Meeting on Light Water Reactor Fuel Performance*. American Nuclear Society, pp. 685-692.

Papin, J., et al. 1996. "French Studies on High-Burnup Fuel Transient Behavior Under RIA Conditions," *Nuclear Safety*, Vol. 37, No. 4., October-December 1996, pg. 289-327.

Table A.4 Summary of CABRI RIA Test Rod Parameters			
Parameter	CABRI RIA Test		
	REP-Na3	REP-Na4	REP-Na5
Rod Type	PWR	PWR	PWR
Basic Design			
Cladding Type	improved (low tin)	standard Zry	standard Zry
Clad OD, mm	9.508	9.508	9.508
Clad Wall Thickness, mm	0.576	0.575	0.575
Fuel OD, mm	8.192	8.193	8.193
Fuel Length, mm	440	3661	3661
Rod Length, mm			
Fill Gas	He@25 bar air@1 bar	He@25 bar air@1 bar	He@25 bar air@1 bar
Fuel Enrichment, %U-235	4.5	4.5	4.5
Fuel Density, %	95.25	94.75	94.75
SS Irradiation			
Reactor	Gravelines 5	Gravelines 3	Gravelines 3
Rod Number	EDF/segmented, J12 n°5009, Gravelines 5 grid levels 5/6 (span 5)	EDF/Fabrice GRAV 5c, rod 1065, grid levels 5/6 (span 5)	EDF/Fabrice GRAV 5c, rod 1065, grid levels 2/3 (span 2)
Average LHGR, kW/m	19.0 rod-average	19.0 rod-average	19.0 rod-average
Burnup, MWd/kgM	52.8	62.3	64.3
Cladding Corrosion, μm	40	80, no spalling	20
Steady-State Fission Gas Release (calculated), %	1.48	1.84	1.84
RIA Irradiation			
Date of RIA test	10/6/94	7/28/95	5/5/95
Fuel Length, mm	440.4	567.6	563.5
Pre-RIA Rod Length, mm	560	660.1	659.2
Pre-RIA Rod Diameter, mm	9.49	9.52	9.47
Fill Gas	He@0.3 MPa	He@0.3 MPa	He@0.3 MPa
Energy Deposited at peak power, cal/g	120@0.4s	97@1.2s	105@0.4s
Fuel Enthalpy, cal/g	125	99	115
Pulse Height, kW/m	30255	3557	29380
Pulse Width, ms	9.5	64	9
Coolant	flowing sodium @ 280°C, 0.5 MPa	flowing sodium @ 280°C, 0.5 MPa	flowing sodium @ 280°C, 0.5 MPa
RIA Results			
Peak Pellet Stack Elongation, mm	4 (hodoscope)	4 (hodoscope)	2 (hodoscope)
Peak Cladding Elongation, mm	6	4	6.5
Post-RIA Rod Length, mm			not measured?
Post-RIA Rod Diameter, mm	9.68	9.56	9.58
Cladding Residual Hoop Strain, %	2.0	0.4	1.1
Cladding Residual Axial Strain	3.5 mm = 0.8%	0.4 mm = 0.07%	2 mm = 0.35%
Post-RIA Oxide, μm	unchanged	unchanged	unchanged
Peak Gas Pressure Increase, MPa	not measured	not measured	not measured
Fission Gas Release	13.7% FGR	8.3% FGR	15.1% FGR
Peak Cladding Temperature, °C	not measured	not measured	not measured

Papin, J., and F. Schmitz. 1998. "The Status of the CABRI REP-Na Test Programme: Present Understanding and Still Pending Questions," in Proceedings of *Twenty-Fifth Water Reactor Safety Information Meeting*, NUREG/CP-0162, Volume 2. U.S. NUCLEAR REGULATORY COMMISSION, Washington, D.C.

Papin, J., and F. Schmitz. 2000. "Further Results and Analysis of MOX Fuel Behavior Under Reactivity Accident Conditions in CABRI," in Proceedings of *Twenty-Seventh Water Reactor Safety Information Meeting*, NUREG/CP-0169. U.S. NUCLEAR REGULATORY COMMISSION, Washington, D.C.

Schmitz, F., et al. 1996. "New Results from the Pulse Tests in the CABRI Reactor," in Proceedings of *Twenty-Third Water Reactor Safety Information Meeting*, NUREG/CP-0149, Volume 1. U.S. NUCLEAR REGULATORY COMMISSION, Washington, D.C.

Schmitz, F., C. Gonner, and J. Papin. 1997. "The Status of the CABRI Test Program: Recent Results and Future Activities," in Proceedings of *Twenty-Fourth Water Reactor Safety Information Meeting*, NUREG/CP-0157, Volume 1. U.S. NUCLEAR REGULATORY COMMISSION, Washington, D.C.

Schmitz, F., and J. Papin. 1999. "REP-Na 10, Another RIA Test with a Spalled High Burnup Rod and a Pulse Width of 30 ms," in Proceedings of *Twenty-Sixth Water Reactor Safety Information Meeting*, NUREG/CP-0166, Volume 3. U.S. NUCLEAR REGULATORY COMMISSION, Washington, D.C.

A.2.2.1 REP-Na3

The REP-Na3 test rod is a segmented rod that made a portion of a full-length rod irradiated in the Gravelines 5 reactor operated by Electricite de France (EdF). The commercial rod (J12 n°5009) was irradiated for four cycles, in a load-following mode, to a rod-average burnup of 52.8 MWd/kgM at an average linear heat rate of approximately 19 kW/m. The segment was irradiated in span 5. After the steady-state irradiation, the primary post-irradiation characterization of the segment was profilometry and oxide thickness. Calculated steady-state fission gas release for the rod segment was 1.9%.

The REP-Na3 test rod was instrumented only for cladding elongation. The measured cladding elongation during the RIA is presented in Figure A.23, and principal results are summarized in Table A.4. Maximum cladding elongation during the RIA was measured to be 6 mm.

Post-RIA examinations of REP-Na3 included profilometry, rod puncture and fission gas release analysis, and metallography. The residual cladding diametral strain was 2.0% and the residual length strain was 3 mm. The fission gas release was 13.7%.

A.2.2.2 REP-Na4

The REP-Na4 test rod was fabricated from a PWR full-length commercial rod irradiated in the Gravelines 5 reactor operated by Edf. The commercial rod (rod No. 1065) was irradiated for 5 cycles to a rod-average burnup of 63 MWd/kgM at an average linear heat rate of 19.0. The REP-Na4 section was taken

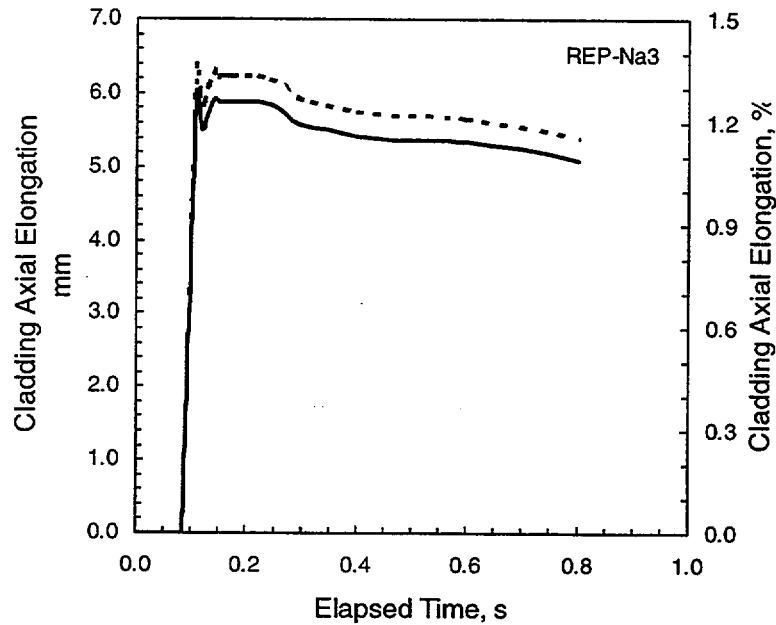


Figure A.23 Cladding Elongation History for REP-Na3

from span 5. After the steady-state irradiation, post-irradiation characterization of the mother rod was performed with examinations including profilometry and oxide thickness. Measured fission gas release for the mother rod was 1.8%.

The REP-Na4 test rod was instrumented only for cladding elongation. Unlike the other RIA cases used for the assessment of FRAPTRAN, the RIA power history for REP-Na4 resulted in a lower, double peak, as illustrated in Figure A.24, because of the approach taken to widen the pulse; total energy was similar to other RIAs. The measured cladding elongation history is presented in Figure A.25, and principal results are summarized in Table A.4. Maximum cladding elongation during the RIA was measured to be 4 mm.

Post-RIA examinations of REP-Na4 included profilometry, rod puncture and fission gas release analysis, and metallography. The residual cladding length strain was 0.4 mm and residual cladding diametral strain was about 0.4%. The fission gas release was 8.1%.

A.2.2.3 REP-Na5

The REP-Na5 test rod was fabricated from a PWR full-length commercial rod irradiated in the Gravelines 5 reactor operated by Edf. The commercial rod (rod No. 1065) was irradiated for 5 cycles to a rod-average burnup of 63 MWd/kgM at an average linear heat rate of 19 kW/m. The REP-Na5 section was taken from span 2. After the steady-state irradiation, post-irradiation characterization of the mother rod was performed with examinations including profilometry and oxide thickness. Measured fission gas release for the mother rod was 1.8%.

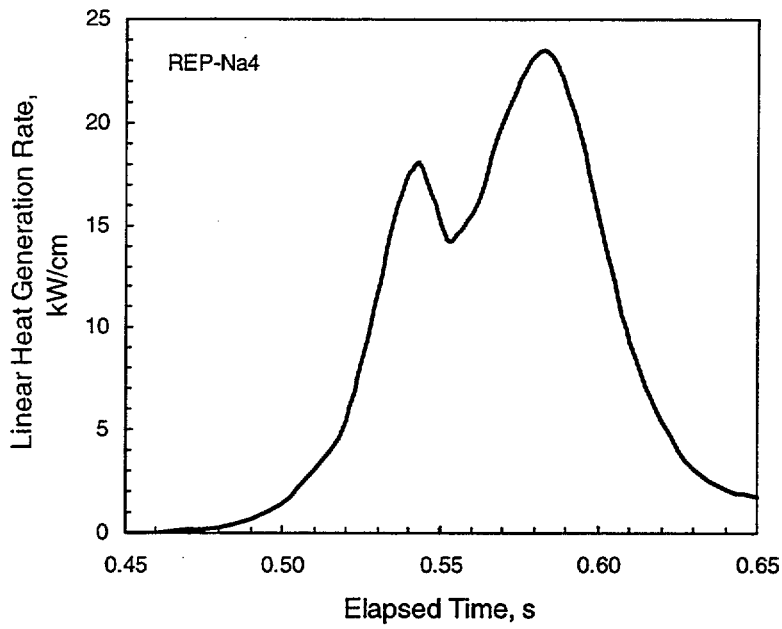


Figure A.24 Double Peak Power History for REP-Na4

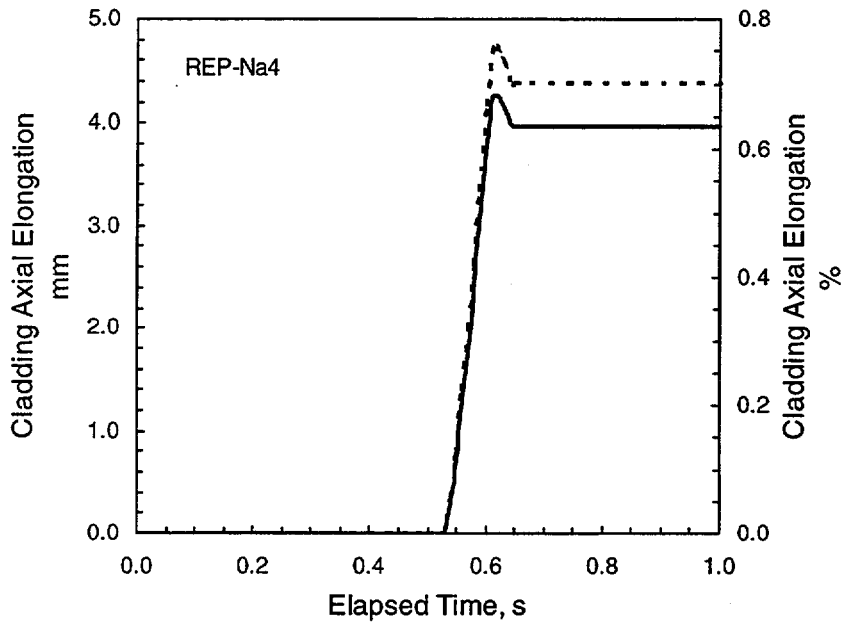


Figure A.25 Cladding Elongation History for REP-Na4

The REP-Na5 test rod was taken from the same mother rod as REP-Na4. Compared to REP-Na4, REP-Na5 had a more typical test reactor power history for an RIA; i.e., a very short pulse. The cladding oxidation for REP-Na5 was much lower than for REP-Na4 (20 μm versus 80 μm). The test rod was instrumented only for cladding elongation. Measured cladding elongation for REP-Na5 is presented in Figure A.26, and principal results are summarized in Table A.4. Maximum cladding elongation during the RIA was measured to be 6 mm.

Post-RIA examinations of REP-Na5 included profilometry, rod puncture and fission gas release, and metallography. The residual cladding length strain was 2 mm and residual cladding diametral strain was about 1.1%. The fission gas release was 15.1%.

A.2.3 IGR, RRC-KI, H5T

The Nuclear Safety Institute of Russian Research Centre “Kurchatov Institute” (RRC-KI) has tested commercial VVER-1000 fuel rods in the Impulse Graphite Reactor (IGR) for comparative studies of the behavior of preirradiated and unirradiated fuel rods under conditions of simulating RIAs. The objectives of the tests included determining the failure threshold for VVER-1000 fuel rods as a function of burnup and determination of failure mechanisms as a function of the test parameters. A total of 23 test rods were subjected to RIA conditions. The test rod selected for the FRAPTRAN assessment was H5T; this rod was refabricated from an irradiated VVER-1000 rod and pulsed in a stagnant water capsule.

The IGR is a pulse uranium-graphite self-quenching reactor of the thermo-capacity type. The core consists of graphite blocks impregnated with uranium salt. The core is located in a leak-tight reactor

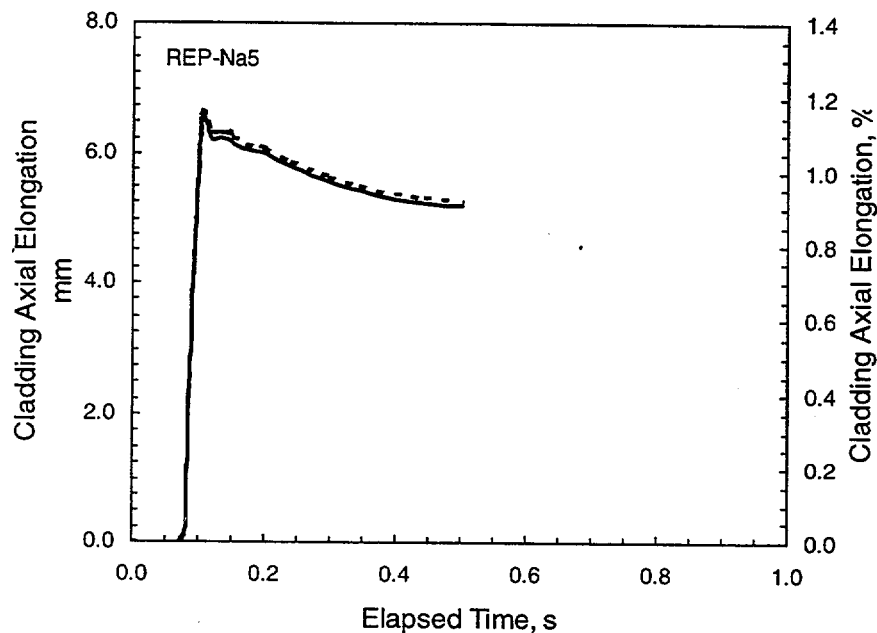


Figure A.26 Cladding Elongation History for REP-Na5

vessel filled with helium. The reactor vessel with the core is located in a water-filled tank. Heat generated during reactor operation is accumulated in the reactor core and then gradually transferred to the coolant circulating in the water tank.

The H5T test rod was refabricated from VVER-1000 rod number 317 irradiated in power unit No. 5 of the NovoVoronezh nuclear power plant. The commercial rod had a rod-average burnup of 49 MWd/kgU after being irradiated for three cycles. Pre-RIA characteristics of H5T are provided in Table A.5.

Rod H5T was tested along with Rod H5C in a stagnant water-filled capsule (the capsules were designed to irradiate two rods at a time) with a small air volume at the top of the capsule. No instrumentation was provided for the rods or the capsules, thus there are no time-dependent fuel behavior data. Total energy deposition for H5T was 237 cal/g at 7 seconds with a peak width of 800 msec; the power history is illustrated in Figure A.27. Rod H5T failed during the RIA test.

Post RIA examinations consisted of visual, X-radiography of intact rods (not H5T), outer diameter of intact rods (but not axial profilometry), metallography, oxide thickness, and rod puncture and fission gas analysis for intact rods.

Sources

Data Base on the Behavior of High Burnup Fuel Rods with Zr-1%Nb Cladding and UO₂ Fuel (VVER Type) Under Reactivity Accident Conditions, NUREG/IA-0156, Volumes 1-3, July 1999. U.S. Nuclear Regulatory Commission, Washington, D.C.

Volume 1: *Review of Research Program and Analysis of Results*

Volume 2: *Description of Test Procedures and Analytical Methods*

Volume 3: *Test and Calculation Results*

Asmolov, V., et al. 2000. "Summary of Results on the Behavior of VVER High Burnup Fuel Rods Tested Under Wide and Narrow Pulse RIA Conditions," in *Proceedings of Twenty-Seventh Water Reactor Safety Information Meeting*, NUREG/CP-0169. U.S. NUCLEAR REGULATORY COMMISSION, Washington, D.C.

Asmolov, V., and L. Yegorova. 1997. "Investigation of the Behavior of VVER Fuel Under RIA Conditions," in *Proceedings of 1997 International Topical Meeting on Light Water Reactor Fuel Performance*. pg. 704-710.

Asmolov, V., and L. Yegorova. 1996. "The Russian RIA Research Program: Motivation, Definition, Execution, and Results," *Nuclear Safety*, Vol. 37, No. 4., October-December 1996, pg. 343-371.

Asmolov, V., and L. Yegorova. 1996. "Recent View to the Results of Pulse Tests in the IGR Reactor with High Burnup Fuel," in *Proceedings of Twenty-Third Water Reactor Safety Information Meeting*, NUREG/CP-0149, Volume 1. U.S. NUCLEAR REGULATORY COMMISSION, Washington, D.C.

Table A.5 Summary of IGR H5T Test Rod Parameters	
Parameter	IGR RIA Test H5T
Rod Type	VVER-1000
Basic Design	
Cladding Type	Zr-1%Nb
Clad OD, mm	9.1
Clad Wall Thickness, mm	0.690
Fuel OD, mm	7.55 annulus of 2.4 mm diameter
Fuel Length, mm	3530
Rod Length, mm	3837
Fill Gas	He@2.0-2.5 MPa
Fuel Enrichment, %U-235	3.58
Fuel Density, %	96.6 BOL/94.1 EOL
SS Irradiation	
Reactor	NovoVoronezh Nuclear Power Plant, Unit 5
Rod Number	Rod 317, assembly 1114 @2550-2700 mm from bottom
Irradiation Dates	6/1984-6/1987
Average LHGR, kW/m	
Burnup, MWd/kgM	49.0
Cladding Corrosion, μm	5, 30-80 ppm H_2
Steady-State Fission Gas Release, %	EOL = 94-99% He
RIA Irradiation	
Data of RIA test	
Fuel Length, mm	156.0
Fuel OD, mm	7.60 radial gap = 30 μm
Pre-RIA Rod Length, mm	300
Pre-RIA Rod Diameter, mm	9.08
Fill Gas	He@1.7 MPa
Energy Deposited, cal/g	237 at 7s
Fuel Enthalpy, cal/g	176
Pulse Height	117 kW/m derived from energy deposition
Pulse Width, ms	800 time of peak = 3.35s
Coolant	stagnant water @ 20°C, 0.1 MPa
RIA Results	
Peak Pellet Stack Elongation, mm	not measured
Peak Cladding Elongation, mm	not measured
Post-RIA Rod Length, mm	not measured?
Post-RIA Rod Diameter, mm	not reported
Cladding Residual Hoop Strain, %	6.5% at failure site 3.1% away from failure site
Cladding Residual Axial Strain, %	not measured
Post-RIA Oxide, μm	8-17
Peak Gas Pressure Increase, MPa	not measured
Fission Gas Release, %	rod failed
Peak Cladding Temperature, °C	not measured

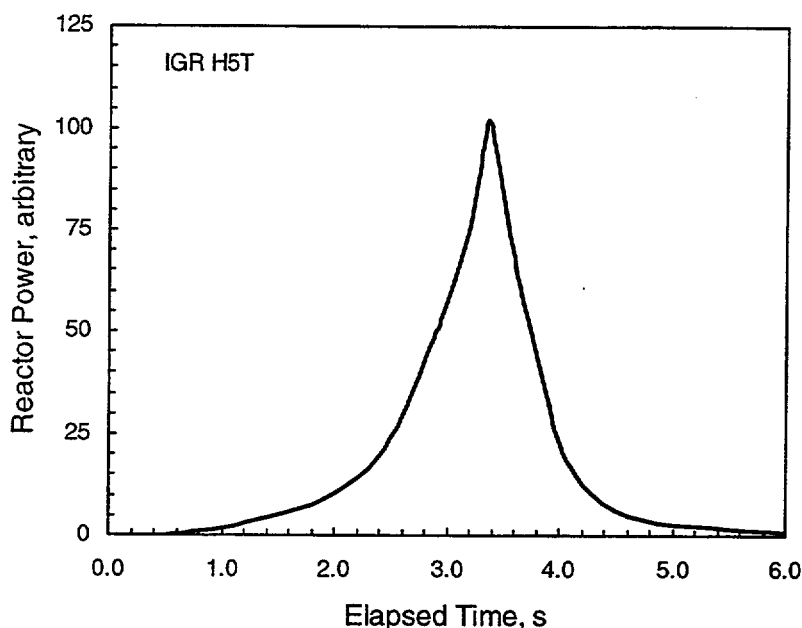


Figure A.27 Power History for IGR H5T

Asmolov, V., and L. Yegorova. 1997. "Recent Results on the RIA Tests in the IGR Reactor," in *Proceedings of Twenty-Fourth Water Reactor Safety Information Meeting*, NUREG/CP-0157, Volume 1. October 1996. U.S. NUCLEAR REGULATORY COMMISSION, Washington, D.C.

Smirnov, V., et al. 1999. "Zr-1%Nb (VVER) High Burnup Fuel Tests Under Transient and Accident Conditions," in *Proceedings of Twenty-Sixth Water Reactor Safety Information Meeting*, NUREG/CP-0166, Volume 3. U.S. NUCLEAR REGULATORY COMMISSION, Washington, D.C.

A.3 Loss-Of-Coolant-Accident (LOCA) Test Cases

A.3.1 Tests Conducted in the NRU

The U.S. Nuclear Regulatory Commission (NRC) conducted a series of thermal-hydraulic and cladding mechanical deformation tests in the National Research Universal (NRU) reactor at the Chalk River National Laboratory in Canada. The objective of these tests was to perform simulated LOCA experiments using full-length light-water reactor fuel rods to study mechanical deformation, flow blockage, and coolability. Three phases of a LOCA (i.e., heatup, reflood, and quench) were performed in situ using nuclear fissioning to simulate the low-level decay power during a LOCA after shutdown. Three materials tests, MT-1, MT-4, and MT-6A, were selected for the assessment of FRAPTRAN. All tests used PWR-type, nonirradiated fuel rods.

The NRU reactor is a heterogeneous, thermal, tank-type research reactor. It has a power level of 135 MWth and is heavy-water moderated and cooled. The coolant has an inlet temperature of 37°C at a pressure of 0.65 MPa. The MT tests were conducted in a specially designed test train to supply the specified coolant conditions.

Typical instrumentation for the MT tests included fuel centerline thermocouples, cladding inner surface thermocouples, cladding outer surface thermocouples, rod internal gas pressure transducers or pressure switches, coolant channel steam probes, and self-powered neutron detectors. This instrumentation allowed for determining rupture times and cladding temperature.

After the experiments, the test train was dismantled and cladding rupture sites were determined and fuel rod profilometry was performed in the spent fuel pool. Only limited destructive postirradiation examination was performed on these three tests.

Initial FRAPTRAN assessment runs for these three cases revealed a significant discrepancy between measured and calculated rod gas pressures prior to the transients. The stated fuel rod fill gas pressures were initially used to define the input fill gas pressure for the FRAPTRAN runs. However, this resulted in FRAPTRAN calculating significantly higher initial gas pressures than were measured. Analyses comparing the stated design data and the FRAPTRAN calculations, based on the perfect gas law, concluded that FRAPTRAN was correctly calculating gas pressure changes with temperature and volume changes and that the stated fill gas pressures were not being interpreted properly.

For tests MT-4 and MT-6A, gas pressure was measured at a manifold in the reactor hall at room temperature. This manifold was connected via a capillary line to the test rods in the reactor core. Therefore, though the pressure in the rods was as-measured, the rods were at higher temperatures in the core than the manifold in the reactor hall. Thus, the quantity of gas actually in the test rods was less than would be calculated from the design parameters and measured pressure at room temperature. Because of this, FRAPTRAN, when using the room temperature design parameters, calculated a higher initial gas pressure than was measured. Therefore, it was decided to set the FRAPTRAN input gas pressures at values that would result in the initial FRAPTRAN-calculated pressures matching those as-measured.

For test MT-1, a similar discrepancy between measured and calculated gas pressures was observed. However, the MT-1 rods were filled and then sealed with gas without the capillary design used for MT-4 and MT-6A. The discrepancy was not resolved, but it was decided to treat MT-1 for the assessment the same as for MT-4 and MT-6A; i.e., set FRAPTRAN input such that measured and calculated pressures match at the beginning of the run.

Summary results of the three tests are provided in Table A-6. A summary of the experimental results for each test will be provided in the following sections.

Table A.6 Summary of NRU Test Parameters and Results			
Parameter/Result	MT-1	MT-4	MT-6A
<i>Basic Rod Design</i>			
Cladding Type	Zry-4	Zry-4	Zry-4
Cladding OD, mm	9.63	9.63	9.63
Cladding ID, mm	8.41	8.41	8.41
Fuel OD, mm	8.26	8.26	8.26
Fuel Length, mm	3658	3660	3660
Total Rod Length, mm	3850	3850	3850
Fill Gas	He @ 3.2 MPa @ 295K	He @ 4.62 MPa @ 296K	He @ 6.03 MPa @ 295K
Fuel Enrichment, % U-235	3	2.93	2.93
Fuel Density, %TD	95	95	95
<i>LOCA Test</i>			
Date of Test	April 1981	May 1982	May 1984
Power Level, kW/m	1.24	1.2	1.2
Pre-Transient Cladding Temperature, K	727	~640	~675-700
Rod Pitch, mm	12.75	12.75	12.75
Steam Pressure, MPa	0.276	0.28	1.72
Delay Time Before Reflood, s	32	57	60 (not stated, inferred from data plots)
Reflood Rate, in./s	2.1	8 in./s for 6 s; 4 in./s for 6 s; 1 in./s for 3 s; then DACS control	8 in./s for 3 s; 7 in./s for 3 s; 2 in./s for balance
Reflood Temperature, K	294 to 328	311	310 (not stated, assumed similar to other tests)
Test Duration, min.	3.2	18.7	5
<i>LOCA Results</i>			
Peak Cladding Temperature, K	1148	1459	~1175
Number of Ruptured Rods	6 of 11	12 of 12	21 of 21
Average Rupture Temperature, K	1145	1094	1050 to 1140
Time to Rod Rupture, s	60 to 95; average of 70	52 to 58; average of 55	58 to 64
Rupture Elevation, mm	2000	2680; strain over ~0.2m	not measured
Average Rupture Hoop Strain, %	43	72	not measured, "large" from visual examination
Maximum Rupture Hoop Strain, %		99	not measured, "large" from visual examination
Rod Pressure @ Rupture, MPa	not stated (peak pressure prior to rupture was 9.66 MPa)	5.58 to 6.48 (peak pressure prior to rupture was 9.31 MPa)	6.07 to 7.93 (peak pressure prior to transient was 9.31 MPa)

A.3.1.1 MT-1

This case consists of 11 full-length PWR rods subjected to adiabatic heatup followed by reflood for providing data for supporting LOCA analyses. The primary objective of the MT-1 test was to determine the effects of fuel cladding dilation and rupture on heat transfer within a full-length fuel bundle during a LOCA. The desired cladding peak temperatures of up to 1172K were selected to allow swelling and rupture of the cladding in the high α , $\alpha+\beta$ microstructure range.

A preconditioning phase for the nonirradiated test rods was conducted at an average fuel rod power of 18.7 kW/m with water cooling at a pressure of 8.62 MPa. Three short runs were made under these conditions to permit the fuel pellets to crack and relocate.

The pretransient phase was conducted with steam cooling at a mass flow rate of 0.378 kg/s and an average fuel rod power of 1.24 kW/m.

In the transient phase, the test assembly was allowed to heat up in stagnant steam. The steam flow was turned off at 10 seconds in Figure A.28. After 32 seconds (42 seconds in Figure A.28), reflood water was introduced at a rate to fill the test section at 0.051 m/s (2 in./s). The test was terminated when all of the thermocouples were quenched. System pressure was held at 0.276 MPa (40 psia) during this phase also.

Provided in Figure A.28 are representative cladding inner surface temperature data for MT-1. A representative measured plenum gas pressure history is provided in Figure A.29. An example of the post-test strain for a rod is provided in Figure A.30.

Sources

Russcher, G. E., et al. 1981. *LOCA Simulation in the NRU Reactor: Materials Test 1*. NUREG/CR-2152 (PNL-3835), Pacific Northwest Laboratory, Richland, Washington.

Uchida, M. 1984. "Application of Two-Dimensional Ballooning Model to Out-Pile and In-Pile Simulation Experiments," *Nuclear Engineering and Design*, 77(1984)37-47.

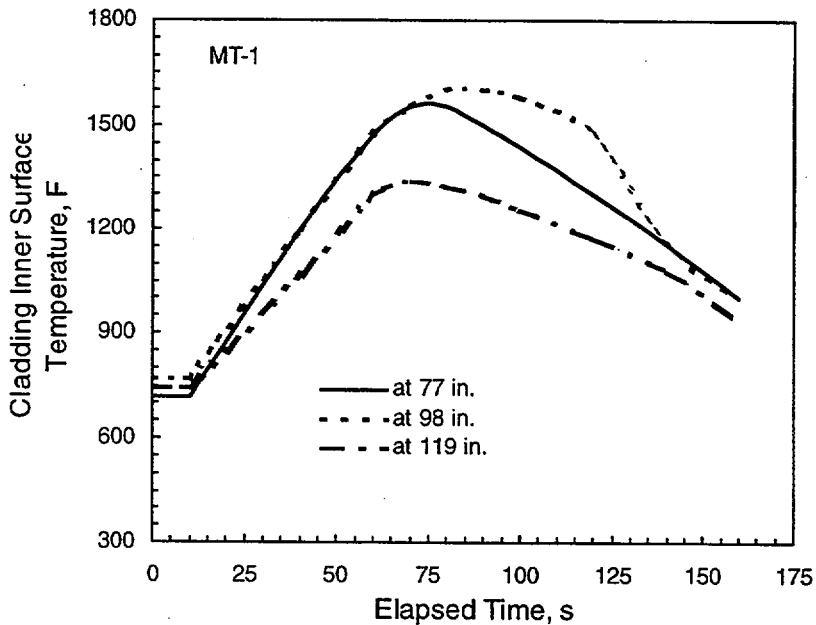


Figure A.28 Cladding Inner Surface Temperature for MT-1

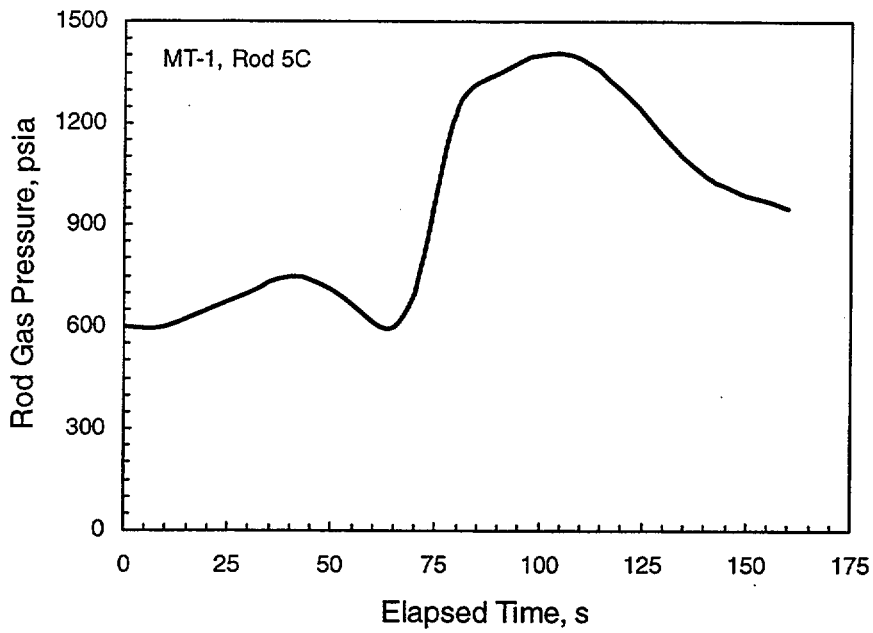


Figure A.29 Representative Plenum Pressure for MT-1, Rod 5C (unfailed)

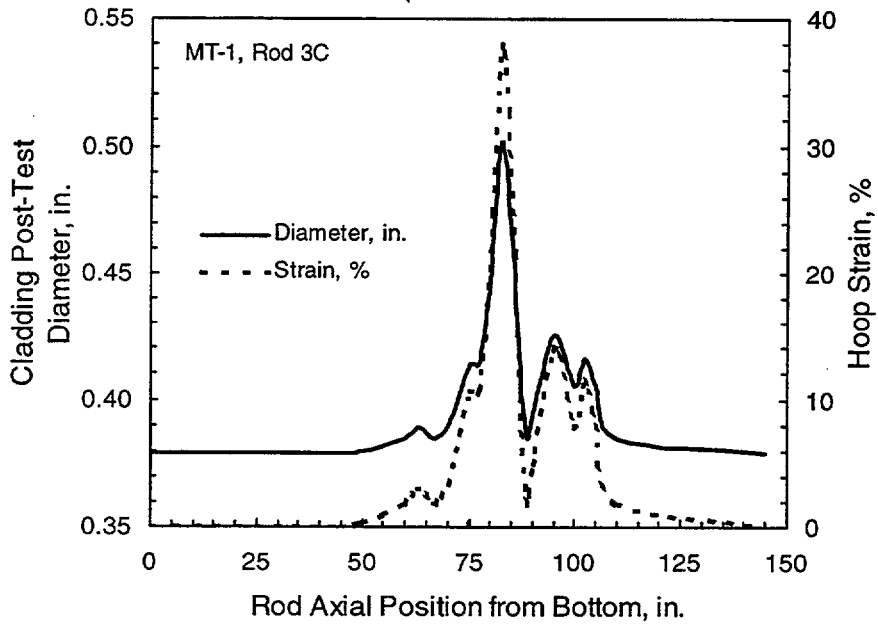


Figure A.30 Representative Post-Test Diameter Profile for MT-1 Rods

A.3.1.2 MT-4

Similar to MT-1, this case consists of 12 full-length PWR rods subjected to adiabatic heatup followed by reflood for providing data for supporting LOCA analyses. The primary objectives of the MT-4 test included providing sufficient time in the α -Zircaloy ballooning window of 1033 to 1200K to allow all 12 pressurized rods to rupture before reflood cooling was introduced, obtaining data to determine heat transfer coefficients for ballooned and ruptured rods, and measuring rod internal gas pressure during rod deformation. All of the objectives for the test were accomplished.

A preconditioning phase for the nonirradiated test rods was conducted for this test with water cooling at a pressure of 8.27 MPa and a flow rate of 16.3 kg/s. Two short runs to full power were made under these conditions to permit the fuel pellets to crack and relocate.

Three transients were run prior to the actual test for MT-4 (designated MT-4.04). These transients were for reflood calibration and assuring that the correct powers were used to obtain the desired cladding heatup rate of ~ 8.3 K/s.

In the desired transient (MT-4.04), there was a short heatup phase of approximately 1.5 minutes and a longer phase at temperature that lasted approximately 20 minutes. Reflood was initiated 57 seconds after steam flow was shutoff. Since the rod failures occurred from 52 to 58 seconds, all but one rod failed during the adiabatic heatup before reflood occurred.

Provided in Figure A.31 are representative cladding inner surface temperature data. Cladding temperatures at time of failure ranged from 1077 to 1114K. Peak internal gas pressures were approximately 8.9

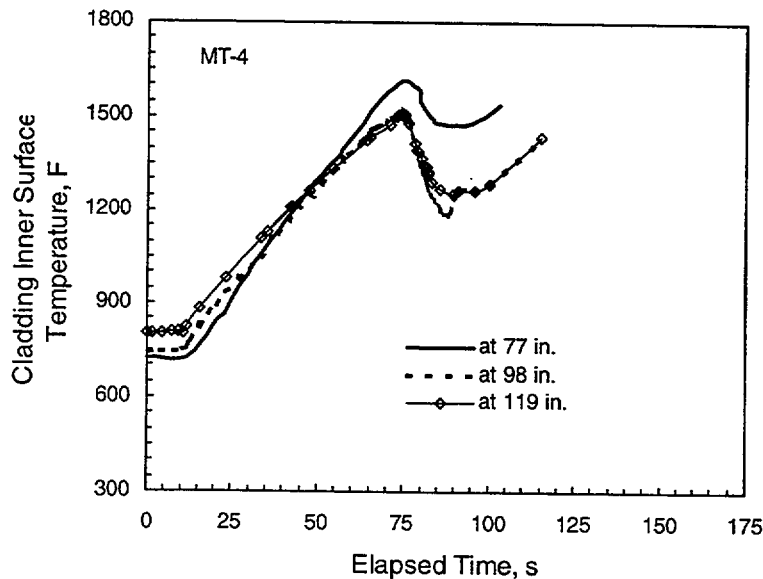


Figure A.31 Cladding Inner Surface Temperature for MT-4

to 9.3 MPa (initial value of 4.62 MPa), with gas pressures at failure of approximately 5.6 to 6.5 MPa. Representative gas pressure histories are provided in Figure A.32. A plot of representative post-test rod strain is provided as Figure A.33.

Sources

Wilson, C. L., et al. 1983. *LOCA Simulation in NRU Program: Data Report for the Fourth Materials Experiment (MT-4)*. NUREG/CR-3272 (PNL-4669), Pacific Northwest Laboratory, Richland, Washington.

A.3.1.3 MT-6A

A principal difference between MT-6A and the other two tests was a redesign of the test train to reduce cladding circumferential temperature gradients and thus induce greater amounts of cladding ballooning and flow blockage. In addition, the 20 guard rods used in the previous tests were replaced with nine pressurized rods that had been used in MT-3. Thus, a total of 21 test rods were in MT-6A.

A malfunction of the computer controlling the test occurred during the test. As a result of this malfunction, system pressure during the transient heat-up was not at 0.28 MPa but was at 1.72 MPa. In addition, the desired temperature control was not achieved.

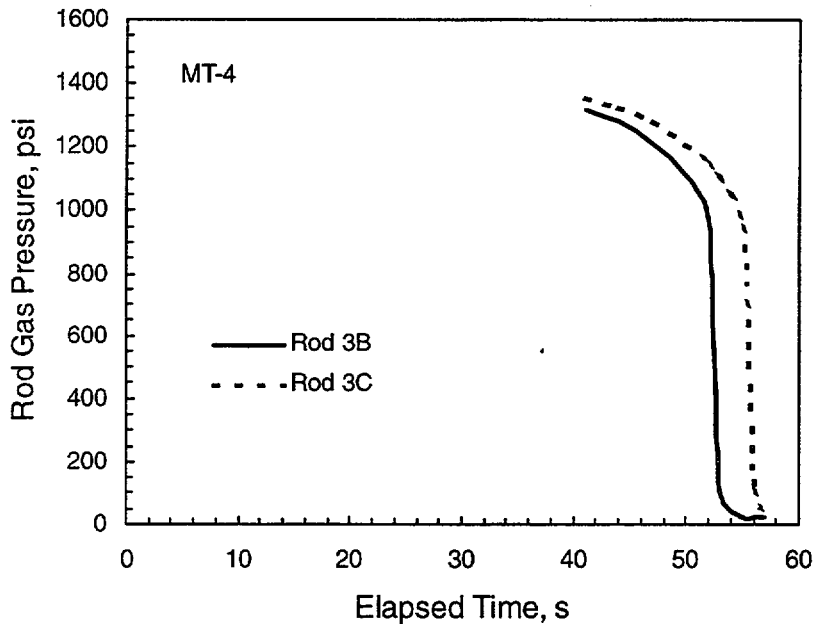


Figure A.32 Rod Gas Pressure for MT-4

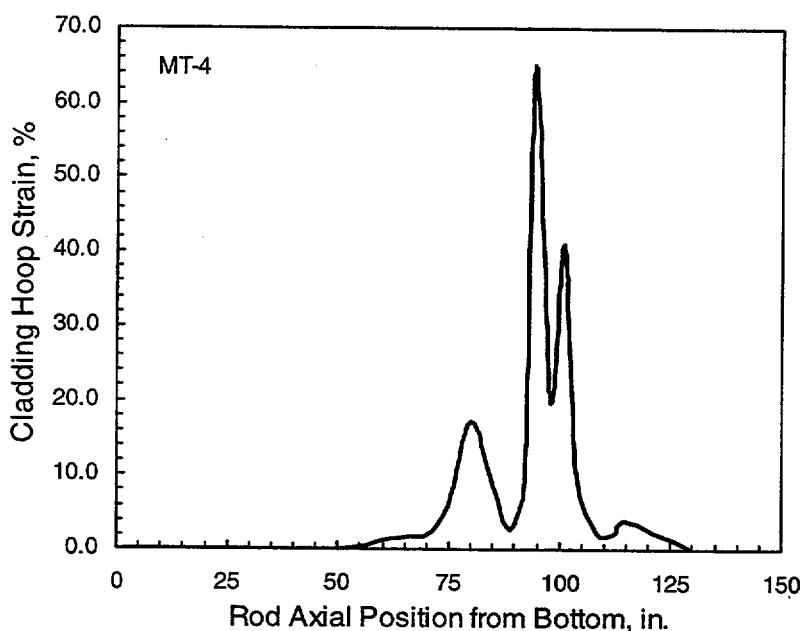


Figure A.33 Representative Permanent Strain for MT-4 Rods

This test was intended to provide the fuel cladding sufficient time in the α -Zircaloy temperature region (1050-1140K) to maximize expansion and to cause the fuel rods to rupture before they were cooled by reflooding. Other objectives included: a) evaluating expansion characteristics of a bundle in which all fuel rods expand and rod-to-rod interaction can occur; and provide data on the rate of cooling for a bundle where all rods have expanded and ruptured.

Representative cladding inner surface temperature histories for MT-6A are provided in Figure A.34. A plenum gas pressure history representative for this test is provided in Figure A.35. No post-irradiation examination data were obtained for this test.

Sources

Wilson, C. L., et al. 1993. *Large-Break LOCA, In-Reactor Fuel Bundle Materials Test MT-6A*. PNL-8829, Pacific Northwest Laboratory, Richland, Washington.

A.3.2 PBF LOC-11C

LOCA testing was conducted in the Power Burst Facility (PBF) as part of the Thermal Fuels Behavior Program (TFBP) for the NRC. The PBF was designed primarily for performing very high-power excursions and consists of a driver core in a water pool and a pressurized-water test loop capable of providing a range of test conditions. The central test space operates as a neutron flux trap that permits high power densities in tested fuel rods relative to the active core. An in-pile tube fits in this central flux trap region and contains the test assemblies.

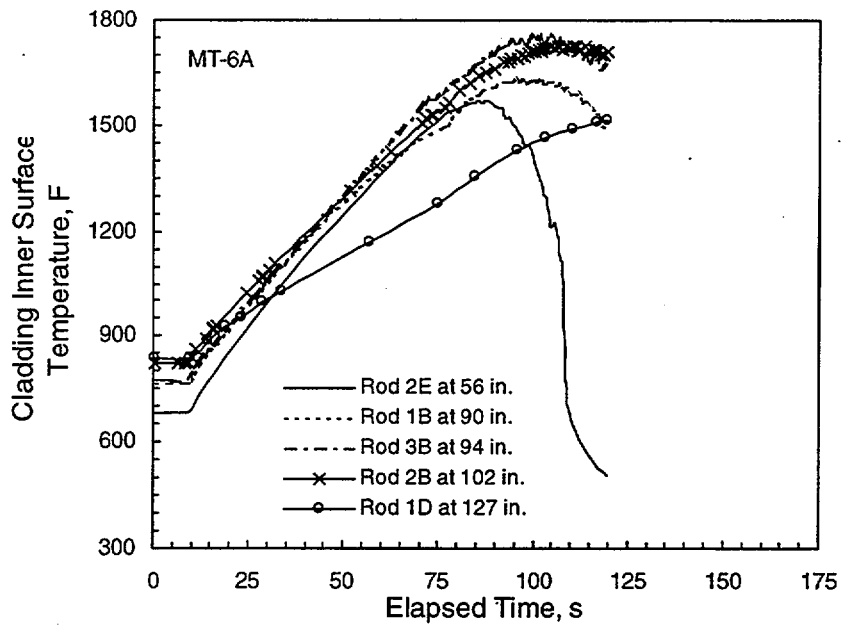


Figure A.34 Cladding Inner Surface Temperatures for MT-6A

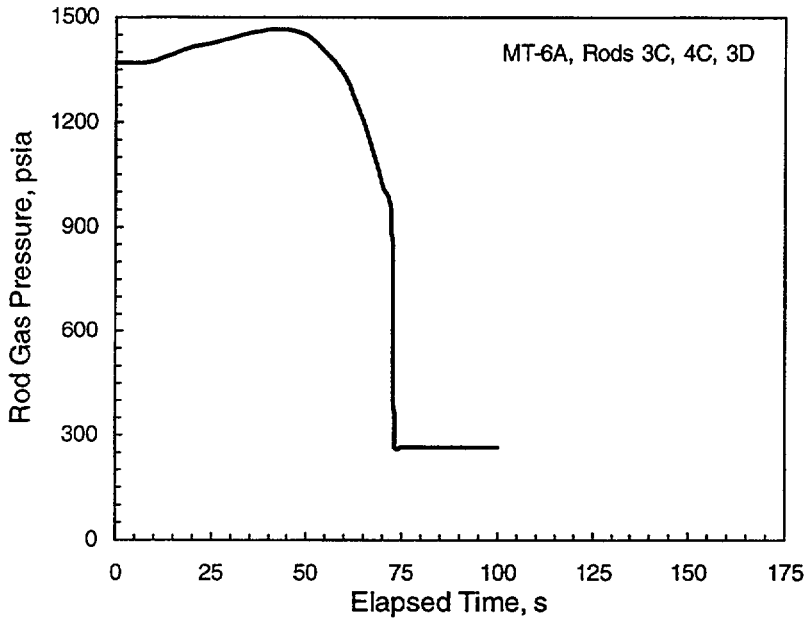


Figure A.35 Plenum Gas Pressure for MT-6A

In the LOC-11 test series, four PWR-type, nonirradiated fuel rods were subjected to cladding temperatures similar to those expected for the highest-powered PWR rods during blowdown and heat-up of a 200% double-ended cold leg break. The test sequence was heat-up, power calibration, pre-conditioning, decay heat buildup, blowdown and quench, and cool down. Three sequential tests were run, LOC-11A, -11B, and -11C. The LOC-11C test was intended to result in peak cladding temperatures of approximately 1030K. There was no indication of fuel rod failure in any of the three tests.

The basic parameters for the rods (same rods used in the -11A and -11B tests), and test conditions for LOC-11C, are provided in Table A.7.

Instrumentation for each test rod included four thermocouples for cladding surface temperature, cladding centerline temperature, cladding axial elongation, and plenum temperature and pressure. The cladding surface temperature histories are provided in Figure A.36, a representative fuel centerline temperature history is provided in Figure A.37 (initial centerline temperatures for the four rods varied from 2450 to 2580K), and the cladding elongation histories are provided as Figure A.38 (strain values are presented in Figure A.39).

Measured post-test cladding outer diameters are presented in Figure A.40 (strain values are presented in Figure A.41). The effect of fuel rod pressurization is easily seen with the two 0.1 MPa (1 atm) rods having diameter decreases and the two pressurized rods (2.41 MPa/24 atm and 4.8 MPa/48 atm) having ballooning at the axial mid-plane where cladding temperatures were the highest.

Parameter	Value (Averaged over four rods)
Rod Overall Length	1003 mm
Active Fuel Length	915.5 mm
Plenum Volume	3.29 cm ³
Cladding Type	Zircaloy-4
Cladding Outer and Inner Diameters	10.72 and 9.50 mm
Radial Gap Thickness	0.105 mm
Pellet Diameter	9.29 mm
Pellet Density	95% TD
Pellet Enrichment	9.6% U-235
Helium Gas Pressure	2 rods at 0.103 MPa (rods 1,4) 1 rod at 2.41 MPa (rod 3) 1 rod at 4.82 MPa (rod 2)
Pre-Transient Coolant	15.2 MPa, 1.01 liter/s, 598K
Pre-Scram/Transient Power	48.8 kW/m average, peak-to-average ratio of 1.4
Transient	Blowdown initiation at scram, Quench 50s after scram

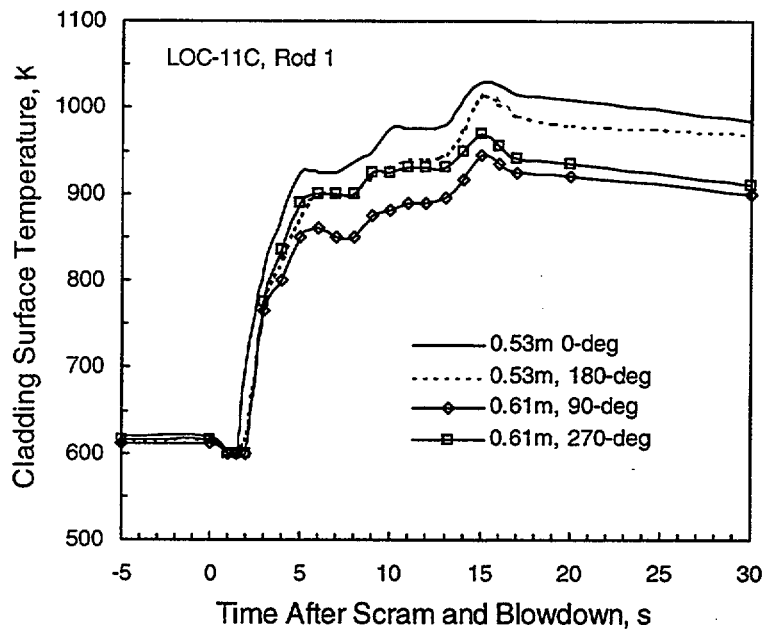


Figure A.36 LOC-11C Cladding Surface Temperature History

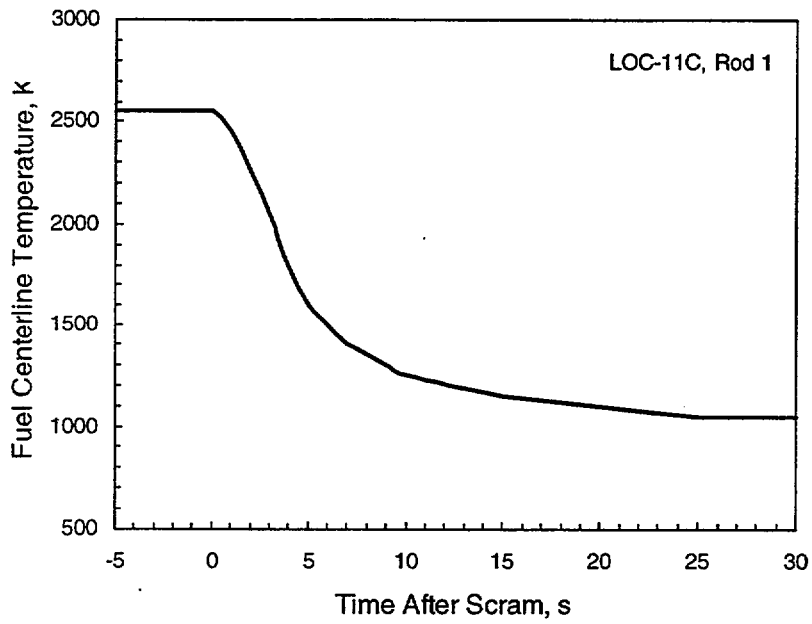


Figure A.37 LOC-11C Fuel Centerline Temperature History

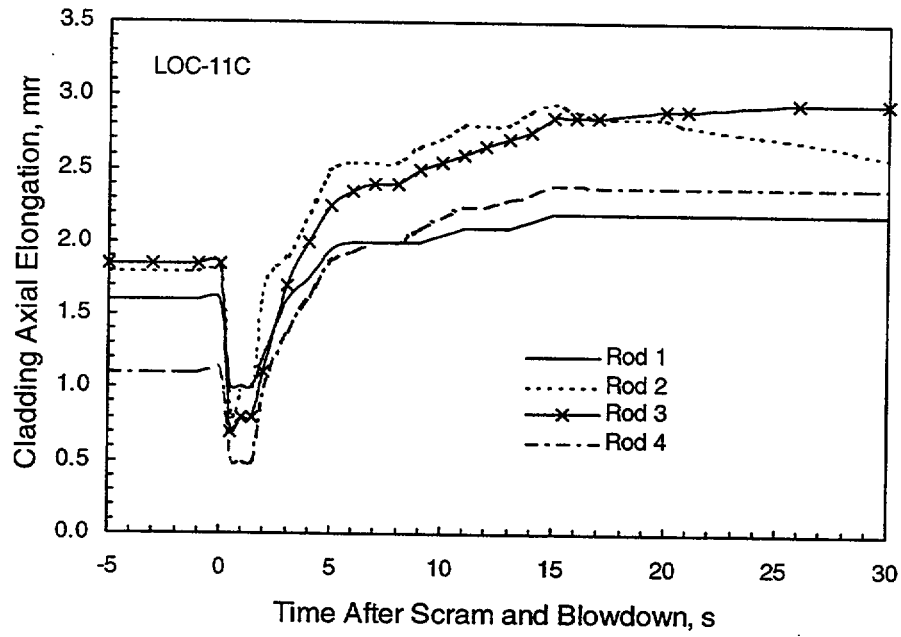


Figure A.38 LOC-11C Cladding Elongation History

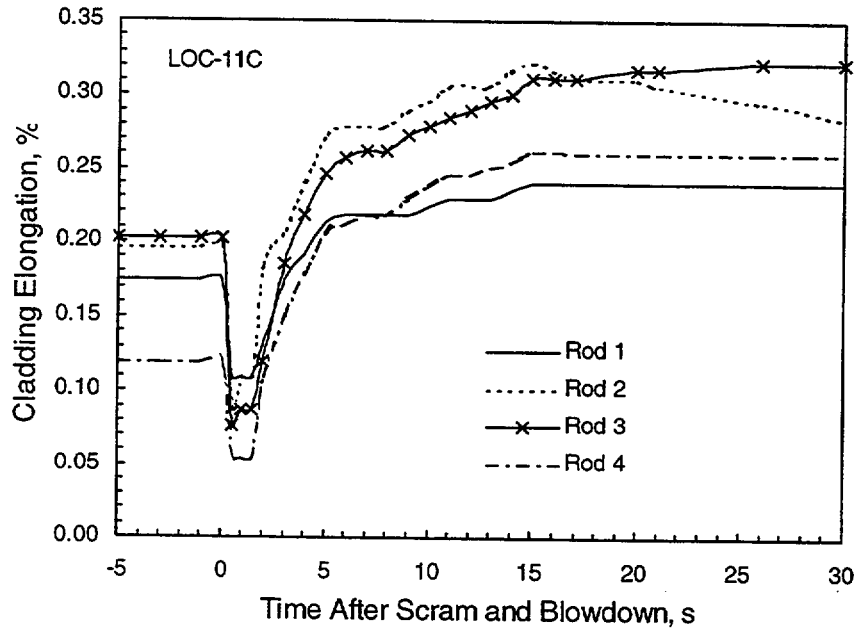


Figure A.39 LOC-11C Axial Strain History

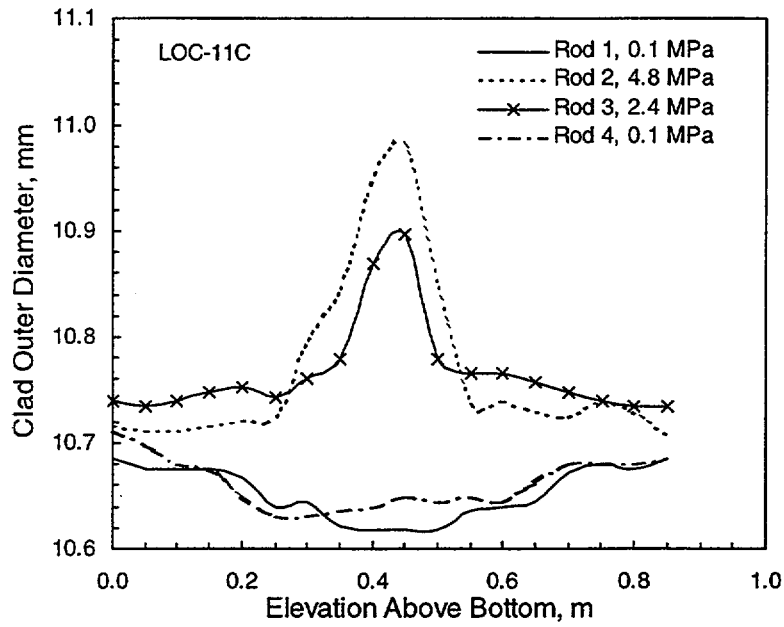


Figure A.40 Post-Test Cladding Diameters for Test Rods in LOC-11C

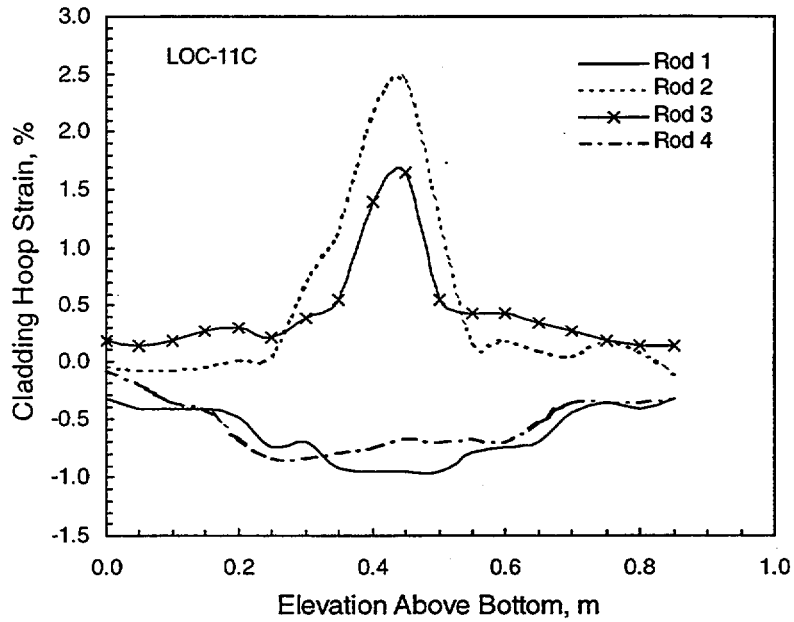


Figure A.41 Cladding Permanent Hoop Strain for Test Rods in LOC-11C

Sources

Buckland, R. J., C. E. Coppin, and C. E. White. 1978. "Experiment Data Report for PBF-LOCA Tests LOC-11b and 11c." NUREG/CR-0303, Idaho National Engineering Laboratory, Idaho Falls, Idaho.

Larson, J. R., et al. 1979. *PBF-LOCA Test Series; Test LOC-11 Test Results Report.*" NUREG/CR-0618, Idaho National Engineering Laboratory, Idaho Falls, Idaho.

A.3.3 TREAT FRF-2

The fuel rod failure (FRF)-2 test was a seven-rod bundle irradiated in the Transient Reactor Test Facility (TREAT) reactor. Power was brought up to 7.16 kW/m for 20 seconds during steam cooling. The purpose of the irradiation was for evaluating code simulations of fuel rod heat capacity by comparing predicted and measured cladding temperatures during beginning-of-life adiabatic heatup.

The TREAT reactor is a solid, graphite-moderated, air-cooled reactor capable of steady-state operation at 0.1 MW or transient operation of 1000 MW-s. Removal of heat from the reactor is the limiting factor for operation. The core has an active height of 48 inches with a central, vertical test hole for materials testing.

The basic design parameters of the test rods, and the test conditions, for the FRF-2 test are provided in Table A.8.

Instrumentation for the test included cladding surface thermocouples on two rods, rod gas pressure for two rods, and coolant conditions. The test rods were examined after irradiation and cladding strain measurements were obtained. Provided in Figure A.42 is the measured cladding surface temperature; peak cladding temperatures were 2400 to 2450 °F. Provided in Figure A.43 is the measured rod gas pressure; gas pressure began to decrease at about 25 seconds when cladding temperatures reached about 1800°F. The rods failed by rupture from 30 to 37 seconds when cladding temperatures were from 2200 to 2400°F. Provided in Figure A.44 is an illustration of the measured permanent hoop strain along the length of a test rod.

Three principal gas volumes are important to the measured gas pressures for rods 11 and 12 in this test; the three volumes are the fuel and gap, the plenum, and an external pressure cell. Particularly because of the external pressure cell, gas pressures did not increase as much as would have been expected had the rods been sealed systems. The three volumes are further described in the following table.

Volume	cm ³ (% of total gas volume)	Temperature History
Fuel and Gap	4.7 (35)	approximately equal to cladding temperature, large increase during transient
Plenum	6.7 (49)	initial temperature of 400K with approximately 33K increase during the transient
Pressure Cell	2.2 (16)	initial temperature of 395K with approximately 8K increase during transient

Table A.8 Basic Parameters for the TREAT FRF-2 Test	
Parameter	Value (Averaged over seven rods)
Rod Overall Length	27 in.
Active Fuel Length	24 in.
Plenum Volume	0.439 in. ³
Cladding Type	Zircaloy-4
Cladding Outer and Inner Diameters	0.5633 and 0.4993 in.
Radial Gap Thickness	0.0024 in.
Pellet Diameter	0.4945 in.
Pellet Density	95% TD
Pellet Enrichment	1.5% U-235
Helium Gas Pressure	75 psia at 77°F
Transient	a) Power started at zero, peaked at 11 kW/ft rod-average, then decreased; b) axial power profile with peak-to-average ratio = 1.06; c) coolant was flowing steam/helium mixture at 10 liters/min.

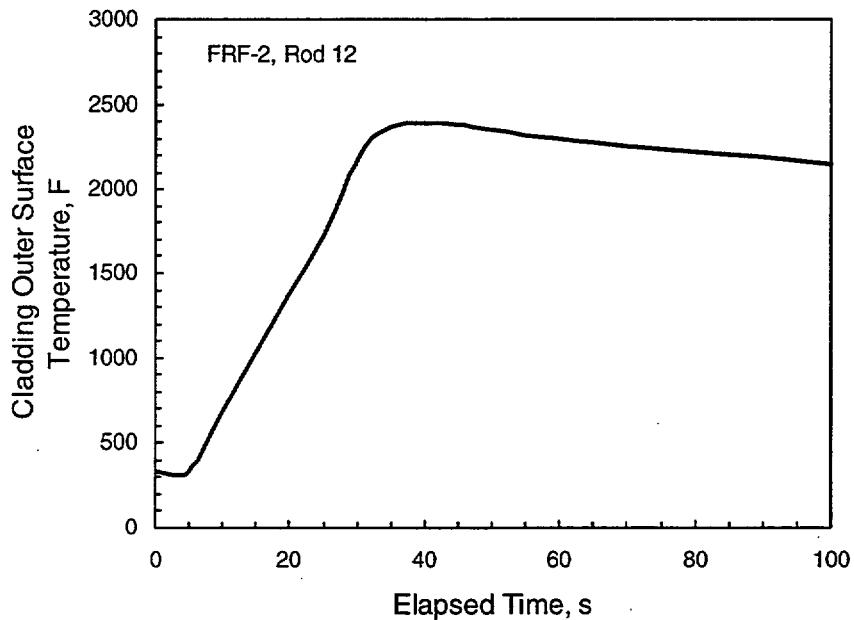


Figure A.42 Cladding OD Temperature History for TREAT FRF-2

For the FRAPTRAN calculation, it is important to note that 65% of the gas volume stayed at relatively low temperatures during the transient. Accounting for these volumes and temperature differences in the FRAPTRAN calculation is discussed further in Section B.5.

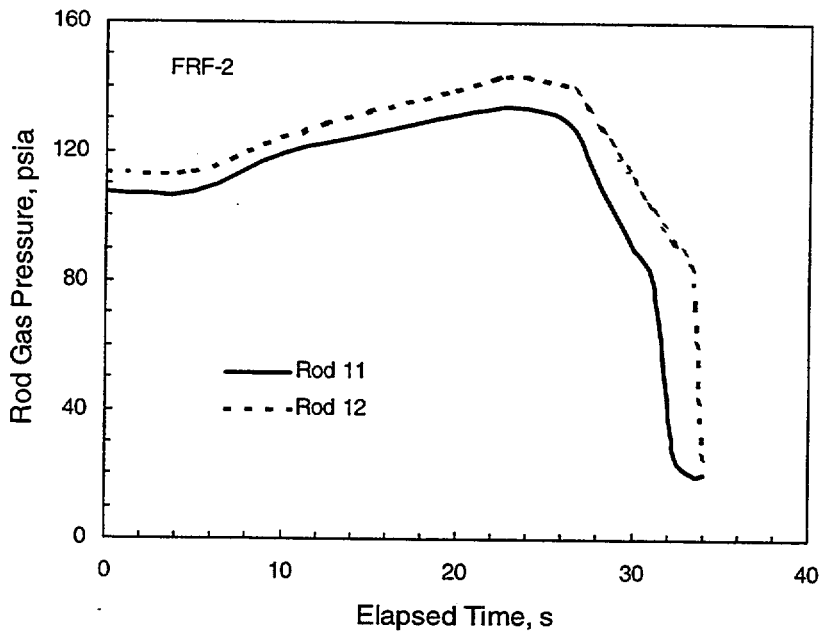


Figure A.43 Rod Plenum Pressure History for TREAT FRF-2

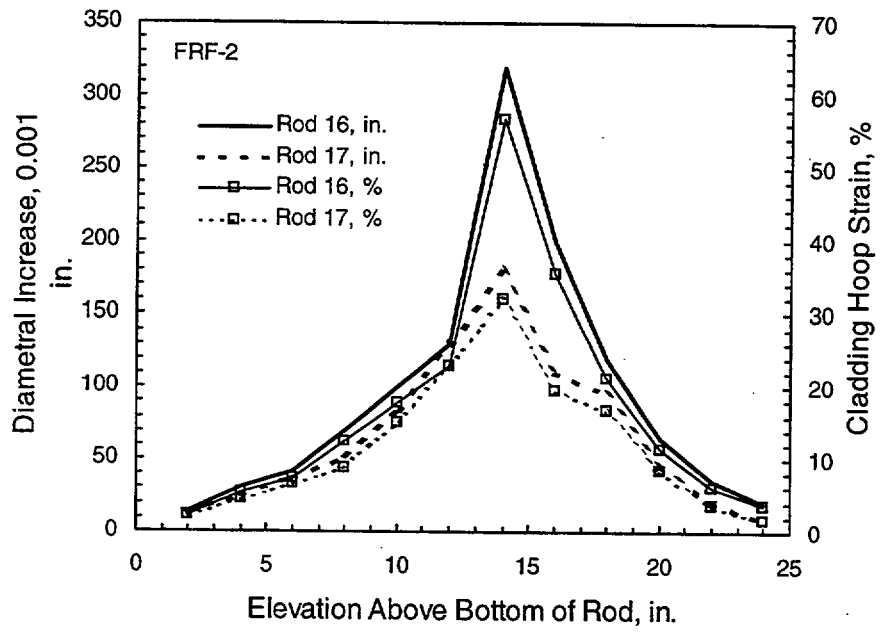


Figure A.44 Cladding Permanent Diameter Increase for FRF-2

Sources

Lorenz, R. A., and G. W. Parker. 1972. *Final Report on the Second Fuel Rod Failure Transient Test of a Zircaloy-Clad Fuel Rod Cluster in TREAT*. ORNL-4710, Oak Ridge National Laboratory, Oak Ridge, Tennessee.

El-Adham, K. 1987. *Extension and Assessment of the Cladding Ballooning Model in the FRAP-T6 Code*. EGG-SSRE-7906, Idaho National Engineering Laboratory, Idaho Falls, Idaho.

A.4 Other Test Cases

A.4.1 FRAP-T6 Standard Problem

This case is a hypothetical double-ended cold leg break in a PWR; input was developed by Idaho National Engineering Laboratory (INEL) and results were reported with the initial release of FRAP-T6 (Siefken et al. 1981). The simulation is of a full-length fuel rod during a 200-second transient. The assumed fuel rod design is summarized in Table A.9. The peak rod power for the assumed nonirradiated fuel rod at the initiation of the accident is 51.9 kW/m. The boundary conditions were determined by a thermal-hydraulic systems analysis code and input by cards for the 1981 FRAP-T6 calculation.

FRAP-T6 calculated results for the peak power node are provided in the following figures: cladding surface temperature in Figure A.45, fuel centerline temperature in Figure A.46, cladding axial elongation in Figure A.47, and rod gas pressure in Figure A.48.

FRAP-T6 calculated localized ballooning and rupture of the cladding 9 seconds after the accident initiation. Rupture was calculated to assume at the peak power location. The calculated maximum uniform cladding hoop strain was 8%.

Calculated peak cladding surface temperature was 1375K at 10.5 seconds after accident initiation. Film boiling caused the cladding surface temperature to rapidly increase.

Parameter	Value
Active Fuel Length	3658 mm
Plenum Volume	10.76 cm ³
Cladding Type	Zircaloy-4
Cladding Outer Diameter	10.72 mm
Cladding Thickness	0.6096 mm
Pellet Diameter	9.30 mm
Pellet Density	93% TD
Helium Gas Pressure	15 MPa
Pre-Transient Coolant	15.2 MPa, 610K
Pre-Transient Power	36.4 kW/m, peak-to-average of 1.4

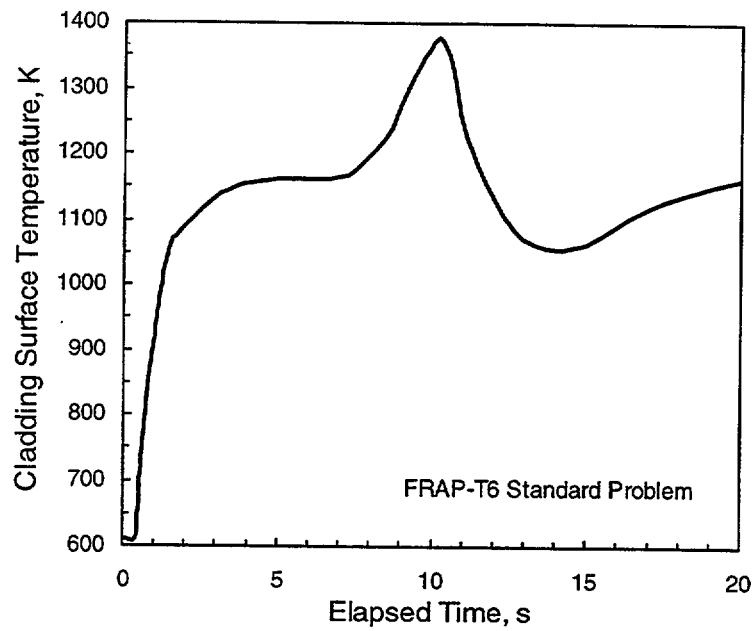


Figure A.45 FRAP-T6 Standard Problem Cladding Temperature History

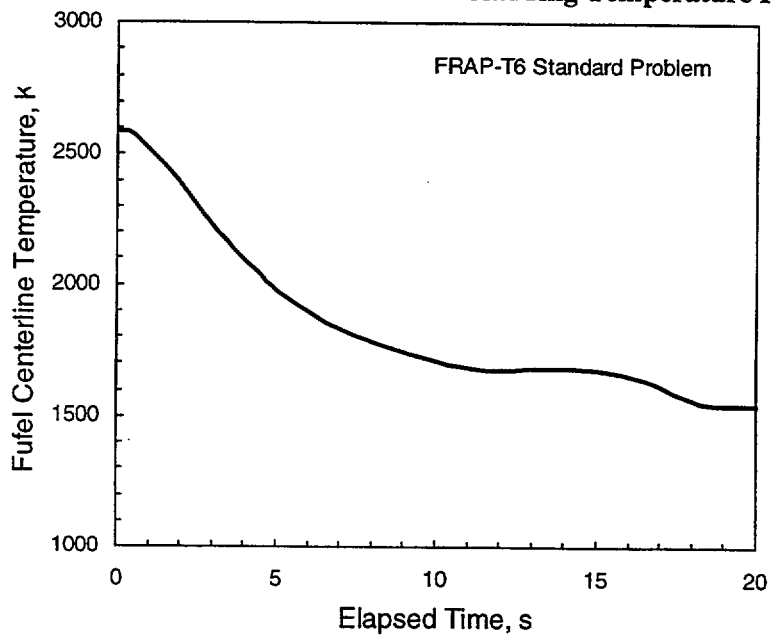


Figure A.46 FRAP-T6 Standard Problem Fuel Centerline Temperature History

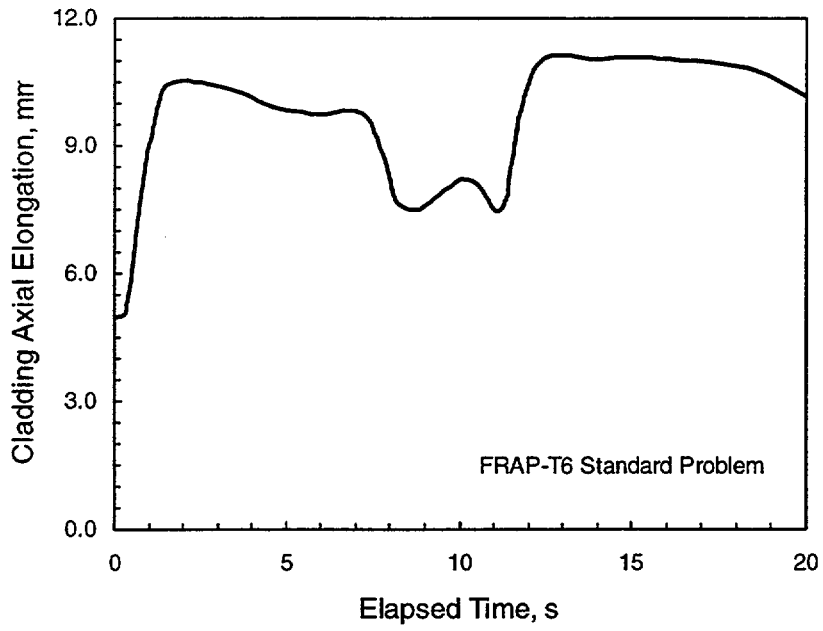


Figure A.47 FRAP-T6 Standard Problem Cladding Elongation History

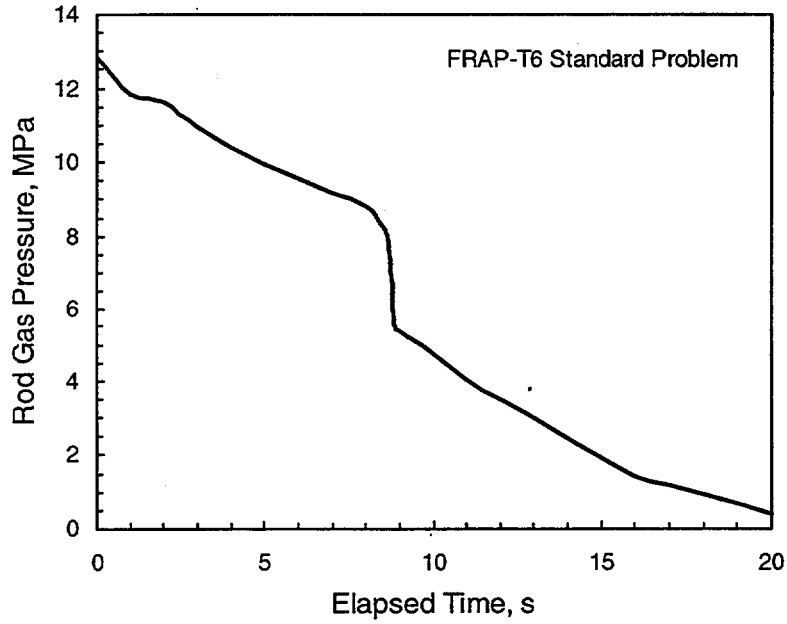


Figure A.48 FRAP-T6 Standard Problem Rod Gas Pressure History

Sources

Siefken, L. J., et al. 1981. *FRAP-T6: A Computer Code for the Transient Analysis of Oxide Fuel Rods*. NUREG/CR-2148. EG&G Idaho, Inc., Idaho Falls, Idaho.

A.4.2 HBWR IFA-508, Rod 11

Instrumented fuel assembly (IFA)-508 was irradiated in the Halden Boiling Water Reactor (HBWR) for the purpose of measuring in-reactor fuel temperatures, rod diameter, and length changes with power and burnup. For the FRAPTRAN assessment, the data of particular emphasis are the cladding axial elongation measurements during the initial stair-step power ascension.

The HBWR is a heavy-water moderated and cooled reactor that is well situated for irradiating instrumented test fuels under both steady-state and moderate transient conditions. Coolant conditions are an inlet temperature of 240°C at a pressure of 3.4 MPa. Each IFA is individually calibrated for total power and power distribution within the assembly.

Three rods were irradiated in IFA-508, but only the small-gap Rod 11 is used in the assessment. This rod was instrumented with a fuel centerline thermocouple and cladding axial elongation sensor. In addition, a traveling, in-reactor rod diameter measurement capability was included. Provided in Table A.10 is a summary of the basic design parameters for the rod and test conditions.

The initial startup of IFA-508 was a stair-step approach to power as illustrated in Figure A.49. Measured centerline fuel temperature at 49 kW/m was approximately 1600K. The resulting cladding axial elongation history is presented in Figure A.50. It may be seen in Figure A.50 that cladding elongation relaxed during each hold at power. FRAPTRAN is not expected to model this behavior because it is indicative of some relaxation process that are not modeled in FRAPTRAN. However, FRAPTRAN, should be expected to model the upper bound of the axial elongation behavior.

Parameter	Value for Rod 11
Rod Overall Length	>755 mm
Active Fuel Length	420 mm
Plenum Volume	
Cladding Type	Zircaloy-2
Cladding Outer and Inner Diameters	12.22 and 10.85 mm
Cladding Thickness	0.685 mm
Pellet Diameter	10.75 mm
Fuel-Cladding Radial Gap	0.050 mm
Fuel Pellet Length	15 mm
Pellet Density	94.8% TD
Pellet Enrichment	10.5% U-235
Fill Gas	100% He, 0.1 MPa at 300K
Coolant Inlet Conditions	240°C at 3.4 MPa

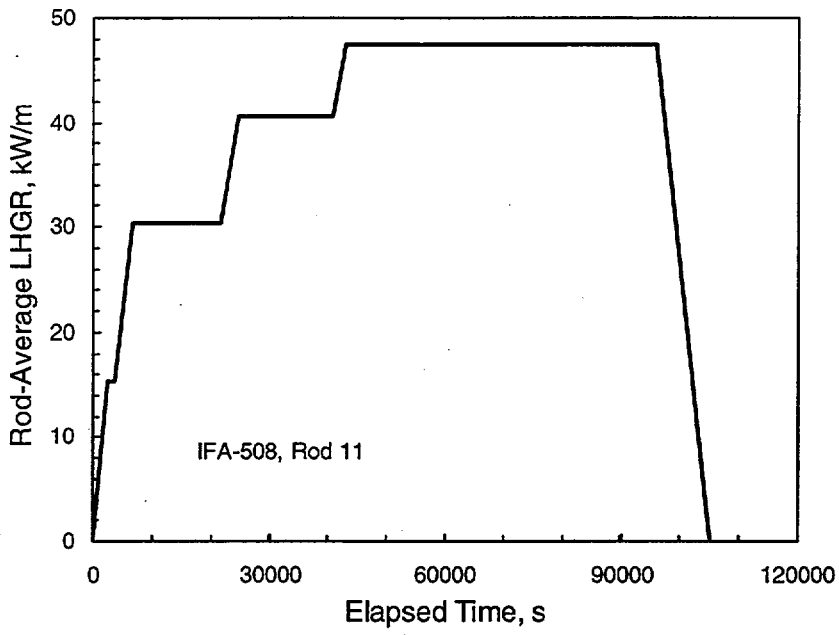


Figure A.49 Initial Power Ascension for IFA-508, Rod 11

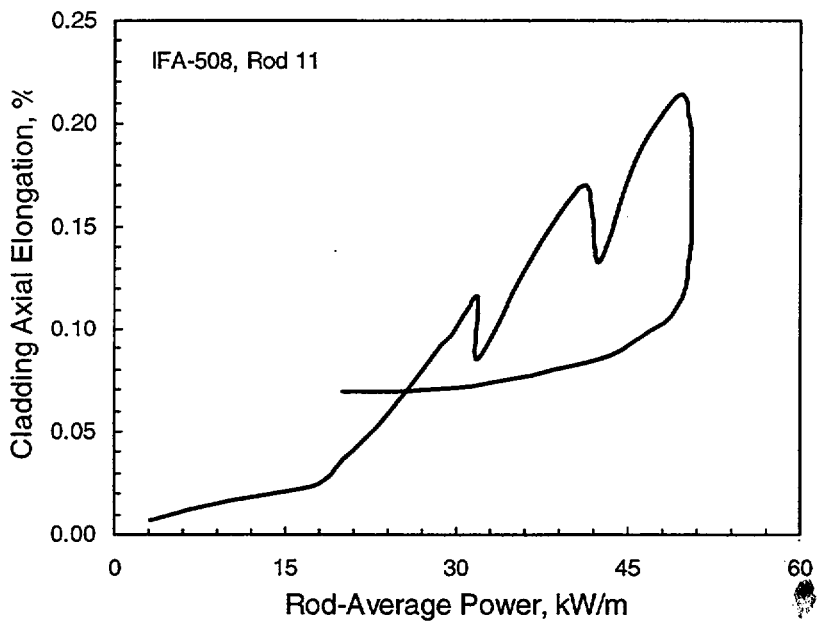


Figure A.50 Initial Cladding Elongation History for HPR-508, Rod 11

Sources

Uchida, M., and M. Ichikawa. 1980. "In-Pile Diameter Measurement of Light Water Reactor Test Fuel Rods for Assessment of Pellet-Cladding Mechanical Interaction," *Nuclear Technology*, 51(1980)33-44.

Yanagisawa, K. 1986. "An Evaluation of the Influence of Fuel Design Parameters and Burnup on Pellet/Cladding Interaction for Boiling Water Reactor Fuel Rod Through In-Core Diameter Measurement," *Nuclear Technology*, 73(1986)361-377.

A.4.3 HBWR IFA-533.2

The second loading of Instrumented Fuel Assembly (IFA)-522 was used to irradiate two irradiated BWR-type rods that were re-instrumented with fuel centerline thermocouples. This allowed acquiring temperature data at high burnup from rods that were not previously instrumented or were irradiated in a different facility. The irradiation of IFA-533.2 included periodic scrams to obtain the transient time constant of the fuel at increasing burnup levels. For the FRAPTRAN assessment, the data collected during the first scram of IFA-533.2 will be used.

The HBWR is a heavy-water moderated and cooled reactor that is well situated for irradiating instrumented test fuels under both steady-state and moderate transient conditions. Coolant conditions are an inlet temperature of 240°C at a pressure of 3.4 MPa. Each IFA is individually calibrated for total power and power distribution within the assembly.

The two BWR-type rods that were irradiated in IFA-533.2 were initially irradiated in IFA-409 at rod-average heat ratings of 30 to 40 kW/m and to a rod-average burnup of approximately 44 MWd/kgUO₂. Halden-calculated fission gas release for the base irradiation was 3%. The rods were then removed from IFA-409 and reinstrumented with fuel centerline thermocouples prior to insertion in IFA-533.2 for continued irradiation. The reinstrumentation process involves drilling out a central well in the fuel so a fuel centerline thermocouple may be installed. The rod was then filled with 100% helium at 0.5 MPa. Only Rod 808R provided good fuel centerline temperature data during the IFA-533.2 irradiation. The thermocouple tip for Rod 808R was located approximately 35 mm below the top of the fuel column.

During IFA-533.2, Rod 808R was subjected to scrams at different burnup levels. The first scram was at a burnup level of 44 MWd/kgUO₂. This occurred about two months after the irradiation of IFA-533.2 began. Provided in Figure A.51 is the fuel centerline temperature history during this scram beginning from an initial linear heat rate of 29 kW/m. The Halden Reactor Project has estimated a fuel time constant for this scram of approximately 9s and a thermocouple time constant of approximately 2s. The thermocouple time constant is manifested in the data as a delay in responding to the actual temperature change.

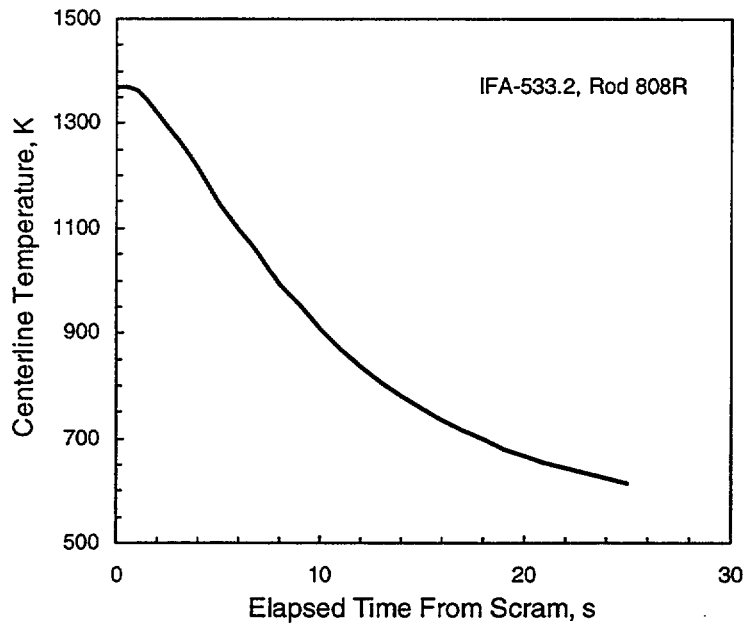


Figure A.51 Fuel Centerline Temperature History for Rod 808R of IFA-533.2 During Scram at 44 MWd/kgUO₂

Provided in Table A.11 is a summary of the design characteristics of Rod 808R; these parameters do not include the changes due to burnup.

A.4.4 PBF IE-1, Rod 7

Four test rods previously irradiated in the Saxton PWR were instrumented and tested in the Power Burst Facility (PBF) for the IE-1 test. Rods were instrumented with gas pressure transducers, cladding surface

Table A.11 Basic Parameters for IFA-533.2, Rod 808R	
Parameter	Value
Cladding Material	Zircaloy-2
Cladding Outer and Inner Diameters	12.52 and 10.80 mm
Cladding Thickness	0.86 mm
Fuel Diameter	10.57 mm
Fuel-Cladding Radial Gap	0.115 mm
Thermocouple Well Diameter	2.5 mm
Thermocouple Well Depth	35 mm
Fuel Pellet Length	12.8 mm
Fuel Density	94.7%TD
Fuel Active Length	400 mm
Rod Total Length	450 mm
Fill Gas (re-instrumented rod)	100% Helium at 0.5 MPa
Coolant Conditions	240°C at 3.4 MPa

thermocouples, and cladding axial elongation detectors. After some conditioning irradiation, the rods were quickly ramped to approximately 70 kW/m peak power and held for 45 minutes to provide data for pellet-cladding mechanical interaction. After 45 minutes, the coolant flow was slowly reduced until film boiling was detected. For the FRAPTRAN assessment, the gas pressure and cladding elongation response for Rod 7 will be used.

The PBF was designed primarily for performing very high-power excursions and consists of a driver core in a water pool and a pressurized-water test loop capable of providing a range of test conditions. The central test space is operated as a neutron flux trap that permits high power densities in tested fuel rods relative to the active core. An in-pile tube fits in this central flux trap region and contains the test assemblies.

The PWR-type rods were initially irradiated in Saxton to burnup levels from 6.8 MWd/kgM for Rod 7 to 16.6 MWd/kgM for the other rods. After the irradiation, the rods were instrumented for the irradiation in PBF. Provided in Table A.12 is a summary of the design characteristics for Rod 7, plus the coolant conditions. Both pre-Saxton and pre-PBF measurements of cladding outer diameter are provided in Table A.12; it can be seen that some creepdown of the cladding occurred during the Saxton irradiation. Measurement of the fuel diameter was not made after the Saxton irradiation, so FRAPTRAN will be assessed using the pre-irradiation fuel diameter.

The irradiation history for IE-1 in the PBF may be characterized with six cycles; the sixth cycle is the one chosen for the FRAPTRAN assessment. Provided in Figure A.52 is an illustration of the rod-average power and coolant flow rate histories for cycle 6 for Rod 7. Power was increased to a peak power of 72 kW/m and then held for approximately 45 minutes. During this period the coolant flow was maintained at a rate of about 900 cm³/s. After the hold, the coolant flow was slowly decreased until film boiling occurred. For Rod 7, this occurred at a flow rate of about 514 cm³/s. Flow was then increased and power decreased. Rod 7 failed with a circumferential crack about three minutes after shutdown. The failure site was at about 0.514 m above the bottom of the rod.

Parameter	Value
Cladding Material	Zircaloy-4
Pre-Saxton Cladding Outer and Inner Diameters	9.930 and 8.750 mm
Cladding Thickness	0.86 mm
Pre-PBF Cladding Outer and Inner Diameters	9.890 and 8.709 mm
Pre-Saxton Fuel Diameter	8.48 mm
Pre-Saxton Fuel-Cladding Radial Gap	0.115 mm
Fuel Pellet Length	12.8 mm
Fuel Density	94%TD
Fuel Active Length	890 mm
Rod Total Length	970 mm
Fill Gas (re-instrumented rod)	78% He and 22% Ar at 1.9 MPa at time of test
Coolant Conditions	600K at 14.8 MPa, 900 cm ³ /s

Provided in Figure A.53 are the measured cladding axial elongation and rod gas pressure histories as a function of rod-average linear heat rate during the cycle 6 ascension to peak power.

Provided in Figures A.54 and A.55 are the measured cladding temperature and rod elongation during the flow rate decrease after reaching peak power. The cladding surface thermocouple was located at the 0.62 m elevation. A correlation between cladding temperature and cladding elongation may be seen when film boiling occurs. During the PBF irradiation, cladding surface temperature for Rod 7 was approximately 625K at peak power and prior to the flow reduction, and then reached a maximum of approximately 660K during the flow reduction. Post-irradiation examination revealed that the film boiling zone was from about 0.445 to 0.685 m along the rod.

Sources

Quapp, W. J., et al. 1977. *Irradiation Effects Test Series, Test IE-1, Test Results Report*. TREE-NUREG-1046, Idaho National Engineering Laboratory, Idaho Falls, Idaho.

A.4.5 PBF PR-1

The PR-1 test was a combination power-cooling-mismatch (PCM) and RIA test performed to characterize the behavior of BWR-type fuel rods under normal and abnormal operating conditions as part of the Thermal Fuels Behavior Program (TFBP) conducted for the NRC. Data from the TFBP experimental effort have been used to determine the completeness and accuracy of the analytical models developed to predict fuel rod behavior for a wide range of postulated reactor operating conditions. This test was

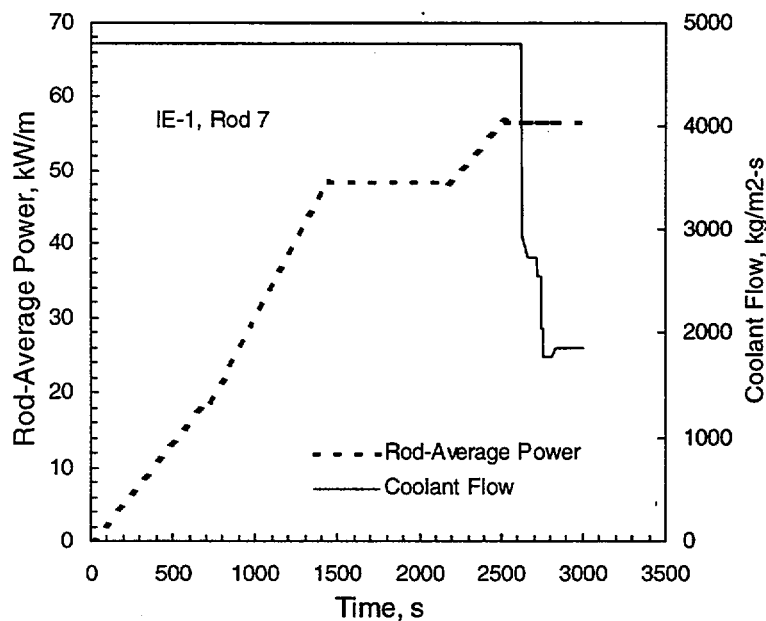


Figure A.52 Rod-Average Power and Coolant Flow History for Rod 7, PBF IE-1

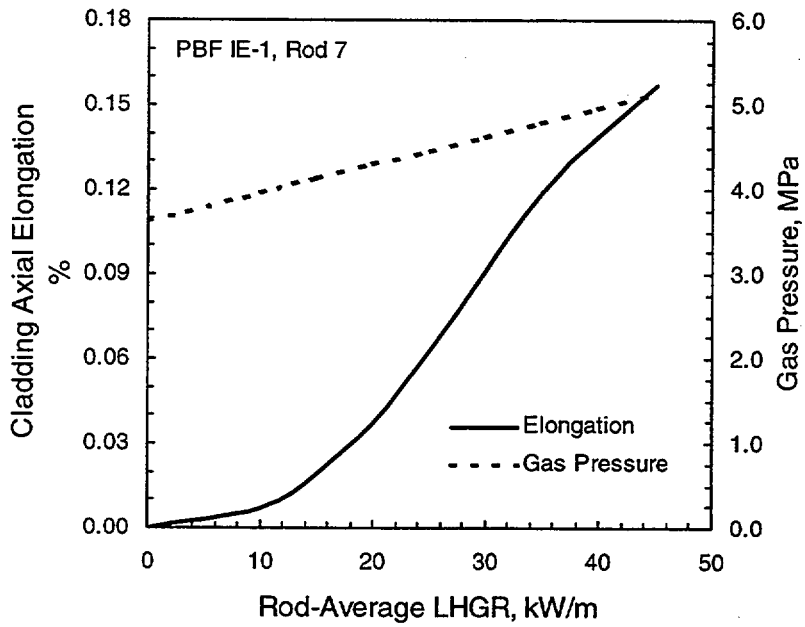


Figure A.53 Measured Cladding Axial Elongation and Gas Pressure During Power Ascension for Rod 7, PBF IE-1

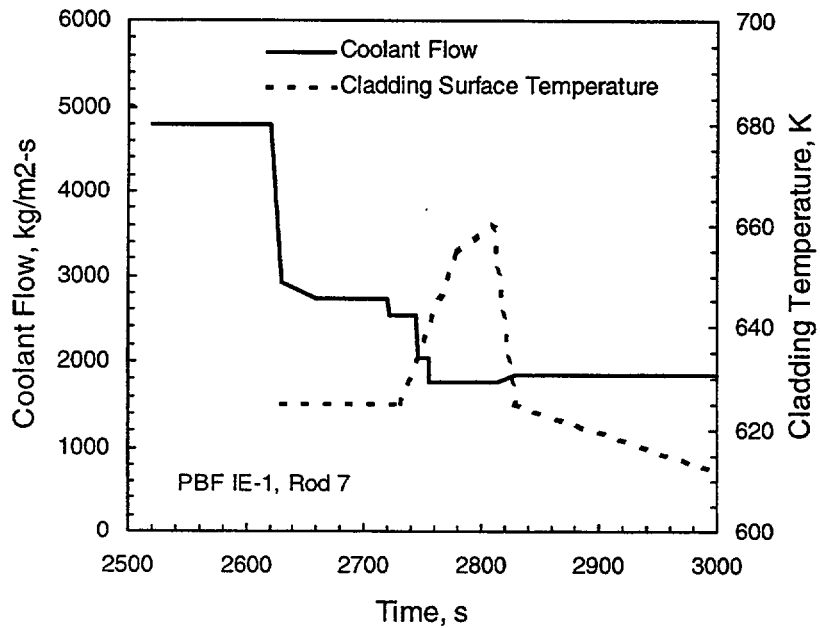


Figure A.54 Measured Cladding Temperature During Flow Reduction for Rod 7, PBF IE-1

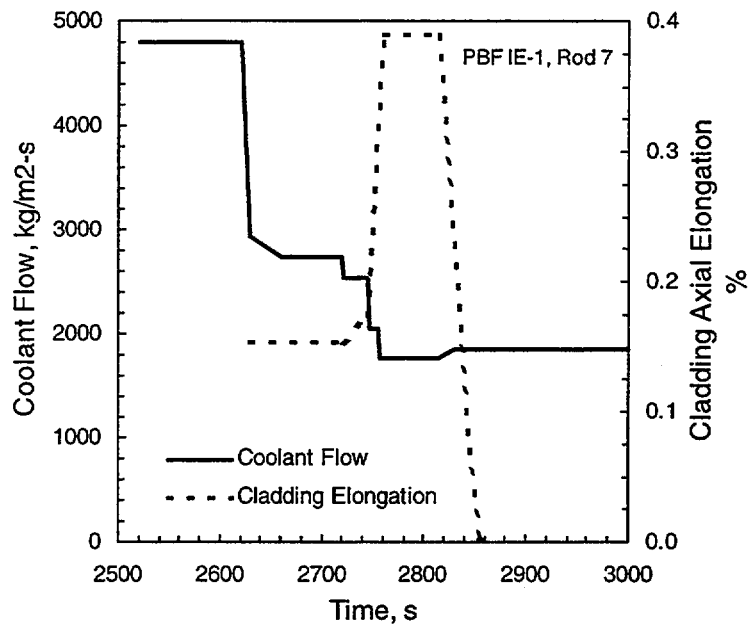


Figure A.55 Measured Cladding Axial Elongation During Flow Reduction for Rod 7, PBF IE-1

designed to characterize LWR fuel rods operated under both normal and abnormal environmental conditions. The specific objectives were to provide fuel rod thermal response under steady-state and oscillating power conditions, to investigate conditions at the on-set of boiling transition, and to provide thermal performance data during RIA excursions. Four non-irradiated BWR-type rods were used, with the rods having both fuel centerline and off-center thermocouples, gas pressure, and cladding elongation instrumentation.

The PBF was designed primarily for performing very high-power excursions and consists of a driver core in a water pool and a pressurized-water test loop capable of providing a range of test conditions. The central test space is operated as a neutron flux trap that permits high power densities in tested fuel rods relative to the active core. An in-pile tube fits in this central flux trap region and contains the test assemblies.

The PR-1 test consisted of four BWR-type rods with three different fuel densities and two different fill gas compositions. There was no steady-state irradiation prior to the calibration and transient irradiations. Rods 524-1 and 524-3 failed during the power-cooling mismatch tests, Rod 524-2 failed during the highest power burst, and Rod 524-4 (argon filled) survived the entire test sequence. Provided in Table A.13 is a summary of the design characteristics for the test rods, plus the coolant conditions.

Cycle 17 was selected for the code assessment. For this cycle, linear heat generation rate was held constant while flow was decreased and then restored. Linear heat generation rate was decreased after full flow was restored, but this portion of the cycle is not modeled for the assessment. The linear heat rate and flow histories for the assessment are presented in Figure A.56.

Table A.13 Basic Design Parameters for PBF PR-1 Test	
Parameter	Value
Cladding Material	Zircaloy-2
Cladding Outer and Inner Diameters	12.50 and 10.79 mm
Cladding Thickness	0.855 mm
Fuel Diameter	10.57 mm
Fuel-Cladding Radial Gap	0.110 mm
Fuel Pellet Length	10.57 mm
Fuel Density	Rod 524-1: 95%TD Rod 524-2: 92%TD Rods 524-3 and 524-4: 97%TD
Fuel Active Length	915 mm
Rod Total Length	1070 mm
Fill Gas (re-instrumented rod)	Rods 524-1, 524-2, 524-3: 100% He at 2.58 MPa Rod 525-4: 100% Ar at 2.58 MPa
Coolant Conditions	604K at 15.6 MPa

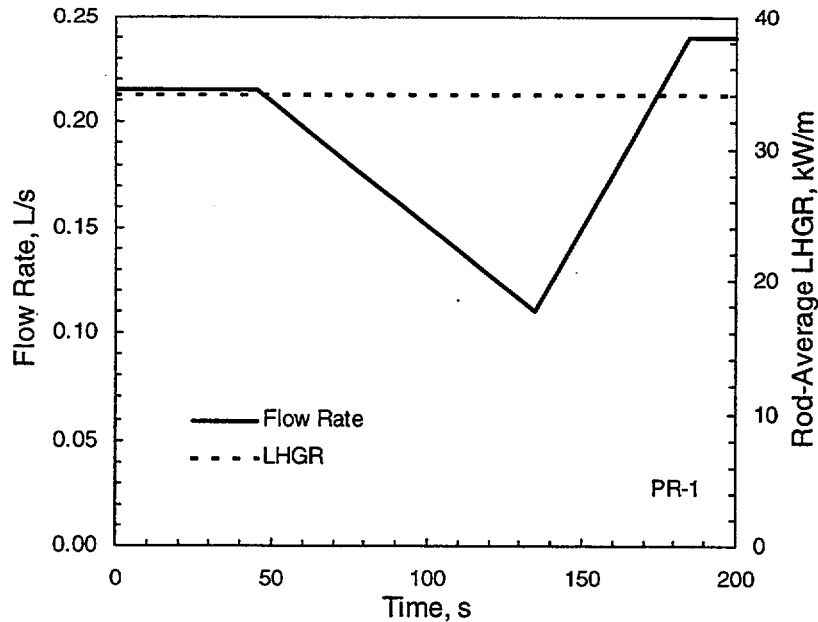


Figure A.56 Linear Heat Rate and Coolant Flow History for PR-1

The measured cladding elongation histories for three of the rods are presented in Figure A.57. Cladding surface temperature data for rod 524-3 are presented in Figure A.58. It may be seen from this figure that one side of the rod apparently went into DNB, while the other side did not. Measured centerline temperature history varied little during this cycle and was approximately 1885K for Rod 524-1 and 1785K for Rod 524-2. Similarly, measured gas pressure also remained fairly constant at approximately 9.0 MPa for Rod 524-1 and 9.7 MPa for Rod 524-2.

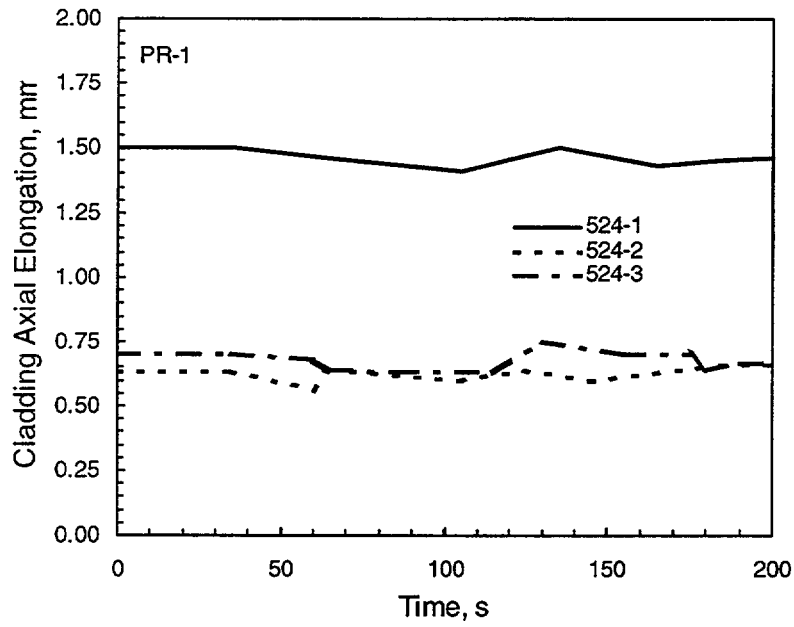


Figure A.57 Measured Cladding Elongation History for PR-1, Cycle 17

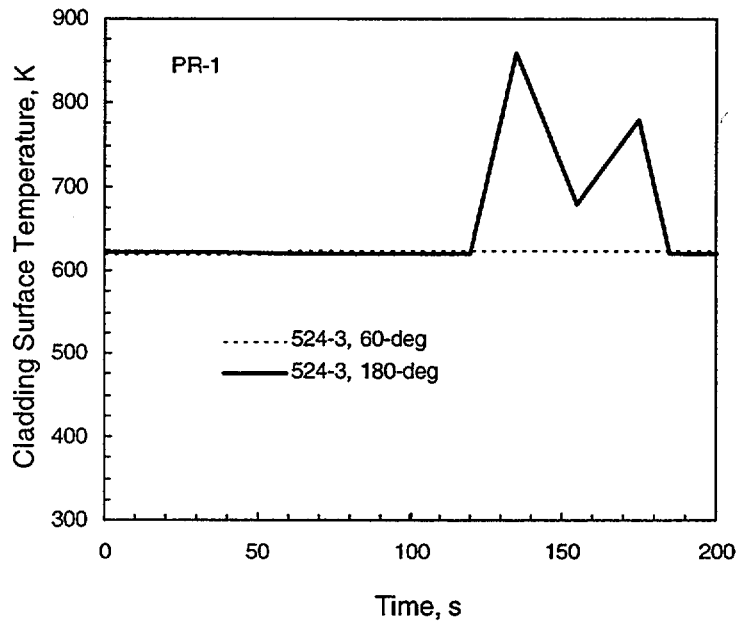


Figure A.58 Measured Cladding Surface Temperature for PR-1, Cycle 17

Sources

Sparks, D. T., R. H. Smith, and R. W. Garner. 1981. *Nuclear Fuel Rod Behavior During Normal and Abnormal Operating Conditions - Results of Test PR-1*. NUREG/CR-2126 (EGG-2102), Idaho National Engineering Laboratory, Idaho Falls, Idaho.

Smith, R. H. 1980. *Power Cooling Mismatch Test Series, Test PR-1, Experiment Predictions*. EGG-TFBP-5056, Idaho National Engineering Laboratory, Idaho Falls, Idaho.

APPENDIX B

FRAPTRAN INPUT FILES

APPENDIX B

FRAPTRAN INPUT FILES

Provided in this appendix are listings of the input files used to make the FRAPTRAN runs for comparison to the integral assessment cases. These input files are supplemented with discussions about how the input files were developed. For some cases, developing the input files was relatively straight forward using the information available in the test reports. For other cases, in order to best control the code and provide a meaningful comparison to the assessment data, development of the input files required additional effort and understanding of the experimental conditions.

An example of additional effort required in developing the input files was defining the coolant temperature history (time and axially) for the RIA and LOCA assessment cases. A decision was made to control the FRAPTRAN calculations for these assessment cases so that the calculated cladding temperatures would match the measured cladding temperature data as closely possible. FRAPTRAN does not have an option to input a cladding temperature history; therefore, the approach was to input coolant temperature histories equal to the measured cladding temperature histories along with a very high cladding-coolant heat transfer coefficient. Thus, the FRAPTRAN-calculated temperature history would be very close to the input coolant temperature history, which was developed from the measured cladding temperature history. This approach was taken to minimize the effect of the thermal-hydraulic models so that the response of the fuel and cladding models could be evaluated during the assessment.

For test rods with burnup, FRAPCON-3 was used to simulate the steady-state irradiation history prior to the transient and then to provide initialization of burnup-dependent variables for FRAPTRAN.

The data written into the file generated by FRAPCON-3 to initialize burnup-dependent parameters for a FRAPTRAN case will over-write any user input data for FRAPTRAN. This can result in a situation where the FRAPCON-3 end-of-life information may not be correct for initializing FRAPTRAN for refabricated rods. This particularly applies to design parameters such as gas composition and pressure where refabricated rods may be backfilled with a different gas composition and pressure than the end-of-life condition for the "mother" rod. The FRAPCON-3 file can be edited by the user to address this problem, and this was done with the FRAPCON-3 files for the NSRR and CABRI RIA cases. The end-of-life FRAPCON-3 results for the steady-state irradiation are based on the initial rod pressures and the calculated fission gas release during the history. It may be seen in Appendix A that the refabricated rods were usually filled with 100% helium and at a pressure different than either the beginning-of-life or end-of-life pressure of the "mother" rod. Therefore, the gas composition and gas moles at the last time step for the FRAPCON-3 file were edited to insert the gas composition used for the refabricated rods and a value for gas moles that would result in FRAPTRAN matching the as-fabricated gas pressure for the refabricated rods.

The following sections in this appendix provide descriptions of how coolant temperatures were specified based on the available cladding or coolant temperature data, and any other unique or important features of setting up the FRAPTRAN runs. In general, all cases were run with 15 radial fuel nodes. The number of axial nodes was dependent on the case, but generally consistent for each rod type/reactor type; i.e., NSRR RIA cases, NRU MT cases, etc.

B.1 Separate Effects Cases

The separate effects cases (IFA-432 and IFA-513) irradiated in the HBWR are straight forward cases to set up. Fuel rod design parameters are provided in Section A.1. Coolant conditions are provided in Table A.1 and do not change during the FRAPTRAN calculations. The axial power profiles are approximately cosine shaped and are provided in Tables B.1 through B.3, which provide the input files for the three cases.

Table B.1 FRAPTRAN Input for IFA-432, Rod 1 Assessment Case	

* FrapTran, transient fuel rod analysis code	*
-----*	
* CASE DESCRIPTION: IFA-432, Rod 1, BOL power ascension	*
* UNIT FILE DESCRIPTION	*
-----*	
* -- Input:	*
* 15 Water properties data	*
* -- Output:	*
* 6 STANDARD PRINTER OUTPUT	*
* 66 STRIPF FILE FOR GRAFITI	*
* -- Scratch:	*
* 5 SCRATCH INPUT FILE FROM ECHO1	*
* Input: FrapTran INPUT FILE	*

* GOESINS:	
FILE05='nullfile', STATUS='scratch', FORM='FORMATTED',	
CARRIAGE CONTROL='LIST'	
FILE15='sth2xt', STATUS='old', FORM='UNFORMATTED'	
* GOESOUTS:	
FILE06='out.ifa432r1bol', STATUS='UNKNOWN', FORMAT='FORMATTED'	
FILE66='stripf.ifa432r1bol', STATUS='UNKNOWN', FORM='FORMATTED',	
CARRIAGE CONTROL='LIST'	
/*****	
IFA-432, Rod 1, BOL power ascension	
\$begin	
ProblemStartTime = 0.0,	
ProblemEndTime = 1000.0,	
\$end	
start	
\$iodata	
unitin=1, dtpoa=50.0,0.0, inp=0, trest=0.0, dtplt=10	

Table B.1 (contd)

```
$end
$solution
  maxit=100, noiter=100, epsht1=1.0,
  naxn=4, nfmesh=15,
$end
$design
  RodLength=0.579, RodDiameter=0.012879,
  pelh=0.0127, FuelPelDiam=0.010681, roughf=2.16, frden=0.955, fgrns=6.0,
  gadoln=0.0,
  gapthk=1.14e-4, coldw=0.2, roughc=0.635, cldwdc=0.04,
  ncs=5, spl=0.05, scd=0.000889, swd=0.000762, vplen=4.74e-6,
  gfrac=1.0,6*0.0, gappr0=1.0e+5, tgas0=300.0,
$end
$power
  RodAvePower=0.0,0.0, 40.0,1000.0,
  AxPowProfile=0.844,0.0, 0.844,0.1448, 1.0,0.2895, 1.156,0.4343, 1.156,0.579,
  RadPowProfile=0.9142,0., 0.9300,0.0020938, 0.9612,0.0030686, 0.9962,0.0038278,
  1.0288,0.0043981, 1.0555,0.0048068, 1.0751,0.0050807, 1.0876,0.0052469,
  1.0942,0.0053322, 1.0967,0.0053400, 1.0971,0.0053500,
$end
$model
  metal='on', cathca=1,
  heat='on',
  cenvoi=1, zvoid1=0.0, zvoid2=0.579, rvoid=8.763e-4,
  deformation='on',
$end
$boundary
  heat='on', nvol2=1, press=2, pbh2=3.45e+6,0.0, 3.45e+6,1000.0,
  zone=1, htclev=0.579, htco=2, htca=3.0e+5,0.0, 3.0e+5,1000.0,
  tem=2, tblka=513.0,0.0, 513.0,1000.0,
$end
$tuning
$end
```

Table B.2 FRAPTRAN Input for IFA-432, Rod 3 Assessment Case

* FrapTran, transient fuel rod analysis code		*

* CASE DESCRIPTION: IFA-432, Rod 3, BOL power ascension		*

* UNIT FILE DESCRIPTION		*

* -- Input:		*
* 15 Water properties data		*

* -- Output:		*
* 6 STANDARD PRINTER OUTPUT		*
* 66 STRIPF FILE FOR GRAFITI		*

* -- Scratch:		*
* 5 SCRATCH INPUT FILE FROM ECHO1		*

* Input: FrapTran INPUT FILE		*

* GOESINS:		
FILE05='nullfile', STATUS='scratch', FORM='FORMATTED',		
CARRIAGE CONTROL='LIST'		
FILE15='sth2xt', STATUS='old', FORM='UNFORMATTED'		

* GOESOUTS:		
FILE06='out.ifa432r3bol', STATUS='UNKNOWN', FORMAT='FORMATTED'		
FILE66='stripf.ifa432r3bol', STATUS='UNKNOWN', FORM='FORMATTED',		
CARRIAGE CONTROL='LIST'		
/*****		
IFA-432, Rod 3, BOL power ascension		
\$begin		
ProblemStartTime = 0.0,		
ProblemEndTime = 1000.0,		
\$end		
start		
\$iodata		
unitin=1, dtpoa=50.0,0.0, inp=0, trest=0, dtplt=10		
\$end		
\$solution		
maxit=100, noiter=100, epsht1=1.0,		
naxn=4, nfmesh=11,		
\$end		
\$design		
RodLength=0.579, RodDiameter=0.012789,		
pelh=0.0127, FuelPelDiam=0.010833, roughf=2.16, frden=0.955, fgrns=6.0, gadoln=0.0,		
gapthk=3.81e-5, coldw=0.2, roughc=0.635, clwdwc=0.04,		
ncs=5, spl=0.05, scd=0.000889, swd=0.000762, vplen=4.74e-6,		
gfrac=1.,6*0., gappr0=1.0e+5, tgas0=300.0,		
\$end		
\$power		
RodAvePower=0.0,0.0, 40.0,1000.0,		
AxPowProfile=0.844,0., 0.844,0.1448, 1.0,0.2895, 1.156,0.4343, 1.156,0.579,		
RadPowProfile=0.9142, 0.0, 0.9300,0.0020938, 0.9612,0.0030686, 0.9962,0.0038278,		

Table B.2 (contd)	
1.0288,0.0043981, 1.0555,0.0048068, 1.0751,0.0050807, 1.0876,0.0052469,	
1.0942,0.0053322, 1.0967,0.0053400, 1.0971,0.0053500,	
\$end	
\$model	
metal='on', cathca=1,	
cenvoi=1, zvoid1=0.0, zvoid2=0.579, rvoid=8.763e-4,	
\$end	
\$boundary	
heat='on', nvol2=1, press=2, pbh2=3.45e+6,0., 3.45e+6,1000.,	
zone=1, htclev=0.579, htco=2, htca=3.0e+5,0., 3.0e+5,1000.,	
tem=2, tblka=513.0,0.0, 513.0,1000.0,	
\$end	
\$tuning	
\$end	

Table B.3 FRAPTRAN Input for IFA-513, Rod 6 Assessment Case	

* FrapTran, transient fuel rod analysis code	*

* /	*
* CASE DESCRIPTION: IFA-513, Rod 6, BOL power ascension	*
* /	*
* UNIT FILE DESCRIPTION	*
* ----	*
* -- Input:	*
* 15 Water properties data	*
* /	*
* -- Output:	*
* 6 STANDARD PRINTER OUTPUT	*
* 66 STRIPF FILE FOR GRAFITI	*
* /	*
* -- Scratch:	*
* 5 SCRATCH INPUT FILE FROM ECHO1	*
* /	*
* Input: FrapTran INPUT FILE	*
* /	*

* /	*
* GOESINS:	
FILE05='nullfile', STATUS='scratch', FORM='FORMATTED',	
CARRIAGE CONTROL='LIST'	
FILE15='sth2xt', STATUS='old', FORM='UNFORMATTED'	
* /	
* GOESOUTS:	
FILE06='out.ifa513r6bol', STATUS='UNKNOWN', FORMAT='FORMATTED'	
FILE66='stripf.ifa513r6bol', STATUS='UNKNOWN', FORM='FORMATTED',	
CARRIAGE CONTROL='LIST'	
/*****	
IFA-513, Rod 6, BOL power ascension	
\$begin	
ProblemStartTime = 0.0,	
ProblemEndTime = 1000.0,	
\$end	
start	
\$iodata	

Table B.3 (contd)	
unitin=1, dtpoa=50.0,0.0, inp=0, trest=0.0, dtplt=10,	
\$end	
\$solution	
maxit=100, noiter=100, epsht1=1.0,	
naxn=4, nfmesh=15,	
\$end	
\$design	
RodLength=0.780, RodDiameter=0.01280,	
pelh=0.0127, FuelPelDiam=0.01070, roughf=2.16, frden=0.955, fgrns=6.0, gadoln=0.0,	
gapthk=1.00e-4, coldw=0.2, roughc=0.635, clwdc=0.04,	
ncs=5, spl=0.05, scd=0.000889, swd=0.000762, vplen=4.74e-6,	
gfrac=0.77,0,0,0.23, gappr0=1.0e+5, tgas0=300.0,	
\$end	
\$power	
RodAvePower=0, 0, 50, 1000,	
AxPowProfile=0.73, 0, 0.94, 0.195, 1.07, 0.390, 1.11, 0.585, 1.04, 0.780	
RadPowProfile=0.9142,0., 0.9300,0.0020938, 0.9612,0.0030686, 0.9962,0.0038278,	
1.0288,0.0043981, 1.0555,0.0048068, 1.0751,0.0050807, 1.0876,0.0052469,	
1.0942,0.0053322, 1.0967,0.0053400, 1.0971,0.0053500,	
\$end	
\$model	
metal='on', cathca=1,	
cenvoi=1, zvoid1=0.0, zvoid2=0.780, rvoid=8.763e-4,	
deformation='on',	
\$end	
\$boundary	
heat='on', nvol2=1, press=2, pbh2=3.45e+6,0.0, 3.45e+6,1000.0,	
zone=1, htclew=0.780, htco=2, htca=3.0e+5,0.0, 3.0e+5,1000.0,	
tem=2, tblka=513.0,0.0, 513.0,1000.0,	
\$end	
\$tuning	
\$end	

B.2 NSRR RIA Cases

Two input parameters of importance for the RIA calculations are the power history and coolant (cladding) temperature history.

Power histories reported for the RIA experiments typically provide the total energy deposited (cal/g), peak fuel enthalpy (cal/g), and a plot of reactor power as a function of time. It is then necessary to convert these data to linear heat generation rate (LHGR) as a function of time to use as the code input. This can be done in a variety of ways and with varying levels of detail. For the FRAPTRAN assessments, detailed and simplified power histories were reviewed and it was decided to model the NSRR RIA power histories with a simple isosceles triangle shape. Peak LHGR values were provided by JAERI through private communication and compared to peak LHGR values derived from the peak fuel enthalpy and stated pulse width values. FRAPTRAN results were compared with the differing assumptions and few differences were found. Therefore, it was decided to use the JAERI-provided peak LHGR values with a pulse half-width for the isosceles triangle shape that resulted in matching the peak fuel enthalpy values. This decision results in triangles that are slightly wider than the stated pulse widths, which then partially approximates the tails on both sides of the power histories. Provided in Figure B.1 is an illustration of

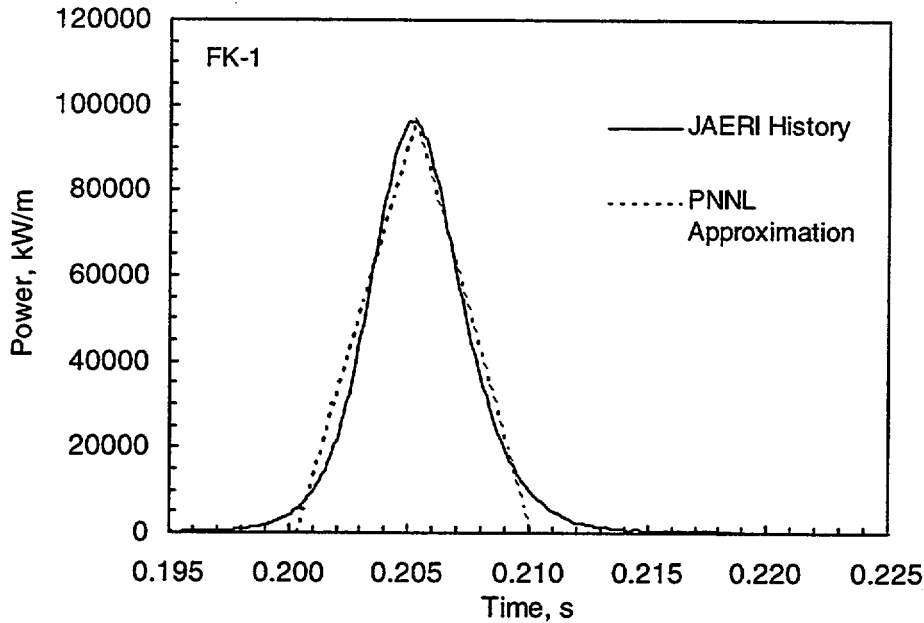


Figure B.1 Comparison of Potential RIA Power Histories for Rod FK-1

the differing possible power histories for Rod FK-1. Provided in Table B.4 is a summary of the experimental data and the assumed power history values used for the FRAPTRAN runs for the NSRR rods.

Because the axial power profile along the test rods was constant during both the steady-state and transient irradiations, a flat axial power profile was assumed for the FRAPTRAN calculations.

To define the burnup-dependent parameters for the FRAPTRAN runs, FRAPCON-3 runs were made for the base irradiations of all six test rods. Design parameters and very simple irradiation histories, with standard PWR or BWR coolant conditions, were used as input for FRAPCON-3. The FRAPCON-3 initialization files were then used with FRAPTRAN. As-fabricated dimensional values (which are in the FRAPTRAN input files) are overwritten when the FRAPCON-3 initialization file is read. The test rods for the RIA cases in the NSRR (Section A.2.1) were irradiated in stagnant water capsules with direct measurement of cladding temperatures using one to five cladding surface thermocouples. Therefore, the FRAPTRAN input coolant temperatures could be easily set equal to the measured cladding temperatures during the transients. The measured cladding temperatures were presented in figures in Section A.2.1. Because of the flat axial profile during the RIA

Table B.4 Measured and Assumed Power Histories for NSRR RIA Cases						
Parameter	HBO-6	MH-3	GK-1	OI-2	TS-5	FK-1
Peak Fuel Enthalpy, cal/g	85	67	93	108	98	130
Measured Pulse Half-Width, s	0.0045	0.0045	0.0045	0.0044	0.0044	0.0044
JAERI Peak LHGR, kW/m	39242	40420	56482	48943	108780	96166
Pulse Half-Width for Isosceles Triangle, s	0.00481	0.00490	0.00487	0.00490	0.00472	0.00492
Time of Peak LHGR, s	0.2069	0.1958	0.1945	0.2015	0.2005	0.2052

irradiations and the approximately adiabatic conditions, it was decided to specify a uniform coolant temperature history along the full length of the NSRR rods. Following is a discussion of the input coolant temperature histories for FRAPTRAN that were developed for each of the six test rods.

HBO-6

Rod HBO-6 was instrumented with three cladding surface thermocouples; however, one of the thermocouples failed early in the irradiation. The remaining two thermocouples were located approximately 32 mm below and above the fuel axial mid-plane (see Figure A.7). For the FRAPTRAN input, the coolant temperature history was specified as the average of the two cladding surface temperature measurements. The measured temperatures and the FRAPTRAN input history are illustrated in Figure B.2. The FRAPTRAN input file for HBO-6 is provided in Table B.5.

MH-3

Rod MH-3 was instrumented with just one cladding surface thermocouple located at the fuel axial mid-plane. Therefore, the coolant temperature history was specified as the measured cladding surface temperature as illustrated in Figure A.9. The FRAPTRAN input file for MH-3 is provided in Table B.6.

GK-1

Rod GK-1 was instrumented with just one cladding surface thermocouple located at the fuel axial mid-plane. Therefore, the coolant temperature history was specified as the measured cladding surface temperature as illustrated in Figure A.11. The FRAPTRAN input file for GK-1 is provided in Table B.7.

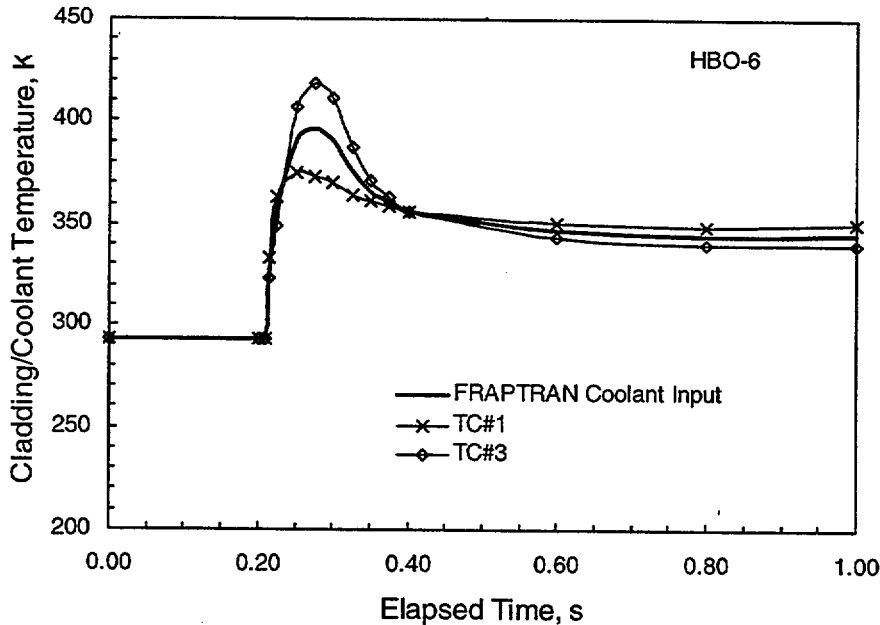


Figure B.2 FRAPTRAN Coolant Temperature Input History for HBO-6

Table B.5 FRAPTRAN Input for HBO-6 Assessment Case

```

*****
* FrapTran, Transient fuel rod analysis code
*
* CASE DESCRIPTION: Assessment - RIA Test HBO-6
*
FILE05='nullfile', STATUS='scratch', FORM='FORMATTED',
CARRIAGE CONTROL='LIST'
FILE15='sth2xt', STATUS='old', FORM='UNFORMATTED'
*
FILE06='out.hbo6', STATUS='UNKNOWN', CARRIAGE CONTROL='LIST'
FILE66='stripf.hbo6', STATUS='UNKNOWN', FORM='FORMATTED',
CARRIAGE CONTROL='LIST'
FILE22='restart.hbo6', STATUS='OLD', FORM='FORMATTED'
/*****
RIA Test Rod HBO-6 Specified Surface Temp
$begin
  ProblemStartTime=0.0,
  ProblemEndTime=1.0,
$end
start
$iodata
  unitin=1, unitout=1, dtpoa(1)=0.01,0.0,0.01,1.0,
  dtpit=0.005, trest=8.4672e07, inp=1,
$end
$solution
  dtmaxa(1)=0.0001, 0.0, 0.00001, 0.2021, 0.0001, 0.3,
  dtss=1.0, prsacc=0.001, tmpacl=0.001, maxit=100, noiter=100, epsht1=1.0,
  naxn=5, nfmesh=15,
$end
$design
  RodLength=0.135, RodDiameter=9.5e-3, rshd=0.003302, dishd=0.0003429,
  pelh=0.01523, dishv0=1.1788e-8, FuelPelDiam=0.00805, roughf=2.12, frden=0.95,
  bup=4354560.0, fotmtl=2.0, tsntrk=1773.0, fgrrns=10.0, gadoln=0.0, ncs=7,
  gapthk=0.85e-4, coldw=0.1, roughc=1.14, cldwdc=0.04, spl=4.57e-2, scd=0.008,
  swd=0.0008, vplen=1.15e-6, gfrac(1)=1.0, gappr0=0.10e6, tgas0=290.0,
$end
$power
  RodAvePower= 0, 0, 0, 0.2021, 39242, 0.2069, 0, 0.2117, 0, 1,
  AxPowProfile=1.0, 0.0, 1.0, 0.135,
  RadPowProfile= 0.8167, 0., 0.8213, 0.0007249, 0.8292, 0.001359,
    0.8412, 0.0019084, 0.8586, 0.0023791, 0.8834, 0.0027772,
    0.9189, 0.0031088, 0.9695, 0.0033802, 1.0414, 0.0035974,
    1.1426, 0.0037664, 1.2829, 0.0038934, 1.4736, 0.0039843,
    1.7249, 0.0040453, 2.0446, 0.0040823, 2.4439, 0.0041012,
    2.911, 0.0041082, 3.2572, 0.0041092,
  CladPower=0.0123,
$end
$model
  internal='on',
  metal='on', cathca=1,
  deformation='on', noball=0,
$end
$boundary
  heat='on'
  zone=1, htclev(1)=0.135,
  press=2, pbh2(1)=101325.0, 0.0, 101325.0, 1.0,

```

Table B.5 (contd)	
htco=2, htca(1,1)=2000000.0, 0.0, 2000000.0, 1.0,	
tem=13, tblka(1,1)= 290, 0, 293, 0.21, 356, 0.225, 391, 0.25, 396, 0.275,	
391, 0.3, 376, 0.325, 366, 0.35, 361, 0.375, 356, 0.4,	
348, 0.6, 345, 0.8, 345, 1.0	
\$end	
\$tuning	
\$end	

Table B.6 FRAPTRAN Input for MH-3 Assessment Case	

* FrapTran, transient fuel rod analysis code	*
-----	*
* CASE DESCRIPTION: JAERI Test Rod MH-3	*
* UNIT FILE DESCRIPTION	*
* ----	*
* -- Input:	*
* 15 Water properties data	*
* -- Output:	*
* 6 STANDARD PRINTER OUTPUT	*
* 66 STRIPF FILE FOR GRAFITI	*
* -- Scratch:	*
* 5 SCRATCH INPUT FILE FROM ECHO1	*
* Input: FrapTran INPUT FILE	*

* GOESINS:	
FILE05='nullfile', STATUS='scratch', FORM='FORMATTED',	
CARRIAGE CONTROL='LIST'	
FILE15='sth2xt', STATUS='old', FORM='UNFORMATTED'	
* GOESOUTS:	
FILE06='out.mh3', STATUS='UNKNOWN', CARRIAGE CONTROL='LIST'	
FILE66='stripf.mh3', STATUS='UNKNOWN', FORM='FORMATTED',	
CARRIAGE CONTROL='LIST'	
FILE22='restart.mh-3', STATUS='OLD', FORM='FORMATTED'	
/*****	
JAERI Test Rod MH-3 Specified Surface Temp	
\$begin	
ProblemStartTime = 0.0,	
ProblemEndTime = 1.0,	
\$end	
start	
\$iodata	
unitin=1, unitout=1, dtpoa(1)=0.01, dtplt=0.005,	
trest = 8.856E7, inp = 1,	
\$end	
\$solution	
dtmaxa(1)=0.0001, 0, 0.00001, 0.1909, 0.0001, 0.3,	
dtss=1.0, prsacc=0.001, tmpacl=0.001	

Table B.6 (contd)					
maxit=100, noiter=100, epsht1=1.0,					
naxn=5, nfmesh=15,					
\$end					
\$design					
RodLength=0.122, RodDiameter=10.72e-3,					
rshd=0.003302, dishd=.0003429, pelh=.01523, dishv0=1.1788e-8,					
FuelPelDiam=0.009290, roughf=2.12, frden=0.95, bup=38900.0, fotmtl=2.0,					
tsntrk=1773.0, fgrns=10.0, gadoln=0.0,					
gapthk=.95e-4, coldw=0.1, roughc=1.14, cldwdc=0.04,					
ncs=7, spl=4.57e-2, scd=.008, swd=.0008, vplen=5.37e-6,					
gfrac(1)=1.0, gappr0=4.57e6, tgas0=300.0,					
\$end					
\$power					
RodAvePower= 0, 0, 0, 0.1909, 40420, 0.1958, 0, 0.2007, 0, 1,					
AxPowProfile=0.9698276, 0.0, 1.0086207, 0.013, 1.0086207, 0.028,					
1.0086207, 0.038, 1.018319, 0.053, 1.018319, 0.073,					
1.0086207, 0.093, 0.9892241, 0.103, 0.9698276, 0.122,					
RadPowProfile=0.979, 0.0, 0.9803, 0.0008192, 0.9835, 0.0015358,					
0.9879, 0.0021568, 0.9929, 0.0026887, 0.998, 0.0031388,					
1.0029, 0.0035137, 1.0073, 0.0038206, 1.0111, 0.0040661,					
1.0142, 0.0042572, 1.0167, 0.0044008, 1.0185, 0.0045038,					
1.0197, 0.0045727, 1.0205, 0.0046145, 1.0209, 0.0046359,					
1.021, 0.0046439, 1.021, 0.004645,					
CladPower=0.0123					
\$end					
\$model					
internal='on',					
metal='on', cathca=1,					
deformation='on', noball=0,					
\$end					
\$boundary					
heat='on'					
press=2, pbh2(1)=101325.0, 0.0, 101325.0, 1.0,					
zone=1, htclev(1)=0.122,					
htco=2, htca(1,1)=2000000.0, 0.0, 2000000.0, 1.0,					
tem=12, tblka(1,1)=					
293, 0, 293, 0.2; 428, 0.238, 417, 0.272, 436, 0.329,					
475, 0.380, 452, 0.507, 428, 0.641, 406, 0.696, 374,					
0.743, 364, 0.8, 358, 1.0					
\$end					
\$tuning					
\$end					

OI-2

Rod OI-2 was instrumented with just one cladding surface thermocouple located at the fuel axial mid-plane. Therefore, the coolant temperature history was specified as the measured cladding surface temperature as illustrated in Figure A.14. The FRAPTRAN input file for OI-2 is provided in Table B.8.

TS-5

Rod TS-5 was instrumented with five thermocouples; two at 32 mm below the fuel axial mid-plane, one at the fuel axial mid-plane, and two at 32 mm above the fuel axial mid-plane. The measured data from

Table B.7 FRAPTRAN Input for GK-1 Assessment Case

* FrapTran, Transient fuel rod analysis code	*
*	*
* CASE DESCRIPTION: Assessment - RIA Test GK-1	*
*	*
FILE05='nullfile', STATUS='scratch', FORM='FORMATTED',	*
CARRIAGE CONTROL='LIST'	*
FILE15='sth2xt', STATUS='old', FORM='UNFORMATTED'	*
*	*
FILE06='out.gk1', STATUS='UNKNOWN', CARRIAGE CONTROL='LIST'	*
FILE66='stripf.gk1', STATUS='UNKNOWN', FORM='FORMATTED',	*
CARRIAGE CONTROL='LIST'	*
FILE22='restart.gk1', STATUS='old', FORM='FORMATTED'	*
/*****	
JAERI Test Rod GK-1 Specified Surface Temp	
\$begin	
ProblemStartTime=0.0,	
ProblemEndTime=1.0,	
\$end	
start	
\$iodata	
unitin=1, unitout=1, dtpoa(1)=0.01, dtplt=0.005, trest = 0.864E8 , inp=1,	
\$end	
\$solution	
dtmaxa(1)=0.0001, 0, 0.000001, 0.1896, 0.0001, 0.3	
dtss=1.0, prsacc=0.001, tmpacl=0.001, maxit=100, noiter=100, epsht1=1.0,	
naxn=5, nfmesh=15,	
\$end	
\$design	
RodLength=0.135, RodDiameter=10.72e-3,	
rshd=0.003302, dishd=.0003429, pelh=.01523, dishv0=1.1788e-8,	
FuelPelDiam=0.00929, roughf=2.12, frden=0.95, bup=3637744.0, fotmt1=2.0,	
tsntrk=1773.0, fgrns=10.0, gadoln=0.0, gapthk=0.95e-4, coldw=0.1, roughc=1.14,	
cldwdc=0.04, ncs=7, spl=4.57e-2, scd=0.008, swd=0.0008, vplen=1.15e-6,	
gfrac(1)=1, gappr0=0.10e6, tgas0=300.0,	
\$end	
\$power	
RodAvePower=0, 0, 0, 0.1896, 56482, 0.1945, 0, 0.1994, 0, 1,	
AxPowProfile=1.0, 0.0, 1.0, 0.135,	
RadPowProfile=0.846, 0.0, 0.8495, 0.0008366, 0.8562, 0.0015684,	
0.8662, 0.0022022, 0.8806, 0.002745, 0.901, 0.0032041,	
0.93, 0.0035865, 0.9716, 0.0038993, 1.0313, 0.0041495,	
1.1164, 0.0043443, 1.2363, 0.0044906, 1.4018, 0.0045954,	
1.6243, 0.0046657, 1.9118, 0.0047082, 2.2605, 0.0047301,	
2.6396, 0.0047382, 2.9367, 0.0047393,	
CladPower=0.0123	
\$end	
\$model	
internal='on',	
metal='on', cathca=1,	
deformation='on', noball=0,	
\$end	
\$boundary	
heat='on'	

Table B.7 (contd)
press=2, pbh2(1)=101325.0, 0.0, 101325.0, 1.0,
zone=1, htclv(1)=0.135,
htco=2, htca(1,1)=2000000.0, 0.0, 2000000.0,1.0,
tem=8, tblka(1,1)=
293, 0, 297, 0.188, 371, 0.212, 371, 0.5, 541, 0.682,
490, 0.842, 352, 0.912, 348, 1,
\$end
\$tuning
\$end

Table B.8 FRAPTRAN Input for OI-2 Assessment Case	

* FrapTran, Transient fuel rod analysis code	*
*	*
* CASE DESCRIPTION: Assessment - RIA Test IO-2	*
*	*
FILE05='nullfile', STATUS='scratch', FORM='FORMATTED',	*
CARRIAGE CONTROL='LIST'	*
FILE15='sth2xt', STATUS='old', FORM='UNFORMATTED'	*
*	*
FILE06='out.oi2', STATUS='UNKNOWN', CARRIAGE CONTROL='LIST'	*
FILE66='stripf.oi2', STATUS='UNKNOWN', FORM='FORMATTED',	*
CARRIAGE CONTROL='LIST'	*
FILE22='restart.oi2', STATUS='old', FORM='FORMATTED'	*
/*****	
JAERI Test OI-2 Specified Surface Temp	
\$begin	
ProblemStartTime=0.0,	
ProblemEndTime=1.0,	
\$end	
start	
\$iodata	
unitin=1, unitout=1, dtpoa(1)=0.01, dtplt=.005,trest = 0.7836E8, inp=1,	
\$end	
\$solution	
dtmaxa(1)=0.0001, 0.0, 0.00001, 0.1966, 0.0001, 0.3,	
dtss=1.0, prsacc=0.001, tmpacl=0.001, maxit=100, noiter=100, epsht1=1.0,	
naxn=5, nfmesh=15,	
\$end	
\$design	
RodLength=0.135, RodDiameter=9.5e-3,	
rshd=0.003302, dishd=.0003429, pelh=.01523, dishv0=1.1788e-8,	
FuelPelDiam=0.00805, roughf=2.12, frden=0.95, bup=4354560.0, fotmt1=2.0,	
tsntrk=1773.0, fgrns=10.0,gadoln=0.0, gapthk=0.85e-4, coldw=0.1, roughc=1.14,	
clwdc=0.04, ncs=7, spl=4.57e-2, scd=0.008, swd=0.0008, vplen=1.15e-6,	
gfrac(1)=1, gappr0=0.10e6, tgas0=300.0,	
\$end	
\$power	
RodAvePower= 0, 0, 0, 0.1966, 48943, 0.2015, 0, 0.2064, 0, 1,	
AxPowProfile=1.0, 0.0, 1.0, 0.135,	
RadPowProfile= 0.8167, 0.0, 0.8213, 0.0007249, 0.8292, 0.0013590,	
0.8412, 0.0019084, 0.8586, 0.0023791, 0.8834, 0.0027772,	
0.9189, 0.0031088, 0.9695, 0.0033802, 1.0414, 0.0035974,	
1.1426, 0.0037664, 1.2829, 0.0038934, 1.4736, 0.0039843,	

Table B.8 (contd)				
1.7249,	0.0040453,	2.0446,	0.0040823,	2.4439,
2.911,	0.0041082,	3.2572,	0.0041092,	0.0041012,
CladPower=0.0123,				
\$end				
\$model				
internal='on',				
metal='on', cathca=1,				
deformation='on', noball=0,				
\$end				
\$boundary				
heat='on'				
press=2, pbh2(1)=101325.0, 0.0, 101325.0, 1.0,				
zone=1, htclev(1)=0.135,				
htco=2, htca(1,1)=2000000.0, 0.0, 2000000.0,1.0,				
tem=11, tblka(1,1)=				
293, 0, 293, 0.2, 311, 0.282, 461, 0.298, 611, 0.316, 649,				
0.371, 638, 0.4, 536, 0.457, 359, 0.5, 329, 0.6, 329, 1,				
\$end				
\$tuning				
\$end				

one thermocouple at each of the axial locations was shown in Figure A.17. The measured cladding temperatures were approximately 373K throughout the first second of the transient, with some apparent oscillations and one apparent spike to 443K. Therefore, the input coolant history for FRAPTRAN is assumed to be a constant 373K after the power pulse. The FRAPTRAN input file for TS-5 is provided in Table B.9.

FK-1

Rod FK-1 was instrumented with three cladding surface thermocouples; each of which showed a different cladding temperature history (see Figure A.20). It was decided to define the input coolant history for FRAPTRAN as the approximate average of TC#1 (32 mm below fuel axial mid-plane) and TC#2 (at fuel axial mid-plane). Provided in Figure B.3 is an illustration of the two measured cladding temperature histories and the assumed input FRAPTRAN coolant temperature history. The FRAPTRAN input file for FK-1 is provided in Table B.10.

B.3 CABRI RIA Cases

Two input parameters of importance for the RIA calculations are the power history and coolant (cladding) temperature history.

Power histories for the RIA experiments typically provide the total energy deposited (cal/g), peak fuel enthalpy (cal/g), and a plot of reactor power as a function of time. It is then necessary to convert these data to LHGR as a function of time to use as the code input. For the FRAPTRAN assessment of the CABRI RIA cases, it was decided to model the power histories with a simple isosceles triangle shape as was done for the NSRR RIA cases. However, CABRI-supplied peak LHGR values were not available.

Table B.9 FRAPTRAN Input for TS-5 Assessment Case

* FrapTran, Transient fuel rod analysis code	*
*	
* CASE DESCRIPTION: Assessment - RIA Test TS-5	*
*	
FILE05='nullfile', STATUS='scratch', FORM='FORMATTED',	*
CARRIAGE CONTROL='LIST'	*
FILE15='sth2xt', STATUS='old', FORM='UNFORMATTED'	*
*	
FILE06='out.ts5', STATUS='UNKNOWN', CARRIAGE CONTROL='LIST'	*
FILE66='stripf.ts5', STATUS='UNKNOWN', FORM='FORMATTED',	*
CARRIAGE CONTROL='LIST'	*
FILE22='restart.ts5', STATUS='old', FORM='FORMATTED'	*
/*****	
JAERI Test Rod TS-5 Specified Surface Temp	
\$begin	
ProblemStartTime=0.0,	
ProblemEndTime=1.0,	
\$end	
start	
\$iodata	
unitin=1, unitout=1, dtpoa(1)=0.01, dtplt=0.01, trest = 0.10584E9, inp=1,	
\$end	
\$solution	
dtmaxa(1)=0.0001, 0.0, 0.00001, 0.1958, 0.0001, 0.3,	
dtss=1.0, prsacc=0.001, tmpac1=0.001, maxit=100, noiter=100, epshtl=1.0,	
naxn=5, nfmesh=15,	
\$end	
\$design	
RodLength=0.135, RodDiameter=14.3e-3,	
rshd=0.003302, dishd=.0003429, pelh=.01523, dishv0=1.1788e-8,	
tsntrk=1773.0, FuelPelDiam=0.01237, roughf=2.12, frden=.95, bup=4354560.,	
fortml=2.0, fgrns=10.0, gadoln=0.0, gapthk=1.6e-4, coldw=0.1, roughc=1.14,	
cldwdc=0.04, ncs=7, spl=4.57e-2, scd=0.008, swd=0.0008, vplen=1.15e-6,	
gfrac(1)=1, gappr0=0.10e6, tgas0=300.0,	
\$end	
\$power	
RodAvePower=0, 0, 0, 0.1958, 108780, 0.2005, 0, 0.2052, 0, 1,	
AxPowProfile=1.0, 0.0, 1.0, 0.135,	
RadPowProfile= 0.8167, 0.0, 0.8213, 0.0007249, 0.8292, 0.001359,	
0.8412, 0.0019084, 0.8586, 0.0023791, 0.8834, 0.0027772,	
0.9189, 0.0031088, 0.9695, 0.0033802, 1.0414, 0.0035974,	
1.1426, 0.0037664, 1.2829, 0.0038934, 1.4736, 0.0039843,	
1.7249, 0.0040453, 2.0446, 0.0040823, 2.4439, 0.0041012,	
2.911, 0.0041082, 3.2572, 0.0041092,	
CladPower= 0.0123,	
\$end	
\$model	
internal='on',	
metal='on', cathca=1,	
deformation='on', noball=0,	
\$end	
\$boundary	
heat='on'	
press=2, pbh2(1)=101325.0, 0.0, 101325.0, 1.0,	

Table B.9 (contd)	
zone=1, htclev(1)=0.135,	
htco=2, htca(1,1)=2000000.0, 0.0, 2000000.0,1.0,	
tem=4, tblka(1,1)= 298, 0, 298, 0.2, 373, 0.25, 373, 1,	
\$end	
\$tuning	
\$end	

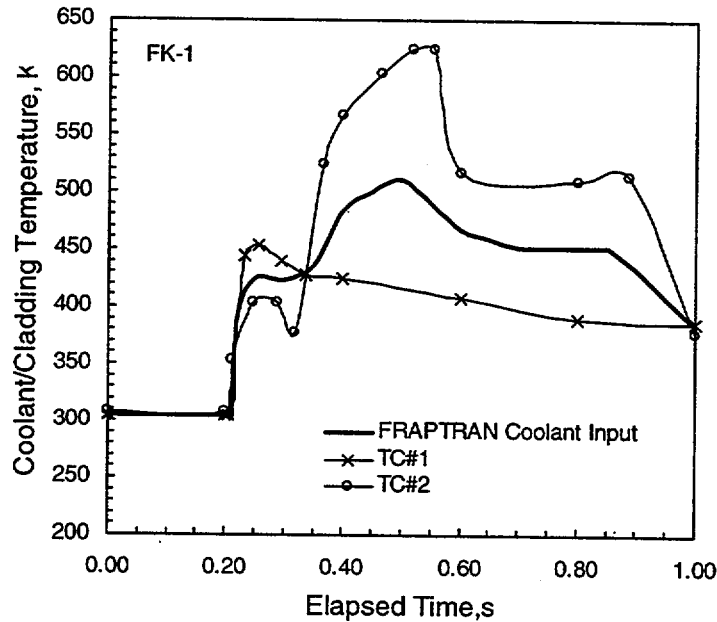


Figure B.3 FRAPTRAN Coolant Temperature Input History for FK-1

Therefore, peak LHGR values were derived using the peak fuel enthalpy, the stated pulse width, and the fuel rod design parameters. Provided in Table B.11 is a summary of the experimental data and the assumed power history values used for the FRAPTRAN runs for the CABRI rods.

The power pulse for Rep-Na4 resulted in a double peak because of the attempt to widen the pulse (see Figure A.24). For modeling the transient with FRAPTRAN, it was decided to model the pulse as a single peak, but with the same total energy deposition as the experiment.

The axial power profiles during the RIA transients were not flat but were peaked (peak to average ratio of approximately 1.1). The axial power profiles are illustrated in Figure B.4. Therefore, five axial nodes were used for the FRAPTRAN calculations to approximately model the axial power profiles during the test irradiation.

To define the burnup-dependent parameters for the FRAPTRAN runs, FRAPCON-3 runs were made for the base irradiations for all three test rods. Design parameters and very simple irradiation histories, with standard PWR coolant conditions, were used as input for FRAPCON-3. The FRAPCON-3 initialization files were then used with FRAPTRAN. As-fabricated dimensional values (which are in the input files) are overwritten when the FRAPCON-3 initialization file is read.

Table B.10 FRAPTRAN Input for FK-1 Assessment Case

* FrapTran, Transient fuel rod analysis code	*
*	*
* CASE DESCRIPTION: Assessment - RIA Test FK-1	*
*	*
FILE05='nullfile', STATUS='scratch', FORM='FORMATTED',	*
CARRIAGE CONTROL='LIST'	*
FILE15='sth2xt', STATUS='old', FORM='UNFORMATTED'	*
*	*
FILE06='out.fk1', STATUS='UNKNOWN', CARRIAGE CONTROL='LIST'	*
FILE66='stripf.fk1', STATUS='UNKNOWN', FORM='FORMATTED',	*
CARRIAGE CONTROL='LIST'	*
FILE22='restart.fk1', STATUS='old', FORM='FORMATTED'	*
/*****	
JAERI Test FK-1 Specified Surface Temp	
\$begin	
ProblemStartTime=0.0,	
ProblemEndTime=1.0,	
\$end	
start	
\$iodata	
unitin=1, unitout=1, dtpoa(1)=0.001, dtplt=0.001, trest = 0.14256E9 ,inp=1,	
\$end	
\$solution	
dtmaxa(1)=0.0001, 0.0, 0.000001, 0.2003,0.0001, 0.3,	
dtss=1.0, prsacc=0.001,tmpacl=0.001, maxit=100, noiter=100, epsht1=1.0,	
naxn=5, nfmesh=15,	
\$end	
\$design	
RodLength=0.135, RodDiameter=12.27e-3,	
rshd=0.003302, dishd=.0003429, pelh=.01523, dishv0=1.1788e-8,	
FuelPelDiam=0.01031, roughf=2.12, frden=0.95, bup=4354560.0, fotmt1=2.0,	
tsntrk=1773.0, fgrns=10.0,gadoln=0.0,	
gapthk=1.2e-4, coldw=.1, roughc=1.14,	
cldwdc=0.04, ncs=7, spl=4.57e-2, scd=0.008, swd=0.0008, vplen=1.15e-6,	
gfrac(1)=1, gappr0=0.10e6, tgas0=300.0,	
\$end	
\$power	
RodAvePower=0, 0, 0, 0.2003, 96166, 0.2052, 0, 0.2101, 0, 1,	
AxPowProfile=1.0, 0.0, 1.0, .135,	
RadPowProfile= 0.8167, 0., 0.8213, 0.0007249, 0.8292, 0.001359,	
0.8412, 0.0019084, 0.8586, 0.0023791, 0.8834, 0.0027772,	
0.9189, 0.0031088, 0.9695, 0.0033802, 1.0414, 0.0035974,	
1.1426, 0.0037664, 1.2829, 0.0038934, 1.4736, 0.0039843,	
1.7249, 0.0040453, 2.0446, 0.0040823, 2.4439, 0.0041012,	
2.911, 0.0041082, 3.2572, 0.0041092,	
CladPower=0.0123	
\$end	
\$model	
internal='on',	
metal='on', cathca=1,	
deformation='on', noball=0,	
\$end	
\$boundary	
heat='on'	
press=2, pbh2(1)=101325.0, 0.0, 101325.0, 1.0,	

Table B.10 (contd)	
zone=1, htclev(1)=0.135,	
htco=2, htca(1,1)=2000000.0, 0.0, 2000000.0,1.0,	
tem=8, tblka(1,1)= 305, 0, 305, 0.21, 393, 0.25, 436,	
0.35, 510, 0.50, 452, 0.70, 452, 0.85, 383, 1.0,	
\$end	
\$tuning	
\$end	

Table B.11 Measured and Assumed Power Histories for CABRI RIA Cases			
Parameter	REP-Na3	REP-Na4	REP-Na5
Peak Fuel Enthalpy, cal/g	125	99	115
Measured Pulse Half-Width, s	0.0095	0.0640	0.0090
Derived Peak LHGR, kW/m	30255	3557	29380
Time of Peak LHGR, s	0.0830	0.5650	0.0800

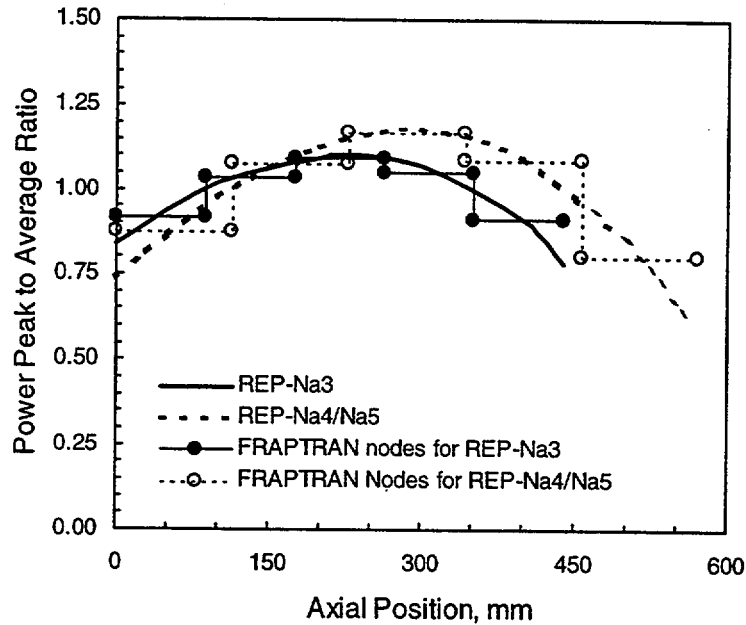


Figure B.4 Axial Power Profiles for CABRI RIA Tests

For the CABRI RIA assessment cases, the FRAPTRAN input coolant temperature histories were based on the measured coolant temperature histories. The test rods for the RIA cases in CABRI (Section A.2.2) were irradiated in flowing liquid sodium with measurement of the coolant temperature but not the cladding temperature. Coolant temperature was measured at input, approximately fuel axial mid-plane, and top of the fuel column. Because of the high heat transfer properties of sodium, the coolant temperature is assumed to be approximately equal to the cladding temperature for these cases. Following is a discussion of the input coolant temperature histories for FRAPTRAN that were developed for each of the three test rods.

REP-Na3

Test REP-Na3 was instrumented with seven coolant thermocouples; one at the test inlet that read a constant 553K, three at the fuel axial mid-plane, and three at the top of the fuel column. Provided in Figure B.5 is an illustration of the average coolant temperatures at each of the three axial positions. To specify the coolant temperature history for REP-Na3, the coolant channel was divided into five axial zones. For FRAPTRAN, the coolant temperature was assumed to simply vary linearly along the test rod from 553K at the inlet to the average measured coolant temperature at the top of the fuel column. The resulting input coolant temperature history is provided in Table B.12 which is a listing of the FRAPTRAN input file for REP-Na3.

REP-Na4

Test REP-Na4 was instrumented with seven coolant thermocouples; one at the test inlet that read a constant 553K, three at the fuel axial mid-plane, and three at the top of the fuel column. Provided in Figure B.6 is an illustration of the average coolant temperatures at each of the three axial positions. To specify the coolant temperature history for REP-Na4, the coolant channel was divided into five axial zones. For FRAPTRAN, the coolant temperature was assumed to simply vary linearly along the test rod from 553K at the inlet to the average measured coolant temperature at the top of the fuel column. The resulting input coolant temperature history is provided in Table B.13 which is a listing of the FRAPTRAN input file for REP-Na4.

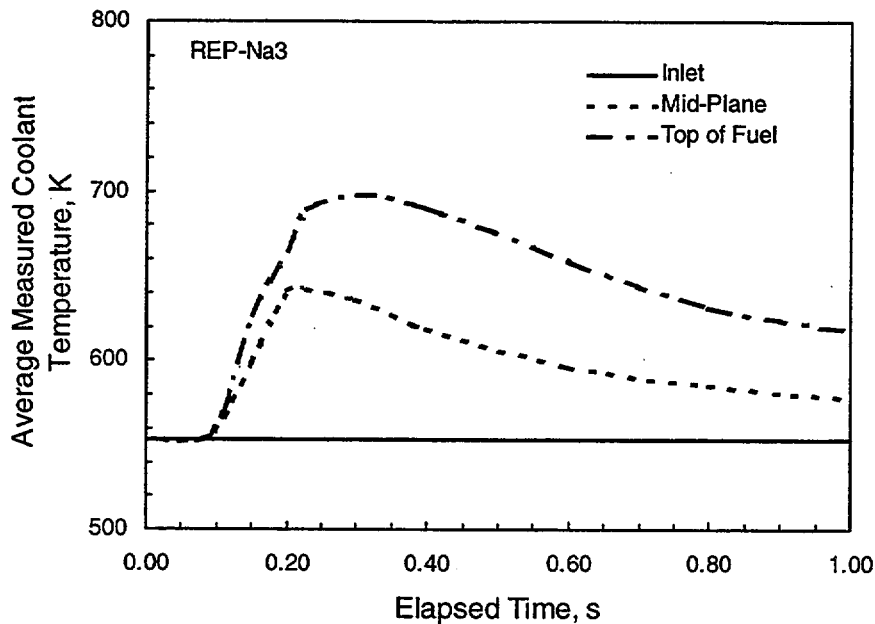


Figure B.5 Coolant Temperature History for REP-Na3

Table B.12 FRAPTRAN Input for REP-Na3 Assessment Case

* FrapTran, Transient fuel rod analysis code	*
*	*
* CASE DESCRIPTION: Assessment - RIA Test Na-3	*
*	*
FILE05='nullfile', STATUS='scratch', FORM='FORMATTED',	*
CARRIAGE CONTROL='LIST'	*
FILE15='sth2xt', STATUS='old', FORM='UNFORMATTED'	*
*	*
FILE06='out.na3', STATUS='UNKNOWN', CARRIAGE CONTROL='LIST'	*
FILE66='stripf.na3', STATUS='UNKNOWN', FORM='FORMATTED',	*
CARRIAGE CONTROL='LIST'	*
FILE22='restart.na3', STATUS='old', FORM='FORMATTED'	*
/*****	
IPNS RIA Test Na-3	
\$begin	
ProblemStartTime=0.0,	
ProblemEndTime=1.0,	
\$end	
start	
\$iodata	
unitin=1, unitout=1, dtpoa(1)=0.01, dtplt=0.001, trest = 0.1037E+09, inp=1,	
\$end	
\$solution	
dtmaxa(1)=0.0001, 0.0, 0.000001, 0.0735, 0.00001, 0.2,	
dtss=1.0, prsacc=0.001, tmpac1=0.001, maxit=100, noiter=100, epsht1=1.0,	
naxn=5, nfmesh=15,	
\$end	
\$design	
RodLength=0.44, RodDiameter=9.508e-3, roughc=1.14,	
rshd=0.003302, dishd=0.0003429, pelh=0.01523, dishv0=1.1788e-8,	
FuelPelDiam=0.0082184, roughf=2.12, frden=0.9475, bup=4354560.0, fotmt1=2.0,	
tsntrk=1773.0, fgrns=10.0, gadoln=0.0, gapthk=0.82e-4, coldw=0.1,	
cldwdc=0.04, ncs=7, spl=4.57e-2, scd=0.008, swd=0.0008, vplen=1.15e-6,	
gfrac(1)=1.0, gappr0=0.10e6, tgas0=300.0,	
\$end	
\$power	
RodAvePower=0, 0, 0, 0.0735, 30255, 0.0830, 0, 0.0925, 0, 1	
AxPowProfile=0.84, 0, 1.02, 0.1, 1.09, 0.2, 1.10, 0.22, 1.07, 0.3, 0.91, 0.4, 0.78;	
0.44,	
RadPowProfile= 0.8167, 0.0, 0.8213, 0.0007249, 0.8292, 0.001359,	
0.8412, 0.0019084, 0.8586, 0.0023791, 0.8834, 0.0027772,	
0.9189, 0.0031088, 0.9695, 0.0033802, 1.0414, 0.0035974,	
1.1426, 0.0037664, 1.2829, 0.0038934, 1.4736, 0.0039843,	
1.7249, 0.0040453, 2.0446, 0.0040823, 2.4439, 0.0041012,	
2.911, 0.0041082, 3.2572, 0.0041092,	
CladPower=0.0123,	
\$end	
\$model	
internal='on',	
metal='on', cathca=1,	
deformation='on', noball=1,	
\$end	
\$boundary	
heat='on'	
press=2, pbh2(1)=101325.0, 0.0, 101325.0, 1.0,	

Table B.12 (contd)	
zone=5, htclev =	0.088, 0.176, 0.264, 0.352, 0.440
htco=2, htca(1,1)=	2000000, 0, 2000000, 1,
	htca(1,2)= 2000000, 0, 2000000, 1,
	htca(1,3)= 2000000, 0, 2000000, 1,
	htca(1,4)= 2000000, 0, 2000000, 1,
	htca(1,5)= 2000000, 0, 2000000, 1,
tem=8,	
tblka(1,1)= 553, 0, 554, 0.1, 564, 0.2, 568, 0.3,	
	567, 0.4, 564, 0.6, 561, 0.8, 560, 1,
tblka(1,2)= 553, 0, 555, 0.1, 586, 0.2, 597, 0.3,	
	594, 0.4, 585, 0.6, 577, 0.8, 573, 1,
tblka(1,3)= 553, 0, 556, 0.1, 608, 0.2, 626, 0.3,	
	621, 0.4, 606, 0.6, 593, 0.8, 586, 1,
tblka(1,4)= 553, 0, 557, 0.1, 630, 0.2, 655, 0.3,	
	648, 0.4, 627, 0.6, 609, 0.8, 599, 1,
tblka(1,5)= 553, 0, 558, 0.1, 652, 0.2, 684, 0.3,	
	675, 0.4, 648, 0.6, 625, 0.8, 612, 1,
\$end	
\$tuning	
\$end	

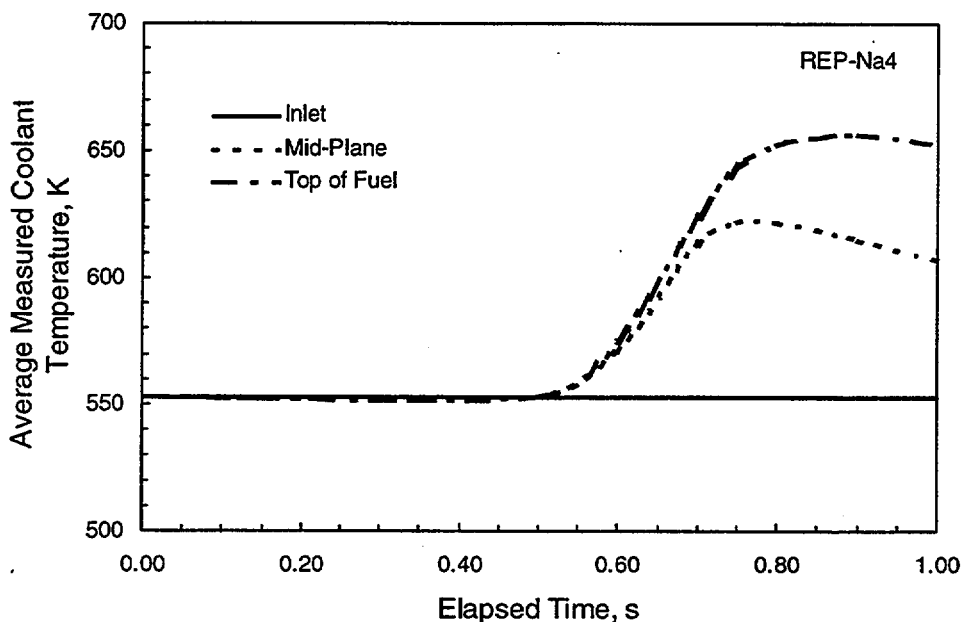


Figure B.6 Coolant Temperature History for REP-Na4

REP-Na5

Test REP-Na5 was instrumented with seven coolant thermocouples; one at the test inlet that read a constant 553K, three at the fuel axial mid-plane, and three at the top of the fuel column (one of the top coolant thermocouples failed). Provided in Figure B.7 is an illustration of the average coolant temperatures at each of the three axial positions. To specify the coolant temperature history for REP-Na5, the coolant channel was divided into five axial zones. For FRAPTRAN, the coolant temperature was

Table B.13 FRAPTRAN Input for REP-Na4 Assessment Case

```

*****
* FrapTran, Transient fuel rod analysis code
*
* CASE DESCRIPTION: Assessment - RIA Test Na-4
*
FILE05='nullfile', STATUS='scratch', FORM='FORMATTED',
CARRIAGE CONTROL='LIST'
FILE15='sth2xt', STATUS='old', FORM='UNFORMATTED'
*
FILE06='out.na4', STATUS='UNKNOWN', CARRIAGE CONTROL='LIST'
FILE66='stripf.na4', STATUS='UNKNOWN', FORM='FORMATTED',
CARRIAGE CONTROL='LIST'
FILE22='restart.na4', STATUS='old', FORM='FORMATTED'
/*****
IPNS RIA Test Na-4
$begin
  ProblemStartTime=0.0,
  ProblemEndTime=1.0,
$end
start
$iodata
  unitin=1, unitout=1, dtpoa(1)=0.01, dtplt=0.005, trest = 8.4672e07, inp=1,
$end
$solution
  dtmaxa(1)=0.0001, 0, 0.000001, 0.501, 0.001, 0.7,
  dtss=1.0, nfmesh=15,
  prsacc=0.001, tmpacl=0.001, maxit=100, noiter=100, epsht1=1.0, maxn=5,
$end
$design
  RodLength=0.571, RodDiameter=9.508e-3, roughc=1.14,
  rshd=0.003302, dishd=0.0003429, pelh=0.01523, dishv0=1.1788e-8,
  FuelPelDiam=0.0082184, roughf=2.12, frden=0.955, bup=4354560.0, fotmt1=2.0,
  tsntrk=1773.0, fgrrns=10.0, gadoln=0.0, gapthk=0.82e-4, coldw=0.1,
  cldwdc=0.04, ncs=7, spl=4.57e-2, scd=0.008, swd=0.0008, vplen=1.15e-6,
  gfrac(1)=1.0, gappr0=0.10e6, tgas0=300.0,
$end
$power
  RodAvePower=0, 0, 0, 0.501, 3557, 0.565, 0, 0.629, 0, 1
  AxPowProfile=0.74,0., 0.98,0.1, 1.12,0.2, 1.18,0.3, 1.09,0.4, 0.85,0.5, 0.61,
0.571,
  RadPowProfile=0.8167, 0.0, 0.8213, 0.0007249, 0.8292, 0.001359,
0.8412, 0.0019084, 0.8586, 0.0023791, 0.8834, 0.0027772,
0.9189, 0.0031088, 0.9695, 0.0033802, 1.0414, 0.0035974,
1.1426, 0.0037664, 1.2829, 0.0038934, 1.4736, 0.0039843,
1.7249, 0.0040453, 2.0446, 0.0040823, 2.4439, 0.0041012,
2.911, 0.0041082, 3.2572, 0.0041092,
  CladPower=0.0123,
$end
$model
  internal='on',
  metal='on', cathca=1,
  deformation='on', noball=0,
$end
$boundary
  heat='on'
  press=2, pbh2(1)=101325.0, 0.0, 101325.0, 1.0,

```

Table B.13 (contd)	
zone=5,	htclew=0.114, 0.228, 0.342, 0.456, 0.571,
htco=2,	htca(1,1)= 2000000, 0, 2000000, 1,
	htca(1,2)= 2000000, 0, 2000000, 1,
	htca(1,3)= 2000000, 0, 2000000, 1,
	htca(1,4)= 2000000, 0, 2000000, 1,
	htca(1,5)= 2000000, 0, 2000000, 1,
tem=7,	
tblka(1,1)=	553.,0., 553.,0.5, 555.,0.6, 560.,0.7, 563.,0.8, 563.,0.9, 563.,1.0,
tblka(1,2)=	553.,0., 553.,0.5, 560.,0.6, 574.,0.7, 583.,0.8, 584.,0.9, 583.,1.,
tblka(1,3)=	553.,0., 553.,0.5, 565.,0.6, 588.,0.7, 603.,0.8, 605.,0.9, 603.,1.,
tblka(1,4)=	553.,0., 553.,0.5, 569.,0.6, 602.,0.7, 622.,0.8, 626.,0.9, 623.,1.,
tblka(1,5)=	553.,0., 553.,0.5, 574.,0.6, 616.,0.7, 642.,0.8, 647.,0.9, 643.,1.,
\$end	
\$stuning	
\$end	

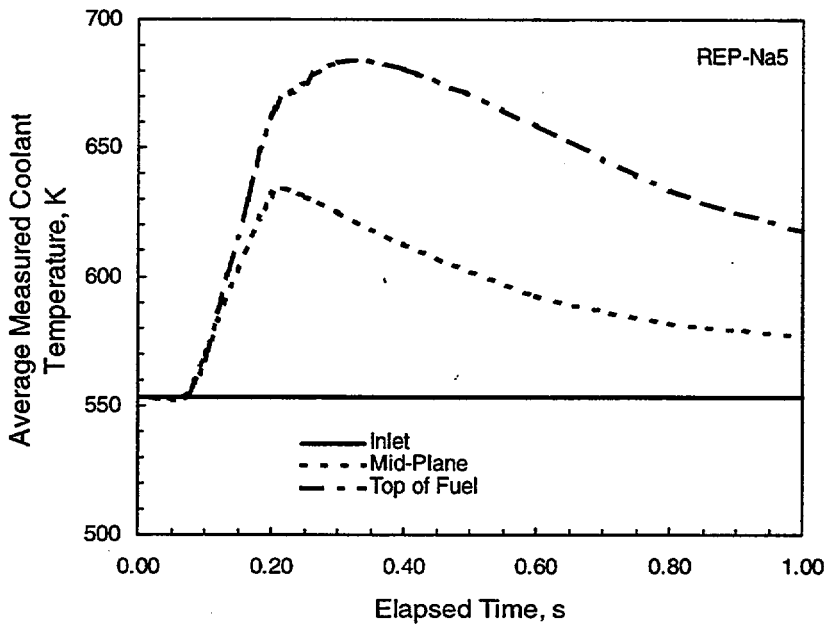


Figure B.7 Coolant Temperature History for REP-Na5

assumed to simply vary linearly along the test rod from 553K at the inlet to the average measured coolant temperature at the top of the fuel column. The resulting input coolant temperature history is provided in Table B.14 which is a listing of the FRAPTRAN input file for REP-Na5.

B.4 IGR RIA Case

For the IGR RIA assessment case, the FRAPTRAN input data were based on the material provided in Section A.2.3, Table A.5, and Volume 3 of NUREG/IA-0156. The power history for this case was illustrated in Figure A.27.

Table B.14 FRAPTRAN Input for REP-Na5 Assessment Case

* FrapTran, Transient fuel rod analysis code	*
*	*
* CASE DESCRIPTION: Assessment - RIA Test Na-5	*
*	*
FILE05='nullfile', STATUS='scratch', FORM='FORMATTED',	*
CARRIAGE CONTROL='LIST'	*
FILE15='sth2xt', STATUS='old', FORM='UNFORMATTED'	*
*	*
FILE06='out.na5', STATUS='UNKNOWN', CARRIAGE CONTROL='LIST'	*
FILE66='stripf.na5', STATUS='UNKNOWN', FORM='FORMATTED',	*
CARRIAGE CONTROL='LIST'	*
FILE22='restart.na5', STATUS='old', FORM='FORMATTED'	*
/*****	
IPNS RIA Test Na-5 Specified Surface Temperature	
\$begin	
ProblemStartTime=0.0,	
ProblemEndTime=0.33,	
ProblemEndTime=1.0,	
\$end	
start	
\$iodata	
unitin=1, unitout=1, dtpoa(1)=0.01, dtplt=0.001, trest = 0.1404E9 ;inp=1,	
\$end	
\$solution	
dtmaxa(1)=0.0001, 0.0, 0.000001, 0.071, 0.0001, 0.2,	
dtss=1.0, prsacc=0.001, tmpacl=0.001, maxit=100, noiter=100, epsht1=1.0,	
naxn=5, nfmesh=15,	
\$end	
\$design	
RodLength=0.571, RodDiameter=9.508e-3, tsnrk=1773.0,	
rshd=0.003302, dishd=0.0003429, pelh=0.01523, dishv0=1.1788e-8,	
FuelPelDiam=0.008193, roughf=2.12, frden=0.955, bup=4354560.0, fotmtl=2.0,	
fgrns=10.0, gadoln=0.0, gapthk=0.82e-4, coldw=0.1, roughc=1.14,	
cldwdc=0.04, ncs=7, spl=4.57e-2, scd=0.008, swd=0.0008, vplen=1.15e-6,	
gfrac(1)=1.0, gappr0=0.10e6, tgas0=300.0,	
\$end	
\$power	
RodAvePower= 0, 0, 0, 0.071, 29380, 0.08, 0, 0.089, 0, 1,	
AxPowProfile=0.74,0., 0.98,0.1, 1.12,0.2, 1.18,0.3, 1.09,0.4, 0.85,0.5, 0.61,	
0.571,	
RadPowProfile=0.8167, 0.0, 0.8213, 0.0007249, 0.8292, 0.001359,	
0.8412, 0.0019084, 0.8586, 0.0023791, 0.8834, 0.0027772,	
0.9189, 0.0031088, 0.9695, 0.0033802, 1.0414, 0.0035974,	
1.1426, 0.0037664, 1.2829, 0.0038934, 1.4736, 0.0039843,	
1.7249, 0.0040453, 2.0446, 0.0040823, 2.4439, 0.0041012,	
2.911, 0.0041082, 3.2572, 0.0041092,	
CladPower=0.0123,	
\$end	
\$model	
internal='on',	
metal='on', cathca=1,	
deformation='on', noball=0,	
\$end	
\$boundary	

Table B.14 (contd)	
heat='on'	
press=2, pbh2(1)=101325.0, 0.0, 101325.0, 1.0,	
zone=5, htclev=0.114, 0.228, 0.342, 0.456, 0.571,	
htco=2, htca(1,1)=2000000.0, 0.0, 2000000.0, 1.0,	
htca(1,2)=2000000.0, 0.0, 2000000.0, 1.0,	
htca(1,3)=2000000.0, 0.0, 2000000.0, 1.0,	
htca(1,4)=2000000.0, 0.0, 2000000.0, 1.0,	
htca(1,5)=2000000.0, 0.0, 2000000.0, 1.0,	
tem=9,	
tblka(1,1)=553.,0., 553.,0.07, 555.,0.1, 564.,0.2, 566.,0.3, 566.,0.4, 564.,0.6, 561.,0.8, 559.,1.0,	
tblka(1,2)=553.,0., 553.,0.07, 558.,0.1, 586.,0.2, 592.,0.3, 591.,0.4, 585.,0.6, 577.,0.8, 572.,1.0,	
tblka(1,3)=553.,0., 553.,0.07, 561.,0.1, 608.,0.2, 618.,0.3, 617.,0.4, 606.,0.6, 593.,0.8, 585.,1.0,	
tblka(1,4)=553.,0., 553.,0.07, 564.,0.1, 629.,0.2, 644.,0.3, 643.,0.4, 627.,0.6, 609.,0.8, 598.,1.0,	
tblka(1,5)=553.,0., 553.,0.07, 567.,0.1, 651.,0.2, 670.,0.3, 668.,0.4, 648.,0.6, 625.,0.8, 611.,1.0,	
\$end	
\$tuning	
\$end	

Although this rod had a burnup of 49 MWd/kgM, no FRAPCON-3 run was performed to provide initialization data because of the different reactor and fuel design. Burnup-dependent radial power profiles are included in the FRAPTRAN input file, which is provided as Table B.15.

Other points to be noted include:

- Standard Zircaloy cladding properties were used even though this rod had Zr-1%Nb cladding.
- There was no measured cladding temperature history, therefore a defined heat transfer coefficient history was used. This history was developed by comparing the FRAPTRAN predicted cladding temperatures to the RRC-KI predicted cladding temperatures (see Volume 3, NUREG/IA-0156). This was done based on the assumption that the RRC-KI had the best understanding of the experiment and their calculated temperatures should be reasonable. The resulting cladding temperatures are high, which is consistent with the oxidation growth and the observed post-test cladding microstructure.
- Radial power and burnup profiles, and the axial power profile, were developed based on the information presented in Volume 3 of NUREG/IA-0156. The assumed axial power profile, with peak power at the bottom of the test rod, is presented in Figure B.8.
- An assumed fission gas release history during the transient is used for this assessment case. This is based on the RRC-KI conclusion that fission gas release was necessary for the observed cladding strain and failure, and measurements of fission gas release in companion non-failed test rods. The assumed 8% fission gas release is based on fission gas release as a function of energy deposition for the companion non-failed test rods.

Table B.15 FRAPTRAN Input for IGR H5T Assessment Case

* fraptran, transient fuel rod analysis code	*

* CASE DESCRIPTION: IGR test H5T	*
* gas release per suggestion by Dr. Shestopalov	*
* UNIT FILE DESCRIPTION	*

* -- Input:	*
* 15 Water properties data	*

* -- Output:	*
* 6 STANDARD PRINTER OUTPUT	*
* 66 STRIPF FILE FOR XMGR/EXCEL	*

* -- Scratch:	*
* 5 SCRATCH INPUT FILE FROM ECHO1	*

* GOESINS:	
FILE05='nullfile', STATUS='scratch', FORM='FORMATTED',	
CARRIAGE CONTROL='LIST'	
FILE15='sth2xt', STATUS='old', FORM='UNFORMATTED'	

* GOESOUTS:	
FILE06='h5t.out', STATUS='UNKNOWN', CARRIAGE CONTROL='LIST'	
FILE66='stripf.h5t', STATUS='UNKNOWN', FORM='FORMATTED',	
* CARRIAGE CONTROL='LIST'	
/*****	
ria IGR problem #H5T noball=0 cathcart 243-275 Edep	
\$begin	
ProblemStartTime=0.0,	
ProblemEndTime= 7.80,	
\$end	
start	
\$iodata	
unitin=0, unitout=1,	
dtpoa=0.5,0., 0.30,1.80, 0.05,3.6, 0.30,5.0, 0.5,8.0, dtplt=0.004,	
\$end	
\$solution	
dtmaxa=.002,0.,.0002,1.5,.00005,3.45,.0005,4.2,0.001,6.,0.002,8.,	
dtss=5.0,	
maxit=100, noiter=100, epsht1=1.0,	
naxn=5, nfmesh=15,	
\$end	
\$design	
RodLength=0.51, RodDiameter=0.0298, pitch=0.037,totnb=25,	
pelh=0.03, FuelPelDiam=0.0251, roughf=1., frden=0.94, fgrns=6.,	
gapthk=0.80e-4, coldw=0.2, roughc=2.16, cldwdc=0.04,cfluxa=0.87e+18,	
ncs=5, spl=0.1, scd=0.021, swd=0.005, vplen=1.95e-4, tflux=100.e+06,	
gfrac=1.0, gappr0=200.,gsms=0.00405, bup=4.e6,	
\$end	
\$power	
RodAvePower=0.03, 0., 0.2, 1.200, 8.0, 1.820,	

Table B.15 (contd)			
16.0,	2.220,	50.0,	2.870, 117.0, 3.350,
65.0,	3.670,	23.0,	4.060, 8.0, 4.500,
4.0,	4.920,	1.5,	6.220, 0.5, 8.00,
AxPowProfile= .95,.09, 1.18,.17, .96,.33, 1.04,.39, .96,0.52,			
RadPowProfile=			
0.01,	0.0,		
	0.01,	0.00118,	
0.85,	0.00119,		
	0.92,	0.00263,	
1.0,	0.00321,		
1.1,	0.00342,		
1.2,	0.00357,		
1.3,	0.00369,		
1.5,	0.00377,		
2.3,	0.003825,		
.01,0.0,			
	0.01,	0.00118,	
0.85,	0.00119,		
	0.92,	0.00263,	
1.0,	0.00321,		
1.1,	0.00342,		
1.2,	0.00357,		
1.3,	0.00369,		
1.5,	0.00377,		
2.3,	0.003825,		
0.01,	0.0,		
	0.01,	0.00118,	
0.85,	0.00119,		
	0.92,	0.00263,	
1.0,	0.00321,		
1.1,	0.00342,		
1.2,	0.00357,		
1.3,	0.00369,		
1.5,	0.00377,		
2.3,	0.003825,		
0.01,	0.0,		
	0.01,	0.00118,	
0.85,	0.00119,		
	0.92,	0.00263,	
1.0,	0.00321,		
1.1,	0.00342,		
1.2,	0.00357,		
1.3,	0.00369,		
1.5,	0.00377,		
2.3,	0.003825,		
0.01,	0.0,		
	0.01,	0.00118,	
0.85,	0.00119,		
	0.92,	0.00263,	
1.0,	0.00321,		
1.1,	0.00342,		
1.2,	0.00357,		
1.3,	0.00369,		
1.5,	0.00377,		
2.3,	0.003825,		
0.01,	0.0,		
	0.01,	0.00118,	
0.85,	0.00119,		
	0.92,	0.00263,	
1.0,	0.00321,		
1.1,	0.00342,		
1.2,	0.00357,		
1.3,	0.00369,		
1.5,	0.00377,		
2.3,	0.003825,		
butemp=	0.01	,	0.0

Table B.15 (contd)

	0.01	, 0.0011,
42430	,	0.0013,
43050	,	0.001967,
43910	,	0.002427,
44100	,	0.002804,
45820	,	0.003108,
48340	,	0.003342,
55100	,	0.003560,
57700	,	0.003605,
65840	,	0.003630,
77220	,	0.003730,
92110	,	0.003781,
101400,	0.003808,	
113700,	0.003825,	
	0.01	, 0.0
	0.01	, 0.0011,
42430	,	0.0013,
43050	,	0.001967,
43910	,	0.002427,
44100	,	0.002804,
45820	,	0.003108,
48340	,	0.003342,
55100	,	0.003560,
57700	,	0.003605,
65840	,	0.003630,
77220	,	0.003730,
92110	,	0.003781,
101400,	0.003808,	
113700,	0.003825,	
	0.01	, 0.0
	0.01	, 0.0011,
42430	,	0.0013,
43050	,	0.001967,
43910	,	0.002427,
44100	,	0.002804,
45820	,	0.003108,
48340	,	0.003342,
55100	,	0.003560,
57700	,	0.003605,
65840	,	0.003630,
77220	,	0.003730,
92110	,	0.003781,
101400,	0.003808,	
113700,	0.003825,	
	.01	, 0.0
	0.01	, 0.0011,
42430	,	0.0013,
43050	,	0.001967,
43910	,	0.002427,
44100	,	0.002804,
45820	,	0.003108,
48340	,	0.003342,
55100	,	0.003560,
57700	,	0.003605,
65840	,	0.003630,
77220	,	0.003730,

Table B.15 (contd)	
92110	, 0.003781,
101400,	0.003808,
113700,	0.003825,
0.01	, 0.0
0.01	, 0.0011,
42430	, 0.0013,
43050	, 0.001967,
43910	, 0.002427,
44100	, 0.002804,
45820	, 0.003108,
48340	, 0.003342,
55100	, 0.003560,
57700	, 0.003605,
65840	, 0.003630,
77220	, 0.003730,
92110	, 0.003781,
101400,	0.003808,
113700,	0.003825,
\$end	
\$model	
internal='on',	
presfgr=1,	
relfrac=.0,.0,0.0,3.1,0.02,3.2,0.05,3.4,.07,3.6,0.08,4.1,.08,8.,	
metal='on', cathca=1,	
deformation='on', noball=0,	
heat='on',	
cenvoi=1, zvoid1=0.0, zvoid2=0.51, rvoid=0.0039,	
\$end	
\$boundary	
heat='on',	
press=3, pbh2(1)= 100.0, 0.0, 30.0, 0.70, 30.0, 9.0,	
zone=1, htclef(1)= .52,	
htco=10, htca(1,1)= 4000., 0.0, 4000., 3.0,	
3400., 3.2, 2800., 3.3, 2000., 3.35,	
1400., 3.4, 500., 3.6, 150., 3.7,	
150., 4.3, 600., 9.0,	
tem=2, tblka(1,1)= 77.0, 0.0, 77.0, 9.0,	
\$end	
\$tuning	
\$end	

B.5 NRU LOCA Cases

For the NRU LOCA assessment cases, the FRAPTRAN input coolant temperature histories were based on the measured cladding temperature histories. The test rods for the LOCA cases in the NRU reactor (Section A.3.1) were irradiated in flowing steam prior to the transient, stagnant steam prior to reflood, and then reflood conditions. Both cladding inner surface and outer surface temperatures were measured, in addition to coolant temperatures. However, only cladding inner surface temperatures were generally presented in the three reports on the tests. In addition, cladding temperature histories were presented at only three axial locations for MT1 and MT-4, while a more extensive presentation of the axial temperature distribution was provided for MT-6A. Therefore, it was necessary to make numerous assumptions to develop the input coolant temperature histories for these three cases for the FRAPTRAN assessment runs.

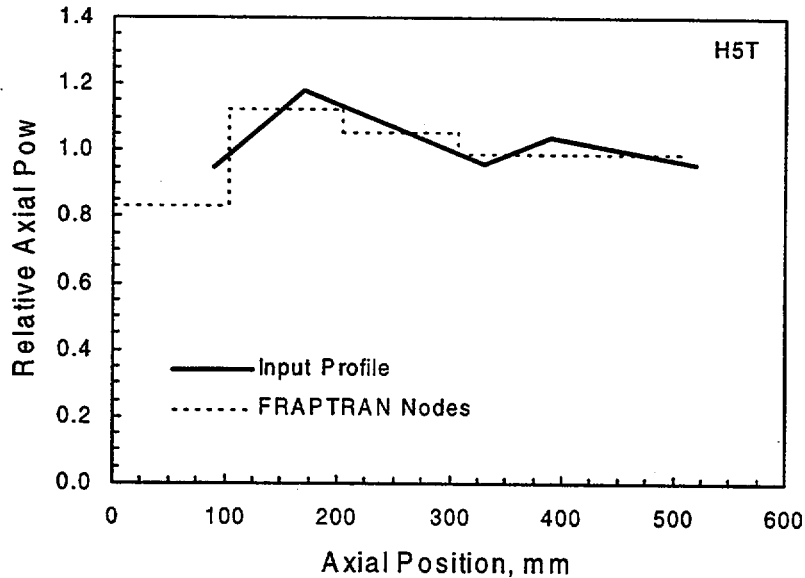


Figure B.8 Axial Power Profile for IGR HST

The development of the input coolant temperature histories is presented in the following. Because the amount of available data for defining the cladding/coolant history for MT-4 and MT-1 is less than for MT-6, the defined histories for MT-4 and MT-1 are dependent on the history for MT-6.

MT-6A

Measured cladding inner surface temperature data are available in graphical form (Wilson et al. 1993) at elevations of 56, 74, 90, 102, 115, and 172 inches. At each of these elevations, cladding inner surface thermocouples were present in three different test rods (see Figure A.34). To develop the cladding/coolant temperature history, the cladding temperature was averaged at each elevation. The resulting axial and time history for MT-6A cladding temperature is presented in Figure B.9.

For the FRAPTRAN input, the coolant input history was assumed equal to the cladding inner surface temperature history illustrated in Figure B.9. The coolant channel was divided into seven axial zones and the histories in Figure B.9 define the temperature history for each coolant axial zone. The resulting input coolant temperature history is provided in Table B.16, which is a listing of the FRAPTRAN input file for MT-6A.

MT-4

Measured cladding inner surface temperature data are available in graphical form (Wilson et al. 1983) at elevations of 77, 98, and 119 inches; these data were presented in Figure A.31. In addition, a pretransient axial temperature profile is available (Figure B.12 of Wilson et al. 1983). To expand the available data to provide a more comprehensive coolant temperature history input for FRAPTRAN, the following approach was taken. First, the axial profile data from Figure B.12 of Wilson et al (1983) were used to

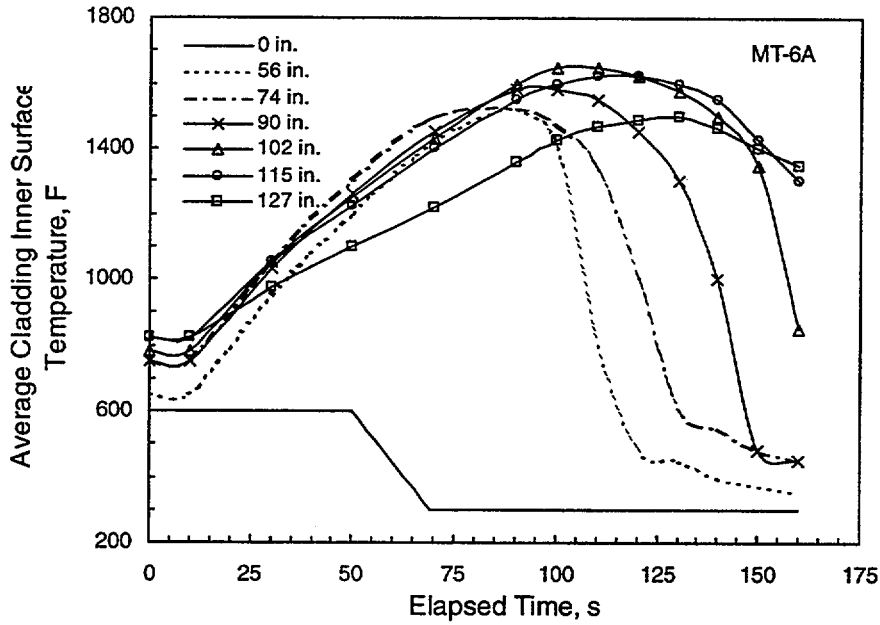


Figure B.9 MT-6A Cladding Temperature History

Table B.16 FRAPTRAN Input for MT-6A Assessment Case		

* FrapTran, transient fuel rod analysis code		*

* CASE DESCRIPTION: MT-6A BR Input		*
* UNIT FILE DESCRIPTION		*

* -- Input:		*
* 15 Water properties data		*

* -- Output:		*
* 6 STANDARD PRINTER OUTPUT		*
* 66 STRIPF FILE FOR GRAFITI		*

* -- Scratch:		*
* 5 SCRATCH INPUT FILE FROM ECHO1		*

* Input: FrapTran INPUT FILE		*

* GOESINS:		
FILE05='nullfile', STATUS='scratch', FORM='FORMATTED',		
CARRIAGE CONTROL='LIST'		
FILE15='sth2xt', STATUS='old', FORM='UNFORMATTED'		

* GOESOUTS:		
FILE06='out.MT6ABR', STATUS='UNKNOWN', CARRIAGE CONTROL='LIST'		
FILE66='stripf.MT6ABR', STATUS='UNKNOWN', FORM='FORMATTED',		

Table B.16 (contd)

CARRIAGE CONTROL='LIST'
/*****
LOCA rod MT-6A British Units Input and SI Units Output
\$begin
ProblemStartTime = 0.0,
ProblemEndTime = 100.0,
\$end
start
\$iodata
unitout=1, dtpoa(1)=2.5, dtplt=2.5
\$end
\$solution
dtmaxa(1)=0.05, dtss=1.e5
prsacc=0.001, tmpacl=0.001, maxit=100, noiter=100, epsht1=3.6,
naxn=12, nfmesh=8,
\$end
\$design
pitch=0.041831, pdrato=1.324, rnbnt=1.0, totnb=12,
RodLength=12.0, RodDiameter=0.03159,
rshd=1.125e-2, dishd=110.0e-5, pelh=3.127e-2, dishv0=43.868e-8,
FuelPelDiam=2.71e-2, roughf=1.0, frden=0.95, fotmt1=2.0, tsntrk=1773.0,
fgrns=10.0,
gapthk=24.6e-5, coldw=0.1, roughc=1.0, cfluxa=0.16e15, tflux=0.2e3, cldwdc=0.04,
ncs=59, spl=0.7513, scd=2.583e-2, swd=4.2494e-3, vplen=48.1e-5,
gfrac(1)=1.0, gappr0=4.801e2, tgas0=80.33,
\$end
\$power
RodAvePower=0.375, 0.0, 0.375, 1000.0,
AxPowProfile=0.09, 0.0, 0.56, 1.0, 0.99, 2.0, 1.34, 3.0, 1.44, 4.0, 1.47, 5.0,
1.46,
6.0, 1.38, 7.0, 1.23, 8.0, 0.98, 9.0, 0.71, 10.0, 0.37, 11.0, 0.03, 12.0,
RadPowProfile=1.0, 0.0, 1.0, 1.36e-2,
\$end
\$model
internal='on',
metal='on', cathca=1,
deformation='on',
\$end
\$boundary
coolant='on',
geomet=1, dhe=0.0389, dhy=0.0389, achm=96.6e-5,
lowpl=2, hinta(1)=1273.0, 0.0, 1273.0, 1000.0,
pressu=2, pbhl(1)=40.0, 0.0, 40.0, 1000.0,
massfl=2, gbh(1)=97200.0, 0.0, 97200.0, 1000.0,
reflood='on'
geometry=1, hydiam=0.0389, flxsec=0.03477, nbundl=6,
time=1, emptm=1.0, refdtm=80.0,
ruptur=1,
inlet=7, temptm= 250.0, 0.0, 129.0, 10.0,
81.6, 105.0, 115.0, 180.0,
210.0, 265.0, 120.0, 275.0,
75.0, 315.0,
pressure=2, prestm(1)=40.0 , 0.0, 40.0 , 1000.0,
reflo=2, fldrat(1)=2.0, 0.0, 2.0, 1000.0,
zone=7, htclev=2.33, 5.42, 6.83, 8.00, 9.08, 10.08, 12.,
htco=2, htca(1,1)= 2.e6, 0., 2.e6, 160.,

Table B.16 (contd)	
htca(1,2)=	2.e6, 0., 2.e6, 160.,
htca(1,3)=	2.e6, 0., 2.e6, 160.,
htca(1,4)=	2.e6, 0., 2.e6, 160.,
htca(1,5)=	2.e6, 0., 2.e6, 160.,
htca(1,6)=	2.e6, 0., 2.e6, 160.,
htca(1,7)=	2.e6, 0., 2.e6, 160.,
tem=13, tblka(1,1)=	625, 0., 625., 10., 775., 30., 900., 50., 860., 70., 910., 90.,
tblka(1,2)=	650., 0, 650.,10., 950.,30., 1200.,50., 1420.,70., 1525.,90., 1400.,100.,
tblka(1,3)=	750.,0., 750.,10., 1050.,30., 1300.,50., 1500.,70., 1525.,90., 1475.,100.,
tblka(1,4)=	750.,0., 750.,10., 1030.,30., 1260.,50., 1450.,70., 1580.,90., 1580.,100.,
tblka(1,5)=	780.,0., 780.,10., 1050.,30., 1250.,50., 1430.,70., 1600.,90., 1650., 100., 1650.,110., 1625.,120., 1575.,130., 1500.,140., 1350.,150., 850.,160.,
tblka(1,6)=	825.,0., 825.,10., 1050.,30., 1225.,50., 1400.,70., 1550.,90., 1600.,100.,
tblka(1,7)=	825.,0., 825.,10., 975.,30., 1100.,50., 1220.,70., 1360.,90., 1425.,100.,
tblka(1,8)=	1470.,110., 1490.,120., 1500.,130., 1460.,140., 1400.,150., 1350.,160.,
\$end	
\$tuning	
\$end	

define the axial cladding temperature profile along the test rod at the time of steam flow being turned off; this assumed profile is illustrated in Figure B.10. Next, from the data presented in Figure A.31, it was assumed that the rate of temperature rise at elevations below 108 inches was 13.5 °F/sec, while for higher

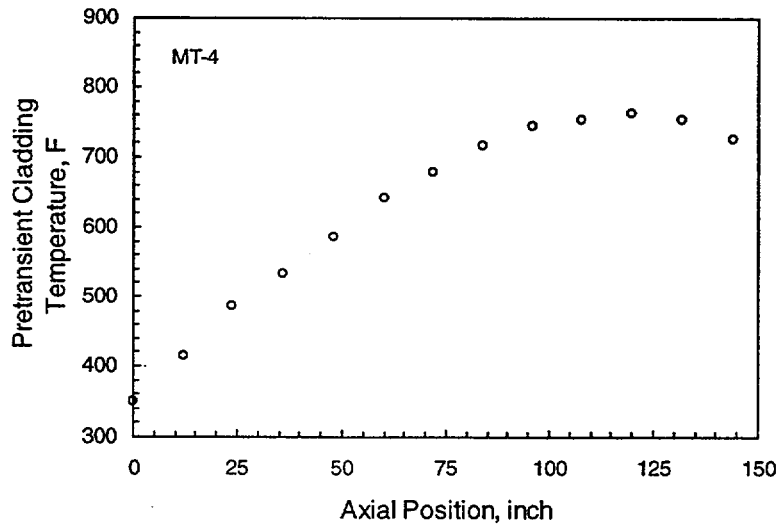


Figure B.10 Pretransient Axial Temperature Profile for MT-4

elevations it was assumed to be 12.3 °F/sec. For the time history, it was assumed that steam-off occurred at 10 seconds and reflood began at 67 seconds (57 seconds after steam-off). From additional data in Wilson et al. (1983), the quench front cycled between 60 and 100 inches during the test until scram and test shutdown at 1050 seconds. For the regions of quench, cladding temperatures went quickly to about 450°F and then further decreased to about 300°F. Using the above observations, and dividing the coolant channel into 12 zones, a cladding temperature history was defined as presented in Figure B.11 and Table B.17, which is a listing of the FRAPTRAN input file for MT-4.

MT-1

Measured cladding inner surface temperature are available in graphical form (Russcher et al. 1981) at elevations of 77, 98, and 119 inches; these data were presented in Figure A.28. To expand the available data to provide a more comprehensive coolant temperature history input for FRAPTRAN, the following approach was taken. First, an initial axial temperature profile for MT-1 was not available; therefore, the initial temperature profile was assumed to be similar to the initial axial temperature profile for MT-4 (see Figure B.10).^a Second, from the data presented in Figure A.28, it was assumed that the rate of temperature rise at elevations below 77 inches was approximately 15.0 °F/s and at an elevation of 119 inches the rate of rise was 11.2 °F/s. For the time history, it was assumed that steam-off occurred at 10 seconds and reflood began at 40 seconds (30 seconds after steam-off). Data on the quench front were not available, therefore the quench front behavior was assumed to be similar to that deduced for MT-4. Using these

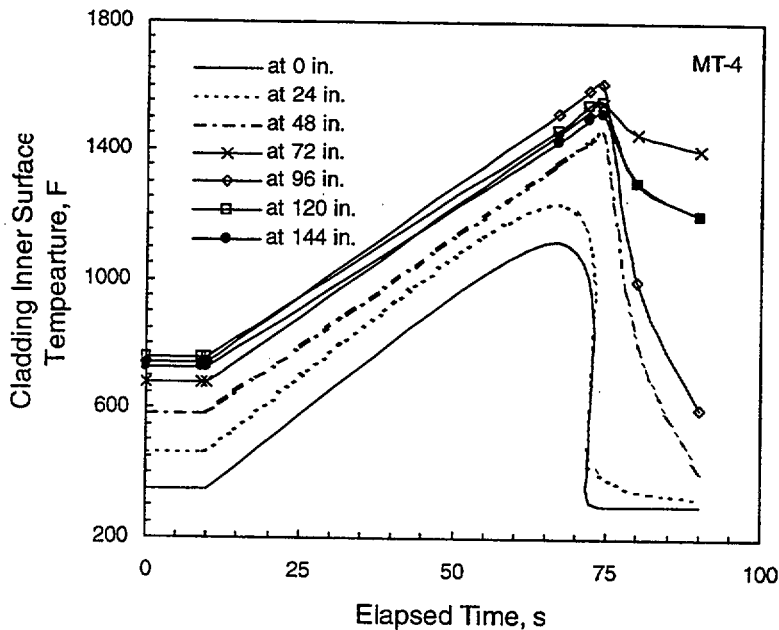


Figure B.11 Assumed MT-4 Cladding/Coolant Temperature History

^aNote that the graphical data presented in Russcher et al. (1981), for example, see data reproduced in Figure A.28, do not appear to support an initial cladding temperature of 861°F reported in Table 3.1 of Russcher et al. An assumed initial cladding temperature of 861°F was not used for the FRAPTRAN input.

Table B.17 FRAPTRAN Input for MT-4 Assessment Case

* FrapTran, transient fuel rod analysis code		*

* CASE DESCRIPTION: MT-4 BR Input		*
* UNIT FILE DESCRIPTION		*

* -- Input:		*
* 15	Water properties data	*
* -- Output:		*
* 6	STANDARD PRINTER OUTPUT	*
* 66	STRIPF FILE FOR GRAFITI	*
* -- Scratch:		*
* 5	SCRATCH INPUT FILE FROM ECHO1	*
* Input: FrapTran INPUT FILE		*

* GOESINS:		
FILE05='nullfile', STATUS='scratch', FORM='FORMATTED',		
CARRIAGE CONTROL='LIST'		
FILE15='sth2xt', STATUS='old', FORM='UNFORMATTED'		
* GOESOUTS:		
FILE06='out.MT4BR', STATUS='UNKNOWN', CARRIAGE CONTROL='LIST'		
FILE66='stripf.MT4BR', STATUS='UNKNOWN', FORM='FORMATTED',		
CARRIAGE CONTROL='LIST'		
/*****		
LOCA rod MT4 British Units Input and SI Units Output		
\$begin		
ProblemStartTime = 0.0,		
ProblemEndTime = 100.0,		
\$end		
start		
\$iodata		
unitout=1, dtpoa(1)=5.0, dtplt=2.5		
\$end		
\$solution		
dtmaxa(1)=2.5, 0.0, 2.5, 59.0, 0.05, 60.0, 0.05, 100.0,		
dtss=1.e5, prsacc=0.001, tmpacl=0.001, maxit=100, noiter=100, epsht1=3.6,		
naxn=12, nfmesh=8,		
\$end		
\$design		
pitch=0.041831, pdrato=1.324, rnbnt=1.0, totnb=12,		
RodLength=12.0, RodDiameter=0.03159,		
rshd=1.125e-2, dishd=110.0e-5, pelh=3.127e-2, dishv0=43.868e-8,		
FuelPelDiam=2.71e-2, roughf=1.0, frden=0.95, fotmtl=2.0, tsntrk=1773.0, fgrrns=10.0,		
gapthk=24.6e-5, coldw=0.1, roughc=1.0, cfluxa=0.16e15, tflux=0.2e3, cldwdc=0.04,		
ncs=59, spl=0.7513, scd=2.583e-2, swd=4.2494e-3, vplen=48.1e-5,		
gfrac(1)=1.0, gappr0=490.23, tgas0=80.33,		
\$end		
\$power		

Table B.17 (contd)				
RodAvePower=0.37,	0.0,	0.37,	1000.0,	
AxPowProfile=0.09,0.,	0.56,1.,	0.99,2.,	1.34,3.,	1.44,4., 1.47,5., 1.46,6.,
1.38,7.,	1.23,8.,	0.98,9.,	0.71,10.,	0.37,11., 0.03,12.,
RadPowProfile=1.0,	0.0,	1.0,	1.36e-2,	
\$end				
\$model				
internal='on',				
metal='on',	cathca=1,			
deformation='on',				
\$end				
\$boundary				
coolant='on',				
geomet=1,	dhe=0.0389,	dhy=0.0389,	achn=96.6e-5,	
lowpl=2,	hinta(1)=1273.0,	0.0,	1273.0,	1000.0,
pressu=2,	pbhl(1)= 40.0,	0.0,	40.0,	1000.0,
massfl=2,	gbh(1)=97200.0,	0.0,	97200.0,	1000.0,
reflood='on'				
geometry=1,	hydiam=0.0389,	flxsec=0.03477,	nbundl=6,	
time=1,	emptm=1.0,	refdtm=58.0,		
ruptur=1,				
inlet=7,	temptm= 250.0,	0.0,	129.0,	10.0,
	81.6,	105.0,	115.0,	180.0,
	210.0,	265.0,	120.0,	275.0,
	75.0,	315.0,		
pressure=2,	prestm(1)=40.0,	0.0,	40.0,	1000.0,
reflo=2,	fldrat(1)= 2.0,	0.0,	2.0,	1000.0,
zone=6,	htclev=2.,	4.,	6.,	8., 10., 12.,
htco=2,	htca(1,1)= 2.e6,0.,	2.e6,90.,		
	htca(1,2)= 2.e6,0.,	2.e6,90.,		
	htca(1,3)= 2.e6,0.,	2.e6,90.,		
	htca(1,4)= 2.e6,0.,	2.e6,90.,		
	htca(1,5)= 2.e6,0.,	2.e6,90.,		
	htca(1,6)= 2.e6,0.,	2.e6,90.,		
tem=6,	tblka(1,1)=466.0.,	466.,10.,	1236.,67.,	400.,74., 350.,80., 325.,90.,
	tblka(1,2)=588.,0.,	588.,10.,	1358.,67.,	1452.,74., 800.,80., 400.,90.,
	tblka(1,3)=680.,0.,	680.,10.,	1450.,67.,	1544.,74., 1450.,80., 1400.,90.,
	tblka(1,4)=744.,0.,	744.,10.,	1514.,67.,	1608.,74., 1000.,80., 600.,90.,
	tblka(1,5)=762.,0.,	762.,10.,	1463.,67.,	1550.,74., 1300.,80., 1200.,90.,
	tblka(1,6)=726.,0.,	726.,10.,	1427.,67.,	1513.,74., 1300.,80., 1200.,90.,
\$end				
\$tuning				
\$end				

observations and assumptions, and dividing the coolant channel into 12 zones, a cladding temperature history was defined as presented in Figure B.12 and Table B.18, which is a listing of the FRAPTRAN input for MT-1.

Other Considerations for the NRU Assessment Runs

See Section A.3.1 for a discussion of the measured gas pressures and the decision to not set the FRAPTRAN initial gas pressure at the stated design pressure, but instead at a pressure that would provide a match between the data and calculation at the beginning of the transient.

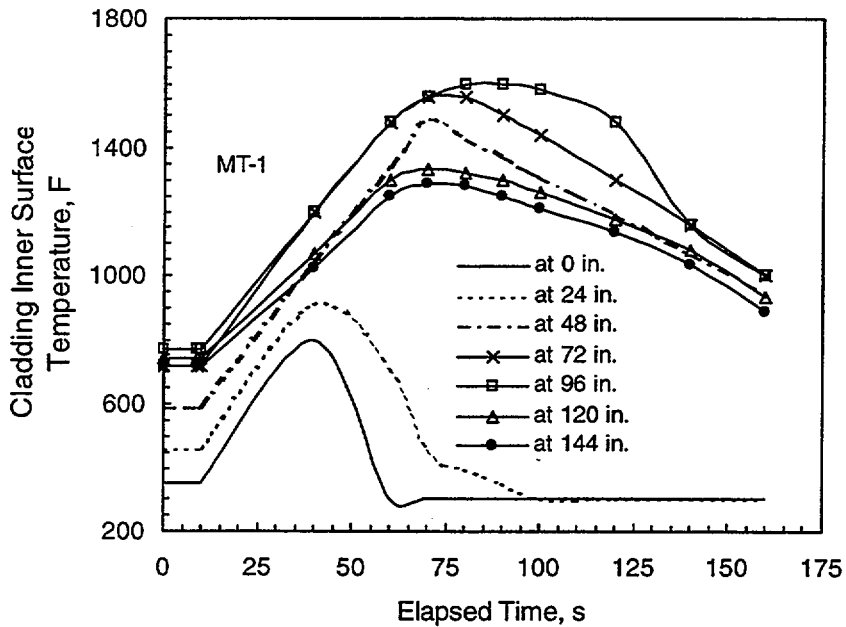


Figure B.12 Assumed MT-1 Cladding/Coolant Temperature History

Table B.18 FRAPTRAN Input for MT-1 Assessment Case		

* FrapTran, transient fuel rod analysis code		*
-----*		
* CASE DESCRIPTION: MT-1 BR Input		*
* UNIT FILE DESCRIPTION		*
* ---- -----*		
* -- Input:		*
* 15 Water properties data		*
* -- Output:		*
* 6 STANDARD PRINTER OUTPUT		*
* 66 .STRIPF FILE FOR GRAFITI		*
* -- Scratch:		*
* 5 SCRATCH INPUT FILE FROM ECHO1		*
* Input: FrapTran INPUT FILE		*

* GOESINS:		
FILE05='nullfile', STATUS='scratch', FORM='FORMATTED',		
CARRIAGE CONTROL='LIST'		
FILE15='sth2xt', STATUS='old', FORM='UNFORMATTED'		
* GOESOUTS:		
FILE06='out.MT1BR', STATUS='UNKNOWN', CARRIAGE CONTROL='LIST'		
FILE66='stripf.MT1BR', STATUS='UNKNOWN', FORM='FORMATTED',		

Table B.18 (contd)

CARRIAGE CONTROL='LIST'
/*****
LOCA rod MT1 British Units Input and SI Units Output
\$begin
ProblemStartTime = 0.0,
ProblemEndTime = 160.0,
\$end
start
\$iodata
unitout=1, dtpoa(1)=5.0, dtplt=2.5,
\$end
\$solution
dtmaxa(1)=2.5, 0.0, 2.5, 15.0, 0.01, 16.0, 0.01, 60.0, 1.0, 160.0,
prsacc=0.001, tmpacl=0.001, maxit=100, noiter=100, epsht1=2.5,
naxn=12, nfmesh=8, dtss=1.e5,
\$end
\$design
pitch=0.041831, pdrato=1.324, rnbnt=1.0, totnb=11,
RodLength=12.0, RodDiameter=0.03159,
rshd=1.125e-2, dishd=110.0e-5, pelh=3.127e-2, dishv0=43.868e-8,
FuelPelDiam=2.71e-2, roughf=1.0, frden=0.95, bup=0.0, fotmtl=2.0, tsntrk=1773.0,
fgrns=10.0, gadoln=0.0, cldwdc=0.04,
gapthk=24.6e-5, coldw=0.1, roughc=1.0, cfluxa=0.16e15, tflux=0.2e3,
ncs=59, spl=0.7513, scd=2.583e-2, swd=4.2494e-3, vplen=48.1e-5,
gfrac(1)=1.0, gappr0=217.56, tgas0=80.33,
\$end
\$power
RodAvePower= 0.378, 0.0, 0.378, 1000.0,
AxPowProfile=0.09, 0., 0.56,1., 0.99,2., 1.34,3., 1.44,4., 1.47,5.,
1.46,6., 1.38,7., 1.23,8., 0.98,9., 0.71,10., 0.37,11., 0.03,12.,
RadPowProfile=1.0, 0.0, 1.0, 1.355e-2,
\$end
\$model
internal='on',
metal='on', cathca=1,
deformation='on'
\$end
\$boundary
coolant='on',
geomet=1, dhe=0.0389, dhy=0.0389, achn=96.6e-5,
lowpl=2, hinta(1)= 1273.0, 0.0, 1273.0, 1000.0,
pressu=2, pbhl(1)= 40.0, 0.0, 40.0, 1000.0,
massfl=2, gbh(1)= 97200.0, 0.0, 97200.0, 1000.0,
reflood='on',
geometry=1, hydiam=0.0389, flxsec=0.03477, nbundl=6,
time=1, emptm=1.0, refdtm=33.0,
ruptur=1,
inlet=7, temptm= 250.0, 0.0, 129.0, 10.0,
81.6, 105.0, 115.0, 180.0,
210.0, 265.0, 120.0, 275.0,
75.0, 315.0,
pressure=2, prestm(1)= 40.0, 0.0, 40.0, 1000.0,
reflo=2, fldrat(1)= 2.0, 0.0, 2.0, 1000.0,
zone=6, htclev=2., 4., 6., 8., 10., 12.,
htco=2, htca(1,1)= 2.e6, 0., 2.e6, 160.,
htca(1,2)= 2.e6, 0., 2.e6, 160.,

Table B.18 (contd)	
htca(1,3)=	2.e6, 0., 2.e6, 160.,
htca(1,4)=	2.e6, 0., 2.e6, 160.,
htca(1,5)=	2.e6, 0., 2.e6, 160.,
htca(1,6)=	2.e6, 0., 2.e6, 160.,
tem=11, tblka(1,1)=	460.,0., 460.,10., 910.,40., 700.,60., 450.,70.,
	400.,80., 350.,90., 100.,300., 300.,120., 300.,140., 300.,160.,
tblka(1,2)=	590.,0., 590.,10., 1040.,40., 1340.,60., 1490.,70.,
	1430.,80., 1370.,90., 1310.,100., 1190.,120., 1070.,140., 950.,160.,
tblka(1,3)=	716.,0., 716.,10., 1200.,40., 1477.,60., 1555.,70.,
	1555.,80., 1500.,90., 1439.,100., 1300.,120., 1155.,140., 1000.,160.,
tblka(1,4)=	767.,0., 767.,10., 1200.,40., 1477.,60., 1555.,70.,
	1600.,80., 1600.,90., 1581.,100., 1477.,120., 1155.,140., 1000.,160.,
tblka(1,5)=	742.,0., 742.,10., 1065.,40., 1297.,60., 1335.,70.,
	1323.,80., 1297.,90., 1258.,100., 1174.,120., 1077.,140., 935.,160.,
tblka(1,6)=	720.,0., 720.,10., 1025.,40., 1250.,60., 1290.,70.,
	1280.,80., 1250.,90., 1210.,100., 1135.,120., 1035.,140., 885.,160.,
\$end	
\$tuning	
\$end	

The assumed axial power profile for the three MT tests is illustrated in Figure B.13.

These rods were tested at zero burnup; therefore, no FRAPCON-3 calculation was performed to initialize FRAPTRAN.

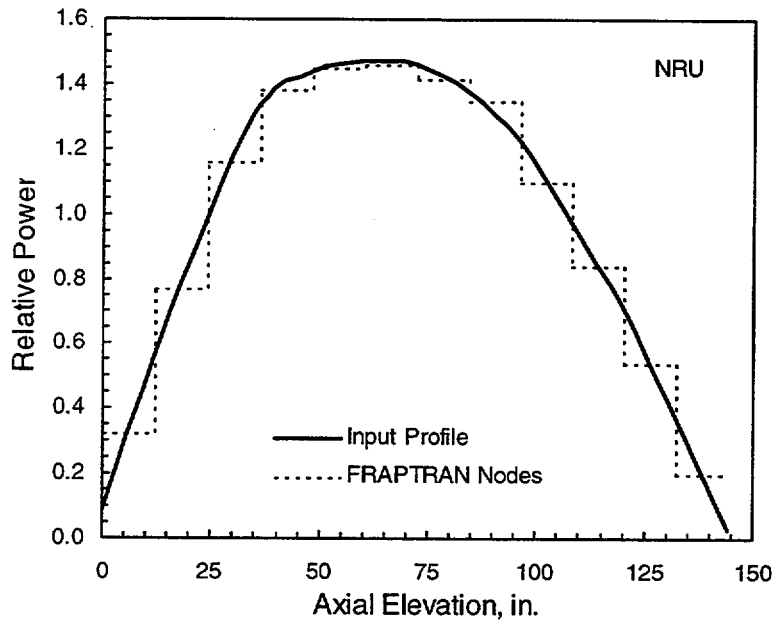


Figure B.13 Assumed Axial Power Profile for NRU LOCA Tests.

B.6 Other LOCA Cases

Two additional LOCA cases were used for the FRAPTRAN assessment. The LOC-11C test was run in the PBF and the FRF-2 test was run in TREAT. Provided in the following are descriptions of how the FRAPTRAN assessment runs were set up for these cases.

PBF LOC-11C

For the PBF LOC-11 assessment case, the FRAPTRAN input coolant temperature history was based on the measured cladding temperature histories. The four test rods for LOC-11C (Section A.3.2) were irradiated in flowing steam following the scram that initiated the transient. Initial cladding temperatures were approximately 620K and increased to peak of approximately 950 to 1050K (see Figure A.36). Cladding outer surface temperatures were measured on all four test rods at elevations of 0.53 and 0.61 m, and all four rods showed similar temperature behavior during the transient.

The input cladding/coolant temperature history for FRAPTRAN was developed as follows. First, the initial cladding temperature was assumed to 620K along the full-length of the rods; this is based on FRAPCON3 calculation that showed minimal axial variation in cladding outer surface temperature prior to the transient. Next, cladding temperatures are assumed to remain constant for the first two seconds of the transient. The input coolant temperature history is then a lineal approximation of the measured cladding temperatures. The history at 0.5m is approximates the measurements at 0.53 m; the history at 0.3 and 0.6 m approximates the measurements at 0.61 m; and the history at the top of the fuel column (1.0 m) is assumed to be approximately 75K less than the measured history at 0.61 m. The assumed input coolant temperature history is presented in Figure B.14, including a comparison to measured cladding temperatures.

The assumed axial power history is presented in Figure B.15.

The input design parameters are generally the average of the as-measured values for the four test rods. The input design gas pressure is for Rod 3 at 2.4 MPa. A listing of the FRAPTRAN input file is provided as Table B.19.

TREAT FRF-2

For the TREAT FRF-2 assessment case, the FRAPTRAN input coolant temperature history was based on the measured cladding temperature histories. The seven test rods for FRF-2 (Section A.3.3) were irradiated in a flowing steam/helium mixture during the transient. To achieve the desired cladding peak cladding temperature of approximately 2400°F, rod-average power levels up to approximately 11 kW/ft were induced during the transient; the transient power history is provided in Figure B.16. and the axial power profile is provided in Figure B.17. Cladding outer surface temperatures were measured on two rods (Rods 12 and 13) at elevations of 11, 14, 15, and 19 inches below the top of the rods; a representative cladding temperature history was provided in Figure A.42. The pretransient cladding axial temperature profile was approximately constant at 335°F.

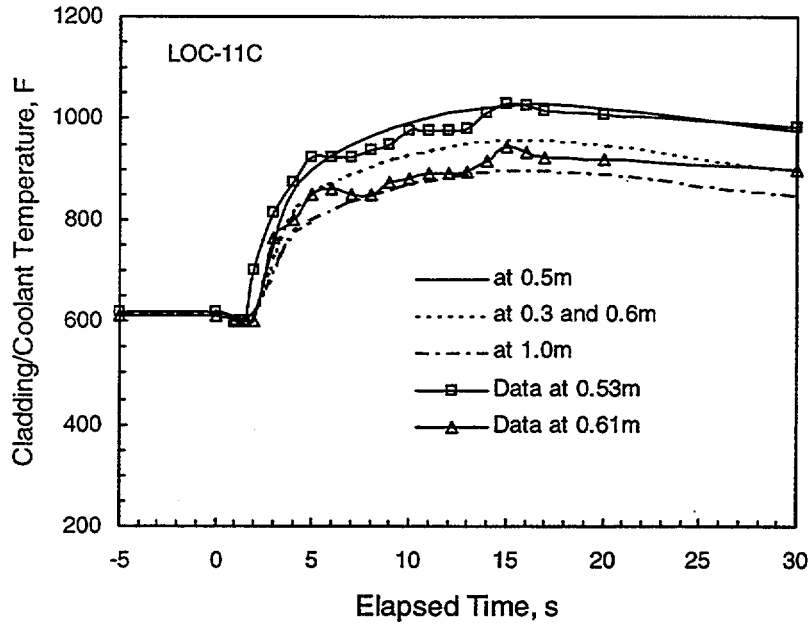


Figure B.14 Assumed Coolant Temperature History for LOC-11C

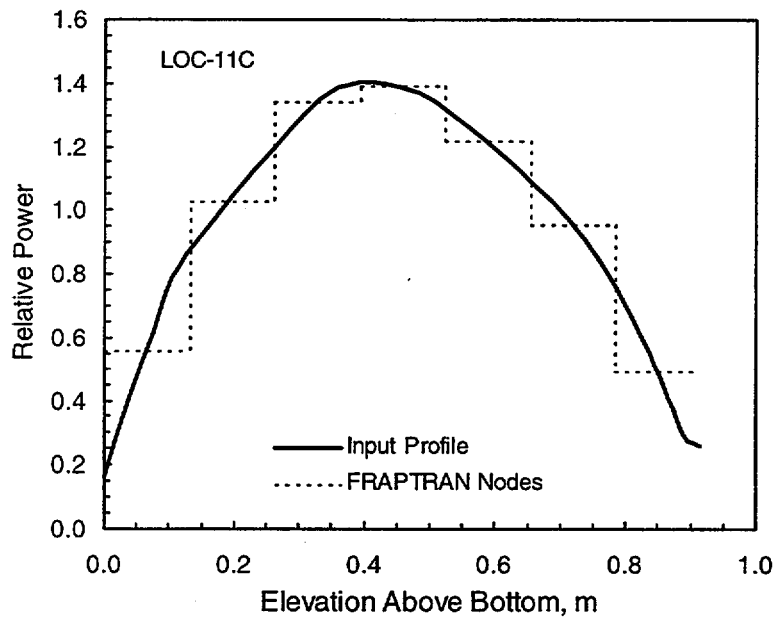


Figure B.15 Assumed Axial Power Profile for LOC-11C

Table B.19 FRAPTRAN Input for LOC-11C Assessment Case

* FrapTran, transient fuel rod analysis code		*

* CASE DESCRIPTION: PBF Test LOC 11C		*
* UNIT FILE DESCRIPTION		*

* -- Input:		*
* 15 Water properties data		*
* -- Output:		*
* 6 STANDARD PRINTER OUTPUT		*
* 66 STRIPF FILE FOR GRAFITI		*
* -- Scratch:		*
* 5 SCRATCH INPUT FILE FROM ECHO1		*
* Input: FrapTran INPUT FILE		*

* GOESINS:		
FILE05='nullfile', STATUS='scratch', FORM='FORMATTED',		
CARRIAGE CONTROL='LIST'		
FILE15='sth2xt', STATUS='old', FORM='UNFORMATTED'		
* GOESOUTS:		
FILE06='out.PBF11C', STATUS='UNKNOWN', CARRIAGE CONTROL='LIST'		
FILE66='stripf.PBF11C', STATUS='UNKNOWN', FORM='FORMATTED',		
CARRIAGE CONTROL='LIST'		
/*****		
PBF Test LOC 11C Specified Surface Temperature		
\$begin		
ProblemStartTime = 0.0,		
ProblemEndTime = 30.0,		
\$end		
start		
\$iodata		
unitout=1, dtpoa(1)=0.5, dtplt=0.1,		
\$end		
\$solution		
dtmaxa(1)=0.0001,0.0, 0.0001,8.0, 0.01,8.01, 0.01,30.0,		
prsacc=0.001, tmpacl=0.001, maxit=200, noiter=200, epsht1=1.0,		
nfmesh=15, naxn=7,		
zelev = 0.25, 0.75, 1.25, 1.50,		
1.73884, 2.0013, 2.25, 2.75,		
\$end		
\$design		
RodLength=3.0, RodDiameter=0.03517,		
rshd=0.0108, dishd=0.001083, pelh=0.05, dishv0=4.473e-7,		
FuelPelDiam=0.03051, roughf=2.159, frden=0.94432, bup=15412.0, fotmtl=2.0,		
fgrns=10.0, gadoln=0.0, tsntrk=1873.0, clwdwc=0.0,		
gapthk=3.3e-4, coldw=0.2, roughc=1.143,		
ncs=17, spl=.19792, scd=.0307, swd=3.38e-3, vplen=1.2e-4,		
gfrac(1)=1.0, gappr0=322.0, tgas0=80.33,		

Table B.19 (contd)

\$end						
\$power						
RodAvePower=	16.368,	0.0,	0.92,	0.01,	0.9,	0.1,
	0.82 ,	1.0,	0.78,	2.0,	0.7,	5.0,
	0.62 ,	10.0,	0.57,	15.0,	0.49,	30.0,
	0.42 ,	60.0,				
AxPowProfile=	0.163,	0.0000,	0.326,	0.0833,	0.620,	0.250,
	0.862,	0.4167,	1.347,	1.0833,	1.396,	1.250,
	1.400,	1.4167,	1.368,	1.5833,	1.304,	1.750,
	1.221,	1.9167,	1.128,	2.0833,	1.028,	2.250,
	0.910,	2.4167,	0.754,	2.5833,	0.548,	2.750,
	0.290,	2.9167,	0.256,	3.0049,		
RadPowProfile=	0.8800,	0.00092878,	0.8810,	0.00130960,	0.886,	0.00168042,
	0.8978,	0.00205124,	0.9095,	0.00242206,	0.929,	
	0.00279288,					
	0.9525,	0.00316370,	0.9825,	0.00252452,	1.031,	
	0.00390534,					
	1.0800,	0.00427616,	1.1460,	0.00530561,		
	CladPower=0.0123,					
\$end						
\$model						
	cenvoi=1,					
	zvoid1=1.6545,					
	zvoid2=3.0034,					
	rvoid =0.00308,					
	gasflo=0,					
	cathca=1,					
	noball=1,					
	internal='on',					
	metal='on',					
	heat='on'					
	deformation='on',					
\$end						
\$boundary						
	coolant='on',					
	heat='on',					
	geomet =1,					
	dhe=0.088, dhy=0.028, achn=0.00243,					
	press=2, pbh2 = 2205, 0, 25, 30,					
	pressu=2, pbh1(1) = 2205, 0, 25, 30,					
	lowpl =2, hinta(1)= 638.9, 0.0, 221.4, 30.0,					
	upppl =2, hupta(1)= 668.2, 0.0, 1184.3, 30.0,					
	zone=4, htclev =0.75, 1.5, 2.25, 3.0,					
	htco=2, htca(1,1)=2000000, 0, 2000000, 30,					
	htca(1,2)=2000000, 0, 2000000, 30,					
	htca(1,3)=2000000, 0, 2000000, 30,					
	htca(1,4)=2000000, 0, 2000000, 30,					
	massfl=8,					
	gbh(1) = 2096609.0, 0.0, 0.0, 0.5, 0.0, 2.0,					
	128160.0, 2.5, 249480.0, 5.0, 36720.0, 7.5,					
	0.0, 8.0, 0.0, 30.0,					
	tem=5, tblka(1,1)= 655, 0, 655, 2, 1070, 5, 1270, 15, 1160, 30,					
	tblka(1,2)= 655, 0, 655, 2, 1160, 5, 1385, 15, 1295, 30,					
	tblka(1,3)= 655, 0, 655, 2, 1070, 5, 1270, 15, 1160, 30,					
	tblka(1,4)= 655, 0, 655, 2, 980, 5, 1160, 15, 1070, 30,					
\$end						

Table B.19 (contd)	
\$	stuning
\$	end

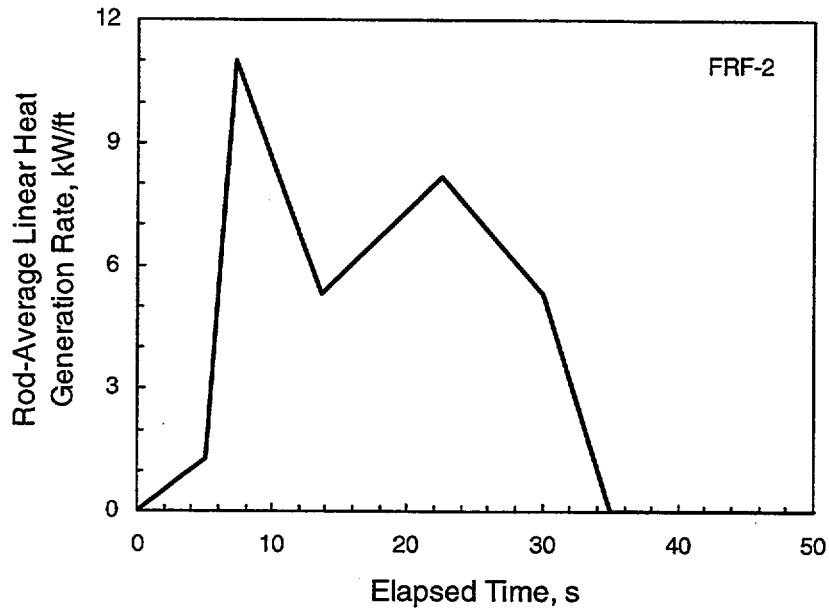


Figure B.16 Transient Power History for FRF-2

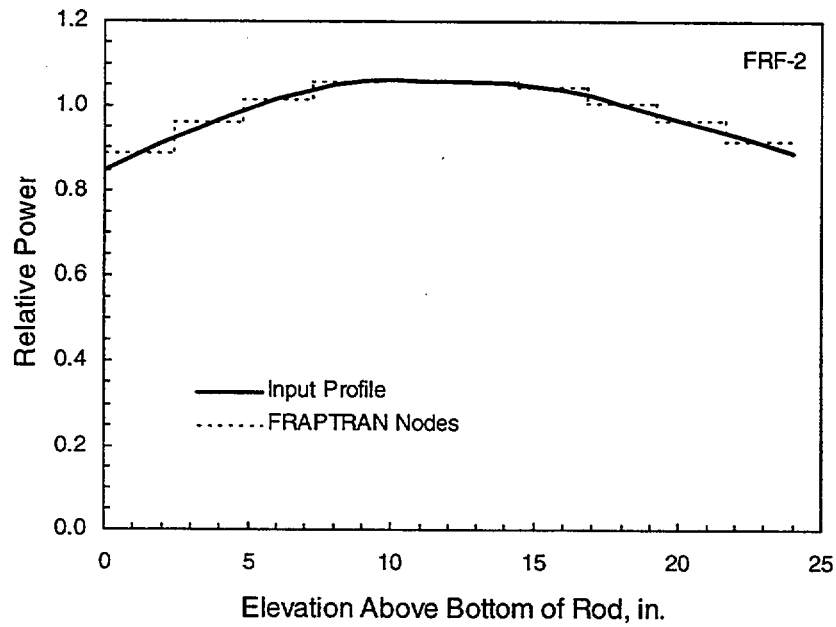


Figure B.17 Axial Power Profile for FRF-2

The input cladding temperature history for FRAPTRAN was developed as follows. Cladding temperatures did not begin to increase until approximately seven seconds into the transient. At that point, cladding temperature increased at an average rate of approximately 80°F/sec till about 30-35 seconds where temperatures reached a maximum and then began to decrease (see Figure A.42). The axial cladding temperature profile at the time of peak cladding temperature may be determined from Figure 15 of Lorenz and Parker (1972). Therefore, it is assumed that cladding temperatures linearly increased from 335°F at 7 seconds to the peak cladding temperatures found in Figure 15 of Lorenz and Parker, at 35 seconds. Temperatures are then assumed to decrease 50°F from 35 to 50 seconds of the transient. This assumed cladding history is provided in Figure B.18 and compared to the measured cladding temperature history for Rod 12. The assumed cladding/coolant temperature history is also provided in Table B.20 which is a listing of the FRAPTRAN input file for the FRF-2 test.

As discussed in Section A.3.3, there were three principal gas volumes in the experimental setup which affect the interpretation of the gas pressure data. The approach used to model this situation with FRAPTRAN was to force the coolant temperature to a low value at the top of the rod to simulate the exterior gas volume that was kept at a low temperature; see Table B.18 for the input used to accomplish this.

B.7 Other FRAPTRAN Assessment Cases

FRAP-T6 Standard Problem

The FRAPTRAN input for the FRAP-T6 Standard Problem is based on the input provided in Appendix B of Siefken et al. (1981). This case is discussed in Section A.4.1 and the FRAPTRAN input file is provided as Table B.21. This is a beginning-of-life case so there is no FRAPCON-3 initialization.

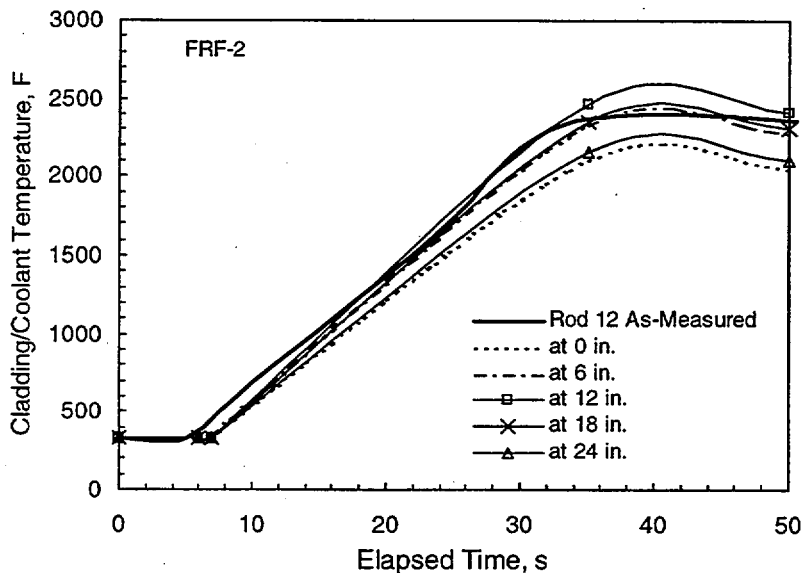


Figure B.18 Assumed Input Cladding Temperature History for FRF-2

Table B.20 FRAPTRAN Input for FRF-2 Assessment Case

```

*****
* FrapTran, transient fuel rod analysis code
*-----*
*
* CASE DESCRIPTION: Treat LOCA experiment FRF-2 with steady state T/H
* zone = 5, htclev = 0.5, 1, 1.5, 2, 2.25,
* UNIT FILE DESCRIPTION
* ----
* -- Input:
* 15 Water properties data
*
* -- Output:
* 6 STANDARD PRINTER OUTPUT
* 66 STRIPF FILE FOR PLOTTER
*
* -- Scratch:
* 5 SCRATCH INPUT FILE FROM ECHO1
*
* Input: FrapTran INPUT FILE
*
*****
* GOESINS:
FILE05='nullfile', STATUS='scratch', FORM='FORMATTED',
CARRIAGE CONTROL='LIST'
FILE15='sth2xt', STATUS='old', FORM='UNFORMATTED'
*
* GOESOUTS:
FILE06='out.treatloca', STATUS='UNKNOWN', CARRIAGE CONTROL='LIST'
FILE66='stripf.treatloca', STATUS='UNKNOWN', FORM='FORMATTED',
CARRIAGE CONTROL='LIST'
/*****
Treat LOCA experiment FRF-2 with steady state T/H
$begin
ProblemStartTime = 0.0,
ProblemEndTime = 50.0,
$end
start
$Iodata
unitout=1, dtpoa(1)=1.0, dtplt=0.1, res=0, pow=1,
$end
$solution
dtmaxa(1)=0.001, 0.0, 0.0001, 20, 0.001, 26.6,
dtss=1.e5
prsacc=0.001, tmpacl=0.001,
maxit=100, noiter=200, epshtl=1.0
naxn=10, nfmesh=15,
$end
$design
RodLength=2, RodDiameter=0.046942,
rshd=0.0136, dishd=0.046942, pelh=0.1, dishv0=0.0,
FuelPelDiam=0.041208, roughf=1.14, frden=0.95, bup=0.0, frpo2=0.0,
fotmtl=2.0, tsntrk=1883.0, fgrrns=10.0, gadoln=0.0,
gapthk=0.0002, coldw=0.1, roughc=2.16, clwdwc=0.04,
ncs=20, spl=.1979, scd=.02958, swd=3.42e-3, vplen=3.178e-4,
gfrac(1)=1.0, gappr0=75.0, tgas0=77.0,

```

Table B.20 (contd)					
\$end					
\$power					
RodAvePower= 0, 0, 1.3, 5, 11, 7.2, 5.3, 13.6,					
8.2, 22.5, 5.3, 30, 0, 35, 0, 50,					
AxPowProfile=0.85, 0, 0.97, 0.333, 1.05, 0.666, 1.06,					
1, 1.04, 1.333, 0.97, 1.666, 0.89, 2,					
RadPowProfile=0.9234, 0.00, 0.9259, 0.003090, 0.9328, 0.005150,					
0.9425, 0.007210, 0.954, 0.009270, 0.969, 0.011330,					
0.986, 0.013390, 1.008, 0.015450, 1.035, 0.017510,					
1.064, 0.019570, 1.0790, 2.0604e-2,					
\$end					
\$model					
internal='on', gasflo=0,					
deformation='on',					
\$end					
\$boundary					
coolant='on' geomet=1, dhe=0.046937, dhy=0.01944, achn=0.01211,					
heat='on',					
lowpl=2, hinta(1)=1215.3, 0.0, 1215.3, 500.0,					
upppl=2, hupta(1)=2500.0, 0.0, 2500.0, 200.0,					
pressu=2, pbh1(1) = 21, 0, 21, 200.0,					
press=2, pbh2(1) = 20, 0, 20, 50,					
zone = 5, htcleve = 0.5, 1, 1.5, 1.8, 2,					
htco=2, htca(1,1) = 2000000, 0, 2000000, 50,					
htca(1,2) = 2000000, 0, 2000000, 50,					
htca(1,3) = 2000000, 0, 2000000, 50,					
htca(1,4) = 2000000, 0, 2000000, 50,					
htca(1,5) = 2000000, 0, 2000000, 50,					
massfl=16, gbh(1)= 87.36, 0.0, 87.36, 5.0,					
98.28, 10.0, 103.74, 15.0,					
103.74, 20.0, 103.74, 25.0,					
132.13, 27.18, 87.36, 30.0,					
65.52, 31.0, 43.68, 37.0,					
27.3, 40.0, 16.38, 50.0,					
50.0, 100.0, 50.0, 110.0,					
51.32, 150.0, 70.98, 200.0,					
tem =5 , tblka(1,1)=335, 0, 335, 7, 2325, 35, 2275, 50,					
tblka(1,2)=335, 0, 335, 7, 2460, 35, 2410, 50,					
tblka(1,3)=335, 0, 335, 7, 2350, 35, 2300, 50,					
tblka(1,4)=335, 0, 335, 7, 2150, 35, 2100, 50,					
tblka(1,5)=335, 0, 335, 7, 370, 35, 370, 50,					
chf=1, jchf='b', filmbo=1, jfb='cl', coldwa=1, axpow=1					
\$end					
\$tuning					
\$end					

Table B.21 FRAPTRAN Input for FRAP-T6 Standard Problem Assessment Case

```

*****
* FrapTran, transient fuel rod analysis code
*-----*
*
* CASE DESCRIPTION: Standard Problem #1
*
* UNIT FILE DESCRIPTION
* ----
* -- Input:
* 15 Water properties data
*
* -- Output:
* 6 STANDARD PRINTER OUTPUT
* 66 STRIPF FILE FOR GRAFITI
*
* -- Scratch:
* 5 SCRATCH INPUT FILE FROM ECHO1
*
* Input: FrapTran INPUT FILE
*
*****
*
* GOESINS:
FILE05='nullfile', STATUS='scratch', FORM='FORMATTED',
CARRIAGE CONTROL='LIST'
FILE15='sth2xt', STATUS='old', FORM='UNFORMATTED'
*
* GOESOUTS:
FILE06='out.stdprobl', STATUS='UNKNOWN', CARRIAGE CONTROL='LIST'
FILE66='stripf.stdprobl', STATUS='UNKNOWN', FORM='FORMATTED',
CARRIAGE CONTROL='LIST'
/*****
Standard Problem #1
$begin
ProblemStartTime = 0.0,
ProblemEndTime = 20.0,
$end
start
$iodata
unitout=1, dtpoa(1)=0.5, dtplt=0.25, pow=1,
$end
$solution
dtmaxa(1)=0.001, 0.0, 0.001, 4.9, 0.01, 5.0, 0.01, 20.0, dtss=1.e5
prsacc=0.001, tmpacl=0.001, maxit=100, noiter=100, epsht1=1.0,
zelev=0.5,1.5,2.5,3.5,4.25,4.75,5.25,5.75,
6.25,6.75,7.25,7.75,8.5,9.5,10.5,11.5,
nfmesh=11,
$end
$design
RodLength=12.0, RodDiameter=0.03517,
rshd=0.01008, dishd=0.000625, pelh=0.0251, dishv0=0.0000002,
FuelPelDiam=0.0305, roughf=1.14, frden=0.932457, fotmt1=2.0, tsntrk=1883.0,
gapthk=3.25e-4, coldw=0.1, roughc=2.16, cldwdc=0.04, fgns=10.0,
ncs=22, spl=0.4583, scd=0.0291, swd=0.006333, vplen=0.00038,
gfrac(1)=1.0, gappr0=2243.0, gsms=0.03,
$end

```

Table B.21 (contd)

\$power					
RodAvePower=11.08,	0.0,	3.695,	0.6,	2.01,	2.3,
1.413,	8.7,	0.815,	10.0,	1.902,	13.0,
0.543,	16.3,	0.402,	45.0,		
AxPowProfile=0.56,					
0.545,	1.17,	1.6333,	1.46,	2.7,	
1.61,	3.8125,	1.58,	4.9,	1.48,	5.99166,
1.34,	7.075,	1.15,	8.15833,	0.94,	9.25,
0.70,	10.3,	0.36,	11.39166,		
RadPowProfile=0.982,					
0.00,	0.983,	0.0022875,	0.984,	0.0038125,	
0.985,	0.0053375,	0.988,	0.0068625,	0.991,	0.0083875,
0.996,	0.0099125,	1.002,	0.0114375,	1.009,	0.0129625,
1.017,	0.0144875,	1.03,	1.525e-2,		
\$end					
\$model					
internal='on',					
metal='on', cathca=1,					
deformation='on',					
\$end					
\$boundary					
heat='on'					
press=12, pbh2(1)=2273.0,	0.00,	1561.0,	0.51,		
1405.0,	1.01,	1198.0,	2.15,		
1166.0,	2.75,	940.0,	6.95,		
908.0,	7.55,	856.0,	8.15,		
686.0,	9.87,	568.0,	11.07,		
206.0,	15.87,	50.0,	20.07,		
zone=3, htco=12, tem=12,					
htclew(1)=3.0, 9.0, 12.0,					
htca(1,1)=51600.0,	0.00,	166.0,	0.51,		
36.0,	1.01,	28.1,	2.15,		
120.0,	2.75,	100.0,	6.95,		
52.0,	7.55,	5.0,	8.15,		
5.0,	9.87,	160.0,	11.07,		
60.0,	15.87,	50.0,	20.07,		
tblka(1,1)=638.3,					
0.0,	601.5,	0.51,			
587.5,	1.01,	743.8,	2.15,		
563.5,	2.75,	537.2,	6.95,		
533.1,	7.55,	553.2,	8.15,		
1333.8,	9.87,	531.0,	11.07,		
384.2,	15.87,	893.2,	20.07,		
htca(1,2)=62300.0,					
0.0,	158.0,	0.51,			
36.0,	1.01,	281.0,	2.15,		
116.0,	2.75,	100.0,	6.95,		
52.0,	7.55,	5.0,	8.15,		
5.0,	9.87,	160.0,	11.07,		
60.0,	15.87,	50.0,	20.07,		
tblka(1,2)=638.3,					
0.00,	601.5,	0.51,			
587.5,	1.01,	743.8,	2.15,		
563.5,	2.75,	537.2,	6.95,		
533.1,	7.55,	553.2,	8.15,		
1333.8,	9.87,	531.0,	11.07,		

Table B.21 (contd)			
384.2,	15.87,	893.2,	20.07,
htca(1,3)=39300.0,	0.0,	250.0,	0.51,
40.0,	1.01,	281.0,	2.15,
128.0,	2.75,	110.0,	6.95,
52.0,	7.55,	5.0,	8.15,
5.0,	9.87,	160.0,	11.07,
60.0,	15.87,	50.0,	20.07,
tblk(1,3)=638.3,	0.0,	601.5,	0.51,
587.5,	1.01,	743.8,	2.15,
563.5,	2.75,	537.2,	6.95,
533.1,	7.55,	553.2,	8.15,
1333.8,	9.87,	531.0,	11.07,
384.2,	15.87,	893.2,	20.07,
\$end			
\$stuning			
\$end			

IFA-508, Rod 11

For the IFA-508 case (Section A.4.2), the FRAPTRAN input is relatively straight-forward. The linear heat rate history was presented in Figure A.49 and the coolant inlet conditions in Table A.10. The axial relative power profile is presented in Figure B.19.

Because the coolant conditions are constant and the power changes are relatively slow, no cladding/coolant temperature history was defined for the FRAPTRAN input; the coolant conditions are defined in the input, as presented in Table B.22 which is the FRAPTRAN input file for IFA-508, Rod 11.

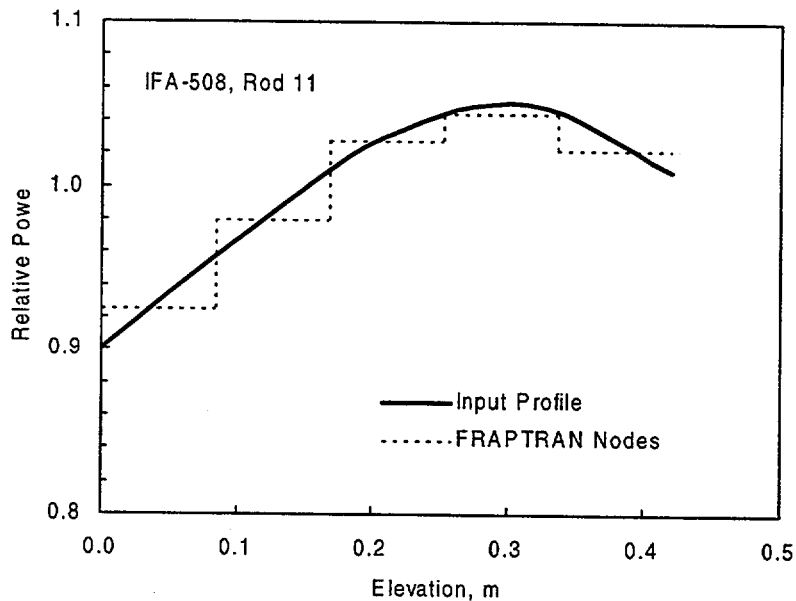


Figure B.19 Axial Power Profile for IFA-508, Rod 11

Table B.22 FRAPTRAN Input for IFA-508, Rod 11 Assessment Case

* FrapTran, transient fuel rod analysis code		*
-----*		
* CASE DESCRIPTION: IFA-508 Test Rod 11		*
* run time 2 hours 40 minutes		*
* UNIT FILE DESCRIPTION		*
-----*		
* -- Input:		*
* 15 Water properties data		*
-----*		
* -- Output:		*
* 6 STANDARD PRINTER OUTPUT		*
* 66 STRIPF FILE FOR GRAFITI		*
-----*		
* -- Scratch:		*
* 5 SCRATCH INPUT FILE FROM ECHO1		*
-----*		
* Input: FrapTran INPUT FILE		*

* GOESINS:		
FILE05='nullfile', STATUS='scratch', FORM='FORMATTED',		
CARRIAGE CONTROL='LIST'		
FILE15='sth2xt', STATUS='old', FORM='UNFORMATTED'		
* GOESOUTS:		
FILE06='out.IFA-508', STATUS='UNKNOWN', CARRIAGE CONTROL='LIST'		
FILE66='stripf.IFA-508', STATUS='UNKNOWN', FORM='FORMATTED',		
CARRIAGE CONTROL='LIST'		
/*****		
HPR-508 Test Rod 11		
\$begin		
ProblemStartTime = 0.0,		
ProblemEndTime = 105000,		
\$end		
start		
\$iodata		
unitin=1, unitout=1, dtpoa(1)=500.0,0.0,1000.0,3.e4,1000.0,10.e5,		
dtplt=100.0,		
\$end		
\$solution		
dtmaxa(1)=0.5,0.0,		
dtss=1.0,		
prsacc=0.001, tmpac1=0.001,		
maxit=100, noiter=100, epsht1=1.0,		
zelev=0.04875, 0.14625, 0.24374, 0.34124, 0.362,		
nfmesh=15, naxn=5,		
\$end		
\$design		
RodLength=0.420, RodDiameter=0.01222,		
rshd=3.65e-3, dishd=0.3990e-3, pelh=1.5e-2, dishv0=2.532e-8,		
FuelPelDiam=0.01075, roughf=2.16, frden=0.948, fotmtl=2.0, tsntrk=1870.0,		
fgrns=10.0, gadoln=0.0		
gapthk=0.00005, coldw=0.1, roughc=1.14, cldwdc=0.04		

Table B.22 (contd)						
ncs=2, spl=6.10e-2, scd=1.02e-2, swd=1.22e-3, vplen=6.2356e-6,						
gfrac(1)=1.0, gappr0=.103e6, tgas0=294.0,						
\$end						
\$power						
RodAvePower=0., 0, 15.38, 2448, 15.38, 3636, 30.34, 6696, 30.34, 21600,						
40.6, 24660, 40.6, 40752, 47.4, 42912, 47.4, 96048, 0, 105156,						
AxPowProfile(1,1) = 0.90, 0, 0.97, 0.105, 1.03, 0.21, 1.05, 0.315,						
1.01, 0.420,						
NumAxProfiles=1,						
RadPowProfile =						
0.85, 0.0, 0.853, 8.8900e-4, 0.88, 1.9761e-3,						
0.902, 2.6518e-3, 0.9270, 3.1852e-3, 0.959, 3.6424e-3,						
0.985, 4.0488e-3, 1.018, 4.4171e-3, 1.055, 4.7574e-3,						
1.095, 5.0749e-3, 1.1375, 5.3721e-3, 1.183, 5.6566e-3,						
\$end						
\$model						
internal='on',						
deformation='on', noball=1,						
heat='on', cenvoi=1, zvoid1=.360, zvoid2=.39, rvoid=.9e-3,						
inst='instrument'						
\$end						
\$boundary						
coolant='on', geomet=1, dhe=1.52e-2, dhy=1.52e-2, achn=1.143e-4,						
lowpl=2, hinta= 1.0352e+6, 0., 1.0352e+6, 10.0e+5,						
pressu=2, pbh1(1)= 3.45e+6, 0., 3.45e+6, 10.0e+5,						
massfl=2, gbh(1)= 3.e+4, 0., 3.e+4, 2e+5, 3.e+4, 4e+5, 3.e+4, 6e+5,						
3.e+4, 8e+5, 3.e+4, 10.0e+5,						
chf=1, jchf='w', filmbo=1, jfb='to'						
\$end						
\$tuning						
\$end						

The relatively high U-235 enrichment (10.5%) and heavy water moderate result in a slightly different radial power profile in the fuel than for a normal light-water reactor. The radial power profile is provided in the input file (Table B.22).

Because this is a beginning-of-life transient, FRAPCON-3 was not used to initialize FRAPTRAN.

IFA-533.2

For the IFA-533.2 case (Section A.4.3), the FRAPTRAN input is relatively straight-forward. The heat rate history is a simple scram from 29 kW/m and assumes a drop to 10% of initial power in the first second. The relative axial power profile is presented in Figure B.20 and coolant inlet conditions were defined in Table A.11.

Because the coolant conditions are constant, no cladding/coolant temperature history was defined for the FRAPTRAN input; the coolant conditions are defined in the input, as presented in Table B.23 which is the FRAPTRAN input file for IFA-533.2, Rod 808R.

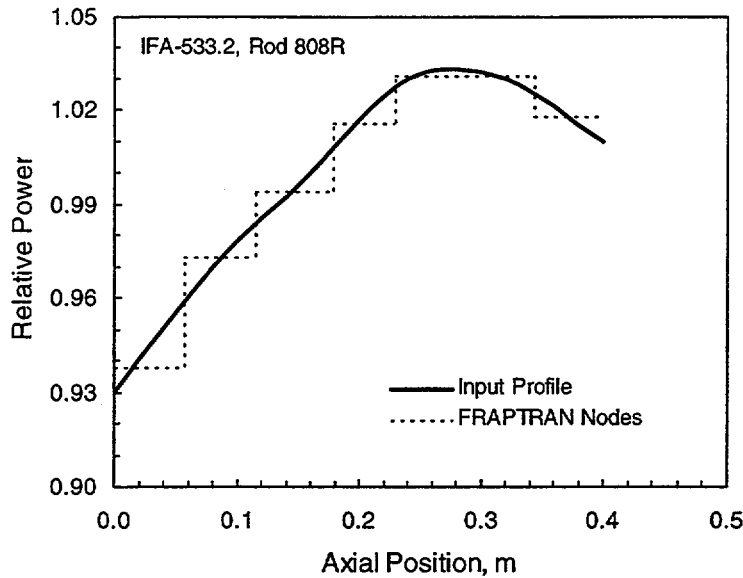


Figure B.20 Axial Power Profile for IFA-533.2

Table B.23 FRAPTRAN Input for IFA-533.2 Assessment Case		

* FRAPTRAN, transient fuel rod analysis code		*
-----		*
* CASE DESCRIPTION: ifa-533.2 scram		*
* UNIT FILE DESCRIPTION		*
* -----*		*
* -- Input:		*
* 15	Water properties data	*
* 22	FRAPCON3 initialization data	*
* -- Output:		*
* 6	STANDARD PRINTER OUTPUT	*
* 13	data file for use in EXCEL	*
* 66	STRIPF FILE FOR GRAFITI	*
* -- Scratch:		*
* 5	SCRATCH INPUT FILE FROM ECHO1	*
* Input: FRAPTRAN Input File plus FRAPCON3 input		*

*		
FILE05='nullfile', STATUS='scratch', FORM='FORMATTED',		
CARRIAGE CONTROL='LIST'		
FILE15='sth2xt', STATUS='old', FORM='UNFORMATTED'		
FILE22='restart.ifa-533HE', STATUS='OLD', FORM='FORMATTED'		
*		
FILE06='out.ifa-533HE', STATUS='UNKNOWN', FORMAT='FORMATTED'		
FILE66='stripf.ifa-533HE', STATUS='UNKNOWN', FORM='FORMATTED',		
CARRIAGE CONTROL='LIST'		

Table B.23 (contd)

```

/*****
ifa-533.2 scram transient
$begin
  ProblemStartTime = 0.0,
  ProblemEndTime = 60,
$end
start
$iodata
  unitin=1, unitout=1, trest = 1.602e08, inp = 1,
  res = 0, pow = 0, dtplt=0.5,
  dtpoa = 0.5,0.0, 0.5,60.0, 0.5,120.0,
$end
$solution
  dtmaxa=0.01,0.0, 0.01,60.0, 0.01,120.0,
  dtss=50.0,
  prsacc = 0.001, tmpacl = 0.001,
  maxit = 100, noiter=100, epshtl = 1.0,
  naxn=7, nfmesh=15,
$end
$design
  RodLength=0.400, RodDiameter=0.01253,
  rshd=0.00, dishd=0.0, pelh=0.0128, dishv0=0.0,
  FuelPelDiam=0.01057, roughf = 2.159, frden = 0.947, bup=3.836e6,
  frpo2=0.0, fotmtl = 2.0,tsntrk = 1883.0,gadoln = 0.0,
  gapthk=0.000115, coldw=0.2, roughc=0.635, cfluxa=0.5e17,
  tflux = 160.e6, clwdc=0.04,
  ncs=5, spl=0.21717, scd=0.00838, swd=0.0014, vplen = 0.0000098,
  gfrac = 1.0,0.0,0.0,0.0,0.0,0.0,0.0,0.0, tgas0=290.0, gappr0 = 0.5e6
$end
$power
  RodAvePower= 28.9, 0, 2.89, 1, 1.45, 60,
  AxPowProfile=0.92, 0, 0.97, 0.08, 1, 0.16, 1.03,
    0.24, 1.03, 0.32, 1.01, 0.4,
  RadPowProfile= 0.9437,    0.,    0.9449, 0.000560,    0.9477 , 0.00107,
    0.9517,    0.00154,    0.9568,    0.00197,    0.9627 ,    0.00235,
    0.9692,    0.00270,    0.9763,    0.00301,    0.9839 ,    0.00328,
    0.9921,    0.00353,    1.0011,    0.00374,    1.0111 ,    0.00392,
    1.0223,    0.00408,    1.0351,    0.00422,    1.0498 ,    0.00433,
    1.0669,    0.00442,    1.0869,    0.00449,    1.1101 ,    0.00455,
    1.1370 ,    0.00459 ,    1.1676 ,    0.00462 ,    1.2018 ,    0.00464,
    1.2390 ,    0.00465 ,    1.2776 ,    0.00466 ,    1.3144 ,    0.004662,
    1.3407 ,    0.004663 ,
$end
$model
  heat='on', cenvoi=1, zvoid1=0.365, zvoid2=0.4,
  rvoid=0.00125, inst='instrument'
$end
$boundary
  heat='on', press=2, pbh2=3360000.0, 0.0, 3360000.0, 120.0,
  zone=1, htclew=0.466, htco=2, htca(1,1)=20000.0, 0.0, 20000.0, 120.0,
  tem=2, tblka(1,1)=513.0,0.0, 513.0,120.0,
$end
$tuning
$end

```

Because this is a transient at a burnup level of 44 MWd/kgUO₂, FRAPCON-3 was used to define the burnup dependent parameter input for FRAPTRAN. The burnup dependent radial power profile model in FRAPCON-3 is able to account for the high initial enrichment and heavy coolant moderator conditions prevalent in the HBWR.

The thermocouple tip was positioned approximately 35 mm below the top of the fuel column. With seven axial nodes used in the FRAPTRAN calculation, axial node 7 is the equivalent position for comparing fuel temperatures.

PBF IE-1, Rod 7

For the PBF IE-1, Rod 7 case, input was developed from the data presented in the data report (see Section A.4.4.). The heat rate history is a rise from zero power to a peak power of 72 kW/m with a hold and subsequent decrease in coolant flow (see Figure A.52). The axial power profile for the IE-1 test is presented in Figure B.21.

No cladding/coolant temperature history was defined for the FRAPTRAN input; the coolant conditions are defined in the input, as presented in Table B.24, which is the FRAPTRAN input file for Rod 7 of test IE-1. The measured cladding temperature history (at 0.622 m) was presented in Figure A.54 for the flow reduction period; otherwise, the cladding surface temperature was constant at about 625K.

Although Rod 7 had a burnup of approximately 6.8 MWd/kgU at the time of the test, no FRAPCON-3 run was made to define burnup dependent parameters for FRAPTRAN. Thus, zero burnup fuel thermal conductivity values were used in the FRAPTRAN calculation. The cladding dimensions were based on

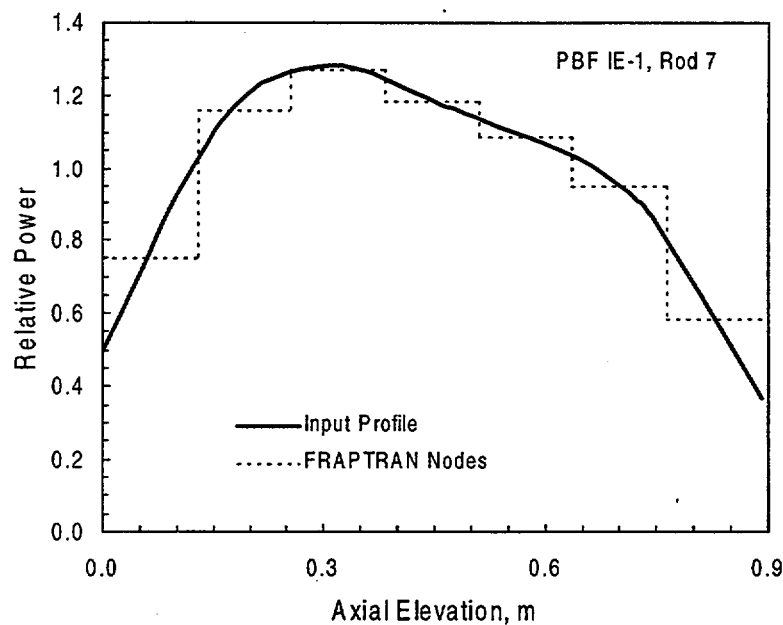


Figure B.21 Axial Power Profile for PBF IE-1, Rod 7

Table B.24 FRAPTRAN Input for PBF IE-1, Rod 7 Assessment Case

* FrapTran, transient fuel rod analysis code		*

* -----		*
* -----		*
* CASE DESCRIPTION: PBF IE-1 Rod 7		*
* -----		*
* UNIT FILE DESCRIPTION		*
* ---- -----		*
* -- Input:		*
* 15 Water properties data		*
* -----		*
* -- Output:		*
* 6 STANDARD PRINTER OUTPUT		*
* 66 STRIPF FILE FOR GRAFITI		*
* -----		*
* -- Scratch:		*
* 5 SCRATCH INPUT FILE FROM ECHO1		*
* -----		*
* Input: FrapTran INPUT FILE		*
* -----		*

* -----		*
* GOESINS:		
FILE05='nullfile', STATUS='scratch', FORM='FORMATTED',		
CARRIAGE CONTROL='LIST'		
FILE15='sth2xt', STATUS='old', FORM='UNFORMATTED'		
* -----		*
* GOESOUTS:		
FILE06='out.IE-1r7', STATUS='UNKNOWN', CARRIAGE CONTROL='LIST'		
FILE66='stripf.IE-1r7', STATUS='UNKNOWN', FORM='FORMATTED',		
CARRIAGE CONTROL='LIST'		
/*****		
PBF IE-1 Rod 7		
\$begin		
ProblemStartTime = 0.0,		
ProblemEndTime = 3000.0,		
\$end		
start		
\$iodata		
unitin=1, unitout=1, dtpoa(1)=100.0,0.0, 500.0,1000.0,500.0,10000.0,		
dtplt=10.0,		
\$end		
\$solution		
dtmaxa(1)=1.0, 0.0, 0.1, 390.0,0.1, 2756		
dtss=5.0,		
prsacc=0.001, tmpacl=0.001, maxit=200, noiter=200, epshtl=1.0,		
naxn=7, nfmesh=15,		
\$end		
\$design		
RodLength=0.89, RodDiameter=0.00989,		
rshd=0.003302, dishd=0.0003429, pelh=0.01564, dishv0=1.18e-8,		
FuelPelDiam=0.00848, roughf=2.16, frden=0.9389, bup=6830.0,		
fotmtl=2.0, tsntrk=1883.0, fgrns=10.0,gadoln=0.0,		
gapthk=0.000115, coldw=0.1, roughc=1.14, cldwdc=0.04,		
ncs=24, spl=0.0572, scd=0.00865, swd=0.001113, vplen=7.098e-6,		
gfrac(1)=0.777,0.223, gappr0=1.9e6, tgas0=300.0,		

Table B.24 (contd)	
\$end	
\$power	
RodAvePower=	0.0, 0.0, 18.8, 720, 48.4, 1440, 48.4, 2160 56.6, 2520, 56.6, 3000,
AxPowProfile=	0.5, 0.000, 1.13, 0.159, 1.28, 0.306, 1.18, 0.452, 1.13, 0.521, 1.07, 0.599, 1.01, 0.662, 0.91, 0.724, 0.86, 0.745, 0.37, 0.890,
RadPowProfile=	0.883, 0.000303, 0.900, 0.000909, 0.904, 0.0015149, 0.925, 0.0021209, 0.956, 0.0027269, 1.006, 0.0033328, 1.2, 0.0042418,
\$end	
\$model	
deformation=	'on'
\$end	
\$boundary	
coolant=	'on'
geomet=	1, dhe=0.0169, dhy=0.00639, achn=0.00013138,
pressu=	2, pbhl(1) = 1.4830e7, 0.0, 1.4830e7, 10000.0,
lowpl=	2, hinta(1)= 1.2473e6, 0.0, 1.2473e6, 10000.0,
uppl=	2, hupta(1)= 1.7e6, 0.0, 1.7e6, 10000.0,
massfl=	14, gbh(1)= 4797, 0.0, 4797, 2620, 2927, 2630, 2731, 2660, 2731, 2720, 2534, 2721, 2534, 2745, 2042, 2746, 2042, 2755, 1000, 2756, 1000, 2815, 1845, 2830, 1845, 3000
\$end	
\$tuning	
\$end	

pre-transient measurements, and did reflect a slight decrease from the as-fabricated measurements. During the steady-state irradiation in the Saxton PWR, the fuel would have undergone some densification, cracking, and outward relocation of fragments; however, the design fuel diameter was used in the FRAPTRAN input.

The test rods were initially filled to a gas pressure of 2.6 MPa for the transient test. However, immediately prior to the test, the pressure for Rod 7 was measured at 1.9 MPa. It is believed that the fill gas leaked into the pressure lines during the period between fabrication and testing. An initial pressure of 1.9 MPa was used for the FRAPTRAN calculations without changing the as-fabricated gas mixture of 78% helium and 22% argon that was used to simulate the thermal conductivity of release fission gases.

PBF PR-1

For the PBF PR-1 case, input was developed from the data presented in the data report (see Section A.4.5). The linear heat rate and coolant flow histories were presented in Figure A.56. The axial power profile for the PR-1 test is presented in Figure B.22.

This was a beginning-of-life test, thus no FRAPCON-3 calculation was made to provide burnup dependent values for parameters for FRAPTRAN.

The basic input used for FRAPTRAN was from Rod 524-2 which had a preirradiation fuel density of 92%TD. However, based on the irradiation history prior to cycle 17 and the observed increases in

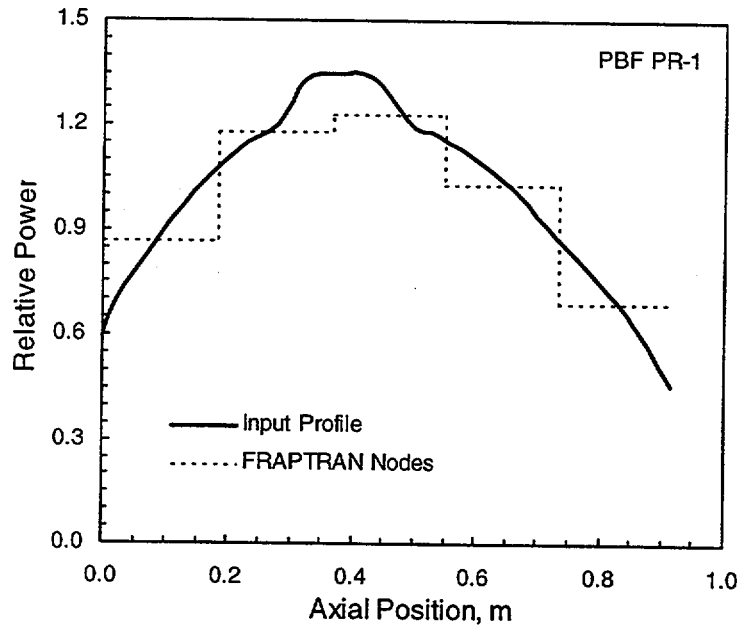


Figure B.22 Axial Power Profile for PBF PR-1.

measured fuel centerline temperature with irradiation cycle, it was assumed for the FRAPTRAN prediction that the fuel had densified to 95%TD. In addition to using a density of 95%TD for the fuel thermal conductivity calculations, the fuel pellet diameter was assumed to decrease from 10.57 mm to 10.50 mm. This density increase with fuel pellet diameter decrease results in widening the fuel-cladding gap and increasing fuel temperatures.

Coolant conditions were specified using temperature and flow rate and then using FRAPTRAN correlations to calculate the heat transfer coefficient and cladding surface temperature. This is different than for many of the other assessment cases where coolant temperature and heat transfer coefficients were input to control cladding surface temperature to closely matched measured data.

The FRAPTRAN input file is provided in Table B.25.

Table B.25 FRAPTRAN Input for PBF PR-1 Assessment Case

* FRAPTRAN, transient fuel rod analysis code		*

* Case name: PBF PR-1		*

* UNIT FILE DESCRIPTION		*

* -- Input:		*
* 15 Water properties data		*

* -- Output:		*
* 6 STANDARD PRINTER OUTPUT		*
* 66 STRIPF FILE FOR PLOT		*

* -- Scratch:		*
* 5 SCRATCH INPUT FILE FROM ECHO1		*

* FILE05='nullfile', STATUS='scratch', FORM='FORMATTED', CARRIAGE CONTROL='LIST'		
* FILE15='sth2xt', STATUS='old', FORM='UNFORMATTED'		
* FILE06='PR1L2a.out', STATUS='UNKNOWN', CARRIAGE CONTROL='LIST'		
* FILE66='stripfPR1L2a', STATUS='UNKNOWN', FORM='FORMATTED', CARRIAGE CONTROL='LIST'		
/*34567890123456789012345678901234567890123456789012345678901234567		
PBF PR-1 PCM transient cycle 17 Rod 524-1 CHF = LOFT FB=CB		
\$begin		
ProblemStartTime=0.,		
ProblemEndTime=184.0,		
\$end		
start		
\$iodata		
unitin=1, dtpoa(1)=3.,0.,2.,95.9, 1.,140.,4.0,185.,		
dtplt=0.125,		
\$end		
\$solution		
dtmaxa(1)=0.005,0.,0.002,20.,0.001,140.,0.1,600.0, dtss=5.0,		
maxit=100, noiter=100, epsht1=1.0, prsacc=0.001,		
nfmesh=17,		
naxn=5,		
\$end		
\$design		
RodLength=0.9144, RodDiameter=0.01235,		
pelh=0.0105, FuelPelDiam=0.0105, roughf=2.12, frden=0.95,		
gapthk=70.e-06, coldw=0.1, roughc=1.1, cldwdc=0.04,cfluxa=.8e+06,		
ncs=16, spl=0.05, scd=0.009, swd=0.001,		
vplen=0.0360e-4,tflux=100.e+01,		
gfrac=1.0, gappr0=2.5e+06, tgas0=300., bup=4.e+01,		
\$end		
\$power		
RodAvePower= 8.0,0.0, 34.0,20.0,33.,165., 23.0,175.,23.0,185.,		
AxPowProfile=0.60,0., 0.79,0.0536, 1.04,0.161, 1.20,0.279,		
1.35,0.375; 1.2, 0.494,		

Table B.25 (contd)	
1.08,0.617, 0.88,0.730, 0.66,0.842, 0.46,0.914,	
RadPowProfile=0.82,0.0010, 0.83,0.0016, 0.85,0.0021,	
0.88,0.0026, 0.91,0.0031, 0.955,0.0035, 1.025,0.0041,	
1.11,0.0045, 1.215,0.00525,	
\$end	
\$model	
internal='on',	
\$end	
\$boundary	
coolant='on',	
geomt=1, dhe=0.0171, dhy=0.00675, achn=0.000169,	
pressu=4,pbh1=15.4e+6,0.,15.4e+6,60.,15.1e+6,135.,15.4e+6,185.,	
massfl=4,gbh=800.,0.0,800.,45.,360.,135.,1000.,185.,	
lowpl=2, hinta=1.52e+6,0.00, 1.52e+6,600.,	
chf=1, jchf='l', filmbo=1, jfb='co',	
\$end	
\$tuning	
\$end	

B.8 References

Lorenz, R. A., and G. W. Parker. 1972. *Final Report on the Second Fuel Rod Failure Transient Test of a Zircaloy-Clad Fuel Rod Cluster in TREAT*. ORNL-4710, Oak Ridge National Laboratory, Oak Ridge, Tennessee.

NUREG/IA-0156, Volume 3, 1999. *Data Base on the Behavior of High Burnup Fuel Rods with Zr-1%Nb Cladding and UO₂ Fuel (VVER Type) Under Reactivity Accident Conditions: Test and Calculation Results.* U.S. Nuclear Regulatory Commission, Washington, D.C.

Russcher, G. E., et al. 1981. LOCA Simulation in the NRU Reactor. Materials Test-1. NUREG/CR-2152 (PNL-3835), Pacific Northwest National Laboratory, Richland, Washington.

Siefken, L. J., et al. 1981. *FRAP-T6: A Computer Code for the Transient Analysis of Oxide Fuel Rods*. NUREG/CR-2148. IG&G Idaho, Inc., Idaho Falls, Idaho.

Wilson, C. L., et al. 1983. LOCA Simulation in NRU Program. Data Report for the Fourth Materials Experiment (MT-4). NUREG/CR-3272 (PNL-4669), Pacific Northwest National Laboratory, Richland, Washington.

Wilson, C. L., et al. 1993. Large-Break LOCA. In-Reactor Fuel Bundle Materials Test MT-6A. PNL-8829, Pacific Northwest National Laboratory, Richland, Washington.

BIBLIOGRAPHIC DATA SHEET

(See instructions on the reverse)

1. REPORT NUMBER
(Assigned by NRC, Add Vol., Supp., Rev.,
and Addendum Numbers, if any.)

NUREG/CR-6739, Vol. 2
PNNL-13576

2. TITLE AND SUBTITLE

FRAPTRAN: Integral Assessment

3. DATE REPORT PUBLISHED

MONTH YEAR

September 2001

4. FIN OR GRANT NUMBER

W6200

5. AUTHOR(S)

M.E. Cunningham, C.E. Beyer, F.E. Panisko, P.G. Medvedev, PNNL
G.A. Berna, GABC
H.H. Scott, NRC

6. TYPE OF REPORT

computer code manual

7. PERIOD COVERED *(Inclusive Dates)*

2000-2001

8. PERFORMING ORGANIZATION - NAME AND ADDRESS *(If NRC, provide Division, Office or Region, U.S. Nuclear Regulatory Commission, and mailing address; if contractor, provide name and mailing address.)*

Pacific Northwest National Laboratory
Richland, WA 99352

Subcontractor:

G.A. Berning Consulting
2060 Sequoia Drive
Idaho Falls, ID 83404

9. SPONSORING ORGANIZATION - NAME AND ADDRESS *(If NRC, type "Same as above"; if contractor, provide NRC Division, Office or Region, U.S. Nuclear Regulatory Commission, and mailing address.)*

Division of Systems Analysis and Regulatory Effectiveness
Office of Nuclear Regulatory Research
U.S. Nuclear Regulatory Commission
Washington, DC 20555-0001

10. SUPPLEMENTARY NOTES

H. H. Scott, NRC Project Manager

11. ABSTRACT *(200 words or less)*

The Fuel Rod analysis Program Transient (FRAPTRAN) is a FORTRAN language computer code that calculates the transient performance of light-water reactor fuel rods during reactor power and cooling transients for hypothetical accidents such as loss-of-coolant accidents (LOCAs) and reactivity-initiated accidents (RIAs), and for anticipated operational occurrences. FRAPTRAN calculates the temperature and deformation history of a fuel rod given time-dependent fuel rod power and coolant boundary conditions. Volume 1 constitutes the code description document and includes the input instructions. Volume 2 (this report) provides the results of the assessment of the code predictions for various performance parameters. An integral assessment has been performed of the FRAPTRAN code to quantify its predictive capabilities. The FRAPTRAN predictions are shown to compare satisfactorily to a substantial set of experimental data. The code assessment data base consists of three separate effects steady-state irradiation tests and twenty integral effects tests. Comparisons were made to RIA test data with rod average burnups to 64 GWd/MTU and to a scram test with rod burnup of 44 GWd/MTU. The LOCA test data were from near-zero burnup experiments.

12. KEY WORDS/DESCRIPTORS *(List words or phrases that will assist researchers in locating the report.)*

Computer Code, Code Assessment, Axial Elongation, Rod Gas Pressure, Fuel Rod Performance, Cladding Oxidation, Cladding Deformation, High Burnup, Pellet Centerline Temperature

13. AVAILABILITY STATEMENT

unlimited

14. SECURITY CLASSIFICATION

(This Page)

unclassified

(This Report)

unclassified

15. NUMBER OF PAGES

16. PRICE

UNITED STATES
NUCLEAR REGULATORY COMMISSION
WASHINGTON, DC 20555-0001

OFFICIAL BUSINESS
PENALTY FOR PRIVATE USE, \$300